AD_____

Award Number: **W81XWH-09-2-0105**

TITLE: **Nrdp1-mediated ErbB3 increase during androgen ablation and its contribution to androgen-independence.**

PRINCIPAL INVESTIGATOR: **Paramita M. Ghosh, PhD**

CONTRACTING ORGANIZATION: **University of California, Davis**
Davis, CA 95616

REPORT DATE: **April 2013**

TYPE OF REPORT: **FINAL**

PREPARED FOR: U.S. Army Medical Research and Materiel Command
Fort Detrick, Maryland 21702-5012

REPORT DOCUMENTATION PAGE

Form Approved
OMB No. 0704-0188

1. REPORT DATE	2. REPORT TYPE	3. DATES COVERED
February 2013	FINAL	15 August 2012 -28 January 2013

4. TITLE AND SUBTITLE
Nrdp1-mediated ErbB3 increase during androgen ablation and its'contribution to androgen-independence.

5a. CONTRACT NUMBER

5b. GRANT NUMBER
W81XWH-09-2-0105

5c. PROGRAM ELEMENT NUMBER

5d. PROJECT NUMBER

5e. TASK NUMBER

5f. WORK UNIT NUMBER

6. AUTHOR(S)
Paramita M. Ghosh, Ph.D.

E-Mail:

7. PERFORMING ORGANIZATION NAME(S) AND ADDRESS(ES)
University of California, Davis
Davis, CA 95616

8. PERFORMING ORGANIZATION REPORT NUMBER

9. SPONSORING / MONITORING AGENCY NAME(S) AND ADDRESS(ES)
U.S. Army Medical Research and Materiel Command
Fort Detrick, Maryland 21702-5012

10. SPONSOR/MONITOR'S ACRONYM(S)

11. SPONSOR/MONITOR'S REPORT NUMBER(S)

12. DISTRIBUTION / AVAILABILITY STATEMENT
Approved for Public Release; Distribution Unlimited

13. SUPPLEMENTARY NOTES

14. ABSTRACT
Our data for the first time identifies Nrdp1 as an AR target that is androgen-regulated in castration resistant cells, but not in castration insensitive cells. Our new data shows that in cells where the AR is stabilized, and does not undergo degradation despite androgen withdrawal, it is able to transcribe PSA but not Nrdp1, whereas in cells where the AR is not stabilized, it can transcribe Nrdp1 and thereby regulate ErbB3 levels. Since we also showed earlier that ErbB3 signaling increase cell growth and suppress apoptosis, our results indicate that AR suppression of ErbB3 is a mechanism for keeping cells castration sensitive, whereas when this effect is lost, the cells become castration resistant. Further, we show that Filamin A nuclear localization keeps cells androgen responsive by destabilizing the AR, and maintaining its ability to transcriptionally regulate Nrdp1.

15. SUBJECT TERMS
ErbB3, Akt, cell proliferation, cell survival, androgen withdrawal, androgen receptor, EGFR, ErbB2, LNCaP, Nrdp1, RNF41, HER2, HER3, androgen response element, FKHRL1, transcriptional activity.

16. SECURITY CLASSIFICATION OF:			17. LIMITATION OF ABSTRACT	18. NUMBER OF PAGES	19a. NAME OF RESPONSIBLE PERSON
a. REPORT	b. ABSTRACT	c. THIS PAGE			USAMRMC
U	U	U	UU	177	19b. TELEPHONE NUMBER *(include area code)*

Table of Contents

INTRODUCTION: Patients with advanced prostate cancer (PCa) are initially susceptible to androgen withdrawal therapy (AWT), but ultimately develop resistance to this therapy (castration-resistant PCa, CRPC). The treatment options for patients who fail AWT are limited; hence the long-term goal of these studies is to identify therapeutic strategies to prolong the effectiveness of AWT. The ErbB receptor tyrosine kinase (RTK) family regulates proliferation and survival in PCa. Multiple studies suggested that ErbB3 plays a role in promoting PCa, however, its mechanism of action and the pathways mediating its effects were unknown. Hence, we investigate the role of ErbB3 in PCa progression.

BODY: Specific Aim 1. To test the hypothesis that increased ErbB3 during androgen ablation results in androgen independence of prostate cancer cells.

Task 1: *We will examine in paraffin embedded prostate cancer tissues whether there is increased ErbB3 and decreased Nrdp1 expression in androgen independent tumors from human patients.*

Patient Characteristics

Number of patients		78
RACE	Caucasian	38
	African American	17
	Others	23
Mean BMI		28.47 ± 4.48
Mean Pre-op PSA		7.99 ± 6.48
GLEASON	Gleason 5-6	35
	Gleason 7	33
	Gleason 8-9	9
STAGE	STAGE T1	43
	STAGE T2	35
POSITIVE MARGINS		27
PSA FAILURE		23

TABLE 1

We showed in a publication in 2010 that ErbB3 increases in castration-resistant prostate cancer. At that time, we did not have the antibody to Nrdp1 that can be used in IHC. Since then this antibody has been developed and is now reported here.

Nrdp1 expression in human prostate cancer correlates with nuclear AR levels. We previously showed that ErbB3 plays a major role in PCa progression and that ErbB3 levels are elevated during AWT due to suppression of the E3 ubiquitin ligase Nrdp1, which enables ErbB3 degradation (Chen, et al. 2010). Hence we investigated the expression of Nrdp1 in primary prostate tumor and surrounding non-tumor tissues available from the archives of the VA Northern California Health Care System (VANCHCS), Laboratory and Pathology Services. Sections from prostate tumors of 78 patients who underwent radical retropubic prostatectomy at VANCHCS between 1996 and 2002 were analyzed for these studies. Patient characteristics are described in **Table 1.** The specimens were stained with antibodies to Nrdp1 and AR. The specificity of the Nrdp1 staining was verified in HEK 293T cells with a control or Nrdp1 shRNA **(Figure 1).**

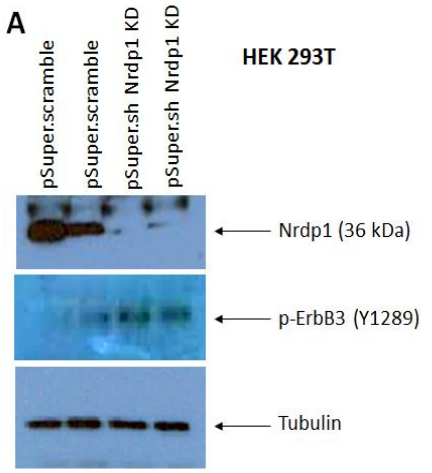

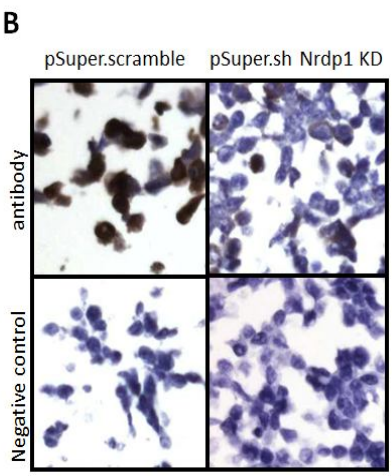

Figure 1. Nrdp1 Antibody Characterization. 293T HEK cells were transfected with control or Nrdp1 shRNA to show the specificity of a rabbit polyclonal anti-Nrdp1 antibody. **(A)** Western blot analysis showed Nrdp1 staining as a non-specific 65 KDa and a specific 36 KDa bands. Specificity of the lower band was determined by knockdown of Nrdp1 upon shRNA use, and a corresponding increase of p-ErbB3. 293T HEK cells were grown in FBS media. Cell lystaes were immunoblotted with andti-Nrdp1, anti-p-Erb3 and anti-tubulin antibodies. **(B)** 293T HEK cell pellets (similarly treated) were paraffin embedded, sectioned and stained with the same Nrdp1 antibody. Lack of background staining in the shRNA-treated cells denotes that the IHC staining was more specific.

Using a scoring system based on immunohistochemistry (IHC) intensity from 0 to 3, where 0 represents no staining and 3 represents the highest protein levels, we observed that Nrdp1 was expressed in the nucleus, the cytoplasm or both **(Figure 2A)**. Nrdp1 nuclear protein levels remains consistent between tumor and non-tumor tissue, whereas cytoplasmic Nrdp1 was significantly increased in tumor tissue compared to non-tumor ($p<0.001$) **(Figure 2B, Table 2)**.

Figure 2. Nrdp1 levels in human prostate tumor tissue correlate positively with nuclear AR expression and negatively with PSA failure. (A). Formalin fixed paraffin-embedded human localized prostate cancer specimens obtained by prostatectomy were arranged in a tissue microarray and stained with anti-Nrdp1 antibody. Nrdp1 expression was observed in the nucleus, cytoplasm or both and was scored in both benign and cancerous prostate tissues. **(B).** Boxplots showing distribution of Nrdp1 and in the nucleus or cytoplasm of cancer compared to non-tumor tissue. The expression of nuclear Nrdp1 remains the same in both cancer and non-tumor tissues, whereas cytoplasmic expression of Nrdp1 increases in tumor compared to non-tumor tissue.

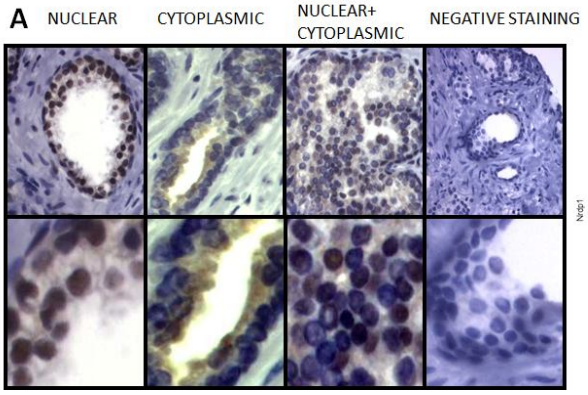

Supplementary Table 2: Staining in Cancer and Non-Cancer Cells

	Cytoplasm			Nucleus		
Protein	Median in Cancer Cells	Median in Non-Cancer Cells	P-Value (Wilcoxon Signed Rank Test)	Median in Cancer Cells	Median in Non-Cancer Cells	P-Value (Wilcoxon Signed Rank Test)
Nrdp1	1.0	0.5	<0.001	0.3	0.3	0.134
AR	1.0	0.8	<0.001	2.0	2.0	0.071

Examination of Oncomine datasets showed a similar trend in mRNA levels from human prostate as determined by various investigators; however, the same datasets also showed that AR levels were increased in tumor tissue vs. non-tumor **(Figure 3).**

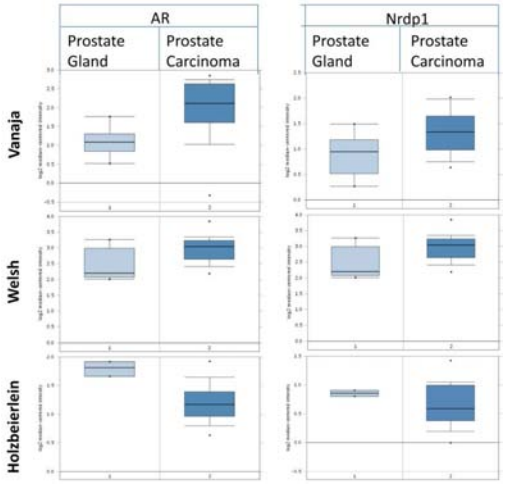

Figure 3. AR and Nrdp1 expression in cancer and normal cells. Confirmation of the up regulation of Nrdp1 and AR in cancer vs. normal prostate and the correlation between three Oncomine datasets. (For AR, p = 3.26 x 10^-8; for Nrdp1, p = 1.62 x 10^-6; values calculated using Fisher's combined probability test). Box plots shown are from studies in the Oncomine database representative of overall trend. Note that Nrdp1 levels correspond to AR values.

Hence, we investigated the protein levels of AR in our TMA tissues **(Figure 4)**.

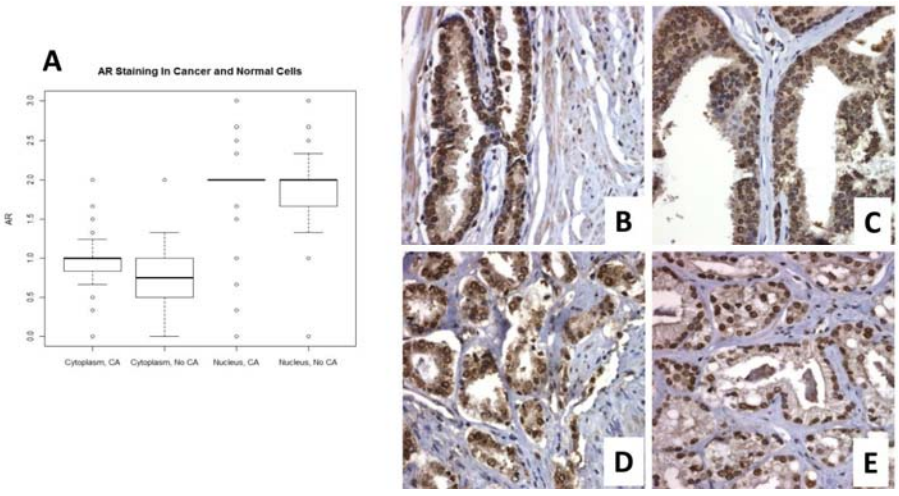

Figure 4. AR Staining in tumor and non-tumor prostate. (A) Boxplots showing distribution of AR in the nucleus and cytoplasm of cancer tissue compared to non-tumor tissue. The expression of nuclear AR and remains the same in both cancer and non-tumor tissues, whereas cytoplasmic expression increases in cancer. **(B-E)** Examples of immunohistochemistry of various types of prostate tissue. **(B)** Benign prostatic hyperplasia, **(C)** high grade prostatic intraepithelial neoplasia, **(D, E)** prostatic neoplasia.

Supplementary Table 3: Pairwise Correlations Between Staining Factors in Cancer Cells				
Spearman's Rho (P-Value)	Nrdp1 Nucleus	Nrdp1 Cytoplasm	AR Nucleus	AR Cytoplasm
Nrdp1 Nucleus		**0.6 (<0.001)**	**0.26 (0.035)**	**0.27 (0.026)**
Nrdp1 Cytoplasm	**0.6 (<0.001)**		**0.42 (<0.001)**	0.23 (0.058)
AR Nucleus	**0.26 (0.035)**	**0.42 (<0.001)**		0.06 (0.617)
AR Cytoplasm	**0.27 (0.026)**	0.23 (0.058)	0.06 (0.617)	

Comparison of AR and Nrdp1 levels revealed a significant correlation between Nrdp1 levels (both nuclear and cytoplasmic) and nuclear (active) AR (cytoplasmic: pairwise correlation coefficient: 0.42; p<0.001; nuclear: pairwise correlation coefficient: 0.26; p=0.035) **(Figure 5A, Table 3)**. Hence we postulated that Nrdp1 levels may be upregulated in prostate tumor in comparison with non-tumor tissue due to an increase in AR levels, perhaps in an attempt to suppress the levels of ErbB3.

The levels of cytoplasmic Nrdp1 were also considerably lower in patients with PSA failure **(Figure 5B)**. Taken together, these results indicated an overall increase of Nrdp1 in cancer, coincidental with increased AR, but a trend towards lower Nrdp1 with tumor progression despite high AR.

Figure 5. (A). Boxplot showing correlation between levels of cytoplasmic Nrdp1 with nuclear AR (p<0.001). **(B).** Boxplot showing the decrease in Nrdp1 expression in patients who later underwent PSA failure (biochemical recurrence) compared to those who did not. Both nuclear and cytoplasmic levels of Nrdp1 decrease.

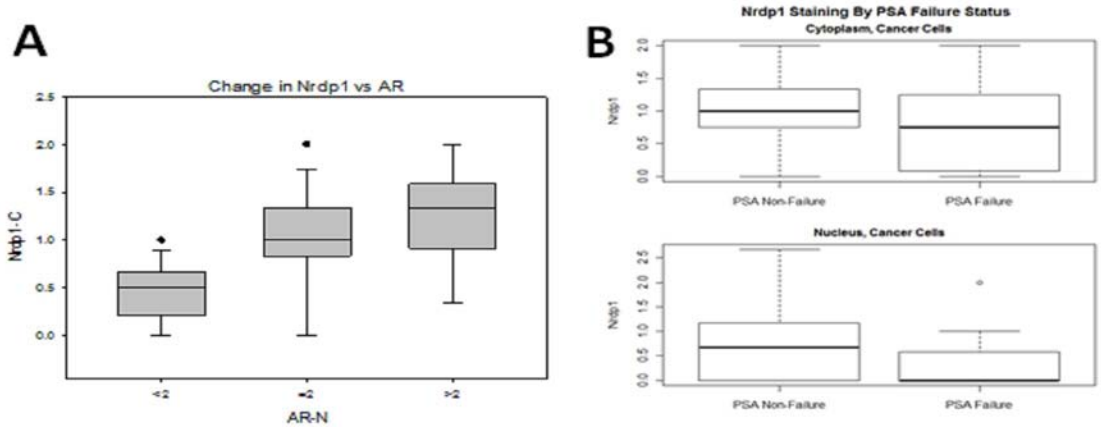

Task 2: *In an animal model of prostate cancer progression, we will investigate whether inhibition of ErbB3 during androgen ablation prevents the development of CRPC tumors.*

AWT suppresses Nrdp1 levels in an androgen-dependent, but not castration-resistant mouse model of PCa progression. To confirm AR regulation of Nrdp1 *in vivo*, athymic nu/nu mice were subcutaneously implanted with CWR22 tumor cells and the engrafted mice were subjected to either castration (n=6) or a sham operation (n=6). CWR22 tumors did not grow in castrated male mice (Mean increase after 14 days = 1.12-fold), while those in intact animals continued to grow (Mean increase after 14 days = 2.2-fold, p=0.02); (after 1 month these tumors would increase 3-fold), indicating that the CWR22 tumors were androgen-dependent **(Figure 6A)**. At the end of the study, the tumors were collected, paraffin embedded, sectioned, and stained by IHC. The levels of nuclear AR were significantly lower in castrated mice compared to the intact animals (p=0.016) while the cytoplasmic AR levels were higher **(Figure 6B),** indicating AR translocation from nucleus (active site) to cytoplasm (inactive site) upon castration. As in the patient tissues, Nrdp1 was observed in both the nucleus and the cytoplasm **(Figure 6C)**, but a strong decrease in cytoplasmic Nrdp1 was observed after castration **(Figure 6D)**. Importantly, a strong correlation between nuclear AR and cytoplasmic Nrdp1 was observed in CWR22 tumors in the castrated animals only (Pearson correlation = 0.734; p=0.0028) **(Figure 6E),** but not in the intact animals**,** confirming the observation in cell lines that androgen ablation caused a decrease in Nrdp1.

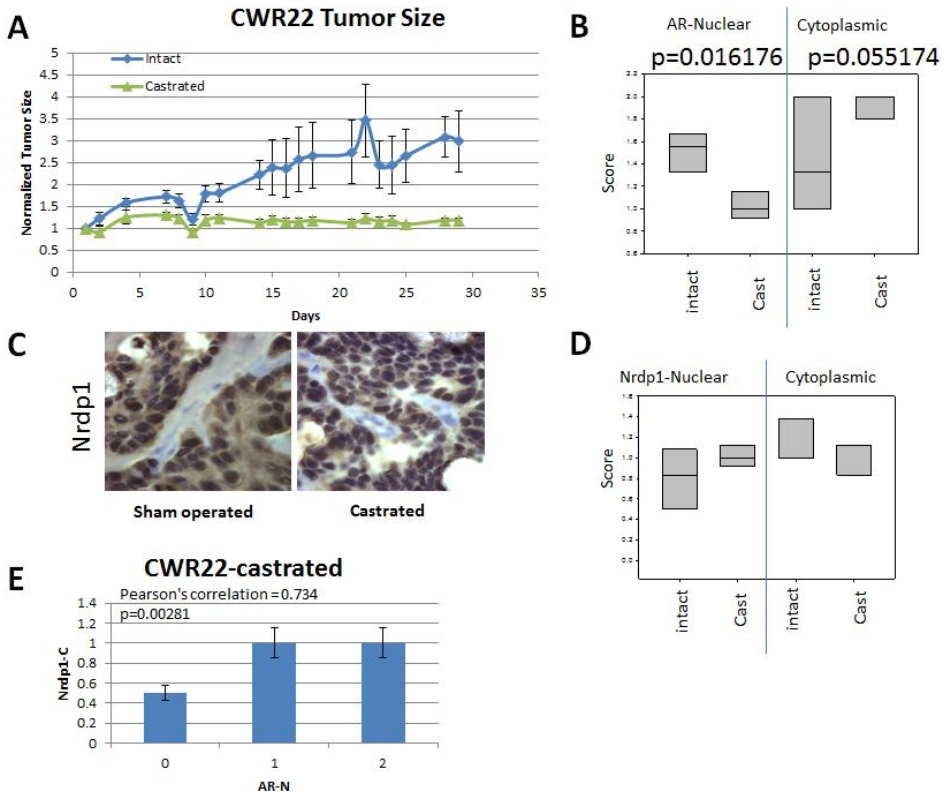

Figure 6. Androgen withdrawal therapy (AWT) suppresses Nrdp1 levels in a mouse model of prostate cancer progression. (A). Nude mice were injected with CWR22 tumors and either castrated (n=6) or left intact (n=6). Tumor volume was measured periodically and expressed as mean ± Std error of volume normalized to day of castration. Note that tumor size in the intact mice increased by 3-fold within 29 days, whereas in the castrated mice they did not grow (max growth 1.2-fold after 10 days from day of castration) (p=0.02)**. (B).** Boxplot showing nuclear and cytoplasmic AR levels in the intact (sham-operated) and castrated mice bearing CWR22 xenografts. AR levels in the nucleus where significantly lower in the castrated group (mean score 1.03 ± 0.298) vs. the intact group (mean score 1.55 ± 0.272) (p=0.0162), while AR levels in the cytoplasm were slightly higher in the castrated group (mean score 1.9 ± 0.2236) vs. the intact group (mean score 1.38 ± 0.49) (p=0.0552). **(C).** Immunohistochemistry of CWR22 tumors from a castrated mouse **(right)**, and an intact mouse **(left),** demonstrating higher levels of cytoplasmic Nrdp1 in the intact mouse, but not nuclear Nrdp1, compared to castrated mice. **(D).** Boxplot showing nuclear and cytoplasmic Nrdp1 levels in the intact (sham-operated) and castrated mice bearing CWR22 xenografts. Nrdp1 levels in the nucleus where higher in the castrated group (mean score 1.0 ± 0.00) vs. the intact group (mean score 0.78 ± 0.455) (p>0.05), while Nrdp1 levels in the cytoplasm were lower in the castrated group (mean score 0.9 ± 0.074) vs. the intact group (mean score 1.14 ± 0.22) (p=0.05). **(E).** Comparison of AR vs. cytoplasmic Nrdp1 levels in castrated CWR22 mice showing that as AR increases, so do cytoplasmic Nrdp1**.**

In contrast, CWR22Rv1 tumors (derived from castrated mice growing relapsed CWR22 tumors) expressed decreased Nrdp1 levels (both nuclear and cytoplasmic) in comparison to CWR22 tumors **(Figure 7A)**. However, CWR22Rv1 tumors did not demonstrate a significant change in Nrdp1 or AR expression after castration **(Figure 7B)**. These results confirm androgen regulation of Nrdp1 in androgen-dependent PCa but not in CRPC.

Figure 7. Comparison of Nrdp1 expression in androgen-dependent vs castration resistant mouse tumors. (A) (upper) Boxplot of Nrdp1 nuclear and cytoplasmic expression levels in nude mice implanted with CWR22Rv1 vs. CWR22 tumors, both showing higher Nrdp1 levels in the cytoplasm vs. the nucleus. Note that the overall Nrdp1 levels are higher in CWR22 compared to CWR22Rv1. **(lower)** immunohistrochemistry demonstrating higher expression of Nrdp1 in CWR22 tumors. **(B) (upper)** Boxplot showing Nrdp1 nuclear and cytoplasmic levels in the castrated and non-castrated CWR22Rv1 mice. Nrdp1 levels remain constant after castration. **(lower)** Boxplot showing AR nuclear and cytoplasmic levels in CWR22Rv1 tumors from castrated and intact mice. AR levels in the nucleus and the cytoplasm remain consistent after castration, indicating castration resistance.

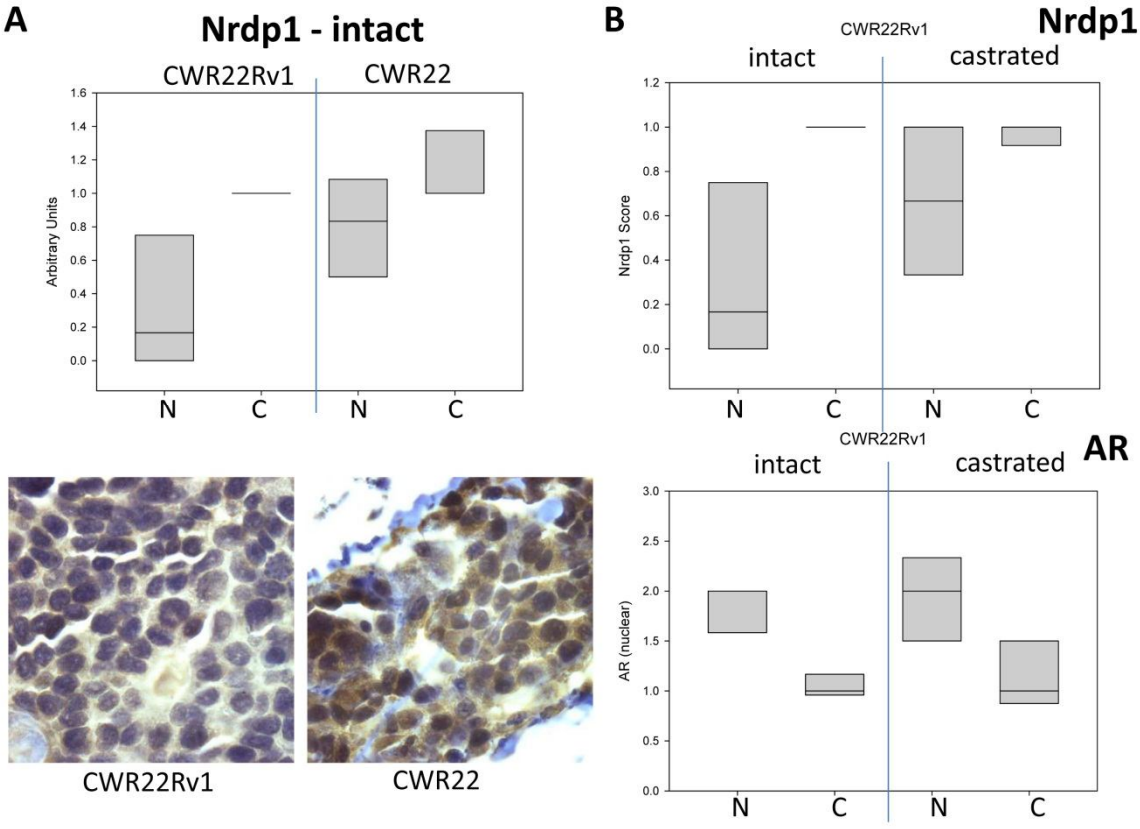

Specific Aim 2. To test the hypothesis that Nrdp1 mediates the regulation of ErbB3 expression by the androgen receptor in androgen dependent cells, but this regulation is lost in androgen independence.

Task 3: *We will identify a role for Nrdp1 in the expression of ErbB3 during androgen withdrawal and in androgen independence.*

Complete – report in previous Annual Report (2010). This topic has already been published in a 2010 paper, this publication is attached.

Task 4: *In androgen dependent cells we will determine how the androgen receptor regulates Nrdp1 transcription.*

Nrdp1 is a direct transcriptional target of the AR. Based on the above, we investigated whether Nrdp1 was a direct transcriptional target of AR. Nrdp1 is known to contain multiple promoters, of which at least one contains the androgen response element (ARE) ARE3, located 209 bp upstream of the transcriptional start site**.** ARE3 is a full 15-bp bipartite palindromic sequence very similar to the AREs found in PSA, the quintessential AR target gene **(Figure 8A, upper)**. Chromatin immunoprecipitation (ChIP) assay showed that AR binding to ARE3 was higher in LNCaP cells (where Nrdp1 is androgen regulated), compared to that in LNCaP-AI cells (derived by continuous culture of LNCaP cells in CSS-containing medium), and in C4-2 cells (where Nrdp1 is independent of androgens) (Chen et al. 2010) **(Figure 8A, lower left)**. To demonstrate androgen-responsiveness of AR binding to ARE3, androgen-dependent LNCaP cells were cultured in fetal bovine serum (FBS) containing high levels of androgens or in low androgen charcoal stripped FBS (CSS) (Sedelaar and Isaacs 2009), in the presence or absence of 1 nM DHT to stimulate AR transcriptional activity. In LNCaP cells the regulation of Nrdp1 is androgen-dependent, with a decrease of AR binding in CSS medium compared to FBS medium and a restoration of AR binding in CSS with DHT added **(Figure 8A, lower right)**. In contrast, in C4-2 cells, AR binding to ARE3 was weak, whereas that to the PSA promoter was strong **(Figure 8B)**. These studies supported previous observation of higher Nrdp1 levels in LNCaP cells compared to C4-2 and explain that lack of AR-binding to ARE3 prevents Nrdp1 transcription in the latter.

To test the potential responsiveness to AR, we created luciferase constructs with the Nrdp1 promoter region containing ARE3. The plasmids were transfected into LNCaP or C4-2 cells which were further treated with DMSO, 1 nM DHT, or the AR antagonist bicalutamde (Casodex; 10μM). The response of LNCaP cells to ARE3 was stronger upon DHT treatment and decreased upon treatment with bicalutamide **(Figure 8C)**. Two luciferase constructs for ARE3 were used - one wild-type and one with several bases mutated to prevent AR binding. Significantly, AR transcriptional activity on the *Nrdp1* promoter increased 3-fold after the addition of DHT ($p=0.046$) but this effect was prevented by bicalutamide ($p>0.05$). In contrast, there was little to no luciferase activity when transfected with the mutated ARE3, indicating that the bases mutated were needed for transcription of Nrdp1 **(Figure 8C)**. This confirmed that ARE3 of *Nrdp1* is indeed a direct transcriptional target of the AR in LNCaP cells. In contrast, in LNCaP-AI cells, the response of ARE3 to DHT was much smaller **(Figure 8D).** Thus, the AR in the CRPC line was still capable of binding to ARE3, however, there was a lack of binding *in situ*.

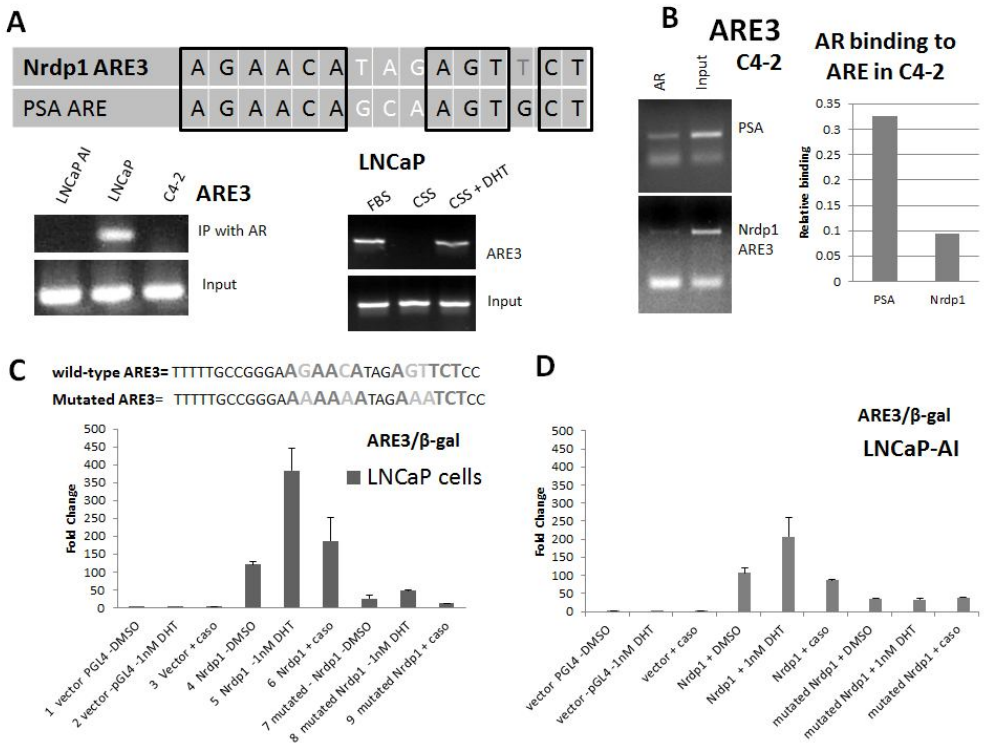

Figure 8. Nrdp1 is a direct transcriptional target of the androgen receptor. (A). (Top). Comparison of *PSA* and *Nrdp1* AREs shows that the *PSA* ARE and *Nrdp1* ARE3 both contain a full palindromic ARE. **(Bottom left).** ChIP assay of AR binding to *Nrdp1* ARE3 in C4-2, LNCaP, and LNCaP AI. AR only binds to *Nrdp1* ARE3 in androgen dependent LNCaP cells and not androgen independent LNCaP AI and C4-2 cells. Cells were cultured in FBS medium. Chromatin samples were immunoprecipitated with anti-AR antibody and analyzed by PCR with primers flanking the *Nrdp1* ARE3 regions. Input is control reactions of genomic DNA prior to immunoprecipitation. **(Bottom right).** ChIP assay of AR binding in LNCaP cells to ARE3. Cells were cultured in FBS medium, CSS medium, or CSS medium with the addition of 1 nM DHT after the first day. Input is control reactions of genomic DNA prior to immunoprecipitation. Chromatin samples were immunoprecipitated with anti-AR antibody and analyzed by PCR with primers flanking the *Nrdp1* ARE3 region**. (B).** ChIP assay of AR binding in C4-2 cells to ARE3 vs. PSA. Note that although AR did not bind to *Nrdp1* ARE3, it did bind to *PSA* in these cells. The upper bands in each panel were quantitated by Image J and normalized to the input. Note that AR binding to *Nrdp1* ARE3 is negligible compared to AR binding to *PSA* ARE. **(C).** Mutation of normal ARE3 to abolish AR binding**. (Top).** Nucleotide sequence of normal *Nrdp1* ARE3 and mutant ARE3 that were inserted into luciferase constructs to test AR transcriptional activity. **(Bottom).** Increased AR transcriptional activity in LNCaP cells on wild-type and mutant ARE3 in the presence of vehicle, 1 nM DHT or 10 μM bicalutamide (caso) compared with control vector and mutant ARE3. **(D)** AR transcriptional activity in LNCaP-AI cells (CRPC subline of LNCaP cells) on wild-type and mutant ARE3 in the presence of vehicle, 1 nM DHT or 10 μM bicalutamide (caso).

Task 5: *In addition, in androgen independent cells we will identify the cause for repression of Nrdp1 expression and investigate whether ErbB3, Akt or its downstream effector FKHRL1 plays a role in this process.*

We found that the structural protein Filamin A (FlnA) regulates Nrdp1 transcription. **Ectopic expression of nuclear FlnA restores AR regulation of Nrdp1 in CRPC cells lacking inherent nuclear FlnA expression.** Previous studies showed that nuclear FlnA interacts with the AR and acts as a co-regulator for transcriptional control (Loy, et al. 2003; Ozanne, et al. 2000). Therefore, we investigated whether FlnA nuclear localization regulated the ability of AR to bind to the *Nrdp1* promoter and coordinate its transcription. As before, the AR failed to bind to *Nrdp1* ARE3 in C4-2 cells, however, transfection of FlnA 16-24 in C4-2 cells, which we have shown earlier to restore nuclear FlnA in C4-2 cells, reestablished AR binding to *Nrdp1* ARE3 **(Figure 9A)**. In order to determine if this reflected a renewal of AR transcriptional activity on *Nrdp1* in C4-2 cells we also performed a luciferase assay on the C4-2 FlnA 16-24 cells using the *Nrdp1* ARE3 luciferase construct and the mutant ARE3 construct. The cells were transfected with either vector and treated with DMSO, DHT, or bicalutamide. The mutant ARE3 construct showed little AR transcriptional activity, while in cells transfected with the wild-type ARE3 vector, transcription of the plasmid was increased in the presence of DHT and inhibited by bicalutamide, indicating a restoration of androgen-sensitivity **(Figure 9B)**. In contrast, other FlnA

constructs that did not restore nuclear FlnA localization (Wang, et al. 2007), did not have as significant an effect on *Nrdp1* transcription. **(Figure 9C)**. We conclude that in androgen-dependent PCa, the AR is able to bind to the *Nrdp1* ARE3 region and cause transcription of *Nrdp1* to downregulate ErbB3. After androgen ablation, the AR is no longer able to bind and prevents *Nrdp1* transcription, which allows ErbB3 to be overexpressed **(Figure 9D)**. These results indicate that FlnA 16-24 is crucial for AR regulation of Nrdp1 in PCa and that introduction of nuclear FlnA can restore androgen regulation of Nrdp1.

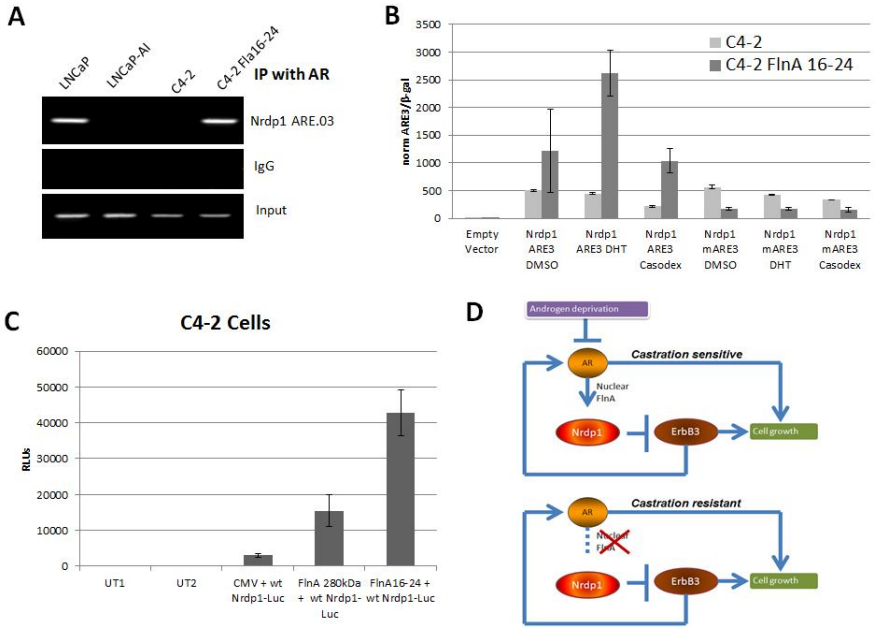

Figure 9. Nuclear Filamin A restores androgen receptor regulation of Nrdp1 in androgen independent cells. (A). AR binds to ARE3 in in the presence of 90 kDa FlnA. ChIP assay of AR binding in LNCaP, LNCaP AI, C4-2, and C4-2 FlnA 16-24 cells. Chromatin samples were immunoprecipitated with anti-AR antibody and analyzed by PCR with primers flanking the *Nrdp1* ARE3 region. Input is control reactions of genomic DNA prior to immunoprecipitation. **(B).** AR transcriptional activity of *Nrdp1* ARE3 is androgen regulated in the presence of FlnA 16-24. C4-2 cells transfected with vector only or C4-2 FlnA 16-24 were cultured in FBS medium and transfected with the control vector, normal ARE3, or mutant ARE3, and AR transcriptional activity was measured by luciferase assay. Cells were also treated with DMSO, 1 nM DHT, or 10 μM bicalutamide (Casodex). **(C).** FlnA restores AR transcriptional activity on Nrdp1 ARE3 in androgen independent cells. Cells were cultured in FBS medium and transfected with full-length FlnA, FlnA repeats 1-15, or FlnA repeats 16-24, and AR transcriptional activity was measured by luciferase assay. **(D).** Schematic describing AR control of Nrdp1 in castration sensitive vs. castration resistant prostate cancer cells. In castration sensitive tumors, the androgen receptor is regulated by the presence of nuclear FlnA. This allows androgen receptor to bind to the ARE upstream of the Nrdp1 gene, ARE.03, and cause an increase of Nrdp1 expression. This in turn down regulates ErbB3 and prevents cell growth. In castration resistant tumors, nuclear FlnA is no longer present, which causes aberrant binding and androgen receptor no longer binds to ARE.03, preventing Nrdp1 expression. This then allows ErbB3 protein levels to increase and causes increased cell growth.

KEY RESEARCH ACCOMPLISHMENTS:

1. Manuscript(s) submitted for publication.
2. Qualifying Exam: Rosalinda Savoy passed her qualifying exams on this topic. Her thesis will acknowledge the DOD.

CONCLUSION: Our data for the first time identifies Nrdp1 as an AR target that is androgen-regulated in castration resistant cells, but not in castration insensitive cells. Our new data shows that in cells where the AR is stabilized, and does not undergo degradation despite androgen withdrawal, it is able to transcribe PSA but not Nrdp1, whereas in cells where the AR is not stabilized, it can transcribe Nrdp1 and thereby regulate ErbB3 levels. Since we also showed earlier that ErbB3 signaling increase cell growth and suppress apoptosis, our results indicate that AR suppression of ErbB3 is a mechanism for keeping cells castration sensitive, whereas when this effect is lost, the cells become castration resistant. Further, we show that Filamin A nuclear localization keeps cells androgen responsive by destabilizing the AR, and maintaining its ability to transcriptionally regulate Nrdp1.

REFERENCES:

Chen L, Siddiqui S, Bose S, Mooso B, Asuncion A, Bedolla RG, Vinall R, Tepper CG, Gandour-Edwards R, Shi X, Lu XH, Siddiqui J, Chinnaiyan AM, Mehra R, Devere White RW, Carraway KL, 3rd & Ghosh PM 2010 Nrdp1-mediated regulation of ErbB3 expression by the androgen receptor in androgen-dependent but not castrate-resistant prostate cancer cells. *Cancer Res* **70** 5994-6003.

Loy CJ, Sim KS & Yong EL 2003 Filamin-A fragment localizes to the nucleus to regulate androgen receptor and coactivator functions. *Proc Natl Acad Sci U S A* **100** 4562-4567.

Ozanne DM, Brady ME, Cook S, Gaughan L, Neal DE & Robson CN 2000 Androgen receptor nuclear translocation is facilitated by the f-actin cross-linking protein filamin. *Mol Endocrinol* **14** 1618-1626.

Sedelaar JP & Isaacs JT 2009 Tissue culture media supplemented with 10% fetal calf serum contains a castrate level of testosterone. *Prostate* **69** 1724-1729.

Wang Y, Kreisberg JI, Bedolla RG, Mikhailova M, deVere White RW & Ghosh PM 2007 A 90 kDa fragment of filamin A promotes Casodex-induced growth inhibition in Casodex-resistant androgen receptor positive C4-2 prostate cancer cells. *Oncogene* **26** 6061-6070.

APPENDICES:

Khan IH, **Ghosh PM**, Zhao J, Ziman M, Sweeney C, Kung HJ and Luciw PA. Microbead Arrays for the Analysis of ErbB Receptor Tyrosine Kinase Activation and Dimerization in Breast Cancer Cells. *ASSAY and Drug Development Technologies*, 8(1): 27-36. 2010.

Chen H, Libertini SJ, Wang Y, Kung HJ, **Ghosh PM**, Mudryj M. ERK Regulates Calpain 2 Induced AR Cleavage To LMW Forms in CWR22 Relapsed Prostate Tumor Cell Lines. *J Biol Chem*, 285(4): 2368-74. 2010.

Chen L, Siddiqui S, Bose S, Mooso B, Asuncion A, Bedolla RG, Vinall R, Tepper CG, Gandour-Edwards R, Shi X, Lu XH, Siddiqui J, Chinnaiyan AM, Mehra R, Devere White RW, Carraway KL 3rd, **Ghosh PM**. Nrdp1-mediated regulation of ErbB3 expression by the androgen receptor in androgen-dependent but not castrate–resistant prostate cancer cells. *Cancer Research*, 70(14): 5994-6003. 2010.

Mooso BA, Loredo GA, Madhav A, Johnson S, Roy M, Moore ME, Moy CV, Mehta RG, Vaughan ATM, **Ghosh PM**. Androgen Receptor regulation of Vitamin D receptor in response of prostate cancer cells to 1α(OH)D5. *Genes & Cancer*. 1(9):927-940. 2010.

Chen H, Libertini SJ, George M, Dandekar S, Tepper CG, Al-Bataina B, Kung H-J, **Ghosh PM**, Mudryj M. Genome-wide analysis of androgen receptor binding and gene regulation in two CWR22-derived prostate cancer cell lines. *Endocrine-related cancers*, 17(4): 857-873.

Vinall RL, Mahaffey CM, Davis RR, Luo Z, Gandour-Edwards R, **Ghosh PM,** Tepper CG, de Vere White RW. Dual blockade of PKA and NF-B inhibits H2 relaxin-mediated castrate-resistant growth of prostate cancer sublines and induces apoptosis. Horm Cancer. 2011 Aug; 2 (4):224-38. 2011.

Jathal, M.K., Chen,L., Mudryj, M. and **Ghosh, P.M.** Targeting ErbB3: the new RTK(id) on the prostate cancer block. *Immunology, Endocrine & Metabolic Agents in Medicinal Chemistry*, 11(2): 131-149, 2011.

Chen, L., Mooso, B.A., Jathal, M.K., Madhav, A., Johnson, S.D., van Spyk, E., Mikhailova, M., Zierenberg Ripoll, A., Xue, L., Vinall, R. L., deVere White, R.W. and **Ghosh, P.M**. Dual EGFR/HER2 inhibition sensitizes prostate cancer cells to androgen withdrawal by suppressing ErbB3. *Clinical Cancer Research,* 2011, [Epub ahead of print].

Mooso BA, Vinall RL, Tepper CG, Savoy RM, Cheung JP, Singh S, SIddiqui S, Wang Y, Bedolla RG, Martinez A, Mudryj M, Kung HJ, deVere White RW, Ghosh PM. *Enhancing the effectiveness of androgen deprivation in prostate cancer by inducing Filamin A nuclear localization.* Endocr Relat Cancer. 012 Nov 9;19(6):759-77. Doi: 10.1530/ERC-12-0171. PMID: 22993077.

Rosalinda M. Savoy, Liqun Chen, Salma Siddiqui, Frank U. Melgoza, Blythe Durbin-Johnson, Mohana Roy, Maitreyee K. Jathal, Swagata Bose, Yu Wang, Benjamin A. Mooso, Leandro D'Abronzo, William H. Fry, Kermit L. Carraway, III, and Paramita M. Ghosh. *Androgen receptor transcriptionally targets the ErbB3 regulator Nrdp1 in the presence of nuclear Filamin A* Submitted to Cancer Research

Liqun Chen's Ph.D. diploma.

Rosalinda M. Savoy's Ph.D. QE report.

Microbead Arrays for the Analysis of ErbB Receptor Tyrosine Kinase Activation and Dimerization in Breast Cancer Cells

Imran H. Khan,[1,2] Jing Zhao,[1] Paramita Ghosh,[3,4] Melanie Ziman,[1] Colleen Sweeney,[4] Hsing-Jien Kung,[4] and Paul A. Luciw[1,2]

[1]Center for Comparative Medicine, [2]Department of Pathology and Laboratory Medicine, and [3]Department of Urology, UC Davis School of Medicine, University of California, Davis, California, and VA Northern California Health Care System, Mather, California. [4]Department of Biochemistry and Molecular Biology, UC Davis Cancer Center, University of California, Davis, California.

ABSTRACT

Receptor tyrosine kinases (RTKs) in the ErbB family (EGFR, ErbB2, ErbB3, and ErbB4) are implicated in a variety of human malignancies. Accordingly, determination of both expression and activation (dimerization/heterodimerization and phosphorylation) of ErbB proteins is critical in defining their functional role in cancer. Efficient and comprehensive methods to study molecular functions of ErbB family of RTKs are needed not only for improvements in diagnostics but also for early screening of targeted drugs (eg, small molecule inhibitors and therapeutic antibodies). We report development of 3 multiplex microbead immunoassays for simultaneous detection of expression, protein–protein interactions, and phosphorylation of these RTKs. These novel multiplex immunoassays were used to study ErbB RTKs under different cell activation conditions in 2 breast cancer cell lines (MDA-MB-453 and MDA-MB-468) and an epidermoid cancer cell line (A431). The results were confirmed by immunoprecipitation/western blot. Importantly, the multiplex immunoassay facilitated time-course studies in these cell lines after cell activation with EGF and neuregulin, revealing the kinetics of phosphorylation of the ErbB family RTKs. This study demonstrates the utility of the Luminex® multiplex system as an efficient and comprehensive approach to study different aspects of molecular roles of these RTKs. Importantly, the study provides proof-of-concept for the utility of the multiplex microbead immunoassay approach for potential use in efficient, robust, and rapid screening of drugs, particularly those targeting functional aspects of these potent signaling molecules. In addition, the assays described here may be useful for cancer diagnostics and monitoring efficacy of therapy targeting the ErbB family of RTKs.

INTRODUCTION

Overexpression of receptor tyrosine kinases (RTKs) belonging to the ErbB family of receptors (EGFR/ErbB1/HER1, ErbB2/HER2, ErbB3/HER3, and ErbB4/HER4) and/or their aberrant signaling is a major characteristic of many human malignancies.[1–3] Most tumors express more than one of these ErbB family members. Overexpression of EGFR and ErbB2 has been documented in a variety of tumor types including breast tumor (63% of ErbB2-positive tumors were also strongly positive for ErbB3) with poor clinical outcome.[4] EGFR is overexpressed in breast cancers with a positivity rate of 14%–91%, which is associated with a more aggressive phenotype and poor patient prognosis.[5] ErbB2 is overexpressed in 20%–30% of invasive breast tumors[4,6–8] and is a marker of poor prognosis.[9] Although ErbB4 is the least well-understood family member in terms of its role in cancer, its expression in breast tumors has been associated with low cell proliferative index, increased survival, and reduced recurrence of tumors.[4]

ABBREVIATIONS: RTK, receptor tyrosine kinase; PBS, phosphate buffered saline; Sulfo-NHS, N-hydroxysulfosuccinamide; EDC, 1-ethyl-3-[3-dimethylaminopropyl] carbodiimide; RT, room temperature; ECL, enhanced chemiluminescence.

DOI: 10.1089/adt.2009.0208

These ErbB family RTKs are activated by various EGF-like growth factors. Binding of EGF to EGFR induces receptor dimerization and tyrosine autophosphorylation of specific residues within the cytoplasmic tail, initiating a complex cascade of cell signaling events leading to cell proliferation.[1] Similarly, neuregulins transmit intracellular signals within target cells by interacting with ErbB3 and ErbB4.[10] Ligand binding to the ErbB RTKs, followed by heterodimerization[11] and phosphorylation, leads to the activation of downstream targets,[12] resulting in intracellular signals stimulating cell proliferation and survival. Discovery of the role of RTKs in oncogenesis has lead to the development of novel anticancer therapeutics targeting these molecules. The advent of such therapies has in turn helped identify the need for a better understanding of molecular events involving RTK function for a variety of cancers. It is therefore critical to analyze intracellular signals transduced by RTKs under different conditions that may produce different cellular responses. From a mechanistic perspective, ErbB2 is considered to be a major factor in oncogenesis. However, ErbB2, when overexpressed alone, may exhibit different protein–protein interactions and phosphorylation dynamics that may affect its activity in comparison to its overexpression in conjunction with that of EGFR and/or ErbB3. Such differences in association of ErbB2 with other members of the ErbB RTK family may lead to differences in activation of intracellular signaling pathways, thus resulting in different cell behavior. To elucidate molecular events underlying the role of ErbB RTKs in oncogenesis, it is important to study expression of these proteins as well as their activation by dimerization/phosphorylation. Accordingly, capabilities of the multiplex approach to detect and quantitate not only protein expression, but also phosphorylation and protein–protein interactions are useful as tools for screening drugs in the early stage of development, that are designed to target functional properties of these clinically important ErbB signaling proteins.[13,14] In addition, such screening tools may enhance the efficiency of studies on pharmacodynamic effects of small molecule inhibitors on activities of ErbB RTKs. Furthermore, the use of this efficient approach in studies on activation of these RTKs (phosphorylation and dimerization) may evolve into development of procedures for cancer diagnostics and monitoring efficacy of targeted therapy. In this report, we present proof-of-concept studies using a robust and efficient multiplex microbead immunoassay approach for the detection of expression and activation (phosphorylation/heterodimerization) of RTKs in the ErbB family. For each of the 4 ErbB family RTKs, 3 multiplex assays are described that enable the simultaneous detection of expression, heterodimerization, or phosphorylation of these key cell signaling proteins in cell line models.

MATERIALS AND METHODS

Cells and Cell Activation

Breast carcinoma cells (MDA-MB-453 and MDA-MB-468) and human epidermoid carcinoma cells (A431) were cultured in Dulbecco's modified Eagle's medium (DMEM) supplied with 10% heat-inactivated newborn calf serum at 37°C and 5% CO_2. Cells were grown to 65%–70% confluence in 25 or 75 cm^2 tissue culture flasks, then starved in X-vivo medium (A431) or DMEM containing 0.1% FBS (MDA-MB-453 and MDA-MB-468) for 24 h before activation.[15] Cells were treated with optimal concentration of EGF (16.5 nM concentration), neuregulin (1:500), or sodium pervanadate (6.6 mM).[15]

Lysate Preparation

Cells in tissue culture flasks were lysed with ice-cold buffer (PBS containing 1% Nonidet P-40, protease inhibitor cocktail, 0.5 mM sodium orthovanadate, and 1× serine/threonine phosphatase inhibitor). The cell lysate was immediately vortexed and incubated on ice for 15 min. Cell debris was removed by centrifugation at 12,000 rpm for 20 min.[15] Total protein concentration of lysates was determined by BCA reagent kit (Bio-Rad, Laboratories, Hercules, CA). Lysates were aliquoted and stored at −80°C until used.

Antibodies and Reagents

Monoclonal antibodies against EGFR (05-104) for microbead coating and immunoprecipitation and biotinylated anti-phosphotyrosine (4G10) were purchased from Upstate, USA (Lake Placid, NY). Monoclonal antibodies against ErbB2, ErbB3, and ErbB4 for microbead coating and immunoprecipitation were purchased from R&D Systems (MAB1129, MAB3481, and MAB1131, respectively; Minneapolis, MN). Biotinylated antibody for total protein detection for EGFR (E101) was obtained from Leinco Technologies (St. Louis, MO) and those for ErbB2, ErbB3, and ErbB4 were purchased from R&D Systems (BAF1129, BAM3481, and BAF1131, respectively). Protease inhibitor cocktail tablets and purified 10% Nonidet P-40 were purchased from Roche Applied Science (Indianapolis, IN). Halt phosphatase inhibitor cocktail was purchased from Pierce (Rockford, IL). Protein G-conjugated Sepharose was from Sigma (St. Louis, MI). EGF was purchased from Upstate. Neuregulin (recombinant) was expressed and purified as previously described.[16]

Microbead Coating

Monoclonal antibodies against EGFR, ErbB2, ErbB3, and ErbB4 were coated as capture antibodies by conjugation to individual microbead sets. One microbead set was coated with BSA to

control for nonspecific interactions, and another set was coated with biotin-conjugated goat IgG (Jackson Immunoresearch Laboratories, West Grove, PA) to serve as a positive control for the detection reagent (streptavidin-conjugated phycoerythrin). Proteins were conjugated to microbeads as previously described.[15] In brief, microbeads were activated with sulfo-NHS (*N*-hydroxysulfosuccinamide; Pierce, Rockford, IL) and EDC (1-ethyl-3-[3-dimethylaminopropyl] carbodiimide; Pierce). The activated beads were washed with 50 mM MES (pH 6.0) buffer. To coat with antibody (protein), activated beads were resuspended in the relevant protein solution (25–100 µg/mL) in 50 mM MES (pH 6.0) buffer. Mixture of activated beads and antibodies was incubated by shaking on a rocker for 2 h at RT for coupling. After coating, beads were washed twice with wash buffer (0.1% Tween-20 in phosphate-buffered saline [PBS], pH 7.40 and resuspended in 1 mL of blocking buffer (1% BSA; 0.1% Tween-20 in PBS, pH 7.4; 0.05% sodium azide). Blocking was performed by shaking on a rocker at room temperature for 30 min. After blocking, beads were washed twice in 1 mL blocking buffer. Finally, antibody-coated beads were resuspended in 1 mL blocking buffer and stored at 4°C for up to a week. For long-term storage, beads were kept frozen at −80°C for several months.

Microbead Suspension Array Immunoassay of Signaling Proteins

Immunoreactions were set up in 96-well, filter-bottomed plates designed for high-throughput separations (1.2 µm MultiScreen; Millipore Corporation, Billerica, MA) as previously detailed.[15] Microbeads (2,000 beads of each set), coated with a specific antibody, were mixed. This multiplex, microbead mixture was added to each well. To this, 25 µL of cell lysate (0.4 mg/mL total protein) was added. The contents were mixed at 1,400 rpm on a plate shaker (Labnet International Inc., Woodbridge, NJ) for 2 h at room temperature (RT). After incubation with the lysate, liquid was drained from the bottom of the plate under vacuum. The microbeads were washed twice by adding 150 µL of wash buffer per well and draining out under vacuum successively. For detection of tyrosine-phosphorylated signaling proteins bound to antibodies coated on microbeads, 25 µL of biotinylated anti-phosphotyrosine antibody 4G10 (0.5 µg/mL in wash buffer) was added as the detection reagent. To detect biotinylated 4G10, streptavidin conjugated to R-phycoerythrin was added at a dilution of 1:1,000 in wash buffer as the reporter molecule and incubated for 15 min at RT. Microbeads were washed once with wash buffer, resuspended in 100 µL of wash buffer per well, and analyzed in the Luminex-100™ instrument (Luminex Corporation, Austin, TX).

Luminex-100 Operation and Multiplex Data Analysis

The Luminex-100 instrument (Austin, TX) was set at the default settings, set by the manufacturer for routine applications, as directed in the user's manual. Data were acquired by Luminex Data Collection Software (Version 1.0). This software package was used for routine operation of the instrument, data acquisition, and data analysis. The instrument was calibrated with Calibration Beads supplied by the manufacturer to adjust the settings for bead set identification or "Classification" and for the detection of "Reporter" (phycoerythrin). Events were gated to exclude doublets and other aggregates. One hundred independent, gated events were acquired for each bead set. The median fluorescence intensity (MFI) or "signal" of a hundred events (beads) was used as a measure of the detection of protein phosphorylation. After acquisition by Luminex software, the data were further processed by Microsoft Excel software.[15]

Immunoprecipitation and Western Blotting

Immunoprecipitation and Western blotting were performed essentially as described previously.[15] For immunoprecipitation, individual capture antibody (3 µg/mL) was mixed with 250 µL of cell lysates (900–1,500 µg/mL total protein) on a rotator overnight at 4°C. Protein G-conjugated Sepharose was added (90 µL of 20% slurry) and mixed on the rotator for 1 h at 4°C. Sepharose beads were washed 3 times in wash buffer (PBS containing 1% Tween-20, 100 mM NaCl) and resuspended in 24 µL of PBS plus 8 µL 4× sample buffer. The samples were boiled for 5 min. Immunocomplexes were resolved on SDS-polyacrylamide gels (8%–16% precast gradient Tris–glycine gels, Novex Immunodetection; Invitrogen, Carlsbad, CA). Membranes were blocked in 5% BSA (Roche Applied Science, Indianapolis, IN). Tyrosine phosphorylation was detected with biotin-conjugated anti-phosphotyrosine antibody (4G10, 0.5 µg/mL). Blots were developed with Vectastain ABC detection reagent (Vector Laboratories, Burlingame, CA) and ECL Plus Western blotting detection system (Amersham Biosciences, Piscataway, NJ) and visualized on a Typhoon 9410 variable mode imager (Amersham Biosciences).

For Western blotting, 30 µg of cell lysate was electrophoresed on 8%–16% SDS-polyacrylamide gels under reducing conditions for EGFR (biotinylated antibody, Upstate), ErbB3 (biotinylated antibody, Santa Cruz Biotechnology, Santa Cruz, CA), ErbB4 (biotinylated antibody R&D Systems), and actin antibody (R&D Systems), or under nonreducing conditions for ErbB2 (biotinylated antibody R&D Systems). After electrophoresis, proteins were transferred onto polyvinylidene difluoride (PVDF) membranes (Bio-Rad) and nonspecific binding sites were blocked with 5% nonfat dry milk (Oxiod Ltd, Basingstoke, Hampshire, England) in

PBS with 1% Tween-20. Blots were probed with Anti-Mouse HRP-linked IgG (Cell Signaling Technologies, Cambridge, MA) for EGFR and ErbB2, anti-Rabbit antibody HRP-linked IgG (Cell Signaling) for ErbB3. The antibodies were used at a concentration of 0.1 mg/mL. Bands were visualized by horseradish peroxidase/hydrogen peroxide-catalyzed oxidation of luminol in the enhanced chemiluminescence (ECL) reaction.

RESULTS

Expression of ErbB Family Receptors

To demonstrate specific detection of members of the ErbB family of RTKs by multiplex microbead suspension array, their expression was examined in 2 breast cancer cell lines MDA-MB-453 and MDA-MB-468, and a human epidermoid carcinoma cell line A431. The MDA-MB-453 cell line expresses ErbB2 and ErbB3 but does not show detectable amounts of EGFR and ErbB4. The MDA-MB-468 cell line expresses EGFR and ErbB3 receptor but does not produce detectable amounts of ErbB2; A431 cells express EGFR, ErbB2, and ErbB3 receptors.[16,17]

Four sets of microbeads, each set coated with monoclonal antibodies to EGFR, ErbB2, ErbB3, or ErbB4, were mixed and incubated with lysates prepared from nonactivated cells. In addition, a microbead set coated with BSA was included as a baseline control, and a microbead set coated with biotin was added as a positive control in the bead mixture. Total protein expression of EGFR, ErbB2, ErbB3, and ErbB4 was detected with biotin-conjugated detection antibody (distinct from capture antibody coupled to microbeads) against each individual RTK (*Fig. 1A*).

The multiplex immunoassay results were confirmed by IP/WB for the detection of the 4 ErbB family RTKs (*Fig. 1B*). Both methods consistently showed that EGFR was expressed in MDA-MB-468 and A431 cells, but not in MDA-MB-453 cells. This finding is consistent with previous reports.[16,17] MDA-MB-453 and A431 cells expressed ErbB2, whereas MDA-MB-468 cells showed no detectable expression of ErbB2. All 3 cell lines expressed ErbB3, and ErbB4 was not detected in any of the cell lines (*Fig. 1*). Taken together, these results confirmed that the multiplex immunoassay simultaneously detected expression of 3 of the 4 ErbB family RTKs in a single sample of cell lysate.

Phosphorylation of ErbB RTKs

To assess the phosphorylation status of the ErbB receptors for cell activation, cells were treated with physiological ligands (EGF and neuregulin) or the phosphatase inhibitor sodium pervanadate. Pervanadate was used as a general cell activator to produce positive control cell lysates for tyrosine phosphorylated proteins. Treatment with pervanadate inhibits intracellular tyrosine phosphatases, resulting in sustained phosphorylation of various tyrosine kinases and substrates that reflects the activation state of the cells.[15] Tyrosine kinases activated in this manner can also activate downstream serine/threonine kinases. In MDA-MB-468 cells, which express EGFR and ErbB3 but not ErbB2, the phosphorylation

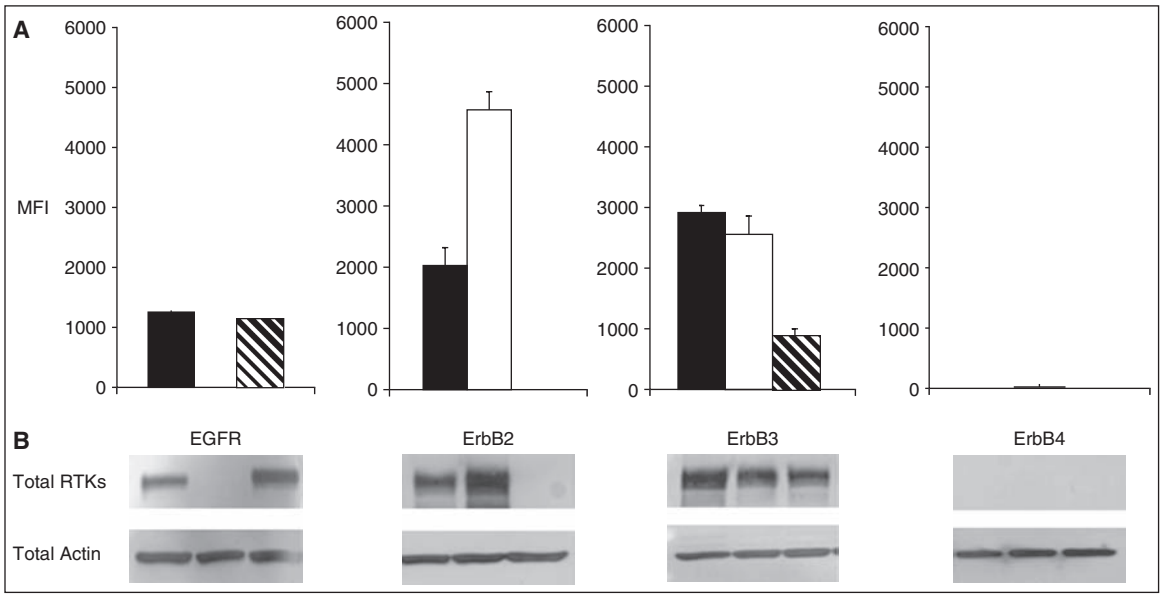

Fig. 1. (**A**) Expression levels of ErbB family of receptors analyzed by multiplex microbead suspension immunoassay in MDA-MB-453 (hashed bars), MDA-MB-468 (open bars), and A431 (closed bars) cells. A mixture of microbeads coated with antibodies to EGFR, ErbB2, ErbB3, and ErbB4 were incubated with lysates from nonactivated cells. Detection of protein expression was achieved by a second antibody against each individual receptor protein. Error bars represent standard error of $n = 4$ values. (**B**) Western blot analysis of EGFR, ErbB2, ErbB3, and ErbB4 expression. Actin expression shows equal loading. Abbreviations: MFI, median fluorescence intensity; RTK, receptor tyrosine kinase.

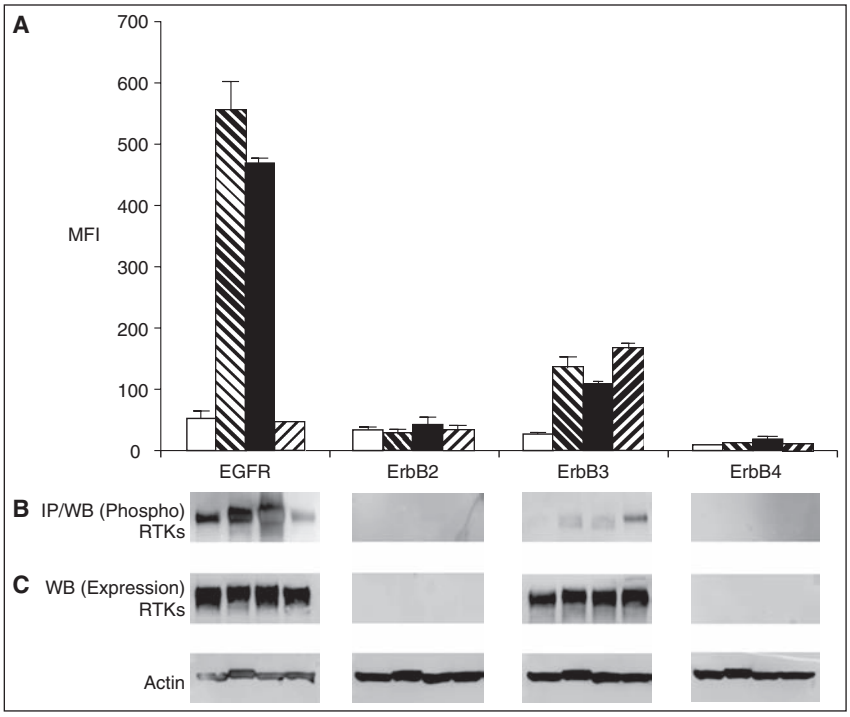

Fig. 2. (**A**) Phosphoproteomic analysis of RTKs by multiplex microbead suspension array immunoassay in MDA-MB-468 cells. Cells were used as untreated (empty bars), treated with 6.6 mM sodium pervanadate for 5 min (hashed bars), 16.5 nM EGF (closed bars), or 1:500 neuregulin for 7 min (reverse hashed bars). A mixture of microbeads coated with antibodies to EGFR, ErbB2, ErbB3, and ErbB4 were incubated with the cell lysates. Error bars represent standard error of $n = 4$ values. (**B**) Immunoprecipitation and western blot analysis of phosphorylation and total ErbB receptors in MDA-MB-468 cells. Antibodies used for immunoprecipitation were the same as those coated on the microbeads for multiplex analysis. (**C**) Western blot analyses were performed for the detection of total RTK proteins (actin shows equal loading). Abbreviations: MFI, median fluorescence intensity; RTK, receptor tyrosine kinase.

level of EGFR increased by 10.3-fold and 8.7-fold upon stimulation following treatment with sodium pervanadate or EGF, respectively (*Fig. 2A*). Activation of ErbB3 was also observed. Pervanadate treatment of these cells resulted in 4.6-fold increase in phosphorylation of ErbB3, and a 5.6-fold increase was observed upon treatment of cells with neuregulin. This cell line does not express the ErbB2 receptor[17,18]; accordingly, phosphorylation of ErbB2 or ErbB4 was not detected (*Fig. 2*).

In MDA-MB-453 cells, treated with sodium pervanadate, levels of phosphorylated forms of ErbB2 and ErbB3 increased by 30.8-fold and 39.4-fold, respectively (*Fig. 3A*). Upon treatment with neuregulin (ErbB3 agonist), ErbB3 phosphorylation increased by 11.3-fold compared to untreated cells. In this experiment, neither expression nor phosphorylation of ErbB4 was detected (*Fig. 3*).

Analysis of A431 cells by multiplex microbead suspension array showed that EGFR, ErbB2, and ErbB3 were hyperphosphorylated upon treatment with pervanadate. Phosphorylation of EGFR increased by 5.5-fold, phosphorylation of ErbB2 receptor increased by 8.2-fold, and phosphorylation of ErbB3 receptor increased by 34.5-fold (*Fig. 4A*). These results confirmed that the multiplex assay was able to detect phosphorylation of 3 of 4 of the ErbB family RTKs. EGF induced phosphorylation of EGFR by 3.8-fold, and ErbB2 receptor by 3.3-fold. However, in the A431 cell line, neuregulin treatment did not increase the level of phosphorylation of ErbB3 as dramatically as in the MDA-MB-468 cell line (*Fig. 4*). This difference is likely due to EGFR sequestering ErbB2 away from ErbB3, and thereby compromising the ability of neuregulin to lead to dimerization of ErbB2 and ErbB3.

To confirm the specificity of antibodies used in coating microbeads for capturing ErbB receptors, lysates of stimulated cells were also tested by IP and WB. Results obtained in IP/WB analysis were generally similar to those in the multiplex microbead assay (*Figs. 2–4, panels B*). However, in the case of MDA-MB-453 cells, increase in phosphorylation of ErbB3 above the baseline was not readily detected by IP/WB even after treatment with pervanadate (*Fig. 3*). The total amount of ErbB receptors in lysates from nontreated and treated cells was similar (*Figs. 2–4*, panel C, lower part). Thus, the results of the multiplex microbead immunoassays are consistent with those obtained by the conventional IP/WB method. However, the advantage of the multiplex microbead immunoassay is that it enables analysis of multiple proteins in a single sample with internal controls and affords a higher throughput.

Phosphorylation Kinetics of RTKs in Cells Treated With EGF or Neuregulin

To study the kinetics of phosphorylation of ErbB family of RTKs upon stimulation with growth factors, a time-course experiment was performed by treating MDA-MB-453, MDA-MB-468, and A431 cells with EGF or neuregulin for various intervals of time ranging from 1 to 60 min. EGF activation induced phosphorylation of EGFR in MDA-MB-468 and A431 cells (*Fig. 5B*) but not in MDA-MB-453 cells that lack EGFR (*Fig. 5A*). Interestingly, patterns of phosphorylation of EGFR in MDA-MB-468 and A431 cells are very similar. After treatment with EGF, phosphorylation

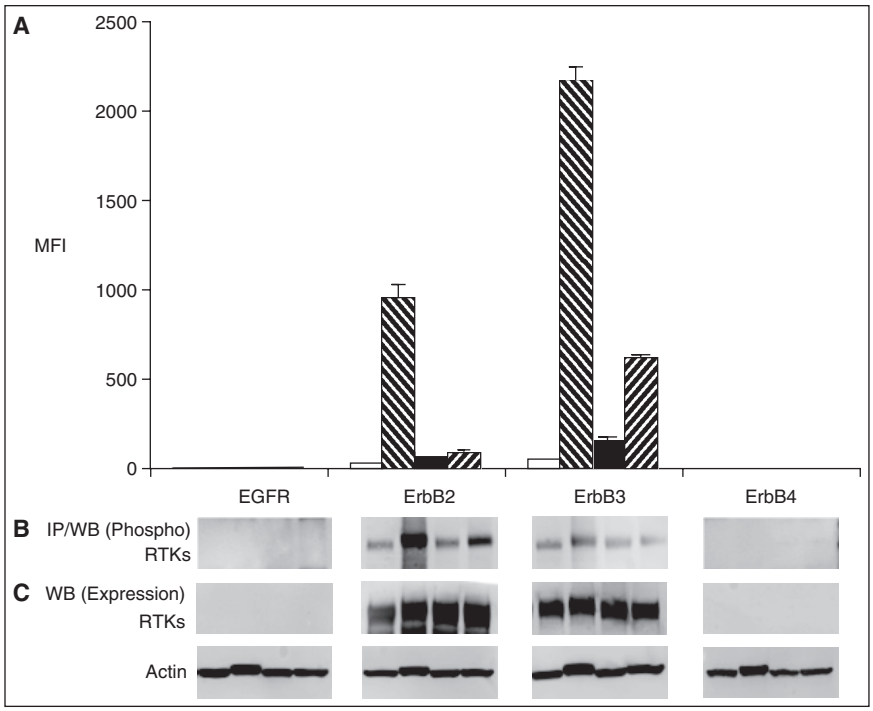

Fig. 3. Phosphoproteomic analysis of RTKs by multiplex microbead immunoassay in MDA-MB-453 cells. Details are the same as described for *Figure 2*. Abbreviations: MFI, median fluorescence intensity; RTK, receptor tyrosine kinase.

of EGFR increased in both MDA-MB-468 and A431 cells within 1 min; tyrosine phosphorylation continued to increase throughout the 60-min period of observation (*Fig. 5*).

Analysis of the time-course treatment with neuregulin revealed the kinetics of phosphorylation of the ErbB3 receptor. A clear increase in phosphorylation was observed in MDA-MB-453 cells that peaked at 15 min and then declined over the next 45 min (*Fig. 5A*). A lower level of increase in phosphorylation of ErbB3 was observed in neuregulin-treated MDA-MB-468 and A431 cells in comparison to untreated cells (*Fig. 5B* and *5C*).

Investigation of Protein–Protein Interactions of RTKs

In breast cancer cell lines, protein–protein interaction between ErbB RTKs, under cell activation conditions were investigated by the multiplex microbead immunoassay. Cell lysates were analyzed from either nonactivated cells, or those treated with pervanadate, EGF, or neuregulin. As expected, when multiplex immunoassay was performed using ErbB2-specific detection antibody, this RTK displayed a strong signal for the microbeads coated with ErbB2 capture antibody (*Fig. 6*). This finding, as expected, shows the presence of ErbB2 in MDA-MB-453 cell lysates (*Fig. 6A*). As expected, the ErbB2 signal intensity on ErbB2-specific microbeads, for each of the 4 lysates, is very high regardless of cell activation condition. However, if heterodimer formation occurred under certain cell activation conditions, ErbB2 detection antibody would also produce a signal above the basal level for a microbead set other than the microbead set specific for capturing ErbB2. Indeed, ErbB2 detection antibody produced a significant signal on ErbB3-specific capture beads (*Fig. 6A*). This signal with ErbB2 detection antibody was only present in lysates obtained from cells that were activated by either neuregulin (11.5-fold signal increase over nonstimulated cells) or pervanadate (5-fold signal increase); that is, these treatment conditions lead to ErbB3 activation. This result indicates that the multiplex microbead immunoassay enabled the detection of ErbB2:ErbB3 heterodimers under the activation conditions that favored these protein–protein interactions.[1] In addition, this result is consistent with the previous demonstration with other methods that neuregulin treatment of cells leads to ErbB2:ErbB3 heterodimer formation.[1] In a reciprocal experiment, ErbB3 was detected on ErbB2-specific capture beads (*Fig. 6B*). Although the signal above background (untreated cell lysate) was lower, it was significant (3-fold signal increase). Note that there are differences in assay reciprocity as well as variability in the assay background for the different microbead sets for detection of ErbB2 and Erb3 in *Figure 6*. These differences could be attributed to the differences in reactivity of the antibodies coated on microbeads as well as differences in the 2 detection antibodies. Nevertheless, it is important to note that the signal for ErbB3 detection on ErbB2-specific beads (and *vice versa*) was observed only in lysates obtained from activated cells. Taken together, the above results indicate that ErbB2 and ErbB3 RTKs actively engaged in heterodimer formation in the MDA-MB-453 cell line when ErbB3 was stimulated. The MDA-MB-468 cell line does not express ErbB2 receptor.[16,17] ErbB2:ErbB3 heterodimers were not detected in this cell line (these authors, data not shown).

DISCUSSION

To understand molecular mechanisms underlying the role of the ErbB family of RTKs in cancer, it is important not only to detect expression but also phosphorylation and heterodimerization of these RTKs.[18,19] Importantly, there is increasing evidence that interplay between the 4 RTKs contributes to more aggressive phenotype and affects response to therapy in breast cancer.[18]

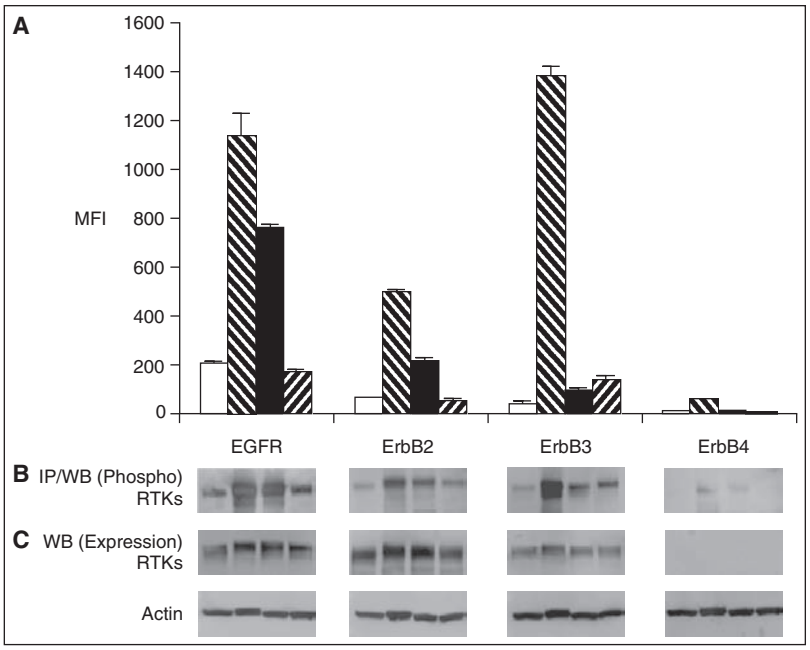

Fig. 4. Phosphoproteomic analysis of RTKs by multiplex microbead immunoassay in A431 cells. Details are the same as described for *Figure 2*. Abbreviations: MFI, median fluorescence intensity; RTK, receptor tyrosine kinase.

A multi-pronged approach, enabling determination of expression as well as function of these potent signaling molecules for drug screening, use as biomarkers in cancer diagnosis/prognosis and monitoring efficacy of therapy, would be more valuable. In this article, we present proof-of-concept studies for the use of the multiplex microbead suspension array method, in 3 multiplex panels that enable detection of expression, phosphorylation, and heterodimerization of ErbB RTKs.

For the detection of expression of RTKs in breast cancer cell lines (MDA-MB-453 and MDA-MB-468) and an epidermoid cell line (A431), multiplex microbead suspension array yielded results similar to those obtained by western blot (*Fig. 1*). As expected, the MDA-MB-453 cell line expressed ErbB2 and ErbB3, and the MDA-MB-468 cell line expressed EGFR and ErbB3. A431 cells expressed 3 RTKs (EGFR, ErbB2, and ErbB3). These RTKs are activated by EGF-like growth factors that promote receptor-mediated homo- and heterodimers.[11] Among ErbB family members, ErbB2 does not have a known growth-factor ligand, whereas ErbB3 has a defective kinase activity but retains the capacity to bind neuregulin.[20] Therefore, these 2 ErbB receptors must heterodimerize with each other, or with other members of this RTK family to transmit signals. These protein–protein interactions may vary from cell type to cell type.[4,20] Neuregulin leads to ErbB2–ErbB3 heterodimerization, which subsequently produces biological effects.[12,20,21] Indeed in MDA-MB-453 cells activated with neuregulin, ErbB2–ErbB3 heterodimers were readily detected by the multiplex assay (*Fig. 6*). Similarly, ErbB2–ErbB3 heterodimers were found in A431 and prostate cancer cell lines (data not shown). In the cell lines used in this study, EGFR–ErbB3 or EGFR–ErbB2 heterodimers were not detected. The simplest explanation for this observation is that the predominant form of activated EGFR may be a homodimer.

Dimerization of ErbB RTKs induces tyrosine kinase catalytic activity, which leads to the autophosphorylation of tyrosine residues at the C-terminus of the kinase.[22] These phosphorylated residues serve as docking sites for recruitment of proteins, which activate downstream signaling cascades,[6,12] including Ras-Raf–mitogen-activated protein kinase (Ras–MAPK), phosphatidylinositol-3 kinase–protein kinase B (PI3K–PKB/Akt, and phospholipase C–protein kinase C (PLC–PKC) pathways.[22,23] We have developed a multiplex assay for the simultaneous detection of phosphorylation for efficient phosphoproteomic profiling of ErbB RTKs under different cell activation conditions. In MDA-MB-453 cells, neuregulin treatment resulted in the phosphorylation of ErbB3. Because EGFR is not present in this cell line, EGF treatment did not result in detectable levels of phosphorylation of RTKs (*Fig. 3*). In contrast, MDA-MB-468 cells displayed a strong increase in phosphorylation of EGFR upon treatment with EGF (*Fig. 2*). In addition, some increase in the phosphorylation of ErbB3 was also observed. EGF treatment of A431 cells also resulted in a robust increase in phosphorylation of EGFR (*Fig. 4*). However, despite the high level of ErbB3 expression in these cells (*Fig. 1*), treatment with neuregulin did not result in phosphorylation of ErbB3. This is surprising because, in pervanadate-treated A431 cells, ErbB3 was found to be heavily phosphorylated (*Fig. 4*). A simple explanation is that in A431 cell line EGFR sequesters ErbB2, and under the conditions of activation with neuregulin, ErbB2 is not available to dimerize with ErbB3. Thus, ErbB3 phosphorylation is inhibited. However, pervanadate is a nonspecific activator that acts by inhibiting tyrosine phosphatases leading to general hyperphosphorylation of tyrosine-phosphorylated signaling proteins. Therefore, in A431 cells treated with pervanadate, phosphorylation of ErbB3 is presumably not ErbB2-dependent.

To illustrate the efficiency of the multiplex microbead suspension array system in studying intracellular signaling, one may consider the example of phosphoproteomic profiling of RTKs by other methods. Phosphoproteomic analysis of the 4 RTKs in breast cancer cell lines needed approximately 8×10^4 cells for the multiplex microbead assay (*Fig. 1*). Importantly, the same number of

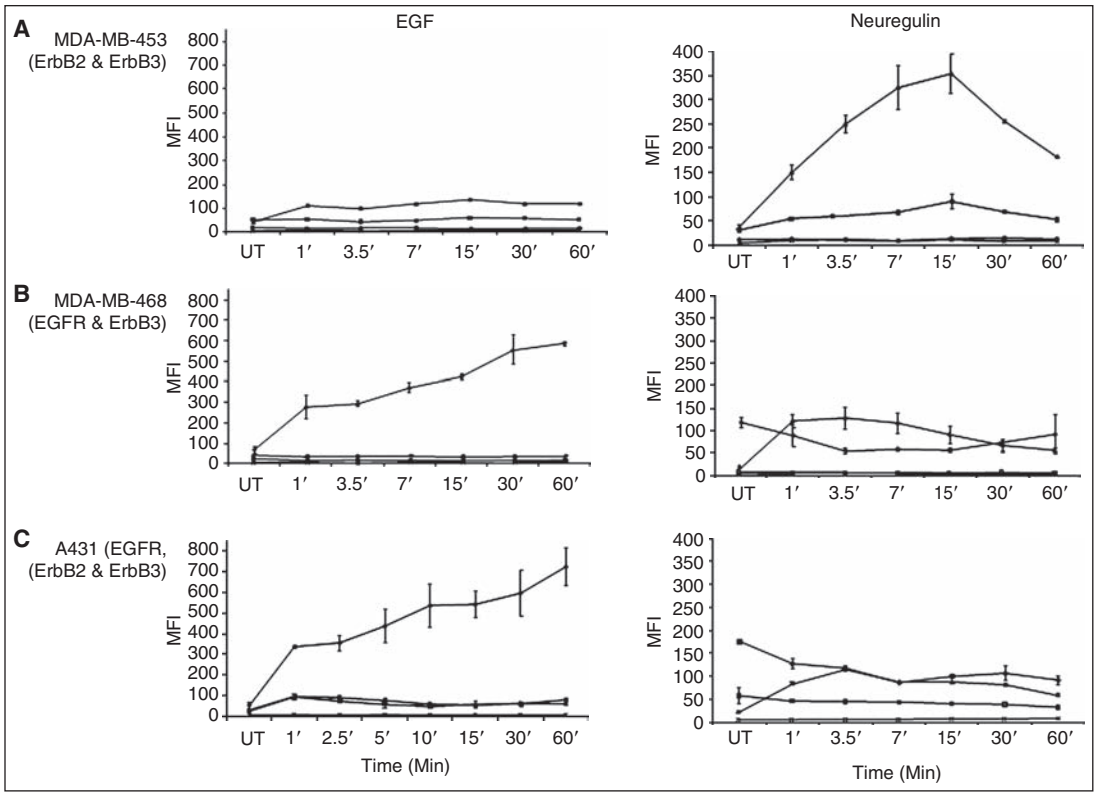

Fig. 5. Kinetics of phosphorylation of RTKs in cells treated with EGF or neuregulin. (**A**) MDA-MB-453, (**B**) MDA-MB-468, and (**C**) A431 cells were activated with 16.5 nM EGF or 1:500 neuregulin for various times ranging from 1 to 60 min. Microbeads used in the multiplex assay were coated with antibodies against EGFR (diamond), ErbB2 (square), ErbB3 (triangle), and ErbB4 (cross). Multiplex microbead immunoassay was performed as described for *Figure 2*. Detection of phosphorylation was performed by 4G10. Error bars represent standard error of $n = 4$ values. Abbreviations: MFI, median fluorescence intensity; RTK, receptor tyrosine kinase.

cells would suffice for the phosphoproteomic analysis of several other downstream signaling proteins simultaneously with ErbB RTKs to obtain more detailed information on intracellular signaling (downstream signaling studies in breast cancer to be published elsewhere).[13] In contrast, to obtain similar information by IP/WB and ELISA analyses of ErbB RTKs, much larger number of cells (4×10^7 and 8×10^6, respectively) were required (*Figs. 2–4*; ELISA data (these authors) not shown). Similarly, expression of a wide variety of cell signaling proteins could be performed in a relatively small number of cells (8×10^4 cells). Thus, the need for only a small amount of sample for profiling of several signaling proteins (theoretically up to 100) is a clear advantage of the multiplex microbead assay system.

Utility and small-sample requirement of this novel multiplex immunoassay for detection of phosphorylation were further demonstrated by the analysis of phosphorylation of ErbB RTKs in a time-course activation of MDA-MB-453, MDA-MB-468, and A431 cell lines. Cells were activated by both agonists (EGF and neuregulin) and samples were collected at 7 time points over a period of 1 h for the phosphoproteomic analysis (56 data points) (*Fig. 5*). The kinetic analysis highlighted the following features of RTK activation: (a) the assay readily enabled investigation of temporal changes in phosphorylation of several proteins simultaneously, involving multiple time points, (b) activation kinetics of EGFR in the 2 cell lines that expressed it (MDA-MB-468 and A431) were similar, displaying a continuous increase in overall tyrosine phosphorylation over 60 min, and (c) the assay was convenient for monitoring signal increase as well as its decay (ErbB3). In comparison to fixed formats such as peptide array systems,[24] the multiplex microbead format offers a flexibility and ease of adaptability where microbead sets coated with capture antibodies can be included or excluded from the mixture at will. Methods based on 2-D gel electrophoresis and mass spectroscopy have recently been applied for simultaneous analysis of multiple signaling proteins in cells.[25–29] However, these methods require complex protocols for sample analysis as well as complicated and very costly instrumentation for biological and clinical applications.

This study outlines an efficient approach for the determination of expression, phosphorylation, and identification of heterodimeric partner(s), performed on the Luminex platform. As shown earlier, results obtained by the multiplex immunoassays can be quantitatively compared across different cell types for each protein individually. For example, the relative expression levels of individual ErbB RTKs in 3 different cell lines are clearly reflected by their respective MFI values (*Fig. 1*). Similarly, phosphorylation

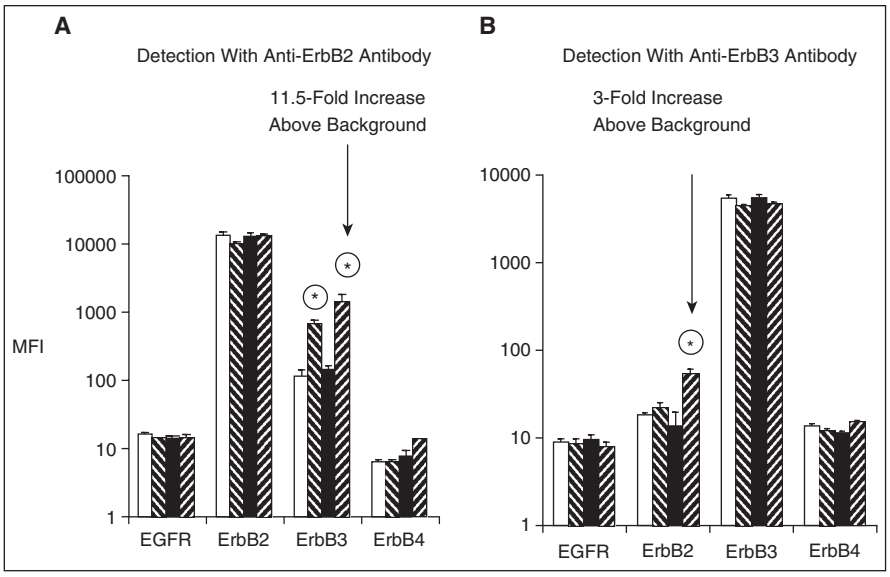

Fig. 6. Detection of heterodimerization of ErbB family of receptors. Cells were used as untreated (open bars), treated with 6.6 mM sodium pervanadate for 5 min (hashed bars), 16.5 nM EGF (closed bars), or 1:500 neuregulin for 7 min (reverse hashed bars). A second antibody (biotinylated), either specific to ErbB2 (**A**) or ErbB3 (**B**), was used for detection of the respective proteins. Treatment of cells by pervanadate, EGF, or neuregulin is indicated. Error bars represent standard deviation error of $n = 4$ values. Significant difference (P value < 0.01) in detection signal for ErbB2 and ErbB3 (between untreated control and activated cell lysates) is indicated by an encircled asterisk.

levels of each of the RTKs in 3 different cell lines are shown by their respective MFI values (*Figs. 2–4*).

In conclusion, the studies reported here provide proof-of-concept for the use of the multiplex microbead suspension array as a highly efficient method for simultaneous detection of expression, phosphorylation, and heterodimerization of the ErbB RTKs in cancer cells. This approach is relatively high throughput and quantitative and enables the study of critically important attributes of ErbB RTKs in cancer. The results presented here demonstrate the feasibility of the multiplex suspension array approach for analysis of molecular mechanisms by which RTKs exert their oncogenic effects. This approach can also be used for the simultaneous detection and quantitation of expression, phosphorylation, and heterodimerization of many other signaling proteins, and hence the multiplex microbead suspension array system holds promise as a novel method for drug screening, cancer diagnosis, and the prediction of outcomes in cancer patients.

ACKNOWLEDGMENTS

We thank the UC Davis Cancer Center and the Department of Pathology and Laboratory Medicine at UC Davis for support.

AUTHOR DISCLOSURE STATEMENT

I.H.K., J.Z., P.G., M.Z., C.S., H.-J.K., and P.A.L. are employees of the University of California Davis.

REFERENCES

1. Stern DF: ERBB3/HER3 and ERBB2/HER2 duet in mammary development and breast cancer. *J Mammary Gland Biol Neoplasia* 2008;13:215–223.
2. Lo HW, Hsu SC, Hung MC: EGFR signaling pathway in breast cancers: from traditional signal transduction to direct nuclear translocalization. *Breast Cancer Res Treat* 2006;95:211–218.
3. Ono M, Kuwano M: Molecular mechanisms of epidermal growth factor receptor (EGFR) activation and response to gefitinib and other EGFR-targeting drugs. *Clin Cancer Res* 2006;12:7242–7251.
4. Sweeney C, Miller JK, Shattuck DL, Carraway KL: ErbB receptor negative regulatory mechanisms: implications in cancer. *J Mammary Gland Biol Neoplasia* 2006;11:89–99.
5. Agrawal A, Gutteridge E, Gee JM, Nicholson RI, Robertson JF: Overview of tyrosine kinase inhibitors in clinical breast cancer. *Endocr Relat Cancer* 2005;12(Suppl 1):S135–S144.
6. Niu G, Carter WB: Human epidermal growth factor receptor 2 regulates angiopoietin-2 expression in breast cancer via AKT and mitogen-activated protein kinase pathway. *Cancer Res* 2007;67:1487–1493.
7. Engel RH, Kaklamani VG: HER2-Positive breast cancer: current and future treatment strategies. *Drugs* 2007;67:1329–1341.
8. Johnston JB, Navaratnam S, Pitz MW, Maniate JM, Wiechec E, Baust H, Gingerich J, *et al.*: Targeting the EGFR pathway for cancer therapy. *Curr Med Chem* 2006;13:3483–3492.
9. Leong TY, Leong AS: Controversies in the assessment of HER-2: more questions than answers. *Adv Anat Pathol* 2006;13:263–269.
10. Britsch S: The neuregulin-I/ErbB signaling system in development and disease. *Adv Anat Embryol Cell Biol* 2007;190:1–65.
11. Stortelers C, van der Woning SP, Jacobs-Oomen S, Wingens M, van Zoelen EJ: Selective formation of ErbB-2/ErbB-3 heterodimers depends on the ErbB-3 affinity of epidermal growth factor-like ligands. *J Biol Chem* 2003;278:12055–12063.
12. Graus-Porta D, Beerli RR, Daly JM, Hynes NE: ErbB-2, the preferred heterodimerization partner of all ErbB receptors, is a mediator of lateral signaling. *EMBO J* 1997;6:1647–1655.
13. Abd El-Rehim DM, Pinder SE, Paish CE, Rampaul RS, Balmey RW, Robertson JFR, *et al.*: Expression and co-expression of the members of the epidermal growth factor receptor (EGFR) family in invasive carcinoma. *Br J Cancer* 2004;91:1532–1542.

14. Normanno N, Maiello MR, De Luca A: Epidermal growth factor receptor tyrosine kinase inhibitors (EGFR-TKIs): Simple drugs with a complex mechanism of action? *J Cell Phys* 2002;194:13–19.
15. Khan IH, Mendoza S, Rhyne P, Ziman M, Tuscano J, Eisinger D, *et al.*: Multiplex Analysis of intracellular signaling pathways in lymphoid cells by microbead suspension arrays. *Mol Cell Proteomics* 2006;5:758–768.
16. Crovello CS, Lai C, Cantley LC, Carraway KL, III: Differential signaling by the epidermal growth factor-like growth factors neuregulin-1 and neuregulin-2. *J Biol Chem* 1998;273:26954–26961.
17. Lupu R, Colomer R, Kannan B, Lippman ME: Characterization of a growth factor that binds exclusively to the erbB-2 receptor and induce cellular responses. *Proc Natl Acad Sci USA* 1992;89:2287–2291.
18. Zaczek A, Brandt B, Bielawski KP: The diverse signaling network of EGFR, Her2, HER3 and HER4 tyrosine kinase receptors and the consequences of therapeutic approaches. *Histol Histopathol* 2005;20:1005–1015.
19. Anido J, Matar P, Albanell J, Guzman M, Rojo F, Arribas J, *et al.*: ZD1839, a specific epidermal growth factor receptor (EGFR) tyrosine kinase inhibitor, induces the formation of inactive EGFR/HER2 and EGFR/HER3 heterodimers and prevents heregulin signaling in HER2-overexpressing breast cancer cells. *Clin Cancer Res* 2003;9:1274–1283.
20. Citri A, Yarden Y: EGF-ERBB signalling: towards the systems level. *Nat Rev Mol Cell Biol* 2006;7:505–516.
21. Karamouzis MV, Badra FA, Papavassiliou AG: Breast cancer: the upgraded role of HER-3 and HER-4. *Int J Biochem Cell Biol* 2007;39:851–856.
22. Jimeno A, Hidalgo M: Pharmacogenomics of epidermal growth factor receptor (EGFR) tyrosine kinase inhibitors. *Biochim Biophys Acta* 2006;1766:217–229.
23. Chan SK, Hill ME, Gullick WJ: The role of the epidermal growth factor receptor in breast cancer. *J Mammary Gland Biol Neoplasia* 2006;11:3–11.
24. Reimer U, Reineke U, Schneider-Mergener J: Peptide arrays: from macro to micro. *Curr Opin Biotechnol* 2002;13:315–320.
25. Imam-Sghiouar N, Laude-Lemaire I, Labas V, Pflieger D, Le Caer JP, Caron M, *et al.*: Subproteomics analysis of phosphorylated proteins: application to the study of B-lymphoblasts from a patient with Scott syndrome. *Proteomics* 2002;2:828–838.
26. Steinberg TH, Agnew BJ, Gee KR, Leung WY, Goodman T, Schulenberg B, *et al.*: Global quantitative phosphoprotein analysis using Multiplexed Proteomics technology. *Proteomics* 2003;3:1128–1144.
27. Brill LM, Salomon AR, Ficarro SB, Mukherji M, Stettler-Gill M, Peters EC: Robust phosphoproteomic profiling of tyrosine phosphorylation sites from human T cells using immobilized metal affinity chromatography and tandem mass spectrometry. *Anal Chem* 2004;76:2763–2772.
28. Veenstra TD, Prieto DA, Conrads TP: Proteomic patterns for early cancer detection. *Drug Discov Today* 2004;9:889–897.
29. Ficarro SB, Salomon AR, Brill LM, Mason DE, Stettler-Gill M, Brock A, *et al.*: Automated immobilized metal affinity chromatography/nano-liquid chromatography/electrospray ionization mass spectrometry platform for profiling protein phosphorylation sites. *Rapid Commun Mass Spectrometry* 2005;19: 57–71.

Address correspondence to:
Dr. Imran H. Khan
Center for Comparative Medicine
University of California at Davis
Hutchison Drive and County Road 98
Davis, CA 95616

E-mail: ihkhan@ucdavis.edu

THE JOURNAL OF BIOLOGICAL CHEMISTRY VOL. 285, NO. 4, pp. 2368–2374, January 22, 2010
Printed in the U.S.A.

ERK Regulates Calpain 2-induced Androgen Receptor Proteolysis in CWR22 Relapsed Prostate Tumor Cell Lines*

Received for publication, July 28, 2009, and in revised form, November 7, 2009 Published, JBC Papers in Press, November 28, 2009, DOI 10.1074/jbc.M109.049379

Honglin Chen[‡], Stephen J. Libertini[‡], Yu Wang[§], Hsing-Jien Kung[¶], Paramita Ghosh[§‖], and Maria Mudryj[‡‖1]

From the [‡]Department of Medical Microbiology and Immunology, [§]Department of Urology, and [¶]Division of Basic Sciences, Cancer Center, and Department of Biochemistry and Molecular Medicine, University of California, Davis, California 19616 and the [‖]Veterans Affairs-Northern California Health Care System, Mather, California 95655

Androgen ablation therapy is effective in treating androgen-dependent prostate tumors; however, tumors that can proliferate in castrate levels of androgen eventually arise. We previously reported that in CWR22Rv1 (Rv1) cells, the protease calpain 2 can cleave the androgen receptor (AR) into a constitutively active ~80,000 low molecular weight (LMW) form. In this study, we further dissect the mechanisms that produce the AR LMW forms using Rv1 cells and the related CWR22-R1 (R1) cells. The 39-amino acid insertional mutation in the Rv1-AR (E3DM-AR) sensitizes this AR to calpain 2 proteolysis. R1 cells encode the same AR molecule as the parental CWR22 xenograft. Using calpain 2 small interfering RNA and calpeptin, we find that calpain 2 plays a role in the generation of the LMW-AR in R1 cells. Furthermore, LMW-AR expression is regulated by the activation of calpain 2 by ERK 1 and 2. Inhibition of ERK phosphorylation or small interfering RNA-mediated decrease of ERK expression reduces LMW-AR levels in R1 cells. Conversely, activation of the MAPK pathway results in increased ERK phosphorylation and increased levels of LMW-AR. Finally, analyses of human tumor samples found that LMW-AR levels are higher in tumors that have an increased calpain/calpastatin ratio and/or increased levels of phospho-ERK (pERK). This suggests that a higher calpain/calpastatin ratio collaborates with activated ERK to promote the generation of the LMW-AR.

Prostate cancer is a commonly diagnosed malignancy that is treated with hormonal therapy aimed at blocking signaling through the androgen receptor (AR).[2] Initially, androgen ablation therapy is effective, but eventually, this treatment leads to the development of aggressive relapsed tumors that thrive in the absence of androgens. Analysis of clinical samples revealed that >90% of the relapsed tumors express AR (1–4). The AR, a member of the steroid hormone superfamily of ligand-activated transcription factors (5, 6) is central to the initiation and growth of prostate tumors and their responses to therapy. In the absence of ligand, the AR is retained in the cytoplasm. The binding of hormone alters the conformation of AR to promote translocation of the AR into the nucleus, where it regulates gene transcription (6–8).

Aberrant AR activity has been postulated to promote proliferation of tumor cells in reduced levels of androgen. Studies have shown that 25–30% of androgen-independent tumors that arose following androgen ablation have AR gene amplification (9, 10). AR mutations are more commonly observed in androgen-independent tumors (11, 12) and usually broaden ligand specificity (13). The AR present in CWR22 xenograft cells has a mutation in the ligand binding domain (LBD; H847Y) that enhances responsiveness to estradiol and progesterone (14). Structure function analysis of the AR showed that deletion of the LBD generates a constitutively active AR molecule (15). A subsequent study identified a nonsense mutation at Q640 that results in a truncated constitutively active AR in a tumor refractory to androgen ablation therapy (16). We and others previously reported that calpain cleaves the AR molecule to produce various LMW isoforms (17–19), including an ~80,000 C-terminally truncated AR. We found that the ~80,000 LMW-AR is present in some human prostate tumors (18). Using the androgen-independent Rv1 cell line that expresses high levels of the LMW-AR, we demonstrated that inhibition of calpain activity induces apoptosis in cells cultured in the absence of androgen. These studies implied that calpain-dependent proteolysis of the AR may play an important role in conferring androgen independence in a subset of prostate cancer cases (18). In this study, we show that calpain 2 and ERK collaborate in the generation of the LMW-AR.

EXPERIMENTAL PROCEDURES

Cell Culture and Pharmacological Agents—LNCaP, Rv1, PC3, and DU145 cells were obtained from American Type Culture Collection. R1 cells were provided by Dr. Elizabeth Wilson (University of North Carolina). Rv1, PC3, DU145, and R1 cells were propagated in RPMI 1640 supplemented with 5% fetal bovine serum, 2 mmol/liter L-glutamine, 100 units/ml penicillin, and 100 μg/ml streptomycin (Invitrogen) at 37 °C and 5% CO_2. LNCaP cells were propagated in 10% fetal bovine serum. RWPE, pRNS-1-1, and PZ-HPV-7, obtained from Dr. Ralph

* This work was supported by Department of Defense Grant PC051049 (to M. M.), Veterans Affairs Merit Award (to M. M.), and Department of Defense Predoctoral Award PC073557 (to H. C.).

[1] To whom correspondence should be addressed: Dept. of Medical Microbiology, 3147 Tupper Hall, University of California, Davis, CA 95616. Fax: 530-752-8692; E-mail: mmudryj@ucdavis.edu.

[2] The abbreviations used are: AR, androgen receptor; Rv1, CWR22Rv1; R1, CWR22-R1; LMW, low molecular weight; FL, full-length; CLDN4, claudin 4; ERK, extracellular signal-regulated kinase; pERK, phospho-ERK; TPA, phorbol ester 12-*O*-tetradecanoylphorbol-13-acetate; MTS, 3-(4,5-dimethyl-thiazol-2yl)-5-(3-carboxymethoxyphenyl)-2-(4-sulfophenyl)-2H-tetrazolium; MTT, 3-(4,5-dimethylthiazol-2-yl)-2,5-diphenyltetrazolium bromide; wt, wild-type; E3DM-AR, exon 3 duplication mutation AR; FAK, focal adhesion kinase; LBD, ligand binding domain; MEK, mitogen-activated protein kinase/extracellular signal-regulated kinase kinase; GAPDH, glyceraldehyde-3-phosphate dehydrogenase; MAPK, mitogen-activated protein kinase.

deVere White, were maintained in a keratinocyte serum-free medium supplemented with 50 mg/ml bovine pituitary extract and 5 ng/ml epidermal growth factor (Invitrogen). All cell lines were incubated at 37 and 5% CO_2. For *in vivo* inhibition of calpain activity, 2×10^5 cells were plated in 35-mm plates and cultured in androgen-containing or androgen-depleted media (phenol red-free media/charcoal-stripped serum) for 48 h. Bicalutamide (Casodex) was from AstraZeneca (Cheshire, UK). For calpain inhibition studies, cells were treated with dimethyl sulfoxide or 40 μmol/L calpeptin (Calbiochem) for 24 or 48 h, washed with cold phosphate-buffered saline, and harvested. For MEK inhibition studies, cells were treated with 20 μM U0126 (Cell Signaling) or dimethyl sulfoxide for 24 and 48 h. Protein kinase C activity was stimulated by treatment with 10 nM 12-*O*-tetradecanoylphorbol-13-acetate (TPA) (LC Laboratories) dissolved in dimethyl sulfoxide.

Western Immunoblot Analysis—Cells were placed in a 4 °C radioimmunoprecipitation lysis buffer that contained calpeptin and a protease inhibitor mixture (Sigma). Thirty micrograms of protein were separated on 8%, 10%, or 12% SDS-PAGE gels and transferred to BA-85 membrane (Schleicher & Schuell) and blocked with 5% nonfat dry milk in phosphate-buffered saline and 0.1% Tween 20. The following antibodies were used: AR (central) clone 441 (Ab-1; Lab Vision Corp.), AR NH_2 terminus (N-20; Santa Cruz Biotechnology), Calpain 2 (Domain III, Sigma), calpastatin (1F7E3D10, Calbiochem), ERK (Cell Signaling), pERK (Thr202/tyr204, Cell Signaling), and FAK (clone 4.47; Upstate), GAPDH (clone 6C5, Santa Cruz Biotechnology). Proteins were detected using Enhanced chemiluminescence (GE Healthcare).

RNA Interference—2×10^5 Rv1 and R1 cells were plated in 60-mm dishes. 24 h later, the cells were transfected with 130 nM calpain 2 siRNA ON-TARGETplus SMARTpool or ERK 1 and 2 siRNA ON-TARGETplus SMARTpool (Dharmacon Research Inc.) with Lipofectamine 2000 (Invitrogen). The ON-TARGETplus nontargeting siRNA was used as a negative control. Cells were harvested for RNA analysis 72 h post-transfection (RNeasy mini kit) (Invitrogen).

In Vitro Calpain Assay—Cells were resuspended in calpain assay buffer (50 mmol/liter HEPES (pH 7.4), 150 mmol/liter NaCl, 1% Triton X-100). Calpain was activated with addition of $CaCl_2$ to 1 mM. The reactions were incubated at 25 °C.

Transfection—Cells were transfected using Lipofectamine 2000 (Invitrogen) following the manufacturer's protocol. Cells were harvested 48 h after transfection and subjected to analysis as described previously (18).

Cell Proliferation Assay—Cellular proliferation was assessed using the 3-(4,5-dimethylthiazol-2yl)-5-(3-carboxymethoxyphenyl)-2-(4-sulfophenyl)-2H-tetrazolium (MTS) or the 3-(4,5-dimethylthiazol-2-yl)-2,5-diphenyltetra-zolium bromide (MTT) assay (Promega) following manufacturer's recommendations.

Real-time PCR—Total cellular RNA was prepared from cells (RNeasy) and cDNA was synthesized from 1 μg RNA using QuantiTect (Qiagen) reverse transcription kit. cDNAs were diluted 1:4 in double distilled H_2O, and 2 μl of cDNA was added to 5 μl of EXPRESS SYBR® GreenER qPCR supermix (Invitrogen) and 200 nM of each primer for a total volume of 10 μl. GAPDH was used as the standard. PCR conditions were as follows: a 20-s initial denaturation step at 95 °C; 40 cycles at 95 °C for 3 s, 60 °C for 30 s, followed by a melt curve at 95 °C for 15 s, 60 °C for 15 s, an increase to 95 °C over 20 min; an additional 95 cycles starting at 60 °C with a 0.5 °C increase per cycle for melt curve analysis. The Eppendorf Mastercycler ep Realplex was used for this study. Primer sequences: GAPDH: 5′-TGCACCACCAACTGCTTA-3′ and 5′-AGAGGCAGGGATGATGTTC-3′; CLDN4: 5′-AACCCTGACTTTGGGATCTG-3′ and 5′-AGATGCAGGCAGACAGAGTG-3′; HPRT1: 5′-TGACACTGGCAAAACAATGCA-3′ and 5′-GGTCCTTTTCACCAGCAAGCT-3′.

Statistics—Analyses using a two-tailed Student's *t* test were used to compare two groups. $p < 0.05$ was considered statistically significant.

RESULTS

Characteristics of the Rv1 and R1 Cell Lines—Two castrate-resistant cell lines, R1 and Rv1, were derived from two independent CWR22 relapsed tumors. The cellular phenotypes of the Rv1 and R1 cells are similar. In the presence of androgen the cells tend to grow in clusters, whereas in the absence of androgens, they tend to be more scattered and less adhesive (Fig. 1*A*). The AR in both lines has the same LBD mutation as the CWR22 xenograft (20, 21). As previously reported, R1 and Rv1 cells express the LMW AR forms (Fig. 1*B*) (20, 21). Western immunoblot analysis indicated that R1 cells expressed higher levels of AR than Rv1 cells, but the ratio of the LMW to full-length (FL)-AR was higher in Rv1 cells. The size of the FL-AR in the R1 cells is smaller than the FL-AR in the Rv1 cells, because R1 cells do not have the 39 amino acid duplication of exon 3. Closer inspection revealed that the ~80,000 LMW forms could be resolved into several discrete bands (Fig. 1*B*). The MTS proliferation assay confirmed that the R1 and Rv1 cell proliferation rates were only slightly slower in androgen-depleted media compared with cells grown in the presence of androgen (Fig. 1*C*). The proliferation assay conducted in the presence of 10 μM Casodex indicated that R1 and Rv1 cells were refractory to the effects of this AR inhibitor (Fig. 1*D*). Although all three lines are responsive to androgen, only LNCaP cells are dependent on androgen to sustain growth.

Generation of the LMW-AR Involves Calpain—We have reported previously that the inhibition of calpain activity by calpeptin reduces the expression of the LMW-AR in Rv1 cells (18). Likewise, treatment of R1 cells, proliferating in the presence or absence of androgen, with calpeptin reduced the levels of LMW-AR in R1 cells (Fig. 2*A*). We previously showed that proteolysis of the calpain substrate focal adhesion kinase (FAK) is a good indicator of calpain activity (22). Calpeptin treatment of R1 cells reduced the levels of LMW-FAK (Fig. 2*A*). To further analyze the role of calpain in the generation of LMW-AR, calpain 2 expression was analyzed in several tumor derived, as well as immortalized, prostate cell lines. R1 cells expressed much higher levels of calpain 2 than Rv1 and LNCaP cells (Fig. 2*B*). Interestingly, the two AR negative and highly metastatic cell lines, PC3 and DU145, expressed the highest levels of calpain 2. Given that calpain activity is regulated by its endogenous inhibitor calpastatin,

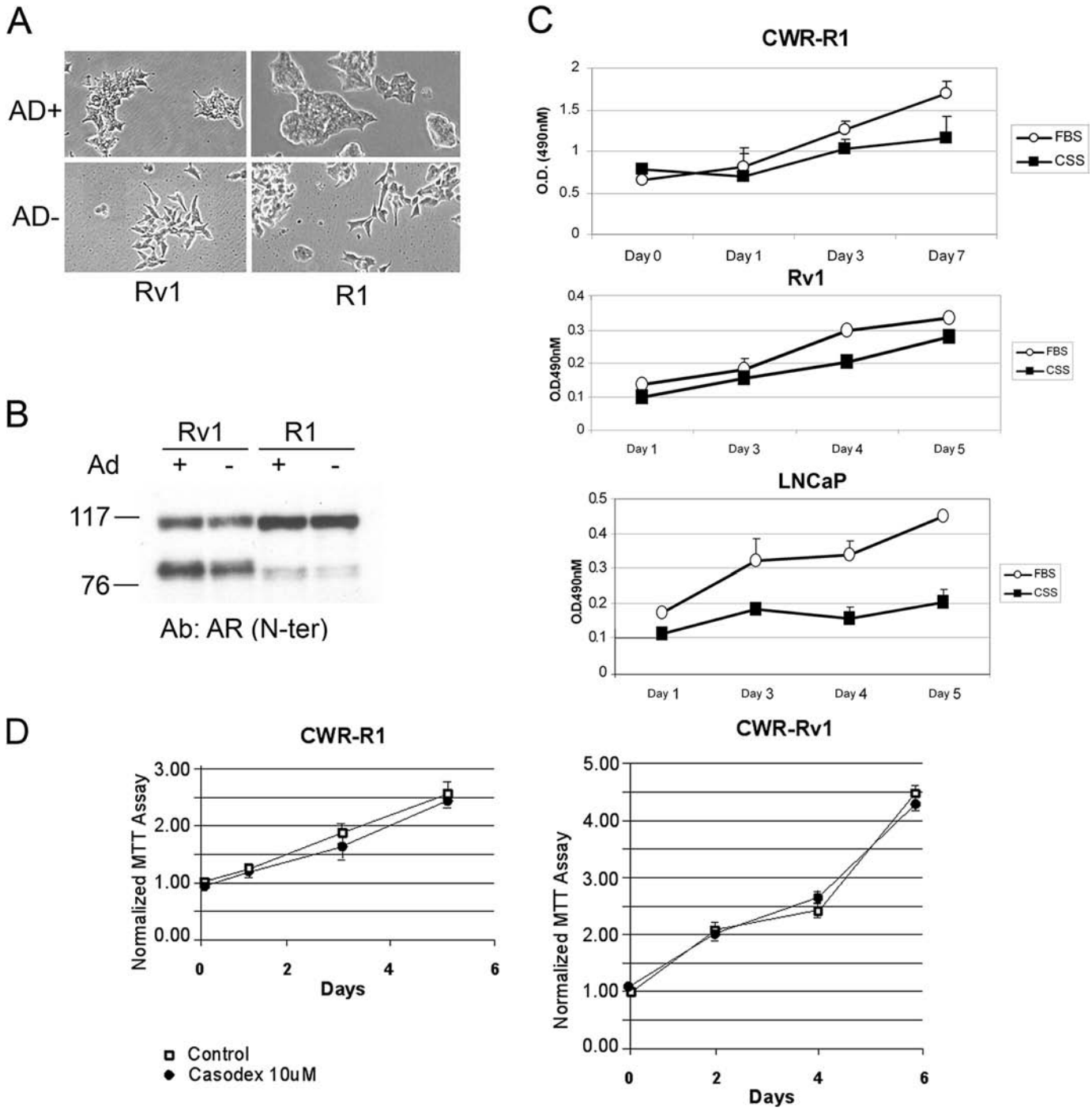

FIGURE 1. **Rv1 and R1 cells proliferate in castrate levels of androgen.** *A*, R1 and Rv1 cells proliferating in the presence of androgen (*AD*+) are less refractile than cells in androgen-depleted media (*AD*−). *B*, AR expression is greater in R1 than in Rv1 cells, but the FL and LMW-AR expressed in R1 cells is slightly smaller that that expressed in Rv1 cells. *C*, R1 and Rv1 cells proliferate in castrate levels of androgen, but proliferation is slightly greater in the presence of androgen. Androgen depletion inhibits LNCaP proliferation. *D*, Rv1 and R1 cells proliferate in the presence of 10 μM Casodex. *Ab*, antibody; *Nter*, N-terminal; *FBS*, fetal bovine serum; *CSS*, charcoal stripped serum.

we analyzed calpastatin levels as well, and found that expression was comparable in all the cell lines (Fig. 2*B*). R1 cells had higher amounts of proteolyzed FAK, indicating greater calpain activity (Fig. 2*C*). The extent of FAK cleavage was greater in the absence of androgen, suggesting that calpain activity may be higher under androgen-depleted conditions. To further confirm the involvement of calpain 2 in the generation of the LMW-AR forms in R1 cells, we used calpain 2 siRNA to reduce calpain 2 expression. A previous study reported that calpain 2 has a very long half-life of 5 days (23). A 6-day treatment resulted in an ~60% reduction of calpain 2 protein levels in R1 cells (Fig. 2*D*) and reduced levels of the LMW-AR forms (Fig. 2*D*). This treatment also reduced FAK proteolysis indicating that calpain 2 activity was reduced. This analysis indicates that calpain 2 plays a role in the generation of the LMW-AR in R1 cells.

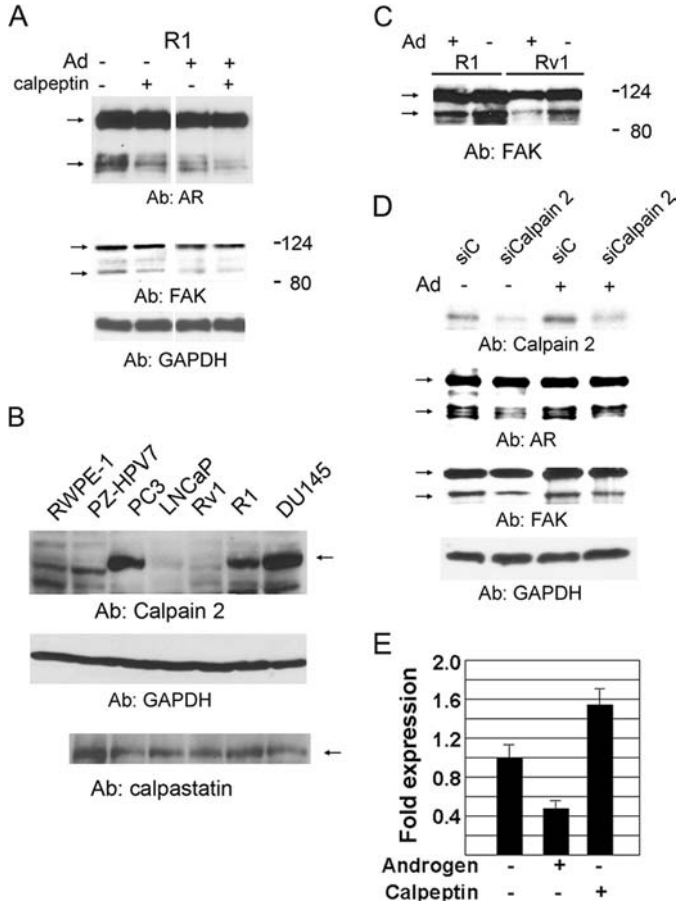

FIGURE 2. **Calpain expression and activity in prostate-derived cells.** *A*, inhibition of calpain activity in R1 cells with calpeptin (40 uM) for 48 h decreases the expression of the LMW-AR (relative to FL-AR) by 55% in the absence of androgen (*Ad*) and 43% in the presence of androgen. *B*, *top panel*, Western blot analysis of calpain 2 levels in nontransformed and tumor prostate cells. *Bottom panel*, Western blot analysis of calpastatin levels in nontransformed and tumor cells. GAPDH served as a loading control. *C*, calpain-dependent proteolysis of FAK from a 120-kDa to a 90-kDa form and ultimately smaller forms is indicative of calpain activity. FAK proteolysis is greater in R1 than in Rv1 cells and is greater in both cells in the absence of androgens. *D*, calpain 2 siRNA down-regulated calpain 2 protein levels 144 h post-transfection in R1 cells. The down-regulation of calpain 2 expression by calpain 2 siRNA reduced the LMW-AR (relative to FL-AR) by 54% in the absence of androgen and 39% in the presence of androgen. Calpain-dependent proteolysis of FAK was also decreased. *E*, expression of CLDN4 in R1 cells culture in androgen-depleted media, following a 2-h stimulation with DHT and a 24-h treatment with 60 μM calpeptin was assessed by real-time PCR. CLDN4 expression was standardized to GAPDH. *Error bars* represent S.D. $p < 0.05$. *Ab*, antibody; *siC*, control siRNA; *siCalapin*, calpain 2 siRNA.

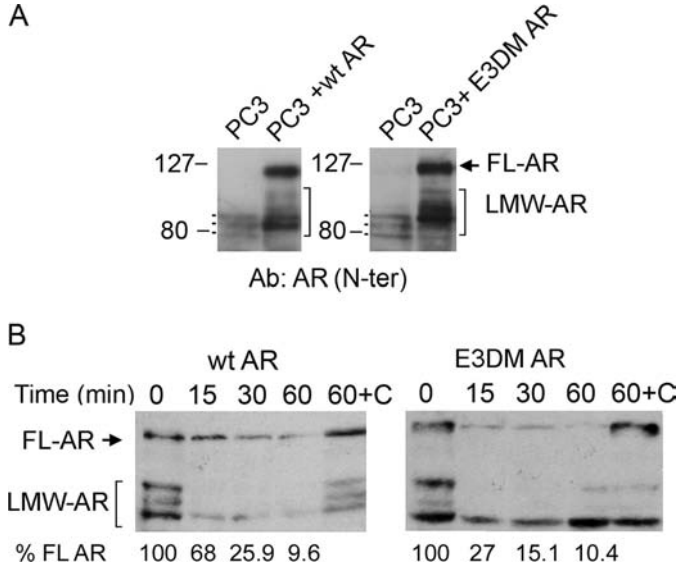

FIGURE 3. **Transient expression of wt and E3DM-AR cDNA in PC3 cells.** *A*, transfection of PC3 cells with wt or E3DM-AR cDNA results in the expression of FL and LMW (denoted by *arrows* and *brackets*) forms of AR. The three nonspecific bands at ~80,000 present in the nontransfected PC3 cells serve as markers (denoted by *dots*). The FL and LMW forms expressed in cells transfected with the E3DM-AR are slightly larger. *B*, extracts prepared from PC3 cells transfected with wt or E3DM-AR were treated with 1 mM $CaCl_2$ to activate calpain activity. The E3DM-AR is degraded more rapidly than the WT AR (compare *lanes 1* and *6*, *lanes 2* and *7*, and *lanes 4* and *9*). *N-ter*, N-terminal; *60+C*, 60 min in presence of calpeptin.

In R1 cells, the expression of claudin 4 (CLDN4) is highly repressed by the addition of androgen (Fig. 2*E*). If calpeptin treatment reduces the levels of LMW-AR, then in the absence of androgen the expression of androgen repressed genes may be further activated. In the absence of androgen calpeptin treatment of R1 cells further increased the expression of CLDN4, thus arguing the LMW-AR has a role in transcription of certain genes.

The Exon 3 Duplication Sensitizes E3DM-AR to Calpain Proteolysis—Rv1 cells express higher levels of the LMW-AR but have low expression of calpain 2 protein and calpain activity (Fig. 2). We hypothesized that the exon 3 duplication sensitizes the E3DM-AR to calpain cleavage. The AR-null PC3 cells expressing high levels of calpain 2 were transfected with cDNA plasmids encoding either the wild-type or E3DM-AR. As expected, the E3DM-AR was slightly larger than the wild-type receptor (Fig. 3*A*). Additionally, the LMW forms generated in cells transfected with the E3DM-AR were larger than the LMW forms generated from the wild-type AR cDNAs. To test the hypothesis that the E3DM-AR is more sensitive to calpain-dependent proteolysis, extracts prepared from the transfected cells were treated with $CaCl_2$ to activate endogenous calpain activity. As shown in Fig. 3*B*, the AR was progressively cleaved into the smaller forms by the addition of $CaCl_2$. The amount of FL-AR remaining was quantitated and indicated that the E3DM-AR was degraded more rapidly than the wt AR. The inclusion of calpeptin retarded proteolysis, indicating that proteolysis was calpain-dependent (Fig. 3*B*). While the ~80,000 forms were present initially and throughout the time course, as proteolysis progressed, the LMW-AR was further proteolyzed to smaller peptides. *In vivo*, the ~ 80,000 LMW-AR forms that are generated by proteolysis can translocate into the nucleus, where they would be less susceptible to further proteolysis. *In vitro*, as was previously observed (17) activated calpain proteolyzes the AR to still smaller forms. The mutant E3DM-AR was cleaved more rapidly than the wild-type FL-AR, resulting in the disappearance of the FL-AR (compare *lanes 4* and *9*).

The Expression of the LMW-AR Is Regulated by ERK—Calpain activity is tightly regulated by various mechanisms, including phosphorylation. Previous studies have shown that ERK can phosphorylate calpain 2 to stimulate protease activity (24). ERK expression was analyzed in immortalized (RWPE-1, PZ-HPV-7, and pRNS-1-1) and tumor derived (PC3, LNCaP, Rv1, R1, and DU145) cell lines. All of the tumor-derived cell lines had higher levels of ERK in comparison to the immortalized cell lines (Fig. 4*A*). A comparison of R1 and Rv1

cells proliferating in the absence and presence of androgen showed that R1 cells had higher levels of the active form of the protein (pERK) under both conditions (Fig. 4*B*).

ERK is phosphorylated and activated by MEK, a dual threonine and tyrosine kinase (24). Treatment of R1 cells with the MEK inhibitor U0126 for 24 or 48 h reduced ERK phosphorylation (Fig. 4*C*). An analysis of AR in the same extracts (Fig. 4*C*) indicated that inhibition of ERK activity reduced the levels of LMW-AR. Similar results were found in Rv1 cells (data not shown). To confirm that LMW-AR expression is dependent on ERK, cells were treated with control siRNA and ERK siRNA. Inhibition of ERK expression resulted in decreased levels of LMW-AR (Fig. 4*D*). This analysis established that ERK activation has a role in the etiology of the LMW-AR forms.

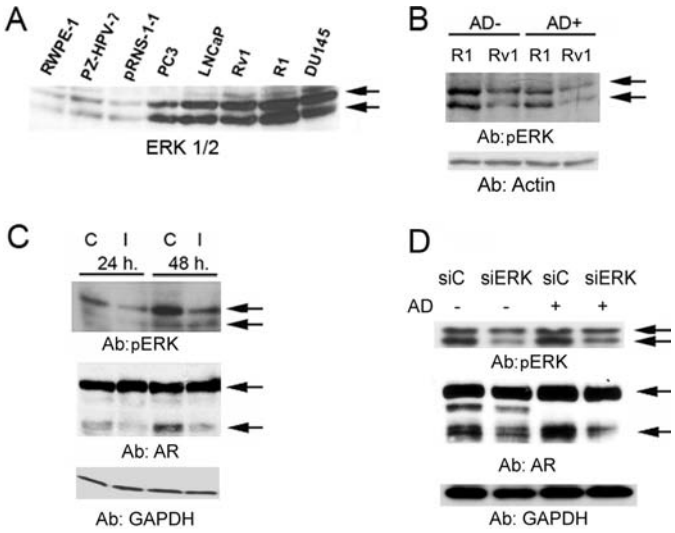

FIGURE 4. **Inhibition of ERK phosphorylation reduces the expression of the LMW-AR.** *A*, Western blot analysis of ERK expression in nontransformed and tumor-derived cell lines. *B*, the pERK levels are higher in R1 than Rv1 cells in the presence or absence of androgen. *C*, R1 cells were treated with 20 μM of the MEK inhibitor U0126 (*I*) or vehicle (*C*) for 24 or 48 h. The *top portion* of the blot shown in the *top panel* was used to detect AR. Inhibition of ERK phosphorylation reduced the expression of the LMW-AR relative to FL-AR by 32% in 24 h and 51% in 48 h. The *arrows* denote the FL and ~80,000 LMW-AR. *D*, ERK-specific siRNA reduced the expression of pERK and the levels of LMW-AR relative to FL-AR to 51.8% in the presence of androgen (*AD*+) and 21% in the absence of androgen (*AD*−). *Ab*, antibody; *si*, small interfering; *siC*, control siRNA.

Because the protein kinase C activator TPA can result in ERK phosphorylation (25), Rv1 and R1 cells were treated with TPA in the absence of androgen for 1 or 2 h to stimulate ERK activity. This treatment promoted an increase in levels of the LMW-AR indicating that activation of this pathway resulted in enhanced AR proteolysis (Fig. 5*A*). TPA treatment of Rv1 cells also resulted in decreased levels of the FL-AR; after a 2-h TPA treatment, the FL-AR was barely discernable, arguing that *in vivo*, as *in vitro*, the Rv1 AR is more sensitive to proteolysis.

To test our hypothesis that an increase in calpain 2 and ERK activity collaborate in promoting LMW-AR expression, we examined calpain 2, calpastatin, and pERK levels in 6 of 13 tumor samples previously analyzed for the expression of the LMW-AR. Three of the thirteen samples that had the highest levels LMW-AR (01, 31, and 94) and three that had low levels of LMW-AR (21, 25, and 28) were used in the analysis (Fig. 5*B*). The expression of LMW-AR was defined as percent of total. Interestingly, the levels of the endogenous calpain inhibitor calpastatin was variable. It was higher in samples 21 and 25, which have lower levels of LMW-AR and lowest in Sample 01. Samples 01 and 31 had high levels of pERK (Fig. 5*C*). The remaining samples had low pERK levels. Therefore, the three samples that had the highest LMW-AR had high levels of pERK or a high amount of calpain 2. Conversely, samples that had low LMW-AR levels had little pERK and elevated calpastatin levels. This limited analysis suggests that in human tumors an increased ratio of calpain to

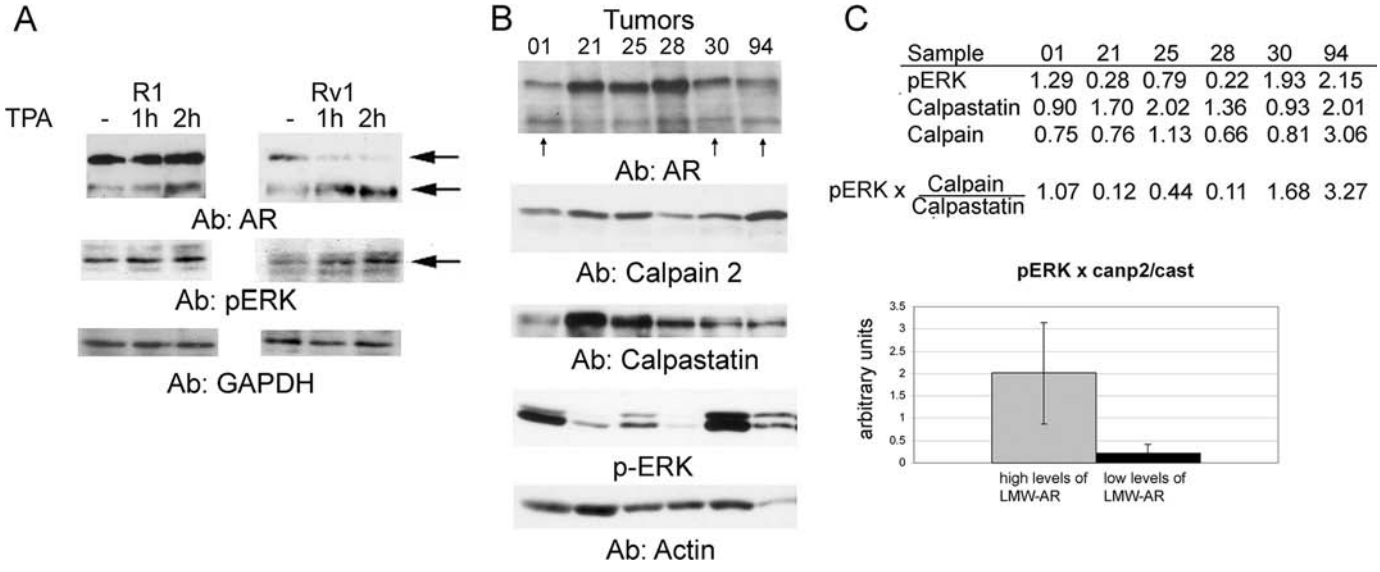

FIGURE 5. **ERK activation and calpain/calpastatin ratios collaborate to promote expression of the LMW-AR.** *A*, treatment of R1 and Rv1 cells with TPA (10 nM) for 1 and 2 h increases the expression of the LMW-AR forms (*top panel*). Control cells were treated with dimethyl sulfoxide. The *bottom panel* shows that TPA treatment increases pERK levels. *Arrows* denote the full length and LMW AR or pERK. *B*, higher calpain/calpastatin and pERK levels together correlate with higher expression of LMW-AR in tumor samples. *Arrows* denote tumors with highest percent of LMW AR. *C*, quantitation of the protein levels in *B*. The calpain/calpastatin ratios multiplied by levels of pERK were calculated for tumors that express high levels of LMW-AR (01, 30, and 94) and samples that had low levels of LMW-AR (21, 25, 28). The average calpain/calpastatin × pERK levels are significantly higher in samples with elevated levels of LMW-AR. *Error bars* represent S.D. $p < 0.05$. *canp2*, calpain 2; *cast*, calpastatin.

calpastatin and increased ERK activity, work in concert contribute to increased LMW-AR expression.

DISCUSSION

R1 and Rv1 cell lines were derived from relapsed CWR22 tumors and express the FL-AR as well as LMW-AR forms. However, the FL and LMW-AR forms expressed in Rv1 cells is larger than those in R1 cells due to a 39-amino acid insertional mutation at the junction of the DNA binding domain and hinge region (21). Transient expression of the E3DM-AR cDNA in PC3 cells also results in the expression of slightly larger LMW forms than transfection of the wt AR cDNA. Activation of calpain AR-transfected PC3 extracts indicates that the E3DM-AR is more susceptible to proteolysis than the wt AR. *In vivo* activation of calpain activity through activation of ERK also promotes a more rapid proteolysis of the E3DM-AR. Early studies reported that a serine protease can proteolyze the AR to generate a ~30,000 or ~40,000 fragment containing the LBD (26). More recently, an independent study found that *in vitro*, calpain proteolyzes the AR to smaller amino-terminal fragments; those fragments include an ~75,000 polypeptide (17). Our data suggest that the junction between the DNA binding domain and LBD might be especially sensitive to proteolysis. Therefore, it is not unexpected that the insertion of 39 additional amino acids near this region would alter AR structure and further sensitizes the molecule to calpain proteolysis (27, 28). Unlike Rv1 cells, R1 cells have an AR that is identical to the AR in the parental CWR22 xenograft. Therefore, we postulated that other molecular alterations must account for the increased expression of the LMW-AR. The current study shows that R1 cells express higher levels of calpain 2 and pERK than Rv1 cells. These two features collaborate to elevate calpain activity and promote proteolysis of the AR and FAK. The role of calpain in the degradation of AR is substantiated by the reduction of LMW-AR caused by inhibition of calpain by calpeptin or a decrease of calpain 2 by siRNA. A comparison of R1 and Rv1 cells indicated that R1 cells had higher levels of ERK and pERK. The participation of ERK in AR proteolysis was demonstrated by an siRNA-mediated decrease of ERK and by the inhibition of ERK phosphorylation by the MEK inhibitor U01286. Therefore, a decrease of ERK levels or ERK activity reduces LMW-AR expression. Activation of ERK by TPA in Rv1 and R1 cells results in a time-dependent increase in the generation of LMW-AR. The short interval required for increased LMW-AR generation is consistent with activation of a signaling cascade that results in the activation of a protease. The MAPK phosphorylation cascade that leads to ERK activation has been well studied and is considered a target for cancer therapeutics (29). Since ERK activation in prostate tumors has been previously reported (30), this is a potential mechanism that could contribute to the expression of LMW-AR in human tumors. Likewise, increased calpain 2 expression has been observed in prostate tumors. Because the activity of calpain 2 is partly regulated by calpastatin, the ratio of calpain/calpastatin affects calpain 2 activity. The expression of calpastatin has not been previously studied in prostate tumors. However, an increase in the calpain/calpastatin ratio has been reported in a study of colorectal cancer (31), which showed that calpastatin levels are high in normal mucosa but decreased in tumor tissue. Moreover, increased expression of calpain 2 was detected in colorectal tumors and polyps, suggesting that the increase of calpain 2 levels may be an early event in the tumorigenesis process. At this point, we cannot rule out that calpain 1 contributes to the generation of the LMW-AR. Interestingly, calpain 1 has been shown to activate ERK (32), and, therefore, all of these molecules may be components of a regulatory pathway. The importance of the calpain/calpastatin equilibrium and the activation of the MAPK signaling pathway in prostate tumorigenesis remain to be defined.

Recent studies reported that the LMW-AR forms expressed in Rv1 cells are derived from an alternatively spliced AR mRNA (33–35). However, the studies do not agree on the identity of the spliced forms that give rise to the LMW-AR forms. Our analysis shows that several LMW-AR forms are expressed in Rv1 and R1 cells. Because we did not completely eliminate the expression of the LMW-AR by inhibiting calpain 2 and pERK, some of the LMW-AR forms could be derived from alternatively spliced AR mRNA. This is analogous to results obtained from studies of cyclin E. In transformed cells, several LMW cyclin E forms can be detected (36). Studies have shown that some of the LMW cyclin E forms are derived from alternatively spliced mRNAs, whereas others are generated by proteolysis of cyclin E protein (22, 37–39). The LMW cyclin E forms have altered cellular localization and are associated with higher kinase activity (40, 41). We agree with the interpretation of Guo *et al.* (35) that several mechanisms can be employed to generate LMW-AR forms. These LMW-AR forms may not be identical, but they would share critical features including the presence of the activation and DNA binding domains and a deletion of the LBD. Such AR molecules would be able to translocate into the nucleus in an androgen-independent manner, bind to DNA, and activate or repress gene transcription. Furthermore, the interaction of the LMW-AR and FL-AR with various AR-interacting proteins may differ, and, therefore, if the LMW-AR and the FL-AR bind to identical DNA sequences, they may have differential effects on gene transcription.

Multiple calpain substrates have been previously implicated in cellular transformation. This suggests that an alteration of the calpain/calpastatin equilibrium, which is observed in some tumors, would affect multiple pathways that drive tumor progression. The modulation of calpain activity could result in a constellation of changes that would be difficult to ascribe to any individual molecule. This feature of calpain-driven deregulation of cell physiology also provides a therapeutic opportunity. The inhibition of calpain activity, even partially, could be sufficient to modify multiple tumor survival and proliferative pathways, which, in synergy with other therapeutics, could be effective in halting tumor progression.

Acknowledgments—We thank Dr. Elizabeth Wilson for the CWR-R1 cells, Dr. Clifford Tepper for the E3DM-AR expression plasmid, and Dr. Hau Nguyen for critical reading of the manuscript. This work was conducted in a facility constructed with support from Research Facilities Improvement Program Grant C06 RR-12088-01 from the National Center for Research Resources, National Institutes of Health.

REFERENCES

1. Chen, C. D., Welsbie, D. S., Tran, C., Baek, S. H., Chen, R., Vessella, R., Rosenfeld, M. G., and Sawyers, C. L. (2004) *Nat. Med.* **10,** 33–39
2. Gregory, C. W., He, B., Johnson, R. T., Ford, O. H., Mohler, J. L., French, F. S., and Wilson, E. M. (2001) *Cancer Res.* **61,** 4315–4319
3. Gregory, C. W., Kim, D., Ye, P., D'Ercole, A. J., Pretlow, T. G., Mohler, J. L., and French, F. S. (1999) *Endocrinology* **140,** 2372–2381
4. Ruizeveld de Winter, J. A., Trapman, J., Vermey, M., Mulder, E., Zegers, N. D., and van der Kwast, T. H. (1991) *J Histochem. Cytochem.* **39,** 927–936
5. Xia, L., Robinson, D., Ma, A. H., Chen, H. C., Wu, F., Qiu, Y., and Kung, H. J. (2002) *J. Biol. Chem.* **277,** 35422–35433
6. Shang, Y., Myers, M., and Brown, M. (2002) *Mol. Cell* **9,** 601–610
7. Berrevoets, C. A., Umar, A., and Brinkmann, A. O. (2002) *Mol. Cell. Endocrinol.* **198,** 97–103
8. Louie, M. C., Yang, H. Q., Ma, A. H., Xu, W., Zou, J. X., Kung, H. J., and Chen, H. W. (2003) *Proc. Natl. Acad. Sci. U.S.A.* **100,** 2226–2230
9. Visakorpi, T., Hyytinen, E., Koivisto, P., Tanner, M., Keinänen, R., Palmberg, C., Palotie, A., Tammela, T., Isola, J., and Kallioniemi, O. P. (1995) *Nat. Genet.* **9,** 401–406
10. Linja, M. J., Savinainen, K. J., Saramäki, O. R., Tammela, T. L., Vessella, R. L., and Visakorpi, T. (2001) *Cancer Res.* **61,** 3550–3555
11. Marcelli, M., Ittmann, M., Mariani, S., Sutherland, R., Nigam, R., Murthy, L., Zhao, Y., DiConcini, D., Puxeddu, E., Esen, A., Eastham, J., Weigel, N. L., and Lamb, D. J. (2000) *Cancer Res.* **60,** 944–949
12. Tilley, W. D., Buchanan, G., Hickey, T. E., and Bentel, J. M. (1996) *Clin. Cancer Res.* **2,** 277–285
13. Taplin, M. E., and Balk, S. P. (2004) *J. Cell Biochem.* **91,** 483–490
14. Tan, J., Sharief, Y., Hamil, K. G., Gregory, C. W., Zang, D. Y., Sar, M., Gumerlock, P. H., deVere, White, R. W., Pretlow, T. G., Harris, S. E., Wilson, E. M., Mohler, J. L., and French, F. S. (1997) *Mol. Endocrinol.* **11,** 450–459
15. Jenster, G., van der Korput, H. A., van Vroonhoven, C., van der Kwast, T. H., Trapman, J., and Brinkmann, A. O. (1991) *Mol. Endocrinol.* **5,** 1396–1404
16. Céraline, J., Cruchant, M. D., Erdmann, E., Erbs, P., Kurtz, J. E., Duclos, B., Jacqmin, D., Chopin, D., and Bergerat, J. P. (2004) *Int. J. Cancer* **108,** 152–157
17. Pelley, R. P., Chinnakannu, K., Murthy, S., Strickland, F. M., Menon, M., Dou, Q. P., Barrack, E. R., and Reddy, G. P. (2006) *Cancer Res.* **66,** 11754–11762
18. Libertini, S. J., Tepper, C. G., Rodriguez, V., Asmuth, D. M., Kung, H. J., and Mudryj, M. (2007) *Cancer Res.* **67,** 9001–9005
19. Yang, H., Murthy, S., Sarkar, F. H., Sheng, S., Reddy, G. P., and Dou, Q. P. (2008) *J. Cell. Physiol.* **217,** 569–576
20. Gregory, C. W., He, B., and Wilson, E. M. (2001) *J. Mol. Endocrinol.* **27,** 309–319
21. Tepper, C. G., Boucher, D. L., Ryan, P. E., Ma, A. H., Xia, L., Lee, L. F., Pretlow, T. G., and Kung, H. J. (2002) *Cancer Res.* **62,** 6606–6614
22. Libertini, S. J., Robinson, B. S., Dhillon, N. K., Glick, D., George, M., Dandekar, S., Gregg, J. P., Sawai, E., and Mudryj, M. (2005) *Cancer Res.* **65,** 10700–10708
23. Zhang, W., Lane, R. D., and Mellgren, R. L. (1996) *J. Biol. Chem.* **271,** 18825–18830
24. Glading, A., Chang, P., Lauffenburger, D. A., and Wells, A. (2000) *J. Biol. Chem.* **275,** 2390–2398
25. Lee, H. W., Ahn, D. H., Crawley, S. C., Li, J. D., Gum, J. R., Jr., Basbaum, C. B., Fan, N. Q., Szymkowski, D. E., Han, S. Y., Lee, B. H., Sleisenger, M. H., and Kim, Y. S. (2002) *J. Biol. Chem.* **277,** 32624–32631
26. de Boer, W., Bolt, J., Kuiper, G. G., Brinkmann, A. O., and Mulder, E. (1987) *J. Steroid Biochem.* **28,** 9–19
27. Goll, D. E., Thompson, V. F., Li, H., Wei, W., and Cong, J. (2003) *Physiol. Rev.* **83,** 731–801
28. Tompa, P., Buzder-Lantos, P., Tantos, A., Farkas, A., Szilágyi, A., Bánóczi, Z., Hudecz, F., and Friedrich, P. (2004) *J. Biol. Chem.* **279,** 20775–20785
29. Roberts, P. J., and Der, C. J. (2007) *Oncogene* **26,** 3291–3310
30. Price, D. T., Della Rocca, G., Guo, C., Ballo, M. S., Schwinn, D. A., and Luttrell, L. M. (1999) *J. Urol.* **162,** 1537–1542
31. Lakshmikuttyamma, A., Selvakumar, P., Kanthan, R., Kanthan, S. C., and Sharma, R. K. (2004) *Cancer Epidemiol. Biomarkers Prev.* **13,** 1604–1609
32. Sawhney, R. S., Cookson, M. M., Omar, Y., Hauser, J., and Brattain, M. G. (2006) *J. Biol. Chem.* **281,** 8497–8510
33. Dehm, S. M., Schmidt, L. J., Heemers, H. V., Vessella, R. L., and Tindall, D. J. (2008) *Cancer Res.* **68,** 5469–5477
34. Hu, R., Dunn, T. A., Wei, S., Isharwal, S., Veltri, R. W., Humphreys, E., Han, M., Partin, A. W., Vessella, R. L., Isaacs, W. B., Bova, G. S., and Luo, J. (2009) *Cancer Res.* **69,** 16–22
35. Guo, Z., Yang, X., Sun, F., Jiang, R., Linn, D. E., Chen, H., Chen, H., Kong, X., Melamed, J., Tepper, C. G., Kung, H. J., Brodie, A. M., Edwards, J., and Qiu, Y. (2009) *Cancer Res.* **69,** 2305–2313
36. Wingate, H., Zhang, N., McGarhen, M. J., Bedrosian, I., Harper, J. W., and Keyomarsi, K. (2005) *J. Biol. Chem.* **280,** 15148–15157
37. Porter, D. C., and Keyomarsi, K. (2000) *Nucleic Acids Res.* **28,** E101
38. Porter, D. C., Zhang, N., Danes, C., McGahren, M. J., Harwell, R. M., Faruki, S., and Keyomarsi, K. (2001) *Mol. Cell. Biol.* **21,** 6254–6269
39. Wang, X. D., Rosales, J. L., Magliocco, A., Gnanakumar, R., and Lee, K. Y. (2003) *Oncogene* **22,** 769–774
40. Bacus, S. S., Gudkov, A. V., Lowe, M., Lyass, L., Yung, Y., Komarov, A. P., Keyomarsi, K., Yarden, Y., and Seger, R. (2001) *Oncogene* **20,** 147–155
41. Delk, N. A., Hunt, K. K., and Keyomarsi, K. (2009) *Cancer Res.* **69,** 2817–2825

Published OnlineFirst June 29, 2010; DOI: 10.1158/0008-5472.CAN-09-4440

Cancer Research

Nrdp1-Mediated Regulation of ErbB3 Expression by the Androgen Receptor in Androgen-Dependent but not Castrate-Resistant Prostate Cancer Cells

Liqun Chen, Salma Siddiqui, Swagata Bose, et al.

Cancer Res 2010;70:5994-6003. Published OnlineFirst June 29, 2010.

Published OnlineFirst June 29, 2010; DOI: 10.1158/0008-5472.CAN-09-4440

Tumor and Stem Cell Biology

Cancer Research

Nrdp1-Mediated Regulation of ErbB3 Expression by the Androgen Receptor in Androgen-Dependent but not Castrate-Resistant Prostate Cancer Cells

Liqun Chen[1,2], Salma Siddiqui[1], Swagata Bose[1,2], Benjamin Mooso[1,2], Alfredo Asuncion[1], Roble G. Bedolla[3], Ruth Vinall[2], Clifford G. Tepper[2], Regina Gandour-Edwards[2], XuBao Shi[2], Xiao-Hua Lu[2], Javed Siddiqui[4], Arul M. Chinnaiyan[4], Rohit Mehra[4], Ralph W. deVere White[2], Kermit L. Carraway III[2], and Paramita M. Ghosh[1,2]

Abstract

Patients with advanced prostate cancer (PCa) are initially susceptible to androgen withdrawal (AW), but ultimately develop resistance to this therapy (castration-resistant PCa, CRPC). Here, we show that AW can promote CRPC development by increasing the levels of the receptor tyrosine kinase ErbB3 in androgen-dependent PCa, resulting in AW-resistant cell cycle progression and increased androgen receptor (AR) transcriptional activity. CRPC cell lines and human PCa tissue overexpressed ErbB3, whereas downregulation of ErbB3 prevented CRPC cell growth. Investigation of the mechanism by which AW augments ErbB3, using normal prostate-derived pRNS-1-1 cells, and androgen-dependent PCa lines LNCaP, PC346C, and CWR22 mouse xenografts, revealed that the AR suppresses ErbB3 protein levels, whereas AW relieves this suppression, showing for the first time the negative regulation of ErbB3 by AR. We show that AR activation promotes ErbB3 degradation in androgen-dependent cells, and that this effect is mediated by AR-dependent transcriptional upregulation of neuregulin receptor degradation protein-1 (Nrdp1), an E3 ubiquitin ligase that targets ErbB3 for degradation but whose role in PCa has not been previously examined. Therefore, AW decreases Nrdp1 expression, promoting ErbB3 protein accumulation, and leading to AR-independent proliferation. However, in CRPC sublines of LNCaP and CWR22, which strongly overexpress the AR, ErbB3 levels remain elevated due to constitutive suppression of Nrdp1, which prevents AR regulation of Nrdp1. Our observations point to a model of CRPC development in which progression of PCa to castration resistance is associated with the inability of AR to transcriptionally regulate Nrdp1, and predict that inhibition of ErbB3 during AW may impair CRPC development. *Cancer Res; 70(14); 5994–6003. ©2010 AACR.*

Introduction

Because prostate cancer (PCa) cells are initially dependent on androgens for growth, the standard therapy for recurrent PCa is the pharmacologic removal of circulating androgens (androgen withdrawal, AW). Although initially effective, this therapy ultimately fails, indicating the development of castration-resistant PCa (CRPC). The treatment options for patients who fail AW therapy are limited; hence, there is an urgent need for the elucidation of molecular pathways leading to CRPC. Previous studies concluded that AW resulted in cell cycle arrest, whereas CRPC is associated with a release from that arrest (1). In this study, we show that AW results in an increase in the receptor tyrosine kinase ErbB3, which induces an increase in androgen receptor (AR) transcriptional activity and cell cycle progression.

The ErbB receptor tyrosine kinase family regulates proliferation and survival in PCa (2). It consists of the type 1 tyrosine kinases ErbB1/human epidermal growth factor receptor (HER)1/epidermal growth factor receptor (EGFR), ErbB2/HER2/neu, ErbB3/HER3, and ErbB4/HER4 (3). PCa cells express EGFR, HER2, and ErbB3, but not ErbB4 (2, 3), which are activated by ligand binding, dimerization, and phosphorylation. ErbB receptors, except HER2, have specific ligands (4); however, ErbB3 is unique in that its tyrosine kinase domain is functionally defective so it must heterodimerize with other ErbB receptors for signaling activity (4). Despite this, multiple studies suggested that ErbB3 plays a role in promoting PCa. Treatment of androgen-dependent LNCaP cells with the cytokine interleukin-6,

Authors' Affiliations: [1]VA Northern California Health Care System, Mather, California; [2]University of California Davis, School of Medicine, Sacramento, California; [3]University of Texas Health Science Center at San Antonio, San Antonio, Texas; and [4]Michigan Center for Translational Pathology, Department of Pathology, University of Michigan Medical School, Ann Arbor, Michigan

Note: Supplementary data for this article are available at Cancer Research Online (http://cancerres.aacrjournals.org/).

Corresponding Author: Paramita M. Ghosh, Department of Urology, University of California Davis School of Medicine, 4860 Y Street, Suite 3500, Sacramento, CA 95817. Phone: 916-843-9336; Fax: 916-364-0306; E-mail: Paramita.Ghosh@ucdmc.ucdavis.edu.

doi: 10.1158/0008-5472.CAN-09-4440

Published OnlineFirst June 29, 2010; DOI: 10.1158/0008-5472.CAN-09-4440

known to promote PCa progression, stimulates HER2 and ErbB3 (5). Phosphatidylinositol 3-kinase, which regulates cell survival by activating Akt, associates with ErbB3 (6), whereas microarray analysis showed increased ErbB3 expression in PCa compared with normal prostate (7), and immunohistochemical analysis showed that ~90% of PCa tissues displayed significant ErbB3 staining (8–10). Alternate splicing caused multiple soluble, truncated forms of ErbB3 (11, 12), and this receptor tyrosine kinase was also shown to localize to the nucleus (8, 13). These studies point to the importance of ErbB3 in PCa signaling.

Substantial evidence also underscores a link between ErbB3 activation and AR activity. The AR is known to remain active in CRPC, and activation of ErbB3 in a mouse model of PCa was associated with AR phosphorylation (10), whereas activation of HER2/ErbB3 heterodimers modulated AR transcriptional activity (14) and promoted AR transactivation of reporter genes (15). The effects of ErbB3 on the AR are likely mediated by suppression of the ErbB3-binding protein Ebp1 (16, 17), which inhibits both E2F1 and AR activity (17).

In this study, we make the novel observation that ErbB3 levels are increased during AW, and that the effect of AR on ErbB3 is mediated by the RING finger E3 ubiquitin ligase neuregulin receptor degradation protein-1 (Nrdp1), which was discovered as an ErbB3-interacting protein by yeast two-hybrid analyses (18), but was not, until now, investigated in PCa. Nrdp1 associates with ErbB3 and mediates its ubiquitination and rapid degradation in a ligand-independent manner (19), thus regulating steady-state levels in breast cancer cells (20). We show that although the AR regulates Nrdp1 transcription in androgen-dependent cells, this regulation is lost in AR-positive CRPC cells due to the suppression of Nrdp1 by elevated ErbB3. Our data explain how ErbB3 levels are increased in CRPC: during AW, AR levels are decreased, and the suppressive effect of the AR on ErbB3 is relieved, resulting in an increase in ErbB3 levels. However, in AR-positive CRPC cells, ErbB3 levels remain high because elevated ErbB3 suppresses Nrdp1 expression and the AR loses control of Nrdp1 transcription; therefore, it cannot suppress ErbB3 levels even when AR levels rebound.

Materials and Methods

Patients and tissues used

Tissue microarrays from the University of Michigan Prostate Cancer Specialized Program of Research Excellence were constructed from benign prostate (n = 36 cores in triplicate, i.e., total 108), high-grade prostatic intraepithelial neoplasia [HGPIN; n = 21 cores in triplicate (63 total)], prostate tumor tissue [n = 65 cores in triplicate (195 total)] obtained by prostatectomy from men with localized PCa, and CRPC metastatic lesions [n = 68 cores in triplicate (204 total)] from "warm" autopsies (mean 3 h lapsed from death to commencement of autopsy) of patients succumbing to castrate-resistant disease (21, 22). Tissue details, immunohistochemical techniques, and statistical analyses were described earlier (23) and in Supplementary Materials.

Cell culture and pharmacologic treatments

LNCaP, PC-3, DU-145, CWR22Rv1, and RWPE-1 cells were purchased from the American Type Culture Collection, whereas C4-2 cells were from UroCor. pRNS-1-1 cells were from Dr. Johng Rhim, University of the Health Sciences, Bethesda, MD (24), whereas PC-346C cells were provided by Dr. W.M. van Weerden, Josephine Nefkens Institute, Erasmus MC, Rotterdam, the Netherlands. All cells were cultivated in RPMI 1640 with 5% serum unless otherwise noted. CRPC sublines of LNCaP cells (LNCaP-AI cells) were developed by prolonged culture of LNCaP cells in phenol red–free RPMI 1640 with 5% charcoal-stripped fetal bovine serum (CSS; ref. 25). The cell lines were not tested or authenticated specifically for this study; however, they have been authenticated elsewhere (24–27). RPMI 1640 and fetal bovine serum (FBS) was from Invitrogen, whereas CSS was from Gemini Bioproducts. 4,5α-Dihydrotestosterone (DHT), cycloheximide, and concanamycin were obtained from Sigma-Aldrich. Casodex (bicalutamide) was from AstraZeneca. Rabbit polyclonal EGFR, HER2, ErbB3, β-actin, AR, and α-tubulin antibodies were from Santa Cruz Biotechnology. Rabbit polyclonal anti–phospho-Akt (Ser 473), anti–phospho-EGFR (Y1068), anti–phospho-HER2 (Y1248), and phospho-ErbB3 (Y1289) were from Cell Signaling Technology. Affinity-purified rabbit antibodies to Nrdp1 were previously described (18).

Transfections, plasmids, and small interfering RNA

Plasmids expressing wtAR or AR(T877A) resulted from cloning, into pCEP4, the full-length wild-type AR cDNA or AR cDNA whose protein product contains a Thr→Ala mutation at the 877 residual position isolated from LNCaP cells (24). pCDNA-HER2 and pCDNA3-ErbB3 plasmids were from Dr. John Koland, University of Iowa, Iowa City, IA (28). Wild-type AR (pAR0) plasmid was from Dr. Albert Brinkman, Erasmus University, the Netherlands (29). Plasmids encoding human Nrdp1 COOH terminally tagged with a FLAG epitope and a pSuper-Nrdp1 RNAI were described earlier (18, 20, 30). Another small interfering RNA (siRNA) pool against human Nrdp1 was from Santa Cruz Biotechnology (against 5′-CAA-GCA-GUA-UCC-CUG-UUC-ATT-3′, 5″-CUG-UGA-CUG-UAG-UUA-GUU-ATT-3′, and 5′-CUU-CCU-CUC-UUC-CUG-UGA-ATT-3′). siRNA against human AR (Invitrogen): hAR1, 5′-GAC-UCC-UUU-GCA-GCC-UUG-CUC-UCU-A-3′ and 5′-UAG-AGA-GCA-AGG-CUG-CAA-AGG-AGU-C-3′; hAR2, 5′-GCC-UUG-CUC-UCU-AGC-CUC-AAU-GAA-C-3′ and 5′-GUU-CAU-UGA-GGC-UAG-AGA-GCA-AGG-C-3′. siRNA against ErbB3 (Santa Cruz Biotechnology): 5′-CCA-AUA-CCA-GAC-ACU-GUA-CTT-3′. Control siRNA: pool of four scrambled nonspecific siRNA (si*CONTROL*, Santa Cruz Biotechnology.). Reverse transcription-PCR (RT-PCR) was carried out using the following primers: c-erbB3-F, 5′-GGA-GTA-CAA-ATT-GCC-AAG-GG-TA-3′; c-ErbB3-R, 5′-CAG-GTC-TGG-CAA-GTA-TGG-AT-3′; EGFR-F, 5′-GAG-AGG-AGA-ACT-GCC-AGA-A-3′; EGFR-R, 5′-GTA-GCA-TTT-ATG-GAG-AGT-G-3′; β-actin-F, 5′-ACT-CTT-CCA-GCC-TTC-GTT-C-3′; β-actin-R, 5′-ATC-TCC-TTC-TGC-ATC-CTG-TC-3′; Nrdp1-F, 5′-GCA-GTG-GAG-TCT-TGG-AGG-AG-3′; Nrdp1-R, 5′-GCC-TTT-AGC-AGC-TGG-ATG-TC-3′.

Published OnlineFirst June 29, 2010; DOI: 10.1158/0008-5472.CAN-09-4440

Mouse studies

Mice (4–5-week-old, *nu/nu* athymic male) were obtained from Harlan Sprague-Dawley, Inc. and implanted s.c. with sustained release testosterone pellets (12.5 mg, 90-d release; Innovative Research of America). Suspensions of CWR22 cells were made in 50% Matrigel solubilized basement membrane (BD Biosciences), and xenografts were established by s.c. injections of 2.5×10^6 cells/site into both flanks. When palpable tumors were observed, animals were treated with (*a*) vehicle or (*b*) bicalutamide, delivered by oral gavage at a dose of 50 mg/Kg, 100 μL per dose, five times per week, dissolved in ethanol, and delivered as a suspension in peanut oil. After 2 weeks, the mice were euthanized, tumors were collected and divided into sections for paraffin embedding, and snap frozen in liquid nitrogen.

For additional methods, see previous publications (31, 32) and Supplementary Text.

Results

Increased expression of ErbB3 in castration-sensitive PCa and CRPC

We stained tissue microarrays representing benign prostates, HGPIN, and localized prostate tumors obtained by prostatectomy, as well as metastatic lesions from warm autopsies of men who died with hormone refractory PCa, with an anti-ErbB3 antibody that recognizes cytoplasmic ErbB3. Only the tumor tissue stained strongly for ErbB3, which was seen exclusively in the epithelial cells (Fig. 1, top). The extent of ErbB3 staining increased from benign prostate (mean staining score, 1.65 ± 0.80) to PIN (1.9 ± 0.61) to localized PCa (2.37 ± 0.63) to metastatic CRPC specimen (2.51 ± 0.74; benign versus localized tumors: $P = 0.0001$; Benign versus CRPC: $P = 0.0001$; PIN versus loc. tumors: $P = 0.0039$; PIN versus CRPC: $P = 0.0005$; Supplementary Table S1; Fig. 1,

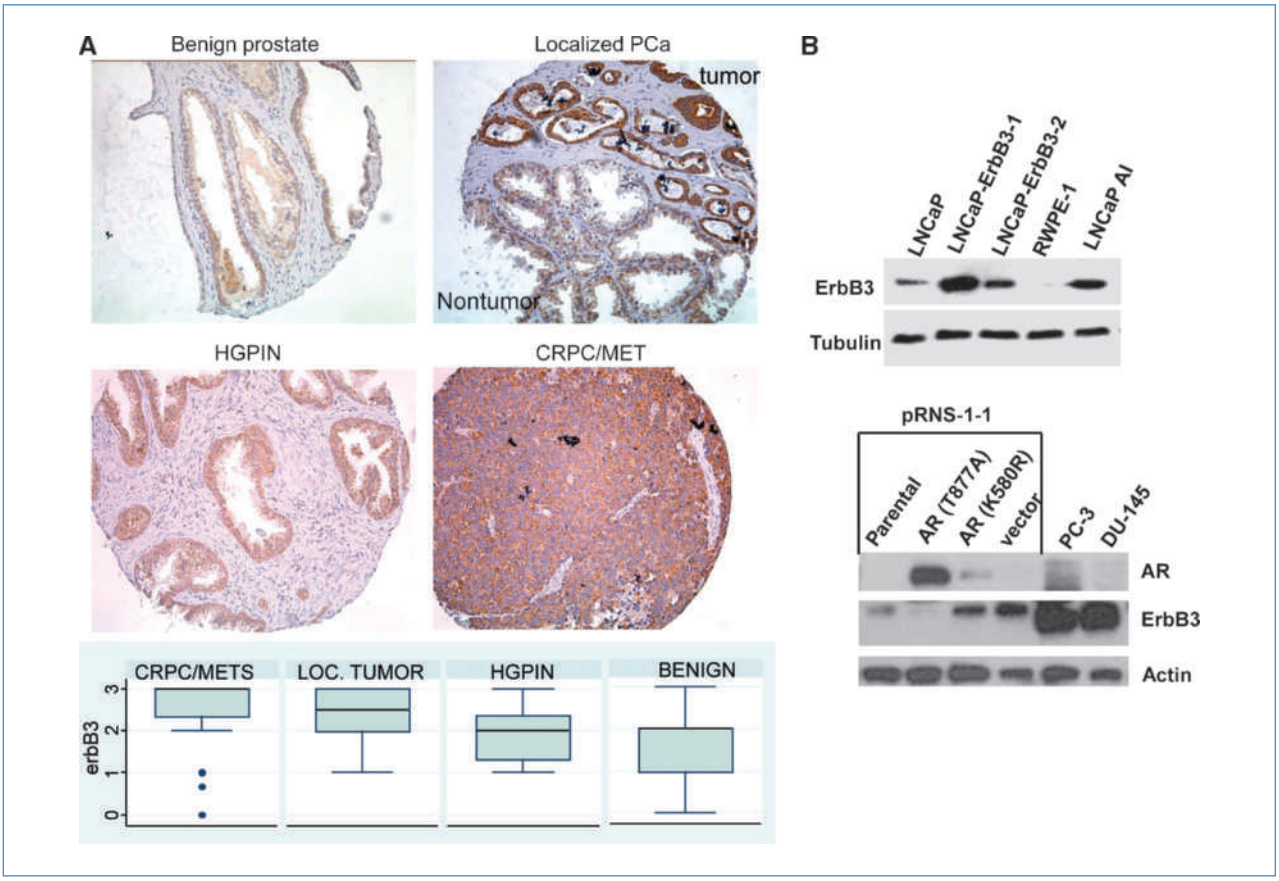

Figure 1. ErbB3 levels increase with PCa progression. A, tissue microarrays representing (*a*) benign prostate ($n = 36$), (*b*) HGPIN ($n = 21$), (*c*) localized tumors ($n = 65$) obtained by prostatectomy, and (*d*) prostatic tissues ($n = 68$; CRPC/MET) from warm autopsies of men who died of CRPC were immunostained with anti-ErbB3 antibody (brown staining) and counterstained with hematoxylin (blue staining). Top, sections stained with anti-ErbB3. Note the strong ErbB3 stain in the tumor containing regions, whereas the benign tissue alongside stained only weakly. The antibody used did not stain the nuclei in these tissues (×20 magnification). Bottom, box plots representing range of ErbB3 expression in benign prostate, HGPIN, localized tumors, and metastatic and localized tissues from warm autopsies of men who died of CRPC. B, increased ErbB3 expression in PCa cells compared with lines derived from normal prostate. Top, normal prostate derived RWPE-1 cells, androgen-dependent LNCaP, and its CRPC subline LNCaP-AI cells compared with stable LNCaP sublines overexpressing ErbB3 (LNCaP-ErbB3-1 and LNCaP-ErbB3-2). Bottom, ErbB3 expression in pRNS-1-1 cells derived from a normal prostate, which upon culture lost the expression of the AR, and AR-null PC-3 and DU-145 cells. pRNS-1-1 cells were transfected with vector only, or mutant AR(T877A) or AR(K580R).

Published OnlineFirst June 29, 2010; DOI: 10.1158/0008-5472.CAN-09-4440

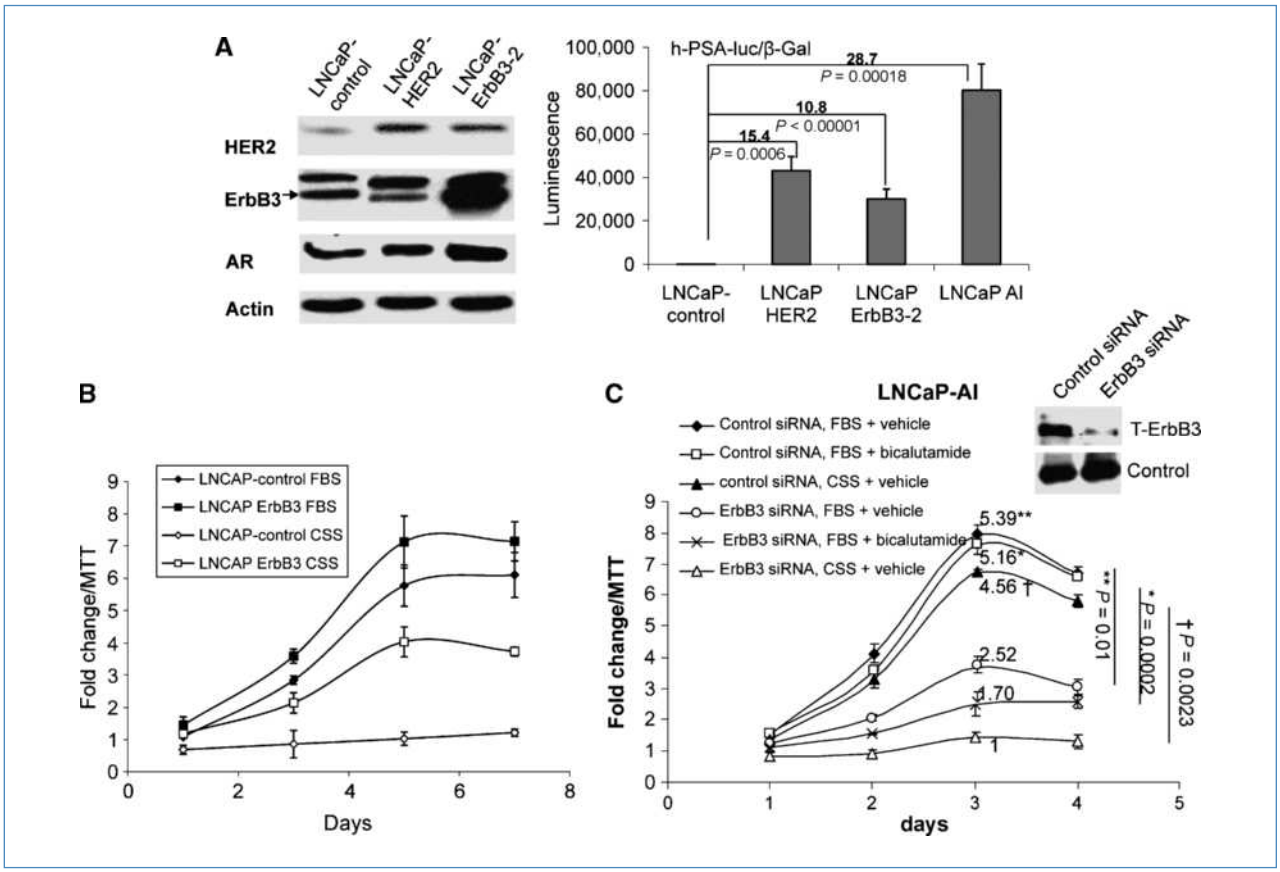

Figure 2. Overexpression of ErbB3 leads to increased AR transcriptional activity and cell proliferation. A, left, increased AR levels in stable LNCaP cell lines overexpressing HER2 or ErbB3 (LNCaP-HER2 and LNCaP-ErbB3) overexpressing plasmids (pcDNA3-HER2 or pcDNA3-ErbB3) in LNCaP cells. Overexpression of HER2 and ErbB3 was confirmed by Western blotting. Right, increased AR transcriptional activity in LNCaP-HER2 and LNCaP-ErbB3 compared with LNCaP. Cells were cultured in CSS-containing medium, and AR transcriptional activity was measured on a prostate-specific antigen promoter by luciferase assay. LNCaP-AI cells were used as positive control. B, ErbB3 overexpression stimulates proliferation in LNCaP cells. MTT assay showed increased growth rates of LNCaP-ErbB3-2 cells versus LNCaP in medium containing FBS versus CSS. Points, mean of three independent readings; bars, SD. C, downregulation of ErbB3 by siRNA suppressed cell growth as estimated through MTT assay in cells cultured in FBS or CSS, in the presence or absence of 10 μmol/L bicalutamide. Points, mean of three independent readings; bars, SD. Inset, immunoblot showing ErbB3 downregulation by siRNA.

bottom). Similarly, comparison of ErbB3 levels in various prostate-derived cell lines revealed that "normal-like" RWPE-1 cells expressed very little ErbB3, whereas its expression was significantly higher in androgen-dependent LNCaP PCa cells and further increased in its castration-resistant subline LNCaP-AI (see Supplementary Fig. S1A and B; Fig. 1A, top). Similarly, CRPC cell lines PC-3 and DU-145 cells expressed very high levels of ErbB3 compared with pRNS-1-1 cells derived from a normal prostate (Fig. 1A, bottom), supporting the assertion that ErbB3 increased with PCa progression.

Overexpression of ErbB3 increased AR transcriptional activity and cell proliferation

To determine the functional significance of ErbB3 increase, LNCaP cells were stably transfected with plasmids encoding ErbB3 (pCDNA3-ErbB3) or HER2 (pCDNA3-HER2; Fig. 2A). The overexpressors used in subsequent experiments were chosen from a screen of multiple clones to select the ones that expressed HER2 and ErbB3 at levels comparable with that in LNCaP-AI cells (two ErbB3 clones shown in Fig. 1B). Overexpression of ErbB3 in LNCaP cells increased AR expression and AR transcriptional activity as determined by reporter gene assay on a prostate-specific antigen promoter construct (Fig. 1B) in an EGFR- and HER2-dependent manner (Supplementary Fig. S1C).

AW in LNCaP cells was induced by culture in CSS-containing medium, causing growth arrest, which was relieved by ErbB3 overexpression, (Supplementary Fig. S2B; Fig. 2A) similar to HER2 (Supplementary Fig. S2A), whereas inhibition of ErbB3 using a human ErbB3 siRNA pool in LNCaP-AI cells significantly decreased their growth rates (Fig. 2C). Overexpression of ErbB3 in normal-like RWPE-1 cells also resulted in increased proliferation (data not shown). These results indicate that ErbB3 regulates cell proliferation in PCa cells.

Published OnlineFirst June 29, 2010; DOI: 10.1158/0008-5472.CAN-09-4440

AW induces ErbB3 increase in androgen-dependent PCa by preventing ErbB3 degradation

We next investigated the cause for ErbB3 increase in PCa cells with a history of AW exposure. Prolonged culture in CSS-containing medium decreased AR expression, but increased ErbB3 levels (Fig. 3A, left). To investigate whether this effect was caused by AR downregulation, AR levels were suppressed in LNCaP cells by two different RNAi, both stimulated ErbB3 levels, although to different extent (Fig. 3A, right). These results indicated that the AR suppresses ErbB3 levels in LNCaP cells, likely to prevent AR-independent cell signaling, whereas AW relieves this suppression.

Similarly, transfection with increasing amounts of wild-type AR (pAR0) in pRNS-1-1, a cell line derived from benign prostate tissue that had lost the expression of its endogenous AR, decreased ErbB3 levels, but not EGFR (Fig. 3B). Stable transfection with AR(T877A) (a mutant AR found in LNCaP cells, which remains ligand dependent), but not the vector alone, also downregulated ErbB3 levels in pRNS-1-1 cells (Fig. 3C, left). DHT, a strong AR ligand, suppressed ErbB3 in pRNS-1-1/AR(T877A), whereas prolonged culture in CSS-containing medium upregulated ErbB3 (Fig. 3C, right). These results show that the AR is a negative regulator of ErbB3 expression in normal prostate also.

Our data indicated that the AR regulated ErbB3 levels by a posttranscriptional, rather than a transcriptional mechanism (Supplementary Fig. S3). To determine whether AR affected ErbB3 degradation, pRNS-1-1 cells transfected with vector alone or with wtAR (Fig. 3D) were treated with the protein synthesis inhibitor cycloheximide, and the rate of ErbB3

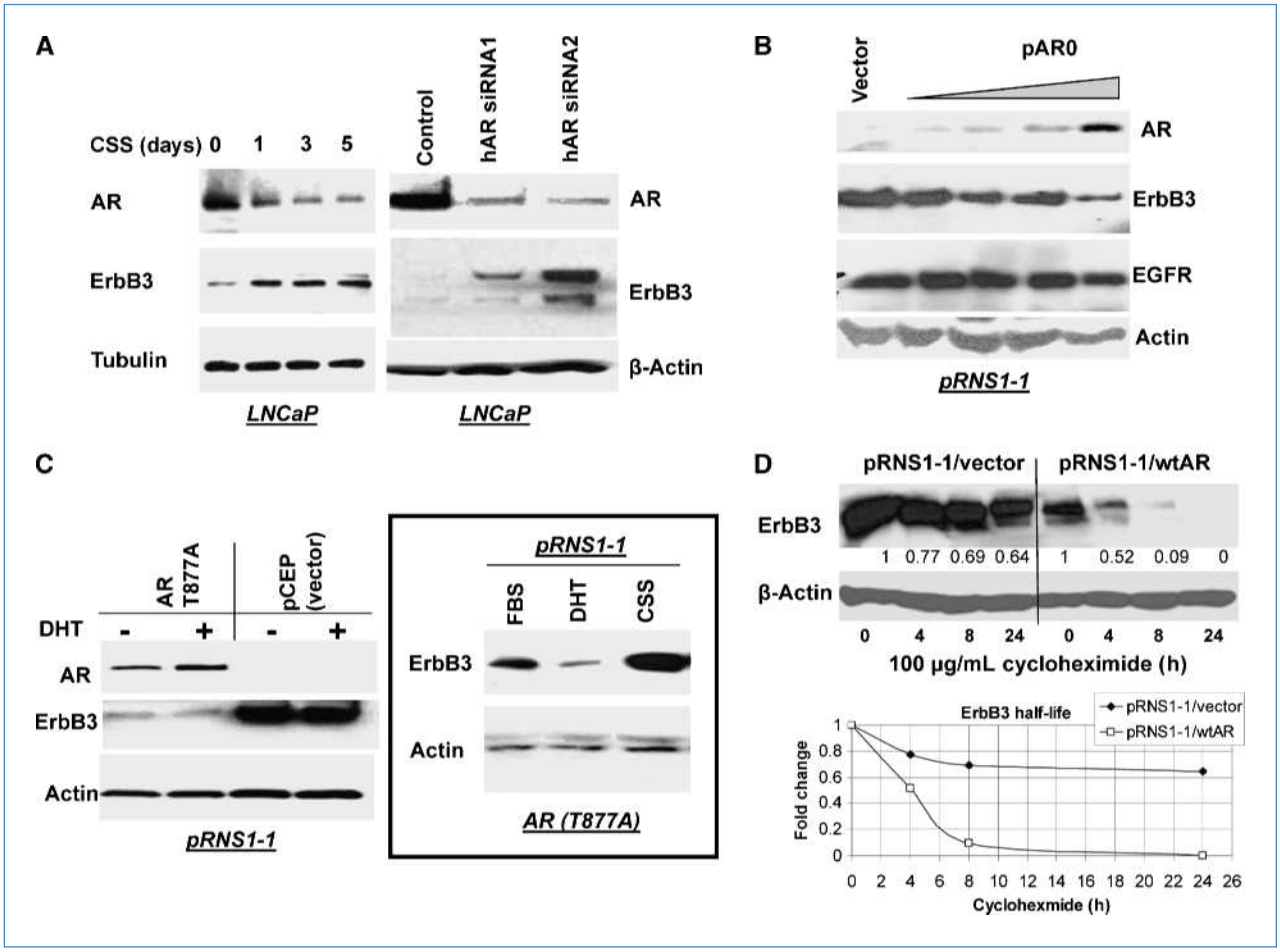

Figure 3. AR negatively regulates ErbB3 expression in androgen-dependent PCa cells. A, left, increased ErbB3 expression with decreasing AR levels in LNCaP cells cultured in CSS-containing medium over a period of 5 d. Right, stimulation of ErbB3 expression in LNCaP cells following AR downregulation with two different AR siRNA duplexes (hAR1 and hAR2). B, increasing AR levels in parental AR-null pRNS1-1 cells transfected with vector alone or with increasing amounts of pAR0 revealed decreasing ErbB3 expression, whereas EGFR levels were not altered. C, expression of AR(T877A) but not vector alone in pRNS1-1 cells caused increased expression of ErbB3. Inset, treatment of pRNS-1-1 cells stably expressing AR(T877A) with 10 nmol/L DHT suppressed ErbB3 levels, whereas 5-d culture in CSS-containing medium stimulated ErbB3. D, decreased ErbB3 half-life upon expression of wild-type AR. pRNS1-1 cells stably transfected with vector only or wtAR were treated with 100 μg/mL cycloheximide for the indicated times. Top, lysates were blotted with anti-ErbB3 or β-actin, and the bands were quantitated. Bottom, ErbB3 half-life was calculated by fitting the data to a single exponential. Results indicate that in pRNS-1-1 cells expressing vector alone, ErbB3 levels were stabilized, whereas in those expressing wtAR, ErbB3 half-life was ~4 h.

Published OnlineFirst June 29, 2010; DOI: 10.1158/0008-5472.CAN-09-4440

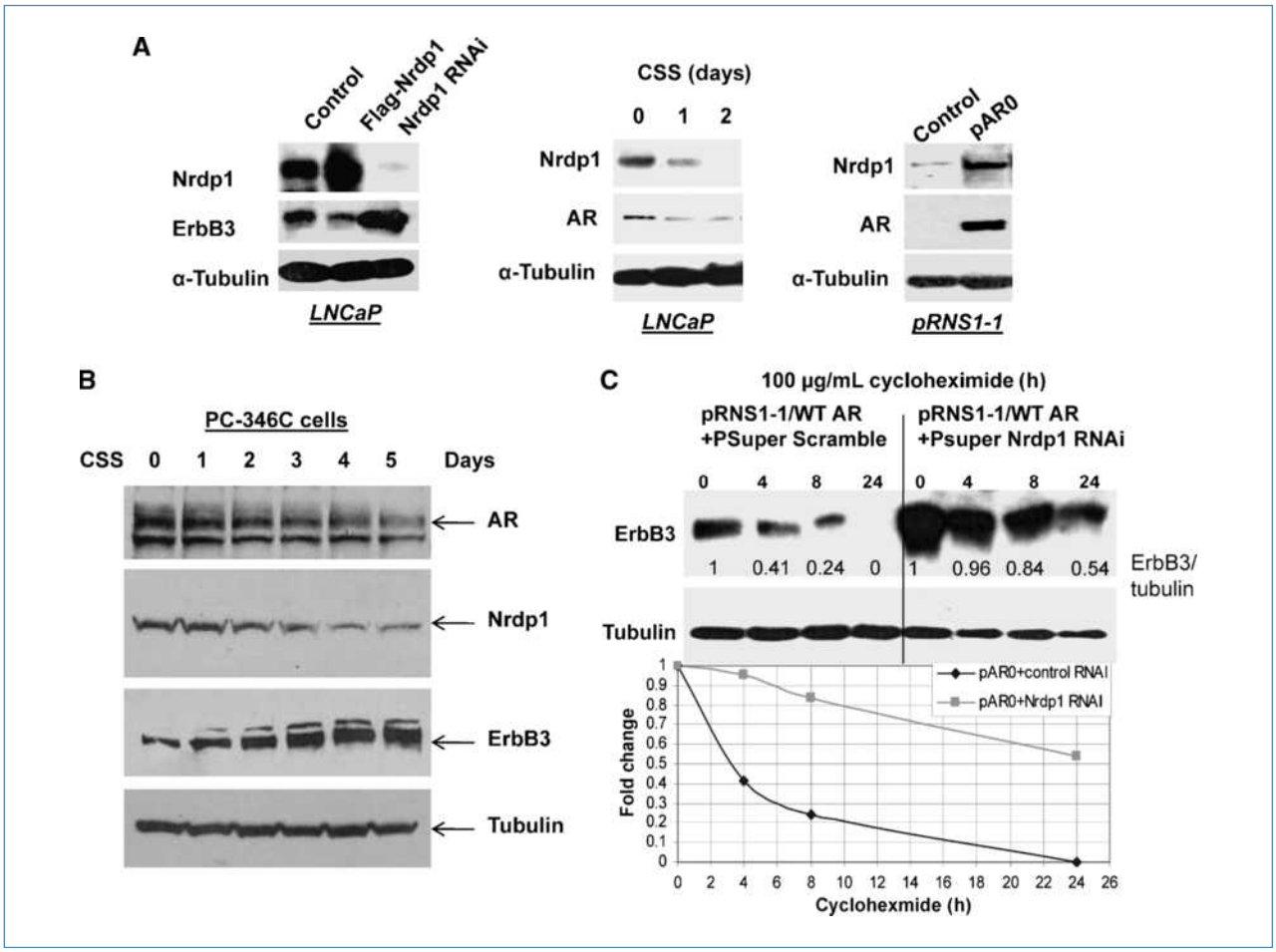

Figure 4. Negative regulation of ErbB3 by AR is mediated by Nrdp1. A, left, expression of the ubiquitin E3 ligase Nrdp1 corresponds to a decrease in ErbB3 expression. LNCaP cells were transiently transfected with plasmids encoding Flag vector, Flag-Nrdp1, or pSuper-Nrdp1 short hairpin RNA for 48 h, after which the lysate was collected and blotted with anti-Nrdp1, anti-ErbB3, or α-Tubulin as control. Middle, Nrdp1 levels correspond to AR expression. Culture of LNCaP cells over 2 d in CSS shows a decrease in Nrdp1 with lower AR. Right, expression of AR in pRNS-1-1 cells stimulates Nrdp1. Parental pRNS1-1 cells were transiently transfected with vector alone or pAR0. Cell lysate was collected after 48 h and blotted with anti-Nrdp1 and anti-AR. B, the AR positively regulates Nrdp1 and negatively regulates ErbB3 levels in androgen-dependent PC-346C cells. Note the expression of a lower molecular weight AR product in these cells. C, decreased half-life of ErbB3 induced by AR expression is mediated by Nrdp1. pRNS1-1 cells stably transfected with wtAR were further transfected with pSuper-scramble or pSuper-Nrdp1 RNAi plasmids for 24 h. ErbB3 half-life in pRNS-1-1/wtAR cells expressing control RNAi remained <4 h, whereas in the absence of Nrdp1 expression, the half-life of ErbB3 increased to >24 h.

degradation in the absence of *de novo* synthesis was determined over time. In cells transfected with vector alone, inhibition of protein synthesis with cyclohexmide caused a 36% decline in ErbB3 after 24 hours; however, transfection with wtAR greatly reduced ErbB3 half-life (<4 h; Fig. 3D). These results show that the increase in ErbB3 expression in the absence of AR is due to a decrease in protein degradation rates.

Nrdp1 mediates AR-induced ErbB3 degradation in androgen-dependent cells

Previous studies identified the RING finger E3 ubiquitin ligase Nrdp1 as a promoter of ErbB3 degradation in breast cancer (18, 20). Nrdp1 overexpression in LNCaP cells decreased ErbB3 levels (Fig. 4A, left) and decreased cell proliferation (Supplementary Fig. S4A), whereas Nrdp1 downregulation (19, 20) increased ErbB3 (Fig. 4A, left), indicating an inverse relationship between ErbB3 and Nrdp1 in PCa as well. Hence, we hypothesized that the effect of AR on ErbB3 may be mediated by Nrdp1.

Culture in CSS medium decreased Nrdp1 expression, whereas transfection of wtAR into AR-null pRNS-1-1 cells increased Nrdp1 expression (Fig. 4A). We also tested this effect in androgen-dependent PC-346C cells derived from a non-treated human prostate tumor extracted by transurethral resection of the prostate (26, 27). Similar to LNCaP, culture of PC-346C cells in CSS medium decreased AR and Nrdp1, whereas ErbB3 increased (Fig. 4B). These results confirmed that the AR positively regulated Nrdp1 expression in androgen-dependent cells. Hence, we investigated whether the effect of AR on ErbB3 half-life is mediated by Nrdp1. ErbB3 half-life in pRNS-1-1 cells stably expressing wtAR was ~3.5 hours, whereas downregulation of Nrdp1 increased ErbB3

Published OnlineFirst June 29, 2010; DOI: 10.1158/0008-5472.CAN-09-4440

half-life to >24 hours (Fig. 4C). Taken together, these results show that AR-regulated decrease in ErbB3 half-life is mediated by AR-induced Nrdp1 transcription. Thus, during AW, AR levels sharply decline, decreasing Nrdp1 levels, which in turn increased ErbB3 levels.

Regulation of Nrdp1 and ErbB3 expression by the AR is lost in AR and ErbB3-overexpressing CRPC cells

If AR always negatively regulated ErbB3 levels, then as AR increased during CRPC development, ErbB3 levels should decrease. However, we see that both LNCaP-AI and C4-2, another androgen-independent subline of LNCaP cells (33), expressed higher AR, as well as ErbB3, compared with LNCaP cells (Fig. 5A). Therefore, we compared the effect of AR stimulation on ErbB3 in LNCaP and LNCaP-AI cells. Increasing doses of DHT in LNCaP stimulated AR, as well as Nrdp1 protein and mRNA levels, but suppressed ErbB3 (Fig. 5B, top left). However, in LNCaP-AI cells, DHT did not affect Nrdp1 or ErbB3 levels (Fig. 5B, top right), although AR activity increased (Fig. 5B, bottom). Our results showed that the AR regulates the levels of Nrdp1, and, as a consequence that of ErbB3 expression, in LNCaP cells, but not in LNCaP-AI.

Both LNCaP-AI and C4-2 expressed higher ErbB3 and lower levels of Nrdp1 compared with LNCaP cells. In addition, overexpression of ErbB3 in LNCaP cells also decreased Nrdp1 (Fig. 5C, top). We conclude that ErbB3 overexpression suppressed Nrdp1 by an AR-independent mechanism, which prevented AR-mediated Nrdp1 transcription, underscored by the observation that AR-independent Nrdp1 decrease by short hairpin RNA prevented stimulation by DHT (Fig. 5C, bottom). Thus, despite increased AR, inability

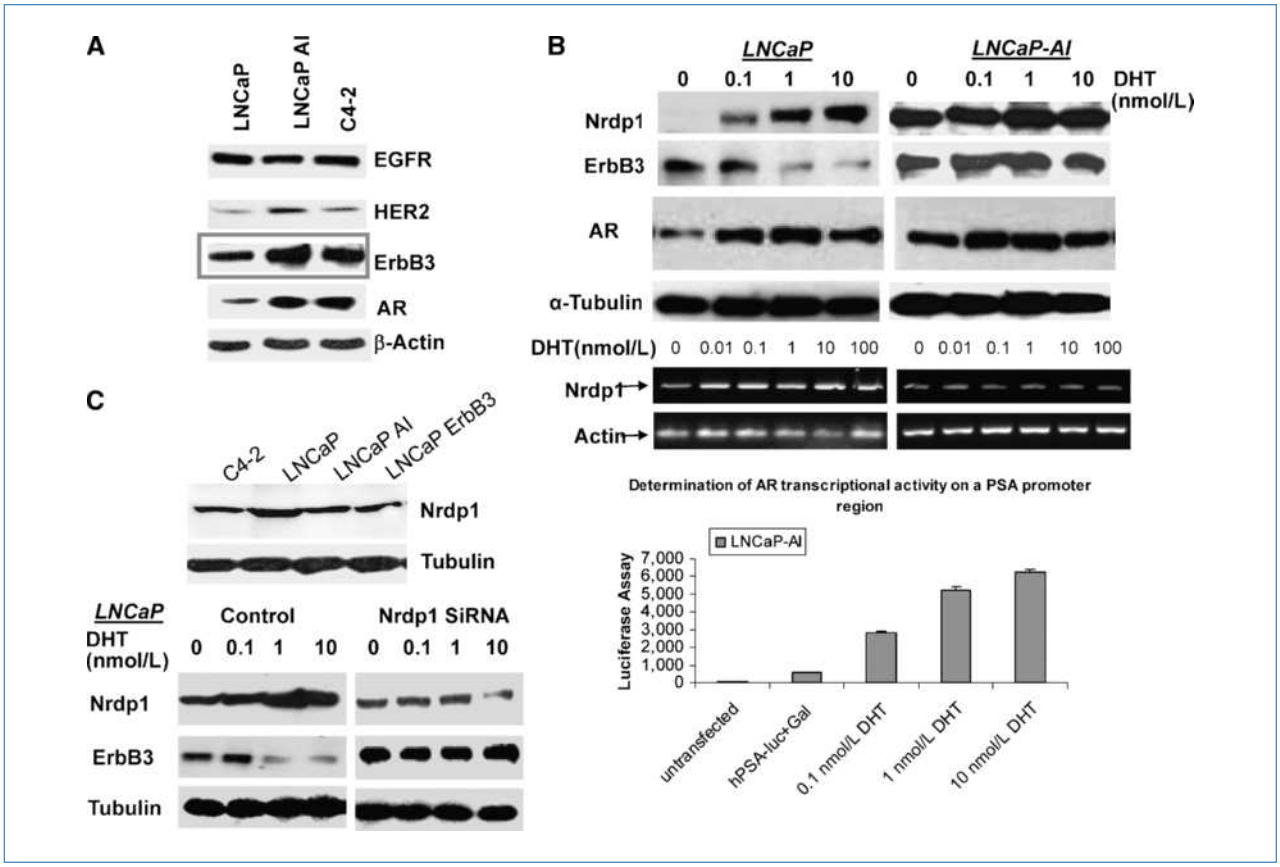

Figure 5. AR regulation of ErbB3 and Nrdp1 is not seen in CRPC cells with high AR transcriptional activity. A, expression of EGFR, HER2, ErbB3, and AR were compared in androgen-dependent LNCaP cells, and its CRPC sublines LNCaP-AI and C4-2 cells by Western blotting, and confirms overexpression of ErbB3 and AR in the CRPC lines. B, stimulation of AR expression with increasing DHT increases Nrdp1 and decreases ErbB3 in LNCaP but not LNCaP-AI. Top, LNCaP and LNCaP AI cells were cultured in CSS-containing medium overnight, then the indicated concentrations of DHT were added for another 48 h. Cell lysates were immunoblotted with anti-ErbB3, anti-Nrdp1, anti-AR, and anti-tubulin antibodies. Middle, AR increases Nrdp1 transcription in LNCaP but not LNCaP AI cells as determined from mRNA levels by RT-PCR after treatment with increasing doses of DHT. Bottom, this is despite increased AR transcriptional activity on a human prostate-specific antigen (PSA) promoter as determined by luciferase assay upon DHT stimulation in LNCaP-AI cells. C, AR fails to regulate Nrdp1 and ErbB3 levels in CRPC cells due to decreased Nrdp1 levels caused by ErbB3 overexpression. Top, suppression of Nrdp1 expression in LNCaP AI, C4-2, and LNCaP-ErbB3 cells compared with LNCaP. Cells were cultured in FBS medium up to 75% confluence and collected for Western blotting. Bottom, DHT-induced suppression of ErbB3 levels in LNCaP cells is mediated by high levels of Nrdp1. This effect was not seen when LNCaP cells were transfected with Nrdp1 siRNA (in CSS) for 24 h, followed by DHT treatment for another 48 h. Cell lysate was collected and blotted with anti-ErbB3 and anti-Nrdp1.

Published OnlineFirst June 29, 2010; DOI: 10.1158/0008-5472.CAN-09-4440

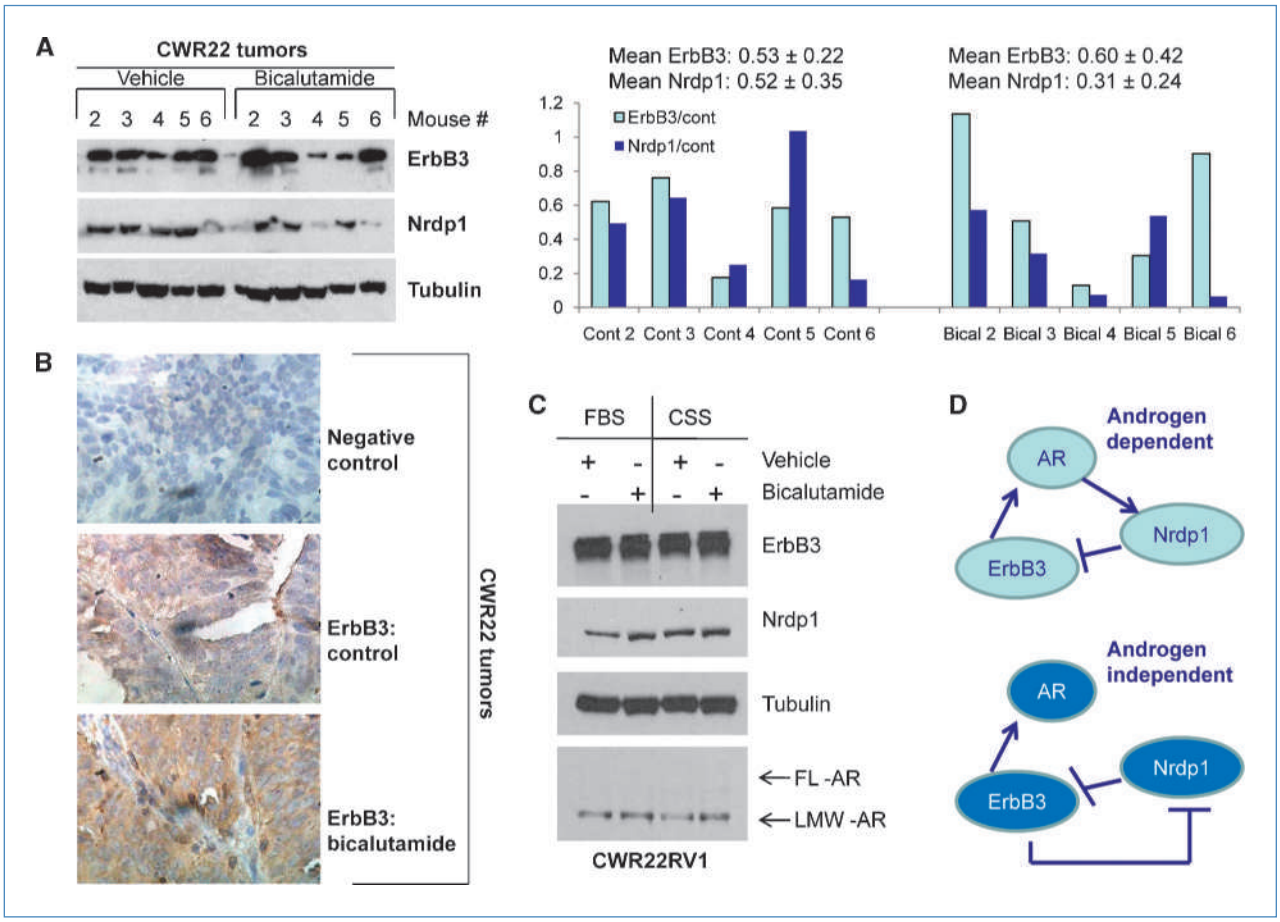

Figure 6. Effect of AR activity on ErbB3 and Nrdp1 expression seen in castration-sensitive CWR22 tumors but not in CRPC cell lines derived from recurrent tumors from castrated mice. A and B, CWR22 xenograft tumors were established by s.c. injections of cell suspensions (2.5×10^6 cells in Matrigel; 1:1, v/v) bilaterally into the flanks of 4- to 5-wk-old *nu/nu* athymic male mice ($n = 10$) previously implanted with sustained release testosterone pellets. When palpable tumors were observed, animals were treated with (*a*) vehicle (peanut oil) or (*b*) the AR antagonist bicalutamide ($n = 5$/group). After 2 wk on this treatment, the mice were euthanized, and tumors were harvested and divided into sections that were paraffin embedded and snap frozen in liquid nitrogen. Paraffin-embedded tumors were analyzed by immunohistochemistry for ErbB3, whereas frozen tumors were excised and lysed, and protein levels were determined by Western blotting. A, Western blotting revealed that ErbB3 levels increased whereas Nrdp1 levels decreased with bicalutamide treatment. B, immunohistochemistry showing that ErbB3 levels increased in tumors extracted from the bicalutamide-fed mice. Brown staining, ErbB3; blue staining, counterstaining with hematoxylin. Negative control showed no ErbB3 staining; the xenograft from the vehicle-fed mouse showed lower ErbB3 expression (scored +1) compared with the bicalutamide-treated one (scored +3). C, in contrast, CWR22Rv1, a CRPC cell line derived from a CWR22-relapsed tumor grown in a castrated mouse, failed to respond to bicalutamide, and in these cells, Nrdp1 and ErbB3 were not androgen regulated. D, scheme describing androgen regulation of Nrdp1 transcription in androgen-dependent but not androgen-independent cells.

of AR to regulate Nrdp1 prolonged ErbB3 half-life in LNCaP-AI (Supplementary Fig. S4B).

Androgen regulation of ErbB3 and Nrdp1 in androgen-dependent CWR22 tumors but not in CRPC CWR22-Rv1 cells

We also tested the effect of AR on Nrdp1 and ErbB3 in androgen-dependent CWR22 tumors in nude mice (34) and in CRPC CWR22Rv1 cells, derived from a relapsed CWR22 tumor (35). CWR22 xenograft tumors were cultivated in the flanks of athymic *nu/nu* mice treated with vehicle or 50 mg/kg bicalutamide (an AR antagonist). Bicalutamide did not affect AR expression but severely decreased AR transcriptional activity in androgen-sensitive cells (32, 36). After 2 weeks, the mice were euthanized and the tumors were extracted, part was paraffin-embedded, and the rest were frozen. ErbB3 levels determined by Western blot (Fig. 6A) reflected only the epithelial cells, as immunohistochemical studies revealed ErbB3 staining only in epithelial cells (Fig. 6B) and showed higher ErbB3 in bicalutamide-treated animals both by immunoblotting and immunohistochemistry, whereas Nrdp1 levels were significantly suppressed. These results indicate that ErbB3 and Nrdp1 levels were regulated by AR in CWR22 tumors as well. However, in CRPC CWR22Rv1 cells, which express very low levels of Nrdp1 (Supplementary Fig. S3C), neither bicalutamide nor culture in CSS medium affected either Nrdp1 or ErbB3 (Fig. 6C). These results show that, similar

Published OnlineFirst June 29, 2010; DOI: 10.1158/0008-5472.CAN-09-4440

to LNCaP and PC-346C cells, AR regulates Nrdp1 and ErbB3 in androgen-dependent CWR22 PCa cells but not in its CRPC subline CWR22Rv1.

Discussion

Men who undergo AW therapy are known to become refractory to this therapy, although investigators continue to debate the causes leading to the development of castration resistance. The present study identifies ErbB3 as a likely mediator of increased proliferation during CRPC development, which releases cells from cell cycle arrest imposed by AW therapy, because increased ErbB3 resulted in enhanced proliferation both in the presence and the absence of androgens. We show that ErbB3 is increased during AW, and that this is caused by a novel mechanism involving the negative regulation of ErbB3 by the AR. In androgen-dependent cells, AR suppresses ErbB3, likely because although the AR promotes androgen-dependent cell cycle progression, it also resists the activation of androgen-independent pathways that promote cell growth. AW therapy relieves this suppression, thereby elevating ErbB3 levels, which stimulate proliferation and likely promote resistance to this therapy. Our data identifies the inability of the AR to suppress ErbB3 expression as one cause of CRPC.

The case for ErbB3 as a mediator of cell cycle release is strengthened by previous studies emphasizing the importance of HER2 in the development of castration resistance (37–45) and by the identification of ErbB3, rather than EGFR, as a major binding partner for HER2 in PCa (5, 14, 15). Reports described transcriptional as well as posttranslational increase of HER2 during AW (46); hence, the major binding partner of HER2 in CRPC would also be expected to increase. Our study shows that the AR regulates ErbB3 levels in PCa by promoting its degradation, whereas during AW, ErbB3 levels are increased due to decreased degradation.

We show that the AR promotes ErbB3 degradation by regulating Nrdp1 transcription. Importantly, we show that the AR transcriptionally regulates Nrdp1 expression in androgen-dependent but not in CRPC cells. Nrdp1 was originally identified as a RING finger domain–containing protein that interacts with ErbB3 (18, 47), binding to the cytoplasmic tail of ErbB3, and promoting its degradation by mediating ligand-independent ubiquitination. Nrdp1 was expressed in multiple androgen-regulated tissues including prostate, testicles (47), and skeletal muscles (18). Our data showed an inverse relationship between ErbB3 and Nrdp1 in androgen-dependent PCa cells. Nrdp1 promotes ErbB3 degradation (19, 47), and we show that it mediates AR regulation of ErbB3 half-life. These results indicate for the first time that Nrdp1 is a transcriptional target of the AR.

We also show that AR regulation of Nrdp1 and ErbB3 is lost in CRPC cells, thereby maintaining elevated ErbB3 in CRPC cells despite high AR activity. Our data show that ErbB3 overexpression suppressed Nrdp1 levels and likely prevented AR regulation of Nrdp1 transcription. This indicates androgen-dependent regulation of Nrdp1 in cells with high Nrdp1 and low ErbB3, and androgen independence of Nrdp1 transcription in cells expressing high ErbB3 and low Nrdp1. Therefore, our data explain why intermittent AW therapy, in which the effects of AW on ErbB3 may be reversed during frequent "off-cycle" phases, while Nrdp1 transcription is still AR regulated, may prolong androgen dependence (48), and indicates Nrdp1 regulation by AR as a hallmark of androgen-sensitive cell growth.

In summary, this study shows that induction of ErbB3 occurs as a result of AR inactivation during AW. However, even after AR levels rebound, ErbB3 remains elevated, eventually promoting castration-resistant proliferation of PCa cells. We show that Nrdp1 mediates the regulation of ErbB3 levels by the AR in androgen-dependent cells and is itself transcriptionally regulated by the AR, whereas this regulation is lost in AR-positive CRPC cells, likely due to high ErbB3 levels caused by AW therapy that may have suppressed Nrdp1 levels in an androgen-independent manner (Fig. 6D). These studies point to the importance of ErbB3 in PCa progression and identify it as a possible target of therapy for prevention of CRPC development.

Disclosure of Potential Conflicts of Interest

No potential conflicts of interest were disclosed.

Acknowledgments

We thank Dr. Hsing-Jien Kung, Department of Biochemistry, UC Davis, for critical reading of the manuscript; Dr. Thomas G. Pretlow (Case Western Reserve School of Medicine, Cleveland, OH) for generously providing the CWR22 human prostate tumor xenograft and protocols for its growth; Rebekah Burich, Department of Hematology/Oncology, and Dr. Yu Wang, currently in Cleveland Clinic, Cleveland, OH, for the assistance with certain experiments; AstraZeneca, Cheshire, UK, for the gift of bicalutamide; Dr. John Koland, University of Iowa, Iowa City, IA, for the gift of the pcDNA3-HER2 and pcDNA3-ErbB3 cDNA; and Dr. Albert O. Brinkman, Erasmus University, the Netherlands, for the wild-type AR plasmid (pAR0).

Grant Support

Department of Defense, Idea Development Award PC081177 (P.M. Ghosh) and by Awards CA133209 (P.M. Ghosh), CA123541 (K.L. Carraway), and GM068994 (K.L. Carraway) from the NIH.

The costs of publication of this article were defrayed in part by the payment of page charges. This article must therefore be hereby marked *advertisement* in accordance with 18 U.S.C. Section 1734 solely to indicate this fact.

Received 12/07/2009; revised 04/27/2010; accepted 05/13/2010; published OnlineFirst 06/29/2010.

References

1. Agus DB, Cordon-Cardo C, Fox W, et al. Prostate cancer cell cycle regulators: response to androgen withdrawal and development of androgen independence. J Natl Cancer Inst 1999;91:1869–76.
2. Robinson D, He F, Pretlow T, Kung HJ. A tyrosine kinase profile of prostate carcinoma. Proc Natl Acad Sci U S A 1996;93:5958–62.
3. Grasso AW, Wen D, Miller CM, Rhim JS, Pretlow TG, Kung HJ. ErbB kinases and NDF signaling in human prostate cancer cells. Oncogene 1997;15:2705–16.
4. Olayioye MA, Neve RM, Lane HA, Hynes NE. The ErbB signaling network: receptor heterodimerization in development and cancer. EMBO J 2000;19:3159–67.

Published OnlineFirst June 29, 2010; DOI: 10.1158/0008-5472.CAN-09-4440

5. Qiu Y, Ravi L, Kung HJ. Requirement of ErbB2 for signalling by interleukin-6 in prostate carcinoma cells. Nature 1998;393:83–5.
6. Lin J, Adam RM, Santiestevan E, Freeman MR. The phosphatidylinositol 3′-kinase pathway is a dominant growth factor-activated cell survival pathway in LNCaP human prostate carcinoma cells. Cancer Res 1999;59:2891–7.
7. Chaib H, Cockrell EK, Rubin MA, Macoska JA. Profiling and verification of gene expression patterns in normal and malignant human prostate tissues by cDNA microarray analysis. Neoplasia 2001;3:43–52.
8. Koumakpayi IH, Diallo JS, Le Page C, et al. Expression and nuclear localization of ErbB3 in prostate cancer. Clin Cancer Res 2006;12:2730–7.
9. Lyne JC, Melhem MF, Finley GG, et al. Tissue expression of neu differentiation factor/heregulin and its receptor complex in prostate cancer and its biologic effects on prostate cancer cells *in vitro*. Cancer J Sci Am 1997;3:21–30.
10. Li Z, Szabolcs M, Terwilliger JD, Efstratiadis A. Prostatic intraepithelial neoplasia and adenocarcinoma in mice expressing a probasin-Neu oncogenic transgene. Carcinogenesis 2006;27:1054–67.
11. Srinivasan R, Leverton KE, Sheldon H, Hurst HC, Sarraf C, Gullick WJ. Intracellular expression of the truncated extracellular domain of c-erbB-3/HER3. Cell Signal 2001;13:321–30.
12. Lee H, Akita RW, Sliwkowski MX, Maihle NJ. A naturally occurring secreted human ErbB3 receptor isoform inhibits heregulin-stimulated activation of ErbB2, ErbB3, and ErbB4. Cancer Res 2001;61:4467–73.
13. Koumakpayi IH, Diallo JS, Le Page C, et al. Low nuclear ErbB3 predicts biochemical recurrence in patients with prostate cancer. BJU Int 2007;100:303–9.
14. Mellinghoff IK, Vivanco I, Kwon A, Tran C, Wongvipat J, Sawyers CL. HER2/neu kinase-dependent modulation of androgen receptor function through effects on DNA binding and stability. Cancer Cell 2004;6:517–27.
15. Gregory CW, Whang YE, McCall W, et al. Heregulin-induced activation of HER2 and HER3 increases androgen receptor transactivation and CWR-R1 human recurrent prostate cancer cell growth. Clin Cancer Res 2005;11:1704–12.
16. Zhang Y, Hamburger AW. Specificity and heregulin regulation of Ebp1 (ErbB3 binding protein 1) mediated repression of androgen receptor signalling. Br J Cancer 2005;92:140–6.
17. Zhang Y, Wang XW, Jelovac D, et al. The ErbB3-binding protein Ebp1 suppresses androgen receptor-mediated gene transcription and tumorigenesis of prostate cancer cells. Proc Natl Acad Sci U S A 2005;102:9890–5.
18. Diamonti AJ, Guy PM, Ivanof C, Wong K, Sweeney C, Carraway KL, III. An RBCC protein implicated in maintenance of steady-state neuregulin receptor levels. Proc Natl Acad Sci U S A 2002;99:2866–71.
19. Cao Z, Wu X, Yen L, Sweeney C, Carraway KL III. Neuregulin-induced ErbB3 downregulation is mediated by a protein stability cascade involving the E3 ubiquitin ligase Nrdp1. Mol Cell Biol 2007;27:2180–8.
20. Yen L, Cao Z, Wu X, et al. Loss of Nrdp1 enhances ErbB2/ErbB3-dependent breast tumor cell growth. Cancer Res 2006;66:11279–86.
21. Rubin MA, Putzi M, Mucci N, et al. Rapid ("warm") autopsy study for procurement of metastatic prostate cancer. Clin Cancer Res 2000;6:1038–45.
22. Shah RB, Mehra R, Chinnaiyan AM, et al. Androgen-independent prostate cancer is a heterogeneous group of diseases: lessons from a rapid autopsy program. Cancer Res 2004;64:9209–16.
23. Bedolla RG, Wang Y, Asuncion A, et al. Nuclear versus cytoplasmic localization of filamin A in prostate cancer: immunohistochemical correlation with metastases. Clin Cancer Res 2009;15:788–96.
24. Shi XB, Xue L, Tepper CG, et al. The oncogenic potential of a prostate cancer-derived androgen receptor mutant. Prostate 2007;67:591–602.
25. Mikhailova M, Wang Y, Bedolla R, Lu XH, Kreisberg JI, Ghosh PM. AKT regulates androgen receptor-dependent growth and PSA expression in prostate cancer. Adv Exp Med Biol 2008;617:397–405.
26. van Weerden WM, de Ridder CM, Verdaasdonk CL, et al. Development of seven new human prostate tumor xenograft models and their histopathological characterization. Am J Pathol 1996;149:1055–62.
27. Limpens J, Schroder FH, de Ridder CM, et al. Combined lycopene and vitamin E treatment suppresses the growth of PC-346C human prostate cancer cells in nude mice. J Nutr 2006;136:1287–93.
28. Vijapurkar U, Cheng K, Koland JG. Mutation of a Shc binding site tyrosine residue in ErbB3/HER3 blocks heregulin-dependent activation of mitogen-activated protein kinase. J Biol Chem 1998;273:20996–1002.
29. Brinkmann AO, Blok LJ, de Ruiter PE, et al. Mechanisms of androgen receptor activation and function. J Steroid Biochem Mol Biol 1999;69:307–13.
30. Wu X, Yen L, Irwin L, Sweeney C, Carraway KL III. Stabilization of the E3 ubiquitin ligase Nrdp1 by the deubiquitinating enzyme USP8. Mol Cell Biol 2004;24:7748–57.
31. Ghosh PM, Malik SN, Bedolla RG, et al. Signal transduction pathways in androgen-dependent and -independent prostate cancer cell proliferation. Endocr Relat Cancer 2005;12:119–34.
32. Wang Y, Mikhailova M, Bose S, Pan CX, deVere White RW, Ghosh PM. Regulation of androgen receptor transcriptional activity by rapamycin in prostate cancer cell proliferation and survival. Oncogene 2008;27:7106–17.
33. Hsieh JT, Wu HC, Gleave ME, von Eschenbach AC, Chung LW. Autocrine regulation of prostate-specific antigen gene expression in a human prostatic cancer (LNCaP) subline. Cancer Res 1993;53:2852–7.
34. Nagabhushan M, Miller CM, Pretlow TP, et al. CWR22: the first human prostate cancer xenograft with strongly androgen-dependent and relapsed strains both *in vivo* and in soft agar. Cancer Res 1996;56:3042–6.
35. Tepper CG, Boucher DL, Ryan PE, et al. Characterization of a novel androgen receptor mutation in a relapsed CWR22 prostate cancer xenograft and cell line. Cancer Res 2002;62:6606–14.
36. Wang Y, Kreisberg JI, Bedolla RG, Mikhailova M, deVere White RW, Ghosh PM. A 90 kDa fragment of filamin A promotes Casodex-induced growth inhibition in Casodex-resistant androgen receptor positive C4-2 prostate cancer cells. Oncogene 2007;26:6061–70.
37. Dankort D, Jeyabalan N, Jones N, Dumont DJ, Muller WJ. Multiple ErbB-2/Neu phosphorylation sites mediate transformation through distinct effector proteins. J Biol Chem 2001;276:38921–8.
38. Klapper LN, Waterman H, Sela M, Yarden Y. Tumor-inhibitory antibodies to HER-2/ErbB-2 may act by recruiting c-Cbl and enhancing ubiquitination of HER-2. Cancer Res 2000;60:3384–8.
39. Myers RB, Brown D, Oelschlager DK, et al. Elevated serum levels of p105(erbB-2) in patients with advanced-stage prostatic adenocarcinoma. Int J Cancer 1996;69:398–402.
40. Osman I, Scher HI, Drobnjak M, et al. HER-2/neu (p185neu) protein expression in the natural or treated history of prostate cancer. Clin Cancer Res 2001;7:2643–7.
41. Oxley JD, Winkler MH, Gillatt DA, Peat DS. Her-2/neu oncogene amplification in clinically localised prostate cancer. J Clin Pathol 2002;55:118–20.
42. Signoretti S, Montironi R, Manola J, et al. Her-2-neu expression and progression toward androgen independence in human prostate cancer. J Natl Cancer Inst 2000;92:1918–25.
43. Wen Y, Hu MC, Makino K, et al. HER-2/neu promotes androgen-independent survival and growth of prostate cancer cells through the Akt pathway. Cancer Res 2000;60:6841–5.
44. Yeh S, Lin HK, Kang HY, Thin TH, Lin MF, Chang C. From HER2/Neu signal cascade to androgen receptor and its coactivators: a novel pathway by induction of androgen target genes through MAP kinase in prostate cancer cells. Proc Natl Acad Sci U S A 1999;96:5458–63.
45. Zhou BP, Hu MC, Miller SA, et al. HER-2/neu blocks tumor necrosis factor-induced apoptosis via the Akt/NF- κB pathway. J Biol Chem 2000;275:8027–31.
46. Berger R, Lin DI, Nieto M, et al. Androgen-dependent regulation of Her-2/neu in prostate cancer cells. Cancer Res 2006;66:5723–8.
47. Qiu XB, Goldberg AL. Nrdp1/FLRF is a ubiquitin ligase promoting ubiquitination and degradation of the epidermal growth factor receptor family member, ErbB3. Proc Natl Acad Sci U S A 2002;99:14843–8.
48. Abrahamsson PA. Potential benefits of intermittent androgen suppression therapy in the treatment of prostate cancer: a systematic review of the literature. Eur Urol 57:49–59.

Genes & Cancer
1(9) 927–940

DOI: 10.1177/1947601910385450
http://ganc.sagepub.com
SAGE

Androgen Receptor Regulation of Vitamin D Receptor in Response of Castration-Resistant Prostate Cancer Cells to 1α-Hydroxyvitamin D5: A Calcitriol Analog

Benjamin Mooso[1,2,*], Anisha Madhav[1,*], Sherra Johnson[1,2], Mohana Roy[1,2], Mary E. Moore[1,2], Christabel Moy[1], Grace A. Loredo[1,2], Rajendra G. Mehta[3], Andrew T.M. Vaughan[1,2], and Paramita M. Ghosh[1,2]

Submitted 15-Jul-2010; revised 26-Aug-2010; accepted 31-Aug-2010

Abstract

Calcitriol (1,25(OH)$_2$D3) is cytostatic for prostate cancer (CaP) but had limited therapeutic utility due to hypercalcemia-related toxicities, leading to the development of low-calcemic calcitriol analogs. We show that one analog, 1α-hydroxyvitamin D5 (1α(OH)D5), induced apoptosis in castration-sensitive LNCaP prostate cancer cells but, unlike calcitriol, did not increase androgen receptor (AR) transcriptional activity. LNCaP-AI, a castrate-resistant (CRCaP) LNCaP subline, was resistant to 1α(OH)D5 in the presence of androgens; however, androgen withdrawal (AWD), although ineffective by itself, sensitized LNCaP-AI cells to 1α(OH)D5. Investigation of the mechanism revealed that the vitamin D receptor (VDR), which mediates the effects of 1α(OH)D5, is downregulated in LNCaP-AI cells compared to LNCaP in the presence of androgens, whereas AWD restored VDR expression. Since LNCaP-AI cells expressed higher AR compared to LNCaP and AWD decreased AR, this indicated an inverse relationship between VDR and AR. Further, AR stimulation (by increased androgen) suppressed VDR, while AR downregulation (by ARsiRNA) stimulated VDR levels and sensitized LNCaP-AI cells to 1α(OH)D5 similar to AWD. Another cell line, pRNS-1-1, although isolated from a normal prostate, had lost AR expression in culture and adapted to androgen-independent growth. These cells expressed the VDR and were sensitive to 1α(OH)D5, but restoration of AR expression suppressed VDR levels and induced resistance to 1α(OH)D5 treatment. Taken together, these results demonstrate negative regulation of VDR by AR in CRCaP cells. This effect is likely mediated by prohibitin (PHB), which was inhibited by AR transcriptional activity and stimulated VDR in CRCaP but not castrate-sensitive cells. Therefore, in castration-sensitive cells, although the AR negatively regulates PHB, this does not affect VDR expression, whereas in CRCaP cells, negative regulation of PHB by the AR results in concomitant negative regulation of the VDR by the AR. These data demonstrate a novel mechanism by which 1α(OH)D5 prolongs the effectiveness of AWD in CaP cells.

Keywords

calcitriol, vitamin D5, androgen receptor, vitamin D receptor, prostate cancer

Introduction

Since the growth of prostate cancer (CaP) is initially dependent on androgens, first-line treatment for recurrent CaP is androgen withdrawal therapy (AWD), to which 95% of tumors initially respond.[1] First-line hormonal therapy usually consists of LHRH agonists, which prevent the production of testicular androgens. However, patients on this treatment relapse within 18 to 24 months, at which time they are placed on complete androgen blockade (CAB) involving the use of androgen receptor (AR) antagonists such as bicalutamide (Casodex, AstraZeneca, London, United Kingdom), a competitive inhibitor of AR ligand binding, together with AWD.[2] Although the majority of these patients continue to express the AR, which transcriptionally regulates the expression of multiple genes, including prostate-specific antigen (PSA),[3] only about 25% to 30% of patients respond to this second-line hormonal therapy, indicating the development of castration-resistant prostate cancer (CRCaP). Therapeutic options for patients who develop CRCaP are limited: clinical trials reveal that United States Food and Drug Administration (FDA)–approved drugs for CRCaP patients, including the chemotherapeutic agent docetaxel,[4,5] and the cancer "vaccine" sipuleucel-T (Provenge, Dendreon Corporation, Seattle,

Supplementary material for this article is available on the *Genes & Cancer* website at http://ganc.sagepub.com/supplemental.

[1]VA Northern California Health Care System, Mather, CA, USA
[2]University of California Davis Medical School, Sacramento, CA, USA
[3]Illinois Institute of Technology Research Institute, Chicago, IL, USA
*These authors contributed equally.

Corresponding Author:
Paramita M. Ghosh, Department of Urology, University of California Davis School of Medicine, 4860 Y Street, Suite 3500, Sacramento, CA 95817
Email: paramita.ghosh@ucdmc.ucdavis.edu

WA),[6] increased survival by only 3 and 4 months, respectively. Hence, the long-term goal of this project is to identify therapeutic targets that would prevent CaP progression to CRCaP.

The naturally occurring active metabolite of vitamin D, 1,25 dihydroxy vitamin D3 (1α,25$(OH)_2D_3$, calcitriol), inhibits CaP growth and induces apoptosis in CaP cells.[7-9] However, the utility of calcitriol has been severely limited because its antitumor activity is achieved at doses that cause toxicity due to hypercalcemia,[10-12] which at high serum calcium levels (≥12.0 mg/dL or 3 mmol/L), leading to increased intestinal and renal calcium absorption, may cause intestinal and renal toxicity, whereas severe hypercalcemia has been known to induce coma and cardiac arrest. Phase III studies in patients with CRCaP utilizing high-dose calcitriol in combination with docetaxel were terminated due to overall decreased survival in comparison with docetaxel alone.[13]

Development of synthetic analogs of the vitamin D molecule that preserve its antiproliferative and cell-differentiating properties while minimizing or eliminating its toxic profile has been ongoing. Calcitrol-induced hypercalcemia is related to the presence of the OH group at C-25 of this compound. To reduce toxicity, a compound of the vitamin D5 family, rather than the D3 family, 1α-hydroxyvitamin D5 (1α(OH)D5), has been constructed and was shown to lack hydroxylation at the C-25 position and to contain an ethyl group at C-24.[14] 1α(OH)D5 (1 μM), similar to calcitriol (100 nM), inhibited the development of DMBA-induced preneoplastic lesions in mouse mammary glands[14] or *N*-methyl-*N*-nitrosourea (MNU)–induced mammary carcinogenesis in female rats.[15] However, unlike calcitriol, 1α(OH)D5 did not increase plasma calcium levels at any dose tested in male rats and did not affect body weight.[14-16] These results indicate the low-calcemic nature of 1α(OH)D5 and lower toxicity, in comparison with calcitriol, despite its tumor-suppressive properties. However, this drug has never been used in prostate cancer cells. The objective of the studies described here is to demonstrate that despite decreased cytotoxicity, 1α(OH)D5 is still as effective as the parent compound, calcitriol, in preventing prostate cancer cell growth.

Studies showed that AWD does not induce cell death but rather results in cell cycle arrest, whereas CRCaP development triggers a release from that arrest, and cell cycle progression, even in the absence of androgens.[17] Thus, the induction of apoptosis during AWD would prevent CRCaP by depleting the system of cells that have the capability to progress. Here, we show that 1α(OH)D5 induced apoptosis in CRCaP cells during AWD, indicating that it would be suitable as adjuvant therapy to improve the effects of AWD. Further, androgens activate the AR, which is required for the growth and survival of not only castrate-sensitive but also CRCaP cells.[18-20] About 30% of CRCaP tumors express higher AR compared to the corresponding androgen-dependent primary tumor.[3] Thus, an increase in AR transcriptional activity would ultimately promote CRCaP cell growth. Calcitriol was shown to induce AR transcriptional activity, especially in LNCaP prostate cancer cells,[21] and this could possibly be a mechanism of resistance to calcitriol in these cells. However, we now show that unlike calcitriol, 1α(OH) D5 did not induce AR transcriptional activity. This indicates an additional benefit of 1α(OH)D5 over calcitriol in the treatment of CaP cells.

The genomic effects of vitamin D are mediated by the vitamin D receptor (VDR), which, like the AR, is a steroid nuclear receptor.[21] Multiple studies reported that calcitriol is more effective in castration-sensitive CaP cell lines such as LNCaP and to some extent in AR-null cell lines such as PC-3, compared to AR-positive CRCaP sublines of LNCaP.[9,21,22] In this study, we observe a similar effect with 1α(OH)D5 and investigate the mechanism. Previous studies indicated negative regulation of VDR transcriptional activity by the AR[23]; however, we now show that the AR is a negative regulator of VDR expression in CRCaP cells but not castrate-sensitive cells. Our results demonstrate that in LNCaP cells, VDR is strongly expressed in the presence of androgens, and 1α(OH)D5, similar to calcitriol, is effective in suppressing proliferation and inducing apoptosis in these cells. However, LNCaP-AI cells, developed by prolonged culture of LNCaP cells in the absence of androgens, express very high levels of AR, which suppressed VDR levels and desensitized the cells to 1α(OH)D5, whereas AWD resensitized CRCaP cells to 1α(OH)D5 by inhibiting the AR and stimulating the VDR.

We also show that the interaction between the AR and the VDR in CRCaP cells is likely mediated by a novel mechanism involving the cell cycle regulator prohibitin (PHB), which was previously shown to interact with the AR in CaP cells. PHB is a highly conserved 32-kDa protein that localizes both in the mitochondria and the nucleus and appears to play different roles at the 2 locations.[24] In the mitochondria, it is a mitochondrial chaperone protein that complexes with BaP37/REA, whereas in the nucleus, it acts as a cell cycle regulator that antagonizes E2F1-mediated gene activation by recruitment of transcriptional repressors including the nuclear corepressor (NCoR), retinoblastoma protein (Rb), and histone deacetylase 1 (HDAC1).[25,26] PHB has been called a tumor suppressor due to its ability to block DNA synthesis and induce apoptosis.[24,27] In prostate tumor cells, PHB was shown to be negatively regulated by androgens[28] and is also a negative regulator of AR transcriptional activity.[29] Suppression of AR activity by AR antagonists required PHB, in complex with the SWI/SNF core protein BRG1.[30] Reduction of PHB promoted both androgen-dependent and -independent tumor growth *in vivo*.[31] Significantly, the growth-inhibitory ability of vitamin D5 in breast cancer cells was also traced to PHB.[32,33]

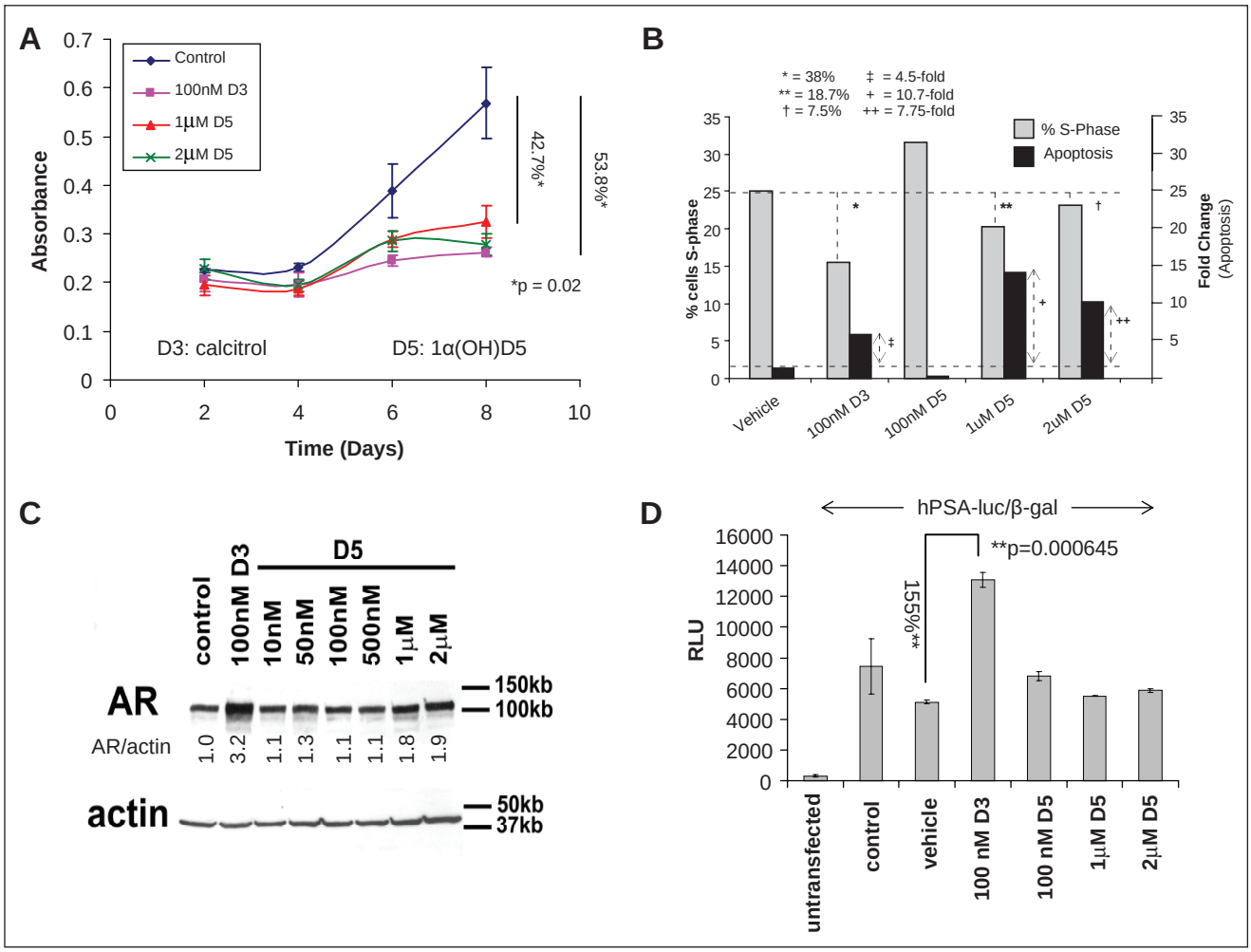

Figure 1. 1α(OH)D5 inhibits cell growth and survival but does not induce AR levels or transcriptional activity in androgen-dependent LNCaP prostate cancer cells. LNCaP cells cultured in medium with androgens (FBS) and exposed to either calcitriol (D3) or 1α(OH)D5 (D5). (**A**) Cell number increase was estimated by MTT assay and indicated comparable cytostatic effects of 100 nM D3 and 1 to 2 μM D5. Data represent mean ± standard deviation (SD) of 3 independent readings. (**B**) Flow cytometric analysis to compare effects of calcitriol versus 1α(OH)D5 on cell proliferation and apoptosis. LNCaP cells were treated with vehicle or calcitriol or different concentrations of 1α(OH)D5 for 48 hours. Change in S-phase is recorded as percentage change over vehicle-treated cells and change in apoptosis as fold change over vehicle-treated cells. (**C**) AR levels assessed by immunoblotting in LNCaP cells showing AR induction by D3 but not by D5. β-actin was assessed as loading control. Numbers under each lane represent fold change in band intensity normalized to that of the control band. These experiments were repeated at least 3 times with similar results. (**D**) LNCaP cells left untransfected or transfected with hPSA-luc and β-gal were treated as shown for 72 hours. AR transcriptional activity was determined by luciferase assay and shows increased activity in D3- but not D5-treated cells. Data of hPSA-gal/β-gal shown as mean ± SD of 3 independent readings.

In this study, we show that in androgen-dependent cells, VDR expression is not regulated by PHB, and the AR does not have an inhibitory effect on VDR. However, CRCaP cells likely undergo a phenotypic change, such that VDR expression is now regulated by PHB; hence, the AR, which is a negative regulator of PHB, also can negatively regulate the VDR. As a result, 1α(OH)D5, in combination with AWD, inhibits growth of CRCaP cells. Taken together, these results show that 1α(OH)D5 prolongs the effectiveness of AWD in CaP cells.

Results

1α(OH)D5 inhibits growth and induces apoptosis in castration-sensitive LNCaP prostate cancer cells. We first investigated whether 1α(OH)D5 was effective in inhibiting the growth of CaP cells. To compare the effects of 1α(OH)D5 with calcitriol in castration-sensitive cells, LNCaP cells were treated in "complete" medium (with fetal bovine serum [FBS] containing androgens) with vehicle (ethanol, control), 100 nM calcitriol, and increasing doses of 1α(OH)D5. At concentrations

<1 μM, 1α(OH)D5 had no significant effect on proliferation (not shown), while 1 to 2 μM 1α(OH)D5 had an equivalent cytostatic effect (42.72% decrease with 1 μM, $P = 0.017$, and 51.18% decrease with 2 μM, $P = 0.015$) as 100 nM calcitriol (53.8% decrease, $P = 0.018$) (Fig. 1A). By flow cytometry, calcitriol (100 nM) was shown to inhibit proliferation (38% decrease in S-phase compared to vehicle-treated cells) and induce apoptosis (4.48-fold increase in apoptosis v. vehicle-treated cells) (Fig. 1B). Compared to calcitriol, 1α(OH)D5 had a smaller effect on cell cycle arrest, but the effect on apoptosis was greater (10.7-fold and 7.5-fold increase in apoptosis compared to vehicle-treated cells, respectively) (Fig. 1B). LNCaP cells were growth arrested (75.36% inhibition after 5 days, $P < 0.0001$) upon culture in medium containing charcoal stripped FBS (CSS), which, among other factors, contain decreased levels of androgens, and neither calcitriol nor 1α(OH)D5 enhanced this effect (calcitriol + CSS, 71.6% inhibition, $P = 0.0004$; 1α(OH)D5 + CSS, 75.81% inhibition, $P < 0.0001$; data not shown).

It is well known that calcitriol upregulates levels of the AR and its transcriptional target, PSA, in LNCaP cells *in vitro*.[9,34,35] Hence, we investigated the same for 1α(OH)D5. Immunoblotting confirmed that in LNCaP cells, calcitriol substantially increased the expression of the AR (3.2-fold) starting 4 days after treatment (not shown) and had a pronounced effect by 8 days (Fig. 1C). However, 1α(OH)D5 at cytostatically equivalent concentrations (1 and 2 μM) showed minimal effect (less than 2-fold increase in AR expression) (Fig. 1C). AR transcriptional activity as determined by luciferase assay on a plasmid encoding for the human PSA promoter tagged to a luciferase construct (hPSA-luc) was increased 155% (2.5-fold) by treatment with 100 nM calcitriol but showed no change with 1α(OH)D5 (Fig. 1D). Taken together, these results indicate that 1α(OH)D5, like calcitriol, had a cytostatic effect on androgen-dependent prostate cancer cells, although by a mechanism different from calcitriol, but, unlike the latter, did not enhance AR transcriptional activity in LNCaP cells.

LNCaP-AI, a CRCaP subline of LNCaP cells, is sensitive to growth inhibition by 1α(OH)D5 in the absence, not presence, of AR transcriptional activity. We next determined whether 1α(OH)D5 was also useful in CRCaP cells. Previous studies had shown that calcitriol was less effective in castrate-resistant sublines of LNCaP cells[21]; hence, we tested the effects of 1α(OH)D5 on one such line, LNCaP-AI, which we had developed by continuous culture of LNCaP cells in CSS medium for prolonged periods of time, as described elsewhere.[36,37] Unlike LNCaP, LNCaP-AI cells were not significantly growth arrested by treatment with 1α(OH)D5 in the presence of FBS (15% inhibition with 1 μM, $P = 0.27$) (Fig. 2A, upper panel). However, in medium containing CSS, which have lower levels of androgens and other hormones, LNCaP-AI cells were significantly growth inhibited by 1 μM 1α(OH)D5 (51.94% inhibition, $P = 0.023$), although vehicle-treated LNCaP-AI cells continued to proliferate (Fig. 2A, lower panel). Flow cytometric analysis indicated that in the presence of FBS, both calcitriol and 1α(OH)D5 failed to induce apoptosis in LNCaP-AI cells, whereas in CSS, substantial apoptosis was observed with both drugs (Fig. 2B). A similar effect was also seen using C4-2 cells, a commercially available CRCaP subline of LNCaP cells obtained from tumors developed in castrated nude mice,[38] which has been extensively described by us previously[39-41] (Suppl. Fig. S1). Thus, our results indicate that CRCaP sublines of LNCaP cells were growth inhibited by 1α(OH)D5 in CSS medium despite neither 1α(OH)D5 nor culture in CSS being individually growth inhibitory in these cells.

Like LNCaP cells, LNCaP-AI experienced no increase in AR activity on a PSA promoter with 1α(OH)D5 as determined by luciferase assay, although calcitriol still increased PSA transcription in FBS medium (110% [2.1-fold] increase, $P < 0.0001$) (Fig. 2C). However, even calcitriol failed to induce AR activity in CSS medium, indicating that the effect was ligand dependent. These results indicate the effectiveness of 1α(OH)D5 in the inhibition of cell growth in CRCaP cells in combination with AWD.

The effects of 1α(OH)D5 are mediated by the VDR, which is suppressed in LNCaP-AI cells by high androgen and AR levels. We next investigated whether there is a link between AR transcriptional activity and the growth inhibitory effect of 1α(OH)D5 in CaP cells. The genomic effects of calcitriol are regulated by the VDR; hence, we determined whether the effects of 1α(OH)D5 were mediated by the VDR as well. LNCaP-AI cells subjected to control siRNA for 48 hours showed approximately 29% reduced growth rates when treated with 2 μM 1α(OH)D5 ($P < 0.0001$) (Fig. 3A, upper), but cells that were depleted of VDR with VDR siRNA for the same time period failed to respond to 1α(OH)D5 (Fig. 3A, lower). The extent of VDR downregulation by VDR siRNA is shown in Supplementary Figure S2. These results indicate that the effects of 1α(OH)D5 on cell growth are mediated by the VDR. Next, we compared the levels of AR and VDR in the 2 cell lines studied. LNCaP-AI cells expressed higher AR and lower VDR levels compared to LNCaP (Fig. 3B, left). Together, these data explain the differential effects of 1α(OH)D5 in LNCaP versus LNCaP-AI cells; in medium with FBS, LNCaP cells responded to 1α(OH)D5 because it expressed high levels of VDR, whereas LNCaP-AI cells did not respond due to lower VDR expression.

Our data indicated that culture in CSS for 24 hours slightly decreased VDR expression (Fig. 3B, left). This observation is in support of previous reports demonstrating positive correlation between AR and VDR expression in LNCaP cells.[23] However, prolonged culture in CSS increased VDR expression in LNCaP-AI cells (Fig. 3B, right), coinciding with a

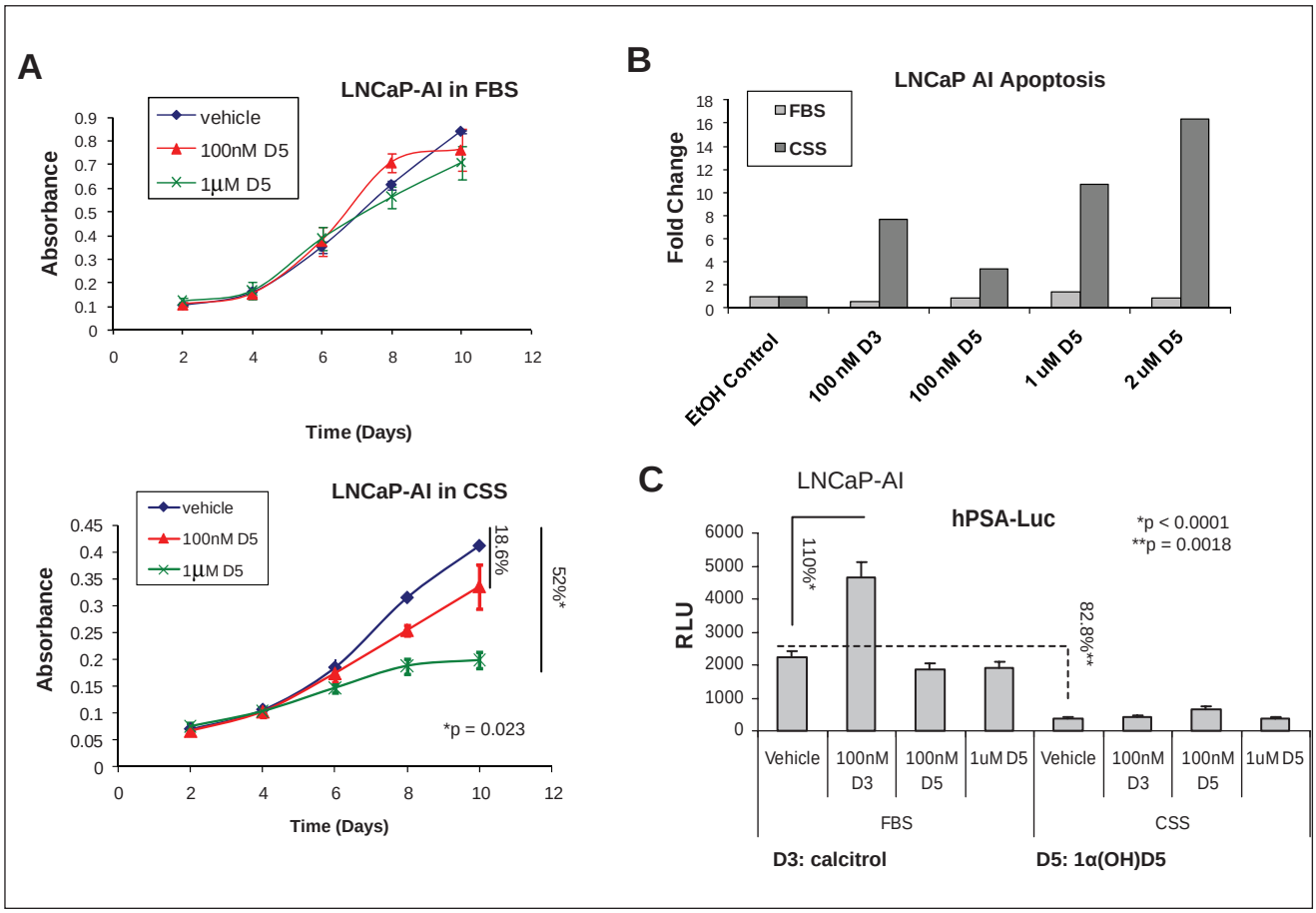

Figure 2. 1α(OH)D5 inhibits growth of LNCaP-AI cells, a castration-resistant subline of LNCaP, in charcoal stripped serum (CSS) but not in complete medium containing FBS. LNCaP-AI cells were cultured in (**A**) complete medium containing FBS (**upper panel**) or phenol red–free medium containing CSS (**lower panel**) for the periods indicated in the presence of vehicle (ethanol) or 100 nM versus 1 μM 1α(OH)D5 (D5). Growth rates estimated by MTT assay indicate greater effect of D5 in CSS compared to FBS. Data represent mean ± standard deviation (SD) (n = 3). (**B**) Flow cytometry to determine the effect of D3 and increasing doses of D5 on LNCaP-AI cell apoptosis. Cells were cultured in medium containing FBS or CSS for 5 days, and the cells were trypsinized and stained with propidium iodide and annexin V prior to flow cytometry. Data represent fold change over number of cells undergoing apoptosis in cells treated with ethanol (EtOH control). (**C**) AR transcriptional activity with calcitriol versus 1α(OH)D5 in FBS versus CSS as determined by luciferase assay in hPSA-luc and β-gal transfected cells. Note the increased AR activity in the presence of D3, which was not apparent in the presence of D5. Data represent mean ± SD of 3 independent readings.

renewed response of these cells to 1α(OH)D5 in CSS medium. Hence, we investigated the cause for CSS-induced increase in VDR expression. Charcoal stripping removes available androgens in FBS, together with other steroids and growth factors; hence, we investigated whether the effects of CSS observed above relate to the removal of androgens from the medium. Prolonged (4-day, but not 2-day) treatment with increasing doses of the androgen dihydrotestosterone (DHT) increased AR and decreased VDR expression (Fig. 3C), indicating that the AR has a suppressive effect on VDR expression in prostate cancer cells.

AR downregulation increased VDR expression in LNCaP-AI cells and sensitized them to 1α(OH)D5. Since LNCaP-AI cells expressed higher AR and lower VDR levels compared to LNCaP, we investigated whether increased AR seen in LNCaP-AI cells suppressed VDR function, thereby desensitizing these cells to 1α(OH)D5. In cells subjected to control siRNA only, treatment with calcitriol, and to some extent, 1α(OH)D5, induced AR expression; however, AR siRNA significantly inhibited AR levels (Fig. 4A, upper panel). VDR expression was induced by both calcitriol and 1α(OH)D5 in cells transfected with control siRNA (Fig. 4A, middle panel). However, inhibition of AR expression by AR siRNA enhanced VDR expression in vehicle-treated, calcitriol, and 1α(OH)D5-treated cells (Fig. 4A, middle panel). This supported our previous observation that the AR antagonized VDR expression in LNCaP-AI cells.

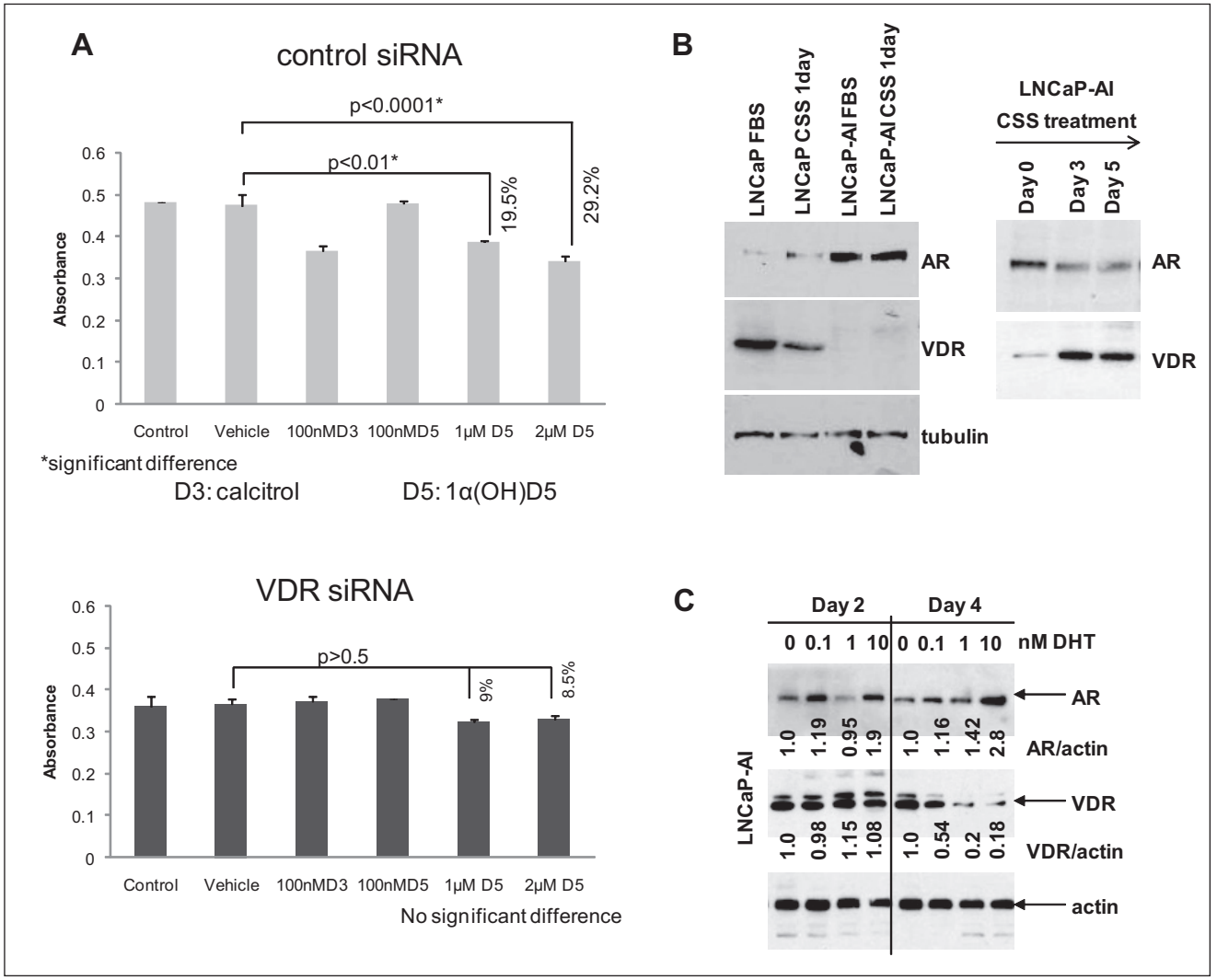

Figure 3. The androgen receptor (AR) negatively regulates the levels of the vitamin D receptor (VDR). (**A**) 1α(OH)D5-induced growth inhibition is mediated by the VDR. (**Upper**) LNCaP-AI cells cultured in CSS medium treated with control siRNA were growth inhibited by 48-hour treatment with 1 to 2 μM 1α(OH)D5, as determined by MTT assay (note that the higher inhibition rates observed in previous figures were achieved after longer periods of treatment), but (**lower**) the same cell line subjected to VDR siRNA for the same time period showed no statistically significant response to 1α(OH) D5. Data represent mean ± standard deviation (SD) (n = 3). (**B**) Negative correlation between the AR and the VDR. (**Left**) LNCaP-AI cells express higher levels of AR and lower levels of VDR compared to LNCaP, (**right**) but when LNCaP-AI cells were cultured for >24 hours in CSS, AR levels declined while VDR levels increased. (**C**) Prolonged treatment with DHT inhibited VDR levels. LNCaP-AI cells were treated with increasing doses of DHT. AR expression increased with increasing concentration of DHT (**upper panel**). In contrast, VDR levels decreased after 4 days but not 2 days of treatment (**middle panel**). Numbers under each lane represent fold change in band intensity normalized to that of control.

The above results predicted that decreased AR expression sensitizes LNCaP-AI cells to the effects of 1α(OH)D5. Hence, we subjected LNCaP-AI cells to control and AR siRNA and determined the growth-inhibitory effects of 1α(OH)D5 under these conditions. As before, LNCaP-AI cells grown in FBS and subjected to control siRNA were resistant to growth inhibition by 1 μM 1α(OH)D5 (14.93% inhibition only, $P > 0.05$) (Fig. 4B, upper). However, down-regulation of AR expression with AR siRNA sensitized these cells to 1α(OH)D5 even in the presence of FBS (41.43% inhibition, $P = 0.0092$) (Fig. 4B, lower). Taken together, these results indicate that the activation of the AR suppresses VDR levels and also the response of LNCaP-AI cells to 1α(OH)D5, whereas AR inhibition relieves this suppression and sensitizes these cells to the drug.

AR overexpression antagonizes the vitamin D receptor, suppresses the expression of prohibitin, and prevents responsiveness to 1α(OH)D5 in pRNS-1-1 cells. Next, we investigated whether an increase in AR expression can suppress VDR

expression. For this purpose, we used pRNS-1-1 cells derived from prostate epithelial cells, which had subsequently lost AR expression and adapted to androgen-independent growth (described by us[36,42]). To determine the effect of AR overexpression on the effect of 1α(OH)D5, pRNS-1-1 cells were stably transfected with vector alone, or wild-type AR (wtAR), and subjected to increasing doses of 1α(OH)D5. However, since the previous figures showed experiments that were all conducted in LNCaP cells and its CRCaP sublines, which endogenously express a mutant AR (T877A), we also used cells stably transfected with the AR mutant to determine whether they behaved similarly to those expressing wtAR. The cells stably transfected with vector alone responded to increasing doses of 1α(OH)D5 (1 μM: 57% decrease after 5 days, $P = 0.0022$; 2 μM: 71.7% decrease, $P = 0.0131$) (Fig. 5A); however, when transfected with wild-type AR (1 μM: 11.2% decrease after 5 days, $P > 0.05$; 2 μM: 15.6% decrease, $P = 0.0013$) (Fig. 5B) or AR T877A (1 μM: 15.9% decrease after 5 days, $P = 0.0254$; 2 μM: 6.01% decrease, $P = 0.0119$) (Fig. 5C), these cells lost the ability to respond to 1α(OH)D5. Investigation into the cause of this loss of response revealed that pRNS-1-1 cells stably expressing wild-type AR or AR(T877A) expressed significantly less VDR compared to those expressing vector alone (Fig. 5D, upper panels). Thus, the expression of the AR prevents sensitivity to 1α(OH)D5 in pRNS-1-1 cells by repressing VDR expression. These results confirm our previous observations that the AR is a suppressor of VDR expression.

Next, we investigated the mechanism by which the AR regulates VDR expression in prostate cancer cells. Previous reports indicated that androgens downregulate the expression of prohibitin (PHB),[28] while 1α(OH)D5 stimulated PHB in breast cancer cells[32]; these reports suggested that PHB may interact with both the AR and VDR. Based on these reports, we investigated the levels of PHB in the various pRNS-1-1 mutant cell lines used. In support of a positive correlation between the VDR and PHB, and a negative effect on both by the AR, expression of wild-type or mutant AR in pRNS-1-1 cells suppressed PHB expression (Fig. 5D, third panel). Taken together, these results indicate a common relationship between the AR, VDR, and PHB.

AR-induced suppression of VDR expression and sensitivity to 1α(OH)D5 are mediated by its effect on prohibitin. Since our previous results indicate a common effect of AR expression on VDR and PHB levels in pRNS-1-1 cells, we investigated whether PHB mediated the interaction between the VDR and the AR. Downregulation of PHB expression with a pool of 3 PHB-specific siRNA duplexes in LNCaP and LNCaP-AI cells not only resulted in an upregulation of AR levels (Fig. 6A, third panel), as previously reported by others,[29,30] but also in downregulation of VDR expression in LNCaP-AI but not in LNCaP cells (Fig. 6A, second panel). On the other hand, downregulation of AR expression in LNCaP-AI cells increased PHB expression (Fig. 6B) in accordance with reports in the literature.[28] Together with a lack of AR regulation of the VDR in LNCaP cells, but strong AR regulation of VDR in LNCaP-AI cells, these results indicate that expression or activation of the AR in CaP cells suppresses PHB expression and that in CRCaP cells, but not in castration-sensitive cells, this in turn prevents the expression of the VDR.

The above indicate that PHB may mediate the interaction between the VDR and the AR; hence, we investigated whether PHB is required for the suppressive effect of the AR on VDR expression. Androgen-independent LNCaP-AI cells, which express a mutant AR(T877A), when cultured in CSS-containing medium, respond to 1α(OH)D5 in the presence of control siRNA (54% inhibition with 2 μM 1α(OH)D5, $P < 0.01$) (Fig. 6C, upper panel). However, upon PHB downregulation using the same siRNA duplex pool described in Figure 6A, these cells became less responsive to 1α(OH)D5 (28% inhibition at the same dose, $P = 0.006$) (Fig. 6C, lower panel). However, a similar response was not seen in LNCaP cells (not shown). These results indicate that PHB mediates androgen-regulated responsiveness of LNCaP-AI, but not LNCaP cells, to 1α(OH)D5.

Discussion

The overall objective of the studies described here is to determine whether 1α(OH)D5 in combination with AWD prevents CRCaP cell growth. The parent compound, calcitriol, has repeatedly demonstrated antiproliferative properties against CaP; however, the antineoplastic activity of calcitriol is achieved at doses that result in hypercalcemia and toxicity. Intermittent dose-intense calcitriol (DN-101), together with the chemotherapeutic agent docetaxel, was relatively successful in a phase II trial (AIPC Study of Calcitriol Enhancement of Taxotere [ASCENT]) but, despite early promise,[43] did not achieve its primary endpoint for PSA response[44]; however, a much larger phase III international trial, ASCENT-2, was halted early due to decreased survival in the ASCENT arm compared to docetaxel alone.[13] As investigators debate the revival of the ASCENT-2 trial, a number of low-calcemic analogs of the parental compound have been placed in clinical development; this includes 1α(OH)D5, which was used in the present studies.

Here, we show that treatment with 1 to 2 μM 1α(OH)D5 and 0.1 μM calcitriol inhibited growth in LNCaP cells to a similar extent. However, the mechanism by which these 2 drugs inhibit cell growth is different; whereas 1α(OH)D5 induced higher levels of apoptosis, calcitriol caused greater cell cycle arrest. It is likely that the difference in response

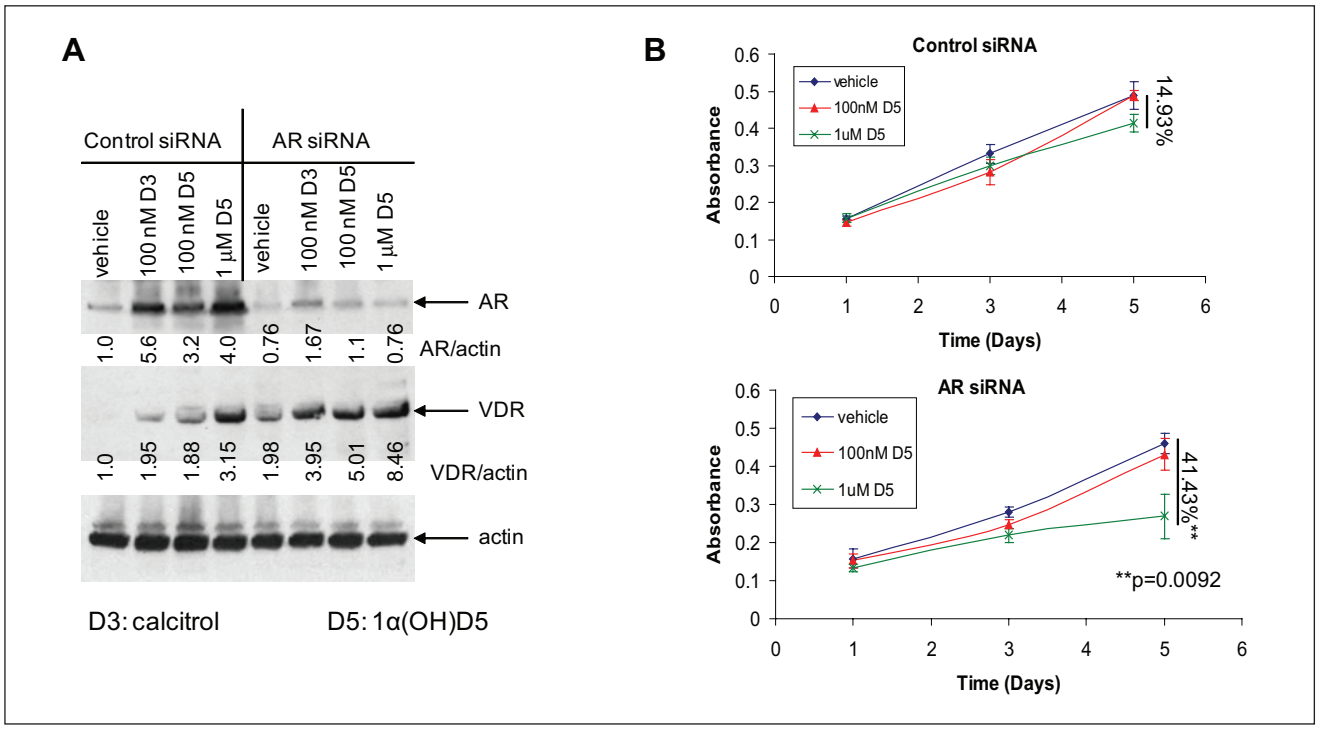

Figure 4. Downregulation of the AR by AR siRNA sensitizes LNCaP-AI cells to 1α(OH)D5. (**A**) An AR siRNA, which downregulated AR expression, but not a pool of control (nonspecific) siRNA duplexes, stimulated VDR levels. The AR siRNA, but not a control siRNA, downregulated AR expression, especially that induced by vitamin D3 and D5 treatment (**upper panel**), and induced VDR expression (**middle panel**). Results were normalized to levels of actin, which acted as loading control (**lower panel**). Numbers under each band represent fold change in band intensity normalized to actin with respect to that of the vehicle-treated control cells. (**B**) LNCaP-AI cells were transfected with control siRNA or AR-specific siRNA in the presence of D5, and changes in cell numbers in the presence of control or AR siRNA were estimated by MTT assay (**upper**). In the presence of the control siRNA, the effect of D5 on the growth of these cells was not significant, (**lower**) but AR downregulation with AR siRNA sensitized these cells to D5, which induced a 41.43% decrease in cell growth rates ($P = 0.0092$) versus 14.93% decrease ($P > 0.5$) with control siRNA (mean ± standard deviation [SD], $n = 3$).

of CaP cells to calcitriol and 1α(OH)D5 is attributable to the difference in binding affinities of these 2 reagents to the VDR since calcitriol has a higher binding affinity to the VDR compared to 1α(OH)D5 (Dr. Rajendra Mehta, unpublished observations). While nongenomic effects of calcitriol are well known,[45] it remains to be seen whether 1α(OH)D5 also has nongenomic effects and whether they affect its induction of apoptosis.

The difference in proliferation versus apoptosis in calcitriol versus 1α(OH)D5 has significant implications regarding their use to prevent the growth of CaP cells. It was previously shown that in castration-sensitive LNCaP cells (but not in CRCaP cells), calcitriol was highly effective in the presence of FBS, whereas it was less effective in LNCaP cells cultured in media containing CSS, where androgen levels were lower.[9,21,22] We hypothesize that if calcitriol at 100 nM mainly induces growth arrest, then it will be effective only against a cycling cell but would not have further effect upon culture in CSS, which is well known to cause LNCaP cells to undergo G1 arrest. Therefore, in castration-sensitive LNCaP cells, the effect of the VDR ligands in FBS versus CSS may be independent of AR regulation of VDR, whereas in castration-resistant cells, the effect is dependent on AR regulation of VDR expression. Since 1α(OH)D5 has a greater effect on LNCaP cells, we hypothesize that its effect in the long term may be greater. The current data could not be used to test this hypothesis because of the lack of sufficient LNCaP cells cultured in CSS-containing media available for flow cytometry in repeated experiments. Although other techniques to test this hypothesis are beyond the scope of this study, they are presently in progress in our laboratory.

It may be noted that while 1α(OH)D5 has a cytostatic effect at 10x the dose used for calcitriol, it is still effective since 100 nM calcitriol has been shown to be cytotoxic, whereas 1 μM 1α(OH)D5 was shown to be nontoxic.[14,15,46] In addition, for a nontoxic drug, 1 μM is not an unrealistic dose; for example, the commonly used antiandrogen Casodex (AstraZeneca), which has a low toxicity profile, is used at a 50-mg daily dose to achieve an intraprostatic dose of approximately 10 μM. Although both calcitriol and 1α(OH)D5 were more effective in LNCaP cells cultured in the

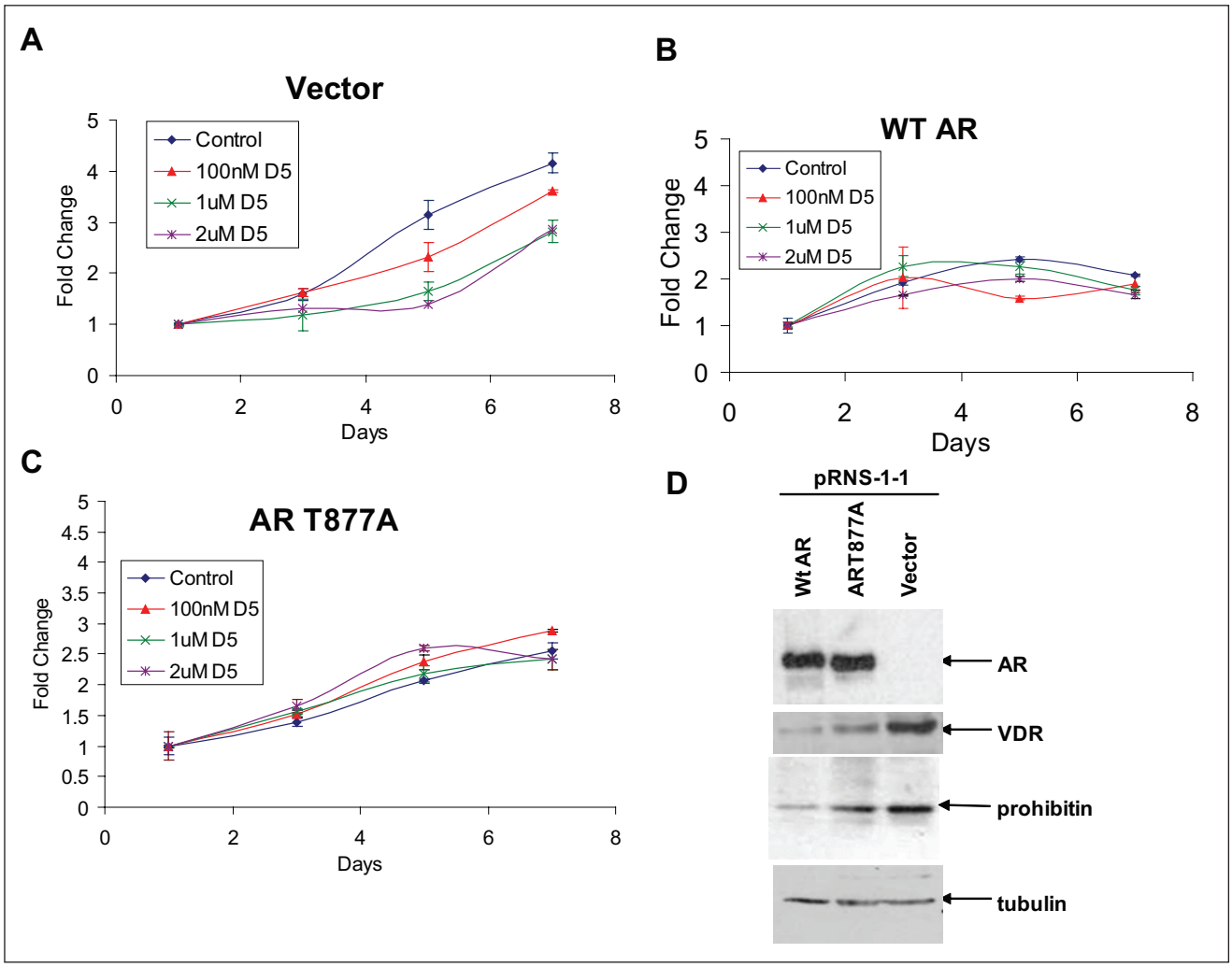

Figure 5. Expression of AR in AR-null pRNS-1-1 cells derived from a normal prostate desensitized these cells to 1α(OH)D5. (**A**) pRNS-1-1 cells stably transfected with vector only responded to 1α(OH)D5. (**B**) pRNS-1-1 cells stably transfected with wild-type AR (wtAR) demonstrated decreased response to 1α(OH)D5. (**C**) pRNS-1-1 cells stably transfected with a mutant AR (T877A) responded even less to 1α(OH)D5. (**D**) Expression of wild-type or mutant AR in pRNS-1-1 cells inhibited VDR and prohibitin expression. (**Upper panel**) Parental pRNS-1-1 cells were transfected with vector only or wild-type or mutant AR. (**Second panel**) Overexpression of AR in pRNS-1-1 cells, but not the vector, suppressed the expression of VDR, (**third panel**) as well as that of prohibitin. (**Bottom panel**) Loading control as detected by the expression of α-tubulin.

presence of androgens compared to its absence, in CRCaP sublines of LNCaP developed in our laboratory by continuous culture in CSS-containing medium (LNCaP-AI), both calcitriol and 1α(OH)D5 were more effective in the absence of AR transcriptional activity compared to its presence. We have described the characteristics of LNCaP-AI cells previously,[36,40] and we have shown that these cells are not growth arrested by culture in CSS or by treatment with bicalutamide (Casodex, AstraZeneca), a competitive inhibitor of AR ligand binding; however, in these cells, CSS or Casodex (AstraZeneca) treatment still inhibits AR transcriptional activity. These cells therefore represent CaP cells that failed first-line hormonal therapy (described in Introduction).

We show that these CRCaP cells do not respond to calcitriol or 1α(OH)D5 because a different effect is now at work, extraordinarily high AR, which suppresses VDR levels. Although growth of these cells is not affected by AWD alone, these treatments still decrease AR transcriptional activity, which stimulates VDR levels; hence, CRCaP LNCaP-AI cells, despite being resistant to AWD and to 1α(OH)D5 individually, are growth inhibited by the combination of these two treatments. Taken together, these results indicate that following the failure of first-line hormonal therapy, 1α(OH)D5 is a good therapeutic agent to prolong the effectiveness of second-line hormonal therapy in CaP cells.

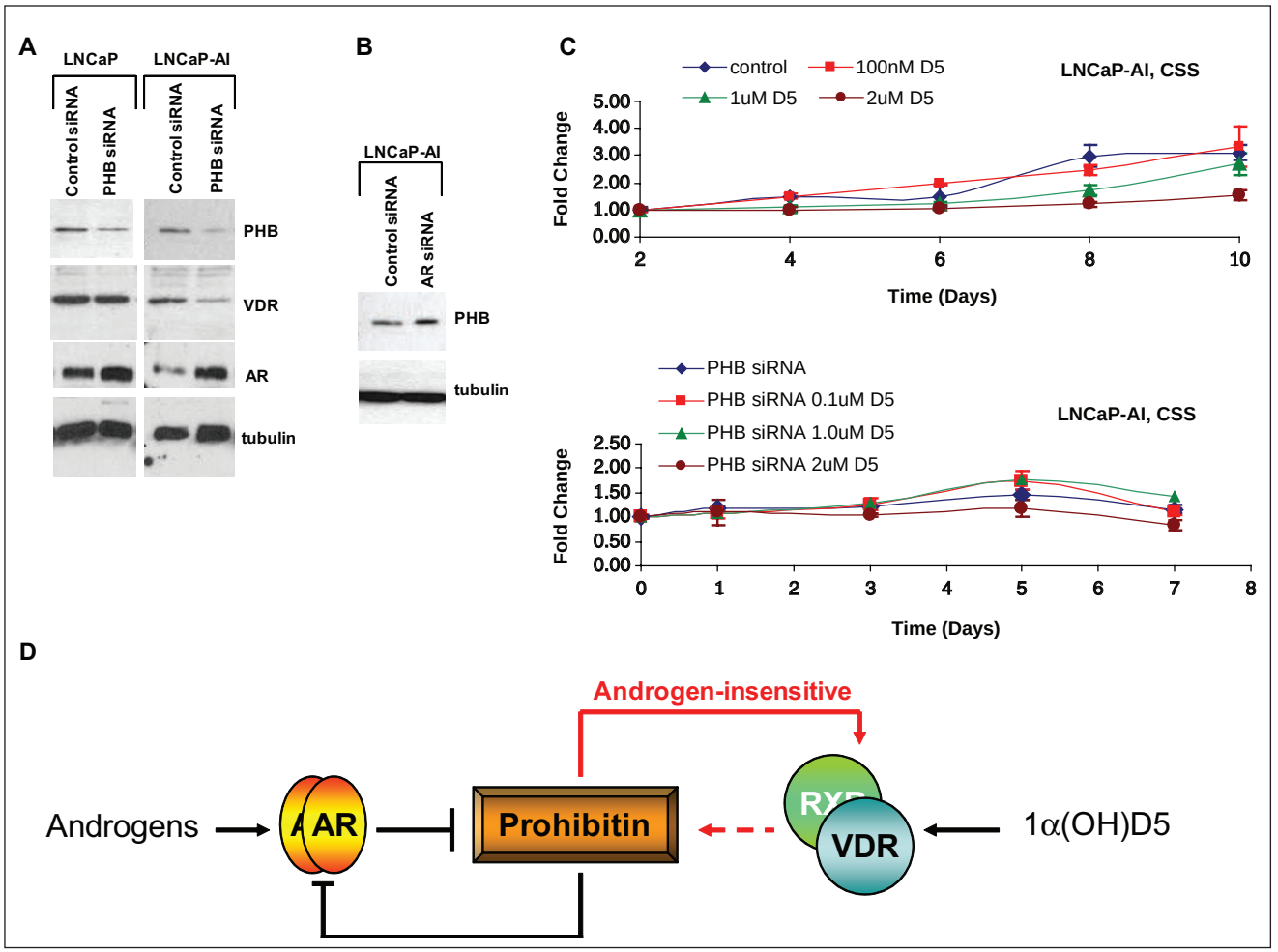

Figure 6. Prohibitin (PHB) mediates the effects of 1α(OH)D5 in androgen-insensitive, but not androgen-sensitive, prostate cancer cells. (**A**) LNCaP (**left**) and LNCaP-AI cells (**right**) were subjected to control (nonspecific) siRNA or PHB siRNA and the effect of these treatments on PHB levels (**upper panel**), VDR levels (**second panel**), AR levels (**third panel**), and tubulin (**fourth panel**) determined by Western blotting. Note that PHB downregulation stimulated AR levels in both LNCaP and LNCaP-AI, as reported by others,[29] but affected VDR expression only in LNCaP-AI. (**B**) Downregulation of AR expression in LNCaP-AI cells increases PHB levels. LNCaP-AI cells were subjected to control or AR siRNA, and PHB levels were determined by Western blotting. Tubulin levels were determined as loading control. (**C**) The growth-inhibitory effect of 1α(OH)D5 in LNCaP-AI cells in CSS medium requires an active PHB. Androgen-independent LNCaP-AI cells treated with control siRNA cultured in CSS medium respond to 1α(OH)D5 as determined by MTT assay (**upper**), whereas those treated with PHB siRNA duplexes do not (**lower**). (**D**) Scheme depicting PHB mediation of the effects of AR on VDR in androgen-insensitive cells. Red lines depict effects seen only in androgen-independent prostate cancer.

Our data show that the AR is a negative regulator of VDR expression in CRCaP cells but not in castration-sensitive cells so that an increase in AR expression, frequently seen in CRCaP cells, caused a decrease in VDR levels, which prevented 1α(OH)D5's growth-inhibitory effects (Fig. 6D). The fact that this effect is seen in CRCaP cells but not in the parental castration-sensitive cells indicates that the ability to regulate the VDR is a mechanism acquired during CRCaP development. The AR does not directly affect VDR transcription; however, we show that the cell cycle regulator PHB likely plays an important role in mediating the effect of the AR on VDR expression in CRCaP cells. AR and PHB were earlier shown to regulate each other,[28,29] and we now show that PHB regulates VDR expression in CRCaP cells but not in castration-sensitive cells. Therefore, in castration-sensitive cells, although the AR negatively regulates PHB, this does not affect VDR expression, whereas in CRCaP cells, negative regulation of PHB by the AR results in concomitant negative regulation of the VDR by the AR.

An investigation of how PHB affects VDR expression in LNCaP-AI, but not LNCaP, cells is beyond the scope of the present study and will be addressed in future projects. However, it may be noted that a previous report, which showed a suppressive effect of AR on VDR transcriptional activity,

suggested that competition for shared coregulators between AR and VDR is a possible mechanism to explain the suppressive effect of androgens on VDR activity.[23] In the current study, we do not examine VDR activity but establish that the AR is a negative regulator of VDR expression in CRCaP cells but not in castration-sensitive cells. The effect of AR on VDR levels is likely by a different mechanism involving PHB. PHB is not a transcription factor, but it represses E2F1-mediated gene transcription by recruitment of transcriptional repressors including the nuclear corepressor 1 (NCoR1).[25,27] It remains to be seen whether PHB regulation of E2F1 activity, and recruitment of NCoR1, plays a role in its regulation of VDR levels. It may be noted that a 2008 study showed that calcitriol treatment recruits the corepressors NCoR and SMRT to the VDR/RXR complex.[47] However, another study showed that overexpression of AR in LNCaP cells induced PHB expression, although the induction was less than 2-fold[48]; this may be a consequence of the biphasic response of these cells to increased AR and an attempt to slow down the growth of the cells at very high AR.

Furthermore, unlike calcitriol at 100 nM, 1α(OH)D5 at the cytostatic equivalent concentration, 1 μM, did not increase AR transcriptional activity. The significance of the increase in AR transcriptional activity by calcitriol, as seen in LNCaP cells, has been debated. A previous study has noted that the onset of calcitriol-induced G0/G1 arrest in LNCaP and CWR22R cells correlated with the onset of increasing AR expression in response to calcitriol treatment and hypothesized that the antiproliferative actions of calcitriol in AR-positive prostate cancer may be mediated through AR expression.[49] While very high levels of androgens, which cause very high levels of AR expression, are known to be antiproliferative,[50,51] low-to-medium levels of AR transcriptional activity in CaP cells are associated with high levels of proliferation,[51] indicating that the increase in AR transcriptional activity by calcitriol may not be as beneficial as previously suggested.[49] On the other hand, this effect may also be an artifact of the cell culture system, as no significant change in serum PSA or free PSA over 8 days was observed in 8 subjects treated with a single dose of 0.5 μg/kg calcitriol.[52] However, it is also true that the phase II ASCENT trial did not achieve its primary endpoint for increased PSA response, although there was a significant trend in PSA response rate in the DN-101 arm.[44] Therefore, the lack of increase in PSA and AR transcriptional activity as seen in 1α(OH)D5-treated cells compared to calcitriol supports its utility as an antitumor agent.

In summary, we have shown here that the vitamin D analog, 1α(OH)D5, similar to calcitriol, has cytostatic effects in androgen-dependent LNCaP cells. However, unlike calcitriol, 1α(OH)D5 does not increase AR transcriptional activity, indicating a mechanism of action distinct from its parental compound. The cytostatic effects of 1α(OH)D5 are not seen in LNCaP-AI, a CRCaP subline of LNCaP cells, in the presence of androgens. However, AWD, which was ineffective by itself, sensitized LNCaP-AI cells to 1α(OH)D5. These cytostatic effects were mediated by an interaction between the AR and the VDR; in the CRCaP cells, increased expression of the AR repressed VDR expression, and inhibition of the AR stimulated VDR expression and sensitized CaP cells to the growth-inhibitory effects of 1α(OH)D5 mediated by the VDR. These effects are likely mediated by the cell cycle regulator PHB, which stimulated VDR expression in CRCaP cells. Our data show that 1α(OH)D5, together with androgen withdrawal, is likely of therapeutic value to prevent the development of CRCaP.

Materials and Methods

Cell Culture and Pharmacological Treatments

Cells were normally cultured in "regular medium": RPMI 1640 medium with 5% fetal bovine serum (FBS) (Invitrogen, Grand Island, NY) unless otherwise specified. LNCaP cells were purchased from American Type Culture Collection (Manassas, VA). Androgen-independent clones of LNCaP cells (LNCaP-AI cells)[36,37] were obtained by prolonged culture of LNCaP cells in "low androgen medium": phenol red–free RPMI 1640 with 5% charcoal stripped FBS (CSS, Hyclone, Logan, UT). The SV40-immortalized human prostate epithelial cell line (pRNS-1-1) developed from a normal prostate has been described elsewhere.[36,42] These cells had lost expression of the AR while in culture, and stable transfectants of pRNS-1-1 cells expressing vector alone, wild-type, or mutant AR were developed and provided by Dr. XuBao Shi (University of California, Davis).[42] Calcitriol and 4,5α-dihydrotestosterone (DHT) were obtained from Sigma-Aldrich (St. Louis, MO) and were dissolved in 200 proof ethanol, as was 1α(OH)D5, which was synthesized as described elsewhere.[14]

Analysis of Cell Growth and Death

Flow cytometry. Cells were grown under desired conditions in 100-mm dishes at 0.5×10^6 cells/dish. Flow cytometry was conducted on FACStar Plus (Becton Dickinson Immunocytometry Systems, San Jose, CA). Cells were illuminated with 200 mW of 488-nm light produced by an argon-ion laser. Fluorescence was read through a 630/22-nm band-pass filter (for propidium iodide) or a 530/30-nm band-pass filter (for annexin V–FITC). Data were collected on 20,000 cells as determined by forward and right angle light scatter and stored as frequency histograms; data used for cell cycle analysis were further analyzed using MODFIT (Verity Software House, Topsham, ME).

MTT Assay. Cells were plated in 24-well plates and treated as indicated. Following treatment, each well was incubated with 25 µL of 5 mg/mL 3-[4,5-dimethylthiazol-2yl]-2,5-diphenyl-tetrazolium bromide (MTT) for 1 hour in a CO_2 incubator at 37°C. The medium was aspirated, and 0.5 mL DMSO was added per well. Proliferation rates were estimated by colorimetric assay reading formazan intensity in a plate reader at 562 nm.

Immunoblotting

These techniques were performed as described elsewhere.[53,54] Mouse monoclonal anti-AR and antitubulin and antirabbit prohibitin antibodies were from Santa Cruz Biotechnology (Santa Cruz, CA). Mouse monoclonal anti-PSA and anti-VDR antibodies were from Neomarkers, Lab Vision Corporation (Fremont, CA). Mouse monoclonal antiactin was obtained from Sigma-Aldrich.

Transfection

Cells were transiently transfected using Lipofectamine 2000 reagent (Invitrogen) according to the manufacturer's specifications using 2 µg plasmid DNA. Wild-type AR (pAR0) plasmid had been obtained from Dr. Albert O. Brinkman (Erasmus University, Rotterdam, the Netherlands).[55] The AR mutant plasmid pCEP4-AR(T877A) was developed and provided by Dr. XuBao Shi (University of California, Davis), as has been described elsewhere.[56] A human PSA reporter plasmid consisting of the human PSA 5′-flanking region (-631/-1) containing androgen response elements I and II (ARE I and ARE II) tagged to a luciferase construct (hPSA-luc) was also provided by Dr. XuBao Shi (University of California, Davis).

AR Transcriptional Activity

Reporter gene activity was determined by luciferase assay as described by us elsewhere.[36] Cells were cotransfected with 2 µg of hPSA-luc with 2 µg of pCMV-βGal using Lipofectamine 2000 (Invitrogen) according to the manufacturer's recommendations. Cells grown in complete medium for 24 hours were treated as required for an additional 48 hours. After 48 hours, cell lysates were prepared for performing luciferase assays using a luciferase enzyme assay system (Promega Corporation, Madison, WI). Each transfection experiment was performed in triplicate on at least 3 separate occasions. Results represent an average of independent experiments with data presented as relative luciferase activity using means of untreated controls as standards.

RT-PCR

RT-PCR was performed as described elsewhere.[36,37] RNA was extracted using TRIzol Reagent (Life Technologies Inc., Grand Island, NY). cDNA synthesis used Moloney murine leukemia virus Reverse Transcriptase (Promega Corporation). The following amplification conditions were used in an MJ PTC-100 thermal cycler (MJ Research, Incline Village, NV): an initial denaturation for 5 minutes at 94°C, 30 cycles at 94°C for 30 seconds, 59°C for 30 seconds, and 72°C for 1 minute, followed by a final extension for 10 minutes at 72°C. The following primers were used: α-actin-F: 5′-ACT CTT CCA GCC TTC GTT C-3′, α-actin-R: 5′-ATC TCC TTC TGC ATC CTG TC-3′, hAR-F: 5′-TCC AAA TCA CCC CCC AGG AA-3′, and hAR-R: 5′-GAC ATC TGA AAG GGG GCA TG-3′.

RNA Inhibition

Cells were transiently transfected using Lipofectamine 2000 reagent (Invitrogen) according to the manufacturer's specifications based on established protocols using 50 pmol (stock: 100 nM) of AR siRNA, VDR siRNA, PHB siRNA, or a control (scrambled) siRNA for 48 to 96 hours (Santa Cruz Biotechnology). Sequences for the siRNA used are the following: anti-AR siRNA sense strands: (A) 5′-CAG UCC CAC UUG UGU CAA A-3′, (B) 5′-CCU GAU CUG UGG AGA UGA A-3′, (C) 5′-GUC GUC UUC GGA AAU GUU A-3′, and (D) 5′-GAC AGU GUC ACA CAU UGA A-3′; VDR siRNA sense strands: (A) 5′-CAU CCG UAG UUC CCU GAA ATT-3′, (B) 5′-CAC GUU CCU UAC UGC AGA ATT-3′, and (C) 5′-GGA ACU CCU GGA AAU AUC ATT-3′; and PHB siRNA sense strands: (A) 5′-CCA UCA CAA CUG AGA UCC U-3′, (B) 5′-GGA AGG AAA CAA AUG UGU A-3′, and (C) 5′-GUG UAU AAA CUG CUG UCA A-3′. Control was a pool of 4 scrambled nonspecific siRNA duplexes. According to the manufacturer, BLAST analysis confirmed at least 4 mismatches with all known human, mouse, and rat genes, and each individual siRNA within this pool was extensively characterized by genome-wide microarray analysis and found to have minimal off-target signatures.

Acknowledgments

The authors thank Dr. XuBao Shi, Department of Urology, University of California, Davis, for pRNS-1-1 cells stably transfected with an empty vector or wild-type or mutant androgen receptor.

Declaration of Conflicting Interests

The author(s) declared no potential conflicts of interest with respect to the authorship and/or publication of this article.

Funding

This work was supported by Award CA133209 from the National Institutes of Health (to P.M.G.).

References

1. Edwards J, Bartlett JM. The androgen receptor and signal-transduction pathways in hormone-refractory prostate cancer. Part 1: modifications to the androgen receptor. BJU Int. 2005;95:1320-6.
2. Klotz L. Maximal androgen blockade for advanced prostate cancer. Best Pract Res Clin Endocrinol Metab. 2008;22:331-40.
3. Feldman BJ, Feldman D. The development of androgen-independent prostate cancer. Nat Rev Cancer. 2001;1:34-45.
4. Petrylak D. Therapeutic options in androgen-independent prostate cancer: building on docetaxel. BJU Int. 2005;96 Suppl 2:41-6.
5. Boehmer A, Anastasiadis AG, Feyerabend S, *et al*. Docetaxel, estramustine and prednisone for hormone-refractory prostate cancer: a single-center experience. Anticancer Res. 2005;25:4481-6.
6. Di Lorenzo G, Buonerba C, Autorino R, De Placido S, Sternberg CN. Castration-resistant prostate cancer: current and emerging treatment strategies. Drugs. 2010;70:983-1000.
7. Leman ES, Arlotti JA, Dhir R, Getzenberg RH. Vitamin D and androgen regulation of prostatic growth. J Cell Biochem. 2003;90:138-47.
8. Murthy S, Agoulnik IU, Weigel NL. Androgen receptor signaling and vitamin D receptor action in prostate cancer cells. Prostate. 2005;64:362-72.
9. Zhao XY, Ly LH, Peehl DM, Feldman D. 1alpha,25-dihydroxyvitamin D3 actions in LNCaP human prostate cancer cells are androgen-dependent. Endocrinology. 1997;138:3290-8.
10. Beer TM, Myrthue A. Calcitriol in cancer treatment: from the lab to the clinic. Mol Cancer Ther. 2004;3:373-81.
11. Johnson CS, Muindi JR, Hershberger PA, Trump DL. The anti-tumor efficacy of calcitriol: preclinical studies. Anticancer Res. 2006;26:2543-9.
12. Trump DL, Hershberger PA, Bernardi RJ, *et al*. Anti-tumor activity of calcitriol: pre-clinical and clinical studies. J Steroid Biochem Mol Biol. 2004;89-90:519-26.
13. Scher HI, Chi KN, De Wit R, *et al*. Docetaxel (D) plus high-dose calcitriol versus D plus prednisone (P) for patients (Pts) with progressive castration-resistant prostate cancer (CRPC): results from the phase III ASCENT2 trial. J Clin Oncol. 2010;28:450-9.
14. Mehta RG, Moriarty RM, Mehta RR, *et al*. Prevention of preneoplastic mammary lesion development by a novel vitamin D analogue, 1alpha-hydroxyvitamin D5. J Natl Cancer Inst. 1997;89:212-8.
15. Mehta R, Hawthorne M, Uselding L, Albinescu D, Moriarty R, Christov K. Prevention of N-methyl-N-nitrosourea-induced mammary carcinogenesis in rats by 1alpha-hydroxyvitamin D(5). J Natl Cancer Inst. 2000;92:1836-40.
16. Mehta RG, Hussain EA, Mehta RR, Das Gupta TK. Chemoprevention of mammary carcinogenesis by 1alpha-hydroxyvitamin D5, a synthetic analog of vitamin D. Mutat Res. 2003;523-524:253-64.
17. Agus DB, Cordon-Cardo C, Fox W, *et al*. Prostate cancer cell cycle regulators: response to androgen withdrawal and development of androgen independence. J Natl Cancer Inst. 1999;91:1869-76.
18. Cheng H, Snoek R, Ghaidi F, Cox ME, Rennie PS. Short hairpin RNA knockdown of the androgen receptor attenuates ligand-independent activation and delays tumor progression. Cancer Res. 2006;66:10613-20.
19. Choudhury A, Charo J, Parapuram SK, *et al*. Small interfering RNA (siRNA) inhibits the expression of the Her2/neu gene, upregulates HLA class I and induces apoptosis of Her2/neu positive tumor cell lines. Int J Cancer. 2004;108:71-7.
20. Haag P, Bektic J, Bartsch G, Klocker H, Eder IE. Androgen receptor down regulation by small interference RNA induces cell growth inhibition in androgen sensitive as well as in androgen independent prostate cancer cells. J Steroid Biochem Mol Biol. 2005;96:251-8.
21. Peehl DM, Feldman D. Interaction of nuclear receptor ligands with the vitamin D signaling pathway in prostate cancer. J Steroid Biochem Mol Biol. 2004;92:307-15.
22. Weigel NL. Interactions between vitamin D and androgen receptor signaling in prostate cancer cells. Nutr Rev. 2007;65:S116-7.
23. Ting HJ, Bao BY, Hsu CL, Lee YF. Androgen-receptor coregulators mediate the suppressive effect of androgen signals on vitamin D receptor activity. Endocrine. 2005;26:1-9.
24. Nuell MJ, Stewart DA, Walker L, *et al*. Prohibitin, an evolutionarily conserved intracellular protein that blocks DNA synthesis in normal fibroblasts and HeLa cells. Mol Cell Biol. 1991;11:1372-81.
25. Wang S, Nath N, Adlam M, Chellappan S. Prohibitin, a potential tumor suppressor, interacts with RB and regulates E2F function. Oncogene. 1999;18:3501-10.
26. Wang S, Fusaro G, Padmanabhan J, Chellappan SP. Prohibitin co-localizes with Rb in the nucleus and recruits N-CoR and HDAC1 for transcriptional repression. Oncogene. 2002;21:8388-96.
27. Joshi B, Ko D, Ordonez-Ercan D, Chellappan SP. A putative coiled-coil domain of prohibitin is sufficient to repress E2F1-mediated transcription and induce apoptosis. Biochem Biophys Res Commun. 2003;312:459-66.
28. Gamble SC, Odontiadis M, Waxman J, *et al*. Androgens target prohibitin to regulate proliferation of prostate cancer cells. Oncogene. 2004;23:2996-3004.
29. Gamble SC, Chotai D, Odontiadis M, *et al*. Prohibitin, a protein downregulated by androgens, represses androgen receptor activity. Oncogene. 2007;26:1757-68.
30. Dai Y, Ngo D, Jacob J, Forman LW, Faller DV. Prohibitin and the SWI/SNF ATPase subunit BRG1 are required for effective androgen antagonist-mediated transcriptional repression of androgen receptor-regulated genes. Carcinogenesis. 2008;29:1725-33.
31. Dart DA, Spencer-Dene B, Gamble SC, Waxman J, Bevan CL. Manipulating prohibitin levels provides evidence for an in vivo role in androgen regulation of prostate tumours. Endocr Relat Cancer. 2009;16:1157-69.
32. Peng X, Mehta R, Wang S, Chellappan S, Mehta RG. Prohibitin is a novel target gene of vitamin D involved in its antiproliferative action in breast cancer cells. Cancer Res. 2006;66:7361-9.
33. Peng X, Mehta RG. Differential expression of prohibitin is correlated with dual action of vitamin D as a proliferative and antiproliferative hormone in breast epithelial cells. J Steroid Biochem Mol Biol. 2007;103:446-50.

34. Esquenet M, Swinnen JV, Heyns W, Verhoeven G. Control of LNCaP proliferation and differentiation: actions and interactions of androgens, 1alpha,25-dihydroxycholecalciferol, all-trans retinoic acid, 9-cis retinoic acid, and phenylacetate. Prostate. 1996;28:182-94.
35. Hsieh TY, Ng CY, Mallouh C, Tazaki H, Wu JM. Regulation of growth, PSA/PAP and androgen receptor expression by 1 alpha, 25-dihydroxyvitamin D3 in the androgen-dependent LNCaP cells. Biochem Biophys Res Commun. 1996;223:141-6.
36. Chen L, Siddiqui S, Bose S, *et al*. Nrdp1-mediated regulation of ErbB3 expression by the androgen receptor in androgen-dependent but not castrate-resistant prostate cancer cells. Cancer Res. 2010;70: 5994-6003.
37. Mikhailova M, Wang Y, Bedolla R, Lu XH, Kreisberg JI, Ghosh PM. AKT regulates androgen receptor-dependent growth and PSA expression in prostate cancer. Adv Exp Med Biol. 2008;617:397-405.
38. Hsieh JT, Wu HC, Gleave ME, von Eschenbach AC, Chung LW. Autocrine regulation of prostate-specific antigen gene expression in a human prostatic cancer (LNCaP) subline. Cancer Res. 1993;53: 2852-7.
39. Ghosh PM, Malik SN, Bedolla RG, *et al*. Signal transduction pathways in androgen-dependent and -independent prostate cancer cell proliferation. Endocr Relat Cancer. 2005;12:119-34.
40. Wang Y, Kreisberg JI, Bedolla RG, Mikhailova M, deVere White RW, Ghosh PM. A 90 kDa fragment of filamin A promotes Casodex-induced growth inhibition in Casodex-resistant androgen receptor positive C4-2 prostate cancer cells. Oncogene. 2007;26: 6061-70.
41. Wang Y, Mikhailova M, Bose S, Pan CX, deVere White RW, Ghosh PM. Regulation of androgen receptor transcriptional activity by rapamycin in prostate cancer cell proliferation and survival. Oncogene. 2008;27:7106-17.
42. Shi XB, Xue L, Tepper CG, *et al*. The oncogenic potential of a prostate cancer-derived androgen receptor mutant. Prostate. 2007;67: 591-602.
43. Beer TM, Ryan CW, Venner PM, *et al*. Intermittent chemotherapy in patients with metastatic androgen-independent prostate cancer: results from ASCENT, a double-blinded, randomized comparison of high-dose calcitriol plus docetaxel with placebo plus docetaxel. Cancer. 2008;112:326-30.
44. Brawer MK. Recent progress in the treatment of advanced prostate cancer with intermittent dose-intense calcitriol (DN-101). Rev Urol. 2007;9:1-8.
45. Ma Y, Yu WD, Kong RX, Trump DL, Johnson CS. Role of nongenomic activation of phosphatidylinositol 3-kinase/Akt and mitogen-activated protein kinase/extracellular signal-regulated kinase kinase/extracellular signal-regulated kinase 1/2 pathways in 1,25D3-mediated apoptosis in squamous cell carcinoma cells. Cancer Res. 2006;66:8131-8.
46. Mehta RG. Stage-specific inhibition of mammary carcinogenesis by 1alpha-hydroxyvitamin D5. Eur J Cancer. 2004;40:2331-7.
47. Sanchez-Martinez R, Zambrano A, Castillo AI, Aranda A. Vitamin D-dependent recruitment of corepressors to vitamin D/retinoid X receptor heterodimers. Mol Cell Biol. 2008;28:3817-29.
48. Urbanucci A, Waltering KK, Suikki HE, Helenius MA, Visakorpi T. Androgen regulation of the androgen receptor coregulators. BMC Cancer. 2008;8:219.
49. Bao BY, Hu YC, Ting HJ, Lee YF. Androgen signaling is required for the vitamin D-mediated growth inhibition in human prostate cancer cells. Oncogene. 2004;23:3350-60.
50. Lin HK, Yeh S, Kang HY, Chang C. Akt suppresses androgen-induced apoptosis by phosphorylating and inhibiting androgen receptor. Proc Natl Acad Sci U S A. 2001;98:7200-5.
51. Hofman K, Swinnen JV, Verhoeven G, Heyns W. E2F activity is biphasically regulated by androgens in LNCaP cells. Biochem Biophys Res Commun. 2001;283:97-101.
52. Beer TM, Garzotto M, Park B, *et al*. Effect of calcitriol on prostate-specific antigen in vitro and in humans. Clin Cancer Res. 2006;12:2812-6.
53. Ghosh PM, Bedolla R, Mikhailova M, Kreisberg JI. RhoA-dependent murine prostate cancer cell proliferation and apoptosis: role of protein kinase Czeta. Cancer Res. 2002;62:2630-6.
54. Ghosh PM, Mikhailova M, Bedolla R, Kreisberg JI. Arginine vasopressin stimulates mesangial cell proliferation by activating the epidermal growth factor receptor. Am J Physiol Renal Physiol. 2001;280:F972-9.
55. Brinkmann AO, Blok LJ, de Ruiter PE, *et al*. Mechanisms of androgen receptor activation and function. J Steroid Biochem Mol Biol. 1999;69:307-13.
56. Shi XB, Ma AH, Xia L, Kung HJ, de Vere White RW. Functional analysis of 44 mutant androgen receptors from human prostate cancer. Cancer Res. 2002;62:1496-502.

Published in final edited form as:
Endocr Relat Cancer. 2010 December ; 17(4): 857–873. doi:10.1677/ERC-10-0081.

Genome-wide analysis of androgen receptor binding and gene regulation in two CWR22-derived prostate cancer cell lines

Honglin Chen[1], **Stephen J Libertini**[1,4], **Michael George**[1], **Satya Dandekar**[1], **Clifford G Tepper**[2], **Bushra Al-Bataina**[1], **Hsing-Jien Kung**[2,3], **Paramita M Ghosh**[2,3], and **Maria Mudryj**[1,4]

[1]Department of Medical Microbiology and Immunology, University of California Davis, 3147 Tupper Hall, Davis, California 95616, USA

[2]Division of Basic Sciences, Department of Biochemistry and Molecular Medicine, Cancer Center, University of California Davis, Sacramento, California 95817, USA

[3]Department of Urology, University of California Davis, Sacramento, California 95817, USA

[4]Veterans Affairs Northern California Health Care System, Mather, California 95655, USA

Abstract

Prostate carcinoma (CaP) is a heterogeneous multifocal disease where gene expression and regulation are altered not only with disease progression but also between metastatic lesions. The androgen receptor (AR) regulates the growth of metastatic CaPs; however, sensitivity to androgen ablation is short lived, yielding to emergence of castrate-resistant CaP (CRCaP). CRCaP prostate cancers continue to express the AR, a pivotal prostate regulator, but it is not known whether the AR targets similar or different genes in different castrate-resistant cells. In this study, we investigated AR binding and AR-dependent transcription in two related castrate-resistant cell lines derived from androgen-dependent CWR22-relapsed tumors: CWR22Rv1 (Rv1) and CWR-R1 (R1). Expression microarray analysis revealed that R1 and Rv1 cells had significantly different gene expression profiles individually and in response to androgen. In contrast, AR chromatin immunoprecipitation (ChIP) combined with promoter DNA microarrays (ChIP-on-chip) studies showed that they have a similar AR-binding profile. Coupling of the microarray study with ChIP-on-chip analysis identified direct AR targets. The most prominent function of transcripts that were direct AR targets was transcriptional regulation, although only one transcriptional regulator, CCAAT/enhancer binding protein δ, was commonly regulated in both lines. Our results indicate that the AR regulates the expression of different transcripts in the two lines, and demonstrate the versatility of the AR-regulated gene expression program in prostate tumors.

Introduction

Multiple studies have demonstrated heterogeneity in prostate carcinoma (CaP), a multifocal disease where tissue architecture and genetic expression are altered not only with disease progression but also between metastatic lesions of patients with prostate cancer (Nwosu *et*

Correspondence should be addressed to M Mudryj at Department of Medical Microbiology and Immunology, University of California, Davis; mmudryj@ucdavis.edu.

Supplementary data

This is linked to the online version of the paper at http://dx.doi.org/10.1677/ERC-10-0081.

Declaration of interest

The authors declare that there is no conflict of interest that could be perceived as prejudicing the impartiality of the research reported.

al. 2001, Beheshti *et al*. 2002, Liu *et al*. 2004, Shah *et al*. 2004). Comparison of metastatic lesions from the same patient as well as different patients showed that metastatic hormone-refractory prostate cancer has a heterogeneous morphology, immunophenotype, and genotype, demonstrating that 'metastatic disease' is a group of diseases even within the same patient (Shah *et al*. 2004). As prostate cancer can progress from an organ-confined, localized state to metastasis, the problem in treating the disease is the identification of therapeutic targets that are common to all the foci within the same patient or in multiple patients. As most CaPs are initially present as androgen-dependent neoplasms, androgen ablation therapy (chemical castration) is an effective treatment, which initially blocks androgen receptor (AR) cell signaling in almost all patients. Although this therapy is initially successful, castration-resistant androgen-independent tumors that are refractory to hormonal therapeutic interventions emerge (Huggins & Hodges 1941, Gittes 1991). Androgen-independent CaPs continue to express the AR and androgen-regulated genes. Thus, a better understanding of the action of AR is a pivotal issue in defining the molecular events that lead to the progression of CaP. However, it is unclear whether requirement for AR function in various foci and metastatic lesions within the same patient or similar groups of patients is the same.

Various studies have indicated that the function of the AR depends on the biochemical environment in which it exists (Ruizeveld de Winter *et al*. 1994, Li *et al*. 2002). As a member of the nuclear receptor superfamily that functions as a ligand-dependent transcription factor, AR mediates androgen-regulated gene expression. Androgen-bound AR is stabilized and translocated into the nucleus to regulate the expression of target genes by binding to androgen response elements (AREs) or by interacting with other transcription factors bound to their specific recognition sites. The role of AR in CaP progression is to promote expression of specific target genes. For example, prostate-specific antigen (*PSA*), the best studied AR target gene, has been reported to contribute to CaP progression through its protease activity and its ability to induce epithelial–mesenchymal transition and cell migration (Borgono & Diamandis 2004, Whitbread *et al*. 2006). Other AR target genes implicated in CaP progression include *FGF8*, *Cdk1* and *Cdk2*, *PMEPA1*, *TMRPSS2*, and amyloid precursor protein (Gregory *et al*. 1998, Lin *et al*. 1999, Gnanapragasam *et al*. 2002, Xu *et al*. 2003, Takayama *et al*. 2009). However, the function of the AR is tightly regulated by the expression of co-factors that are themselves regulated by various transcription factors, including the AR. Studies revealed differential expression of co-regulators with disease progression, which may have led to altered AR function (Li *et al*. 2002). Hence, an important point of investigation in prostate cancer research is to determine whether the AR functions similarly or differently in various metastatic lesions within the same patient.

Since the last decade, microarray techniques have been applied extensively in searching for genes that are AR regulated specifically in prostate tumors. Although gene expression profiling is a powerful technique for depicting the global function of the AR in a specified model, it does not distinguish whether alteration of gene expression is dependent on a direct or indirect action of AR. Moreover, despite the well-characterized AREs in the promoter and enhancer, little is known about AR *cis*-regulatory sites across the human genome. Chromatin immunoprecipitation (ChIP-on-chip) technology has been used for the identification of chromosomal-binding sites of transcription factors to identify novel targets (Cawley *et al*. 2004, Bernstein *et al*. 2005). Therefore, coupling microarray studies with ChIP-on-chip allows the identification of *bona fide* AR target genes. Wang *et al*. (2007) mapped the AR-binding sites on chromosomes 21 and 22 in androgen-dependent LNCaP human prostate cancer cells by combining ChIP with tiled oligonucleotide microarrays. Later, they followed up with comparisons between LNCaP versus a castrate-resistant CaP (CRCaP) variant of LNCaP cells (Wang *et al*. 2009), in an attempt to identify direct AR-dependent target genes in both androgen-dependent CaP as well as in CRCaP, and determined that the role of the

AR in CRCaP is to execute a distinct program resulting in androgen-independent growth. Significantly, targets identified by one group in a CRCaP subline of LNCaP cells (Wang *et al.* 2009) were not identical to those in another LNCaP subline, C4-2B, shown in a different study (Jia *et al.* 2008), which mapped AR-occupied regions as well. A third study, which used PC3 cells transfected with wild-type AR (Lin *et al.* 2009), also identified distinct AR-occupied regions in target genes. The differences in these results may be attributed to differences in the technologies used to study AR-binding sites. An alternative explanation may be that because of the heterogeneity of gene expression in different CaP foci and metastatic lesions, the programs regulated by the AR in each deposit, even within the same patient, may be distinct.

The CWR22 androgen-dependent xenograft model, which mimics human prostate cancer, has been used to study the emergence of CRCaP (Wainstein *et al.* 1994). In male nude athymic mice, this xenograft exhibits androgen-dependent growth and secretes PSA. After androgen withdrawal, the tumors regress and PSA levels plummet. Importantly, the model simulates the clinical course of prostate cancer, in that PSA levels eventually increase and CRCaP tumors emerge (Nagabhushan *et al.* 1996). Similar to most CRCaP tumors, CWR22-recurring tumors continue to express the AR (Gregory *et al.* 1998), which contains a mutation (H847Y) in the ligand-binding domain (LBD) of the molecule (Tan *et al.* 1997). Since this model recapitulates salient features of human prostate tumors, it has been used extensively to study the emergence of CRCaP.

Two cell lines, R1 and Rv1 (van Bokhoven *et al.* 2003), were isolated in separate laboratories from CWR22-relapsed tumors. Several lines of evidence indicate that they were derived from a common ancestor. Karyotypes of the two cell lines are very similar; both lines shared the same structural abnormalities, including a reciprocal translocation between chromosomes 6 and 14 (van Bokhoven *et al.* 2003). Both lines have the same AR (H847Y) mutation that is present in the parental CWR22 cells (van Bokhoven *et al.* 2003). The Rv1 AR also contains a duplication of exon 3 (that encodes the DNA-binding domain), which results in an insertion of 39 additional amino acids (Tepper *et al.* 2002). The insertion mutation was present in the relapse tumor, and the subsequent cell line was established from the tumor, but very low levels of this mutated AR could also be detected by RT-PCR in the parent CWR22 tumor (Tepper *et al.* 2002). Additionally, we and others found that R1 and Rv1 express an ~80 kDa low molecular weight form of AR (LMW-AR) with a deletion of the C-terminal LBD (Gregory *et al.* 2001, Tepper *et al.* 2002). However, though the cell lines have significant similarities, they also exhibit differences. In a recent study, we showed that R1 and Rv1 cells were distinct in their AR expression, characterization, and function (Chen *et al.* 2010). The goals of the current study were to use these two cell lines to determine similarities and differences in AR-regulated programs in two related but distinct systems with a common lineage.

Materials and methods

Cell culture and pharmacological agents

Rv1 cells were obtained from American Type Culture Collection (ATCC, Manassas, VA, USA). CWR-R1 cells were provided by Dr Elizabeth Wilson (University of North Carolina). Rv1 and R1 cells were propagated in RPMI 1640 supplemented with 5% fetal bovine serum, 2 mmol/l L-glutamine, 100 U/ml penicillin, and 100 μg/ml streptomycin (Invitrogen Life Science) at 37 °C and 5% CO_2. For studies in androgen-depleted conditions, cells were propagated in phenol red-free RPMI 1640 supplemented with 5% charcoal-stripped fetal bovine serum, 2 mmol/l L-glutamine, 100 U/ml penicillin, and 100 μg/ml streptomycin at 37 °C and 5% CO_2.

Western immunoblot analysis

Cells were directly placed in a radioimmunoprecipitation assay lysis buffer that contained the Sigma protease inhibitor cocktail (AEBSK, aprotinin, E64, leupeptin, and pepstatin as well as 1 μM calpeptin; Sigma–Aldrich). Thirty micrograms of protein were separated on 8, 10, or 12% SDS-PAGE gels and transferred to 0.22μM nitrocellulose-supported membrane (GE Healthcare, Piscataway, NJ, USA). The membrane was blocked with 5% nonfat dry milk in PBS and 0.1% Tween-20 before the addition of specific antibodies. The following antibodies were used: AR (central) 441 (Ab-1; Lab Vision Corp., Fremont, CA, USA), AR NH_2-terminus N-20 (Santa Cruz Biotechnology, Inc., Santa Cruz, CA, USA), calpain 2 (Sigma), calpastatin, ERK and phosphoERK (Cell Signaling, Danvers, MA, USA), and focal adhesion kinase (clone 4.47; Millipore, Billerica, MA, USA). Proteins were detected using chemiluminescence (GE Healthcare).

Microarray analysis

Labeling of samples, hybridization to U133A Gene-Chips (Affymetrix, Santa Clara, CA, USA), staining, and scanning were performed as described in the Affymetrix Expression Analysis Technical Manual. Fluorescence intensity values (.CEL files) generated from hybridized, stained GeneChips were analyzed with R statistical software (v.2.01, and 'affy' BioConductor package) and BRB Array Tools to identify genes that were differentially expressed. The settings used for Robust Multichip Analysis in R included Microarray Suite 5.0-based background correction, quantile normalization, and Robust Multichip Analysis-based algorithms for calculation of expression values using perfect match only fluorescence intensities. Detection at $P \leq 0.05$ and a mean fold change of ≥1.5-fold were used as criteria for filtering genes for clustering analyses. Hierarchical clustering and comparative fold change analysis were used to identify and group similar patterns of gene regulation. Assignment of genes to functional categories was done by annotation of gene lists with the program, Database for Annotation, visualization, and Integrated Discovery (http://apps1.niaid.nih.gov/david), and literature-based classification was done by hand. Statistically overrepresented (Fisher's exact probability score <0.05) biological processes within clusters were identified using Expression Analysis Systematic Explorer v.1.0 analysis software (Hosack *et al.* 2003).

Quantitative real-time PCR

Total cellular RNA was prepared from Rv1 cells using RNeasy mini kit (Qiagen, Inc.) based on the manufacturer's protocol. cDNA was synthesized from 1 μg RNA using QuantiTect (Qiagen) reverse transcription kit based on the manufacturer's protocol. cDNAs were diluted 1:4 in ddH_2O, and 2 μl diluted cDNA was added to 5 μl of EXPRESS SYBR GreenERTM qPCR supermix (Invitrogen Life Science) and 200 nM of each primer. GAPDH, HPRT, or RPL13A was used as the endogenous expression standards. PCR conditions were initial denaturation step at 95 °C for 20 s, 40 cycles at 95 °C for 3 s, 60 °C for 30 s, followed by additional 95 °C for 15 s and 60–95 °C over 20 min ramp for melt curve analysis. Primer sequences used in the study are provided in Supplementary Methods (see section on supplementary data at the end of this article). Data were collected by the Mastercycler ep Realplex (Eppendorf AG, Hamburg, Germany). Primer sequences are available upon request.

Ingenuity pathway analysis

The microarray expression data were uploaded into ingenuity pathway analysis (IPA) software using Reference sequence (RefSeq). A total of 2322 genes were mapped using the IPA database. Fold change of 1.5 and *P* value of ≤0.05 were applied as the cutoff criteria. Gene networks were algorithmically generated based on their connectivity and were

assigned a score. A score of 3 or higher indicates a 99.9% confidence level that the network was not generated by chance alone. Canonical pathway analysis identifies the pathways from the IPA library of canonical pathways, which are most significant to the input dataset. The significance of the association between the dataset and the canonical pathway is determined based on two parameters: 1) a ratio of the number of genes from the dataset, which map to the pathway, divided by the total number of genes that map to the canonical pathway and 2) a *P* value calculated using Fischer's exact test determining the probability that the association between the genes in the dataset and the canonical pathway is due to chance alone.

ChIP-on-chip analysis

Tiling array analysis was performed with GeneChip Human Promoter 1.0R Arrays (Affymetrix) in order to determine genome-wide analysis of AR recruitment sites. Briefly, AR-associated DNA was enriched by ChIP as described earlier (Louie *et al.* 2003, Desai *et al.* 2006). ChIPs using a pre-immune IgG were used as controls. ChIP DNA (10 μl) and input (10 ng) samples were amplified using the GenomePlex Complete Whole Genome Amplification (WGA) kit (Sigma–Aldrich) with a modification to the manufacturer's protocol to generate product suitable for Affymetrix microarray analysis by including dUTP (80 μM final concentration) in the amplification and re-amplification (if necessary) reactions. WGA products were purified with QIAquick PCR purification kit, eluted in nuclease-free water (Invitrogen), and quantitated with a NanoDrop 2000c spectrophotometer (Thermo Scientific). Target preparation and tiling array-processing procedures were performed according to Affymetrix's standard protocols. Briefly, 7.5 μg DNA was fragmented through the combined actions of uracil DNA glycosylase and human apurinic endonuclease and then end labeled with biotin using terminal deoxynucleotidyl transferase. Labeled target DNA was hybridized to the arrays at 45 °C for 16 h. Subsequently, the arrays were washed and stained using the Fluidics Station 450 (Affymetrics, Santa Clara, CA, USA) according to the manufacturer's protocol and then scanned with the GeneChip Scanner 3000 7G. Data analysis was performed with CisGenome software (Ji *et al.* 2008). AR-binding regions (i.e. ChIP-enriched) were identified by comparing with the nonspecific IgG control using the TileMap peak detection tool (Ji & Wong 2005) with the application of a hidden Markov model. Subsequently, genomic locations of peaks and bound probes were visualized in the CisGenome and UC Santa Cruz genome browsers.

Results

Comparison of the gene expression profiles of R1 and Rv1 cells

We have described earlier the characteristics of R1 and Rv1 cells derived from two different relapsed tumors although both from the same parental CWR22 xenograft (Chen *et al.* 2010). To further define the differences and similarities between the two CWR22 relapsed lines, we used the Affymatix HG-U133 Plus2.0 Gene Chip microarray to identify differences in gene transcription. The analysis was conducted in duplicate in R1 and Rv1 cells cultured in identical conditions, at the same density in charcoal-stripped serum or 2 h after the addition of 10 nM DHT. The 2 h time point was chosen to identify transcripts that are more likely to be direct AR targets, and other laboratories had previously determined this concentration of DHT to be optimal for AR stimulation (Wang *et al.* 2007).

Comparison of R1 and Rv1 gene expression profiles in castrate levels of androgen identified 1275 genes that were differentially expressed (fold change ≥1.5 or ≤−1.5; $P \leq 0.05$) in R1 versus Rv1 cells in the absence of androgens and 1941 transcripts that were differentially expressed (fold change ≥1.5 or ≤−1.5; $P \leq 0.05$) in R1 versus Rv1 cells treated for 2 h with 10 nM DHT (Fig. 1A; Supplementary Table 1, see section on supplementary data given at the

end of this article). Significantly, only 60% of genes differentially expressed in R1 versus Rv1 in the presence of DHT were identical to the transcripts that were differentially expressed in the absence of androgen (Fig. 1A; Supplementary Table 1). These results indicated that the R1 and Rv1 cells were genetically distinct and could serve as models for comparison of two different metastasized CaP lesions derived from the same patient.

We verified the specificity and selectivity of the results obtained with the microarray analysis by comparing these results to known differences between the two lines. We had shown earlier that R1 cells expressed increased levels of calpain 2 mRNA compared to Rv1 cells, whereas the levels of the calpain inhibitor calpastatin were similar in both lines (Chen *et al.* 2010). A similar pattern was seen by the current gene expression studies, thereby authenticating the results (Supplementary Table 1; Fig. 1B). R1 cells also expressed 11.7-fold higher levels of c-MET mRNA (Supplementary Table 1; Fig. 1B). Rv1 cells have more neuroendocrine characteristics than R1 cells because of a greater expression of neuronal-specific enolase (ENO2; 12-fold change; $P = 0.02$; Supplementary Table 1; Fig. 1B), chromogranin A and B (2.74- and 8.69-fold increase respectively), and synaptophysin (3.34-fold increase; Supplementary Table 1). ENO2 expression was not altered by androgen (data not shown). These results also show the accuracy of the gene expression analysis system in these studies.

Based on the gene expression analysis, the most differentially expressed genes between R1 and Rv1 (expression in the absence of androgen) include *TARP*, *IGFBP5*, *STEAP1*, *NMNAT2*, and *SNAI2* (listed in Fig. 1C). To identify patterns in differential gene expressions, IPA was used to identify the pathways that differed in the two cell lines. The Fisher's exact test was used to determine the probability that the association between the dataset and a given pathway is due to chance alone. The most significant pathway differences between R1 and Rv1 cells both in the presence and absence of androgen involved metabolic pathways (Fig. 1D). In summary, the gene expression profiles of R1 and Rv1 indicate that although these two lines were derived from the same CWR22 xenograft and have similar morphologies, at the molecular level, they are distinct.

Analysis of genes differentially regulated in R1 versus Rv1 cell lines in response to androgen treatment

Since the gene expression profile of R1 versus Rv1 cells was vastly different, we investigated whether these genes behaved similarly in response to DHT treatment. Using the same gene expression data that were used in Fig. 1, we analyzed genes that were differentially regulated in the two cell lines in response to a 2 h androgen treatment. Using a cutoff value of fold change ≥ 1.5 or ≤ -1.5 and $P \leq 0.05$, we found that in Rv1 cells, the expression of 854 transcripts was altered by a 2 h DHT treatment, whereas in R1 cells, the expression of only 77 transcripts changed after the addition of DHT for 2 h (Fig. 2A; Supplementary Table 2, see section on supplementary data given at the end of this article). Therefore, the transcriptional response to DHT was greater in Rv1 cells than in R1 cells. A comparison of the DHT-responsive R1 and Rv1 transcripts identified only ten genes that were commonly regulated in both cell lines (Fig. 2B), again indicating the large differences between these two lines. This included seven genes that were upregulated by DHT in both R1 and Rv1 cells, including *CEBPD* and *N*-acetyltransferase type I (*NAT1*), and three that genes were repressed in both cells, including *CLDN4*. Interestingly, the expression of HES1, a component of the Notch signaling pathway (Fischer & Gessler 2007), was DHT regulated in both cell lines, but expression was repressed in R1 cells and activated in Rv1 cells (Fig. 2B). Androgen-dependent regulation of six of these transcripts was validated by real-time PCR, which verified the accuracy of these results (compare Fig. 2C with Supplementary Table 2). The expression of two well-known androgen-responsive genes *KLK3* (*PSA*) and *TMPRSS2* was not significantly altered by DHT in either cell line, thus confirming previous

reports that the transcripts are not androgen regulated in these cell lines (Riegman *et al.* 1991, Lin *et al.* 1999, Tomlins *et al.* 2005).

It is possible that the discrepancy in the number of DHT-regulated transcripts in R1 and Rv1 cells is due to a delay in the DHT response in R1 cells. To address this possibility, we looked at the expression of transcripts that were DHT regulated in R1 and Rv1 cells (NAT1 and TSC22D1), only in R1 cells (FKBP5), or only in Rv1 cells (KRIT1, p27, and FABP7) at 0, 2, 4, and 18 h after DHT addition (Fig. 2D). The time course for transcripts that were regulated in both lines was similar but not identical in the two cell lines. Interestingly, the induction of FKBP5 was more robust in R1 cells than in Rv1 cells; therefore, in the array, study expression in Rv1 cells 2 h after DHT addition was below our cutoff value. In concordance with the array analysis, KRIT1 and p27 were not DHT transactivated in R1 cells. The expression of FABP7 was elevated in Rv1 cells in a time-dependent manner, but in R1 cells, the expression was repressed in a time-dependent manner. This analysis argues that the smaller number of DHT-regulated transcripts in R1 cells is not due to a general delay in response to hormone stimulation.

DHT-regulated pathways in R1 and Rv1 cells

Since the genes regulated by androgens in the two cell lines are different, we asked whether the pathways they regulated were also different, or whether androgen was regulating the same programs in both cells but through different mechanisms. The differentially expressed genes in response to DHT for 2 h were analyzed by IPA to identify most significantly associated biological networks and canonical pathways (metabolic and cell signaling) altered in the two cell lines. The Fisher's exact test was used to determine the probability that the association between the dataset and a given pathway is due to chance alone. IPA identified two significant biological networks associated with the differentially expressed genes in R1 cells (the major one is shown in Fig. 3A, and the other one is shown in Supplementary Figure 1, see section on supplementary data given at the end of this article), whereas in Rv1 cells, a total of 18 biological networks were identified, which are significantly associated with the differentially expressed genes (the major network is shown in Fig. 3A, and the others are shown in Supplementary Figure 2, see section on supplementary data given at the end of this article). In R1 cells, the significantly associated functions affected by DHT treatment include gene expression, cellular development, cell cycle, and embryonic development (Fig. 3B). The canonical pathways most significantly associated with DHT treatment are notch signaling, clathrin-mediated endocytosis, JAK/Stat signaling, and p53 signaling (Fig. 3C). The significantly associated functions in Rv1 cells include cellular development, visual system development and function, cancer, cell cycle, molecular transport, and protein trafficking (Fig. 3B), whereas the most associated canonical pathways include aminoacyl-tRNA biosynthesis, axonal guidance signaling, DNA damage response, cell cycle, p53 signaling, and clatrin-mediated endocytosis (Fig. 3C). These results indicate a greater biological role of AR in Rv1 cells compared to R1 cells. However, a number of cellular functions and canonical pathways regulated by DHT treatment in the two cells lines are similar, suggesting that in the two cell lines, the AR plays a similar role, but employs different mechanisms.

The activity of the AR is affected by multiple co-regulators that serve as co-activators or co-repressors of AR-dependent transcription (Devlin & Mudryj 2009, Heemers *et al.* 2009). Since the differences in DHT-inducible gene expression could be due to the expression of a different cohort of AR co-regulators, we compared the expression of these proteins in the two cell lines in the presence and absence of androgen (Table 1). The number of co-regulators that were expressed at higher levels was greater in R1 than in Rv1 cells. R1 cells had higher levels of 22 co-activators, whereas Rv1 cells had higher levels of 13 co-activators. R1 cells had higher levels of eight co-repressors, and Rv1 cells had higher levels

of seven co-repressors. However, it is notable that there were differences in co-regulator levels in the presence or absence of androgen. Most of these differences were due to the DHT-dependent regulation of co-regulator expression in Rv1 cells. The only AR co-regulator that was differentially expressed after DHT addition in R1 cells was HEY1.

AR chromosomal-binding sites in R1 and Rv1 cells in response to DHT

Next, we asked why the cohort of androgen-regulated transcripts differed in R1 and Rv1 cells. Hence, we determined whether AR binding to regulatory regions differed significantly between the two cell lines. The Human Promoter 1.0R Array (Affymetrix) oligonucleotide (25-mer)-based, high-density tiling array that covers 25 500 promoters with probe sets spanning at least 10 kb of genomic content per gene (~7.5 kb upstream and ~2.45 kb downstream of the transcriptional start site (TSS)) and at a resolution of 35 bp was used to identify AR-binding sites in the entire genome in both cell lines. A total of 1225 and 2021 AR-binding sites (FDR≤0.05) were identified in R1 and Rv1 cells respectively when treated with DHT for 2 h. Figure 4A shows the distribution of the binding sites along chromosomes in two cell lines. A comparison of AR binding across chromosomes in R1 and Rv1 cells treated with DHT showed that AR-binding pattern was similar, but not identical (Fig. 4B). Certain sites were AR bound only in Rv1 cells, whereas others were AR bound only in R1 cells. This analysis indicated that AR binding after the addition of DHT was more extensive in Rv1 than in R1 cells, and most of the R1 AR-bound sites were also AR bound in Rv1 cells. Therefore, although the androgen-regulated gene expression profile of the two cell lines is different, the AR-binding pattern is similar.

To validate our results, we focused on the binding pattern for three well-known androgen-responsive genes *KLK3* (*PSA*; Riegman *et al.* 1991), *NKX3.1* (He *et al.* 1997), and *TMPRSS2* (Tomlins *et al.* 2005) in R1 and Rv1 cells. Gene expression studies had shown that neither *KLK3* nor *TMPRSS2* was androgen regulated in either cell line; however, both genes bound AR. In Rv1 cells, sequences near the *KLK3* (*PSA*) gene bound AR (−4603, −3484, and −2499 upstream of its TSS), whereas there was no AR binding near or in the *KLK3* gene in R1 cells (Fig. 4C). AR binding to *NKX3.1* chromosomal region was identified in both R1 and Rv1 cells. In R1 cells, AR bound in the 3′-UTR (2149 downstream of TSS) of the *NKX3.1* gene, whereas in Rv1 cells, AR bound not only in the 3′-UTR (2059 downstream of TSS) but also in the intron (1164 downstream of TSS) of *NKX3.1* (Fig. 4C). This result is consistent with a recent study that identified androgen-responsive elements in the 3′-UTR of the *NKX3.1* gene (Thomas *et al.* 2010).

AR binding in the 5′-UTR (two sites: 6382 and 7179 downstream of TSS) of the androgen-regulated gene *TMPRSS2* was detected in Rv1 cells, but no binding near or in the *TMPRSS2* gene in R1 cells (Fig. 4B). Previous studies conducted in LNCaP cells detected AR binding to sequences ~14 kb upstream of the *TMPRSS2* TSS, but this sequence was not present in our promoter array. Hence, even if the AR bound to this section of *TMPRSS2* gene in R1 or Rv1 cells, we would not detect AR binding. Therefore, we further analyzed AR binding to the four sites identified in our study using ChIP analysis (Fig. 4D). After the addition of 10 nM DHT for 2 h in Rv1 and LNCaP, AR binding was detected in Rv1 cells, but not in LNCaP cells, further confirming our results.

Motif analysis of AR-binding sites

A motif analysis of the AR-binding sites was conducted to determine whether AR binds to the established consensus ARE in these target genes. Previous studies conducted in LNCaP, LNCaP-derived cells, or AR-transfected PC3 cells (Wang *et al.* 2007, Jia *et al.* 2008, Lin *et al.* 2009) reported that only 10% or less of the AR-binding regions had a canonical class 1 ARE (AGAACAnnnTGTTCT)-binding motif when two positions were allowed to vary

from the palindromic consensus with three nucleotides spacing. Previous studies also found that between 7.8 and 8.4% of the binding regions contained the AR-binding half-site motif (AGAACA). In this study, we found that in Rv1 cells, only 4% (86/2021) of the sites had the canonical ARE and 35% (700/2021) had the AR half-site motif. Likewise, in R1 cells, 6% (76/1225) of the sites had the canonical ARE and 46% (568/1225) had the AR half-site motif (Fig. 5A). These studies indicate that the canonical ARE is not required for AR binding in the majority of the genes examined, and that the half-site is sufficient for AR function.

The expression profile of genes closest to the AR-binding sites in R1 and Rv1 cells in response to DHT

Next, we investigated whether the AR directly regulated the same cohort of genes in the two cell lines. The AR-binding sites identified in R1 and Rv1 cells were closest to 965 and 1518 genes respectively (data not shown). Notably, although some closest genes only contained one AR-binding site, many others had more than one AR-binding sites.

By combining the ChIP-on-chip with microarray expression data, we identified that, of the 854 differentially regulated genes in Rv1 cells in response to DHT for 2 h (Fig. 2A), AR bound to nearby chromosomal sites (FDR≤0.05) of only 53 genes (6%). The location of the AR-binding sites includes intron (15 genes), exon (2 genes), 5′-UTR (9 genes), 3′-UTR (3 genes), and within 5 kb upstream from the TSS (25 genes) (Fig. 5B; Supplementary Table 3A, see section on supplementary data given at the end of this article). Additionally, two genes had AR-binding sites that were more than 10 kb upstream of TSS, whereas three genes had AR-binding sites that were more than 10 kb downstream of the transcriptional end site (TES). The same analysis was performed in R1 cells. Of the 77 differentially regulated genes after adding DHT for 2 h, AR bound to the nearby chromosomal regions (FDR≤0.05) of 32 genes (42%). The identified AR-binding sites include intron (4 genes), 5′-UTR (3 genes), 3′-UTR (2 genes), within 5 kb upstream of the TSS (8 genes), more than 10 kb upstream of the TSS (14 genes), and more than 10 kb downstream of the TES (8 genes) (Fig. 5B; Supplementary Table 3). The AR-binding site that is far upstream or downstream of the androgen-responsive genes resides within or downstream of other annotated genes (Supplementary Table 3). However, the nearest genes are not androgen regulated. The ability of the AR to bind to sequences within one gene, but regulate transcription of a more distant gene has been reported earlier (Wang *et al.* 2009). Taken together, our results indicate that a much higher number of genes are androgen regulated in Rv1 cells compared to R1 cells. However, of the androgen-regulated genes in RV1 cells, only a few are regulated directly by AR, whereas in R1 cells, almost 50% of the genes that are androgen regulated resulted from direct AR transcriptional activity.

IPA analysis showed that the biological functions most prominently associated with these 53 genes in RV1 cells were transcriptional regulation, cell cycle, and metabolic process (Fig. 5C), whereas the major biological functions associated with the 32 genes identified in R1 cells are transcriptional regulation and metabolic process (Fig. 5C); hence, transcriptional regulation and metabolic process are biological functions, which are AR regulated in both cell lines, whereas cell cycle regulation is apparent in Rv1 cells. Therefore, these results support our earlier assertion that the AR regulated multiple common pathways in R1 and Rv1 cells, but that the AR has additional roles in Rv1 cells. The AR effect on gene expression in Rv1 cells is more extensive; however, the effect of the AR on majority of androgen-regulated genes in R1 is through direct transcriptional activity, whereas the effect of the AR on the majority of androgen-regulated genes in Rv1 cells is indirect.

Identification of common genes that are androgen regulated by direct AR transcriptional activity in both R1 and Rv1 cells

A comparison of R1 and Rv1 cells revealed that the majority of the AR-bound sites near the differentially regulated genes were common. However, only two closest genes (CCAAT/enhancer binding protein δ (*CEBPD*) and arylamine *NAT1*) adjacent to the common AR-binding sites in both R1 and Rv1 cells showed correlated transcriptional regulation (fold change 1.5 and $P<0.05$) in both lines. Claudin 4 (*CLDN4*) was androgen regulated in both cell lines, and in both lines, AR binding was detected, but the AR sites were distinct. This argues that only a subset of AR chromosomal-binding sites exhibit transcriptional regulation. Of these three common AR direct targets, *CEBPD* and *NAT1* have been reported to be androgen-responsive genes (Yang *et al.* 2001, Butcher *et al.* 2007), and *CLDN4* has been reported to be deregulated in both primary and metastatic prostate cancer (Landers *et al.* 2008).

Previous studies from other laboratories showed that other transcription factors collaborate with the AR to induce gene regulation (Wang *et al.* 2007, 2009, Jia *et al.* 2008, Lin *et al.* 2009). Considering that other transcription factors might play a collaborative role in AR function, we used a transcription element search system (TESS) to screen for motifs that most frequently co-existing with AR-binding motifs present in the above differentially regulated genes. TESS identifies transcription factor motifs using site or consensus strings and positional weight matrices from the TRANSFAC, JASPAR, IMD, and the CBIL-GibbsMat database (www.cbil.upenn.edu/tess). Using these databases, we found that the transcription factor motifs that most frequently co-exist with AR-binding motifs included GRE, GATA-binding protein (GATA), Sp-1, and forkhead box J2 (FoxJ2) in both R1 and Rv1 cells (not shown). Significantly, previous studies identified GATA- and FoxA1-binding site near AR-binding site (Wang *et al.* 2007, Lin *et al.* 2009).

Our analysis of direct AR target genes in R1 cells revealed that ~25% of genes (seven genes – *NAT1*, *NKX3.1*, *CEBPD*, *HEY*, *POP1*, *PHF20L1*, and *NDRG1*) mapped to chromosome 8 (Fig. 6A), and all were positively regulated by androgen. Hey is one of the primary targets of the Delta-Notch signaling pathway and functions primarily as transcriptional repressors (Fischer & Gessler 2007). Furthermore, one of the AR sites has a single half ARE (*POP1*), whereas all of the other sites have two or three half ARE sites separated by between 40 and several thousand nucleotides. In Rv1 cells, 15% of the genes (eight genes – *NAT1*, *CHRNA2*, *CEBPD*, *RB1CC1*, *ZBTB10*, *PLEKHF2*,*LAPTM4B*, and*MTDH*) mapped to chromosome 8. Seven were positively regulated by androgen, whereas one was repressed (*CHRNA2*). Five of the eight AR-binding sites (NAT1, CHRNA2, CEBPD, RB1CC1, and PLEKHF2) contained at least one ARE half-site. Two of the genes were commonly regulated in both cell lines – *NAT1* and *CEBDP*, whereas the others were not. The high percentage of direct AR target genes on one chromosome indicates that chromosome 8 is exceptionally rich in AR-regulated genes.

Discussion

Outwardly, the morphology and phenotypical characteristics of the R1 and Rv1 cells appear very similar. Both are derived from CWR22-relapsed tumors, are not responsive to the anti-androgen Casodex, and express a LMW-AR that is ligand independent. Both cell lines have the same chromosomal translocations and harbor the same AR and p53 mutations (van Bokhoven *et al.* 2003), indicating they were derived from a common progenitor. However, the extensive difference in gene expression of R1 and Rv1 cells strongly argues that although they are derived from a common progenitor, at the molecular levels, they are very different. This progenitor cell must have had enough plasticity to give rise to cells with distinct molecular phenotypes. We hypothesize that the initial parent xenograft is composed

of several distinct cell types and that the CRCaP cells constitute a small component of morphologically indistinct cells that expanded after the selective pressure of androgen ablation. The current study indicated that even tumors that appear to be homogenous may be composed of several cell types, thus further complicating gene expression analysis.

Most CRCaP tumors and cells continue to express the AR, and the AR continues to regulate gene expression. It was, however, unclear whether in these cells the AR is regulating a distinct set of genes. Previous studies have characterized the gene expression profile of LNCaP-derived CRCaP cells. One study found that the expression of several genes associated with mitosis was AR regulated in the LNCaP-abl cells (Wang *et al.* 2009), whereas an analysis of C4-2B cells identified a different cohort of DHT-regulated transcripts (Jia *et al.* 2008). These studies revealed that AR gene regulation patterns change with disease progression; however, the results from the two studies revealed significant differences in AR-mediated gene regulation in the two LNCaP-derived cell lines. This difference could have arisen because of differences in experimental conditions, or could have been due to inherent alterations in AR-driven programs in the two cell lines. To distinguish between these two possibilities, we analyzed AR-driven gene expression in two related but distinctive cell lines arising from a common progenitor.

The current analysis of androgen-regulated gene transcription in R1 and Rv1 cells revealed that AR-regulated gene expression patterns are very different between these two related cell lines. In R1 cells, the Notch signaling pathway is the most identifiable DHT-regulated pathway. In Rv1 cells, the Notch pathway is not DHT regulated, and the most prominent DHT-regulated pathway includes aminoacyl-tRNA biogenesis, DNA damage response, axonal guidance signaling, and JAK/Stat signaling. However, an analysis of direct AR target genes in R1 (9 mappable genes by IPA analysis) and Rv1 (11 mappable genes by IPA analysis) cells revealed that the most common function by far involved regulation of transcription, whereas the second most common functions were regulation of the cell cycle or metabolism. Therefore, even though the AR uses different tools for gene regulation in the two cell lines, it performs the same function in both, pointing to the versatility in the regulation of cell function. Our results indicate that in the two cell lines, the AR achieves the same goal using different pathways. This may be the reason why so many cancer drugs fail – each drug targets a single pathway, but as soon as one lesion is affected by one drug, other pathways that can bypass the drug target arise.

The most common function of DHT-regulated transcripts involves regulation of transcription. In R1, this includes DHT-mediated regulation of two downstream effectors of Notch signaling, the Hes-1 and Hey-1 transcriptional repressors. However, the DHT-mediated regulation of the two repressors is different. Hes1 expression is DHT repressed, whereas Hey1 levels are higher in R1 cells in the absence of androgen. Hey1 levels are even further elevated after DHT treatment. Moreover, Hey1 has been shown to be an AR co-repressor (Belandia *et al.* 2005); therefore, transactivation of Hey1 may serve as a negative feedback loop to limit AR-regulated transcription. HES1 expression is DHT transactivated in Rv1 and in C4-2B cells (Jia *et al.* 2008). HES1, but not HEY1, knockout mice have defects in neurulation and have premature differentiation of neuronal precursors, suggesting that HES1 has a more prominent role in cells that have a neuronal lineage. It is notable that Rv1 and LNCaP cells have neuroendocrine characteristics. An interaction of HES1 with the AR has not been reported, and the different levels of these two transcriptional co-regulators may be in part responsible for the differences in AR-dependent transcription in the two cell lines.

Mitotic genes identified as DHT targets in LNCaPabl (Wang *et al.* 2009) were not DHT regulated in R1 or Rv1 cells. However, five of the ten transcripts (CEBPD, KCNN2, NAT1,

TSC22D1, and ZBTB16) commonly regulated by DHT in R1 and Rv1 cells were also DHT regulated in C4-2B cells (Jia *et al.* 2008). A comparison of R1 and Rv1 DHT-regulated genes with DHT-regulated transcripts in PC3 cells showed that CEBPD, TSC22D1, and ACTG2 were commonly regulated (Lin *et al.* 2009). This indicates that CEBPD and TSC22D1 are commonly regulated in four different CRCaP cell lines. A further analysis found that NAT1, TSC22, and ZBTB16 (also know as PLZF) are DHT regulated in LNCaP cells or in rat prostatic tissue (Nelson *et al.* 2002, Jiang & Wang 2004, Butcher *et al.* 2007). Previous studies found that the CEBPD was androgen repressed in rat prostatic tissue, but androgen activated in CWR22 cells (Yang *et al.* 2001). It is notable that CEBPD is considered a tumor suppressor, since CEBPD silencing has been detected in cervical and hepatocellular carcinomas and its overexpression is associated with a growth arrest (Ko *et al.* 2008). The expression of CEBPD in CRCaP tumors has not been studied.

So far, the genome-wide studies of AR chromosomal binding have used the androgen-dependant LNCaP cell line, CRCaP LNCaP-derived cell lines (Takayama *et al.* 2007, Wang *et al.* 2007, Jia *et al.* 2008), and PC3 cells transiently expressing the AR (Lin *et al.* 2009). Studies of AR binding in PC3 cells transiently transfected with AR used ChIP followed by sequencing (ChIP-seq) to identify AR-binding sites associated with DHT-dependent gene regulation. The AR-binding sites had varying distances from the TSS but were preferentially located near the TSS of genes that were androgen regulated; 22.4% of the AR sites mapped were within 2 kb of the TSS and ~40% were within 12 kb of the TSS. The current study used the human promoter array with coverage of ~10 kb upstream/downstream of TSS, thus scanned regions proximal to the TSS of known genes throughout the genome. Therefore, although our analysis could not identify all AR-binding sites, it focused on known transcripts throughout the genome. The majority of AR-binding sites were located more than 2 kb upstream of the TSS in both R1 and Rv1 cells, and more AR binding was detected in Rv1 cells than in R1 cells. This correlates with our results that Rv1 cells have a greater number of DHT-regulated transcripts than R1 cells. Most of the AR sites in R1 cells were identical or similar to the sites in Rv1 cells. Consistent with previous findings, the majority of the AR-binding sites did not contain the canonical AREs. However, a significant number of the sites contained an AR half-site motif, and in many cases had more than one half-motif. Therefore, all of the studies so far indicate that the AR half-site is associated with AR binding, where the canonical ARE is rare. As reported earlier, a number of AR binding sites have either a canonical or half-site ARE. The AR may bind directly previously unidentified sequences as has been proposed by Lin *et al.* (2009), the AR may be binding to sites that deviate from the consensus ARE sequence, but binding is stabilized by adjacent co-regulator(s) or, alternatively, the AR may be binding indirectly by interacting with another DNA-binding protein.

An analysis of motifs co-present with the AR identified several transcription factors including GRE, GATA, Sp-1, and FoxJ2 in both R1 and Rv1. The GATA motif has been identified by all previous AR-binding studies (Wang *et al.* 2007, Jia *et al.* 2008, Lin *et al.* 2009). Sp1 is a very common transcription factor-binding site found in many promoter sequences. Moreover, previous studies have shown that Sp1 and the AR interact to promote transcription (Lu *et al.* 2000); therefore, the presence of Sp1 may serve to enhance AR-dependent gene expression. Studies by Jia *et al.* (2008) also found that GRE sites were co-present with AR-binding sites. The FoxJ2, a member of the forkhead family of transcription factors, has a core sequence that is common to other family members, including FoxA1. Therefore, all of the AR-binding studies indicate that GATA and forkhead transcription factor-binding sites are co-present with AR-binding sites. Previous studies have suggested that the forkhead and GATA proteins may act as ‘pioneers’ factors that are capable of initiating chromatin opening (Cirillo *et al.* 2002). GATA proteins have been proposed to play major roles in endocrine function and disease (Viger *et al.* 2008). Forkhead

transcription factors may bind to chromatin before the recruitment of subsequent transcription factors such as AR. The binding of forkhead factors appears to be dependent on histone H3K4 methylation (Lupien *et al.* 2008). The importance of the forkhead factor in AR-dependent gene expression is further substantiated by a recent report that a single nucleotide polymorphism that is associated with an increased prostate cancer risk resides in a FoxA1 site, and this polymorphism facilitates stronger androgen responsiveness (Jia *et al.* 2009). The major role of these proteins may be to open the chromatin and allow AR binding, rather than to specifically promote AR binding. Subsequent events, such as stabilizing AR/DNA interaction and recruiting appropriate co-factors to regulate gene transcription, may rely on additional factors.

A closer analysis of well-studied androgen-regulated genes identified AR binding to sequences near the *PSA* and *TMPRSS2* genes in DHT-treated Rv1 cells, but not in DHT-treated R1 cells. However, DHT treatment of Rv1 cells did not transactivate transcription of either gene. AR binding to the 3′-UTR of the *NKX3.1* gene was detected in DHT-treated R1 and Rv1 cells. A recent report showed that androgen-responsive element of this gene resides in the 3′-UTR (Thomas *et al.* 2010). AR binding to this site was more extensive in Rv1 than in R1 cells, yet NKX3.1 transcription was transactivated only in R1 cells. This indicates that although AR binding is required, it is not sufficient for AR androgen-dependent gene expression and that increased binding does not ensure increased gene expression.

By coupling gene expression profile with ChIP-on-chip analysis, we found that 42% of the differentially expressed transcripts identified in R1 contained AR-binding sites, indicating that they are most likely direct AR targets. Some of the AR-binding sites were actually in adjacent genes that were not AR regulated. In contrast, only 6% of the transcripts identified in Rv1 cells had AR-binding sites. Previous studies have shown that AR-binding sites can be far away from transcription start sites (Takayama *et al.* 2007, Wang *et al.* 2007). The coverage of the promoter array used for this study is limited within ~10 kb of transcription start sites. Therefore, the actual direct AR targets in R1 and Rv1 cells are most likely higher than what we found. Although the number of DHT-regulated genes was much higher in Rv1 cells, the number of genes that are DHT regulated and are associated with an AR-binding site is more comparable in R1 and Rv1 cells. This suggests that AR binding or AR/DNA complex stability in Rv1 cells is greater or that a large number of the DHT-regulated transcripts in Rv1 cells are indirect AR targets. Several mechanisms may account for this discrepancy. The presence of a 39aa insertion mutation in the Rv1 AR that results in the duplication of the DNA domain may facilitate DNA binding, or the interactions with other DNA-binding protein. However, previous studies have found that the 39aa insertion does not increase the sensitivity of the receptor to ligand (Tepper *et al.* 2002). The different complement of AR co-regulators in Rv1 and R1 cells is likely to govern AR binding and AR-dependent gene regulation. Since there are extensive differences in the expression of AR co-regulators in the two cell lines, further analysis will be required to identify the role of the specific co-regulators in regulating transcription of specific genes.

In summary, our study of androgen-responsive CRCaP cells lines that were derived from a common progenitor exhibits similar AR-binding profiles. The GATA, GRE, Foxj2, and Sp1-binding motifs are co-present with AR-binding sites in both cell lines. However, the DHT-dependent gene expression profile of the two cell lines is completely different. The AR is regulating a different program in the two cell lines. The combined ChIP-on-chip with microarray analysis also revealed that only a subset of genes adjacent to AR-binding sites showed differential expression in response to DHT arguing that 1) binding of AR to the vicinity of these genes is insufficient for transcriptional regulation in certain cell context or under the specific experimental conditions applied; or 2) the binding sites are indeed nonfunctional. Similarly, other groups have reported that only a subset of AR-binding sites

in LNCaP cells (Wang *et al*. 2007, Jia *et al*. 2008, Lin *et al*. 2009) or ER in MCF-7 cells (Carroll *et al*. 2006) are functional, as there are many more binding sites identified than differentially regulated genes. It is apparent that the presence of a half-ARE or AR binding is not sufficient for androgen-dependent gene regulation, and AR co-regulators are important in controlling AR-mediated transcription. As more studies of AR binding coupled with expression microarray analysis are conducted in different cellular contexts, the rules that govern AR-dependent gene expression in specific cellular context will become more apparent.

Supplementary Material

Refer to Web version on PubMed Central for supplementary material.

Acknowledgments

We thank Dr Elizabeth Wilson for the CWR-R1 cells and greatly appreciate the expert technical assistance and consultation of Ryan R Davis.

Funding

This study was supported by DOD grants PC051049 (M Mudryj), VA Merit (M Mudryj), and DOD predoctoral award PC073557 (H Chen).

References

Beheshti B, Vukovic B, Marrano P, Squire JA, Park PC. Resolution of genotypic heterogeneity in prostate tumors using polymerase chain reaction and comparative genomic hybridization on microdissected carcinoma and prostatic intraepithelial neoplasia foci. Cancer Genetics and Cytogenetics. 2002; 137:15–22. [PubMed: 12377408]

Belandia B, Powell SM, Garcia-Pedrero JM, Walker MM, Bevan CL, Parker MG. Hey1, a mediator of Notch signaling, is an androgen receptor corepressor. Molecular and Cellular Biology. 2005; 25:1425–1436. [PubMed: 15684393]

Bernstein BE, Kamal M, Lindblad-Toh K, Bekiranov S, Bailey DK, Huebert DJ, McMahon S, Karlsson EK, Kulbokas EJ III, Gingeras TR, et al. Genomic maps and comparative analysis of histone modifications in human and mouse. Cell. 2005; 120:169–181. [PubMed: 15680324]

van Bokhoven A, Varella-Garcia M, Korch C, Johannes WU, Smith EE, Miller HL, Nordeen SK, Miller GJ, Lucia MS. Molecular characterization of human prostate carcinoma cell lines. Prostate. 2003; 57:205–225. [PubMed: 14518029]

Borgono CA, Diamandis EP. The emerging roles of human tissue kallikreins in cancer. Nature Reviews. cancer. 2004; 4:876–890.

Butcher NJ, Tetlow NL, Cheung C, Broadhurst GM, Minchin RF. Induction of human arylamine *N*-acetyltransferase type I by androgens in human prostate cancer cells. Cancer Research. 2007; 67:85–92. [PubMed: 17210686]

Carroll JS, Meyer CA, Song J, Li W, Geistlinger TR, Eeckhoute J, Brodsky AS, Keeton EK, Fertuck KC, Hall GF, et al. Genome-wide analysis of estrogen receptor binding sites. Nature Genetics. 2006; 38:1289–1297. [PubMed: 17013392]

Cawley S, Bekiranov S, Ng HH, Kapranov P, Sekinger EA, Kampa D, Piccolboni A, Sementchenko V, Cheng J, Williams AJ, et al. Unbiased mapping of transcription factor binding sites along human chromosomes 21 and 22 points to widespread regulation of noncoding RNAs. Cell. 2004; 116:499–509. [PubMed: 14980218]

Chen H, Libertini SJ, Wang Y, Kung HJ, Ghosh P, Mudryj M. ERK regulates calpain 2-induced androgen receptor proteolysis in CWR22 relapsed prostate tumor cell lines. Journal of Biological Chemistry. 2010; 285:2368–2374. [PubMed: 19946123]

Cirillo LA, Lin FR, Cuesta I, Friedman D, Jarnik M, Zaret KS. Opening of compacted chromatin by early developmental transcription factors HNF3 (FoxA) and GATA-4. Molecular Cell. 2002; 9:279–289. [PubMed: 11864602]

Desai SJ, Ma AH, Tepper CG, Chen HW, Kung HJ. Inappropriate activation of the androgen receptor by nonsteroids: involvement of the Src kinase pathway and its therapeutic implications. Cancer Research. 2006; 66:10449–10459. [PubMed: 17079466]

Devlin HL, Mudryj M. Progression of prostate cancer: multiple pathways to androgen independence. Cancer Letters. 2009; 274:177–186. [PubMed: 18657355]

Fischer A, Gessler M. Delta-Notch – and then? Protein interactions and proposed modes of repression by Hes and Hey bHLH factors. Nucleic Acids Research. 2007; 35:4583–4596. [PubMed: 17586813]

Gittes RF. Carcinoma of the prostate. New England Journal of Medicine. 1991; 324:236–245. [PubMed: 1985245]

Gnanapragasam VJ, Robson CN, Neal DE, Leung HY. Regulation of FGF8 expression by the androgen receptor in human prostate cancer. Oncogene. 2002; 21:5069–5080. [PubMed: 12140757]

Gregory CW, Hamil KG, Kim D, Hall SH, Pretlow TG, Mohler JL, French FS. Androgen receptor expression in androgen-independent prostate cancer is associated with increased expression of androgen-regulated genes. Cancer Research. 1998; 58:5718–5724. [PubMed: 9865729]

Gregory CW, He B, Wilson EM. The putative androgen receptor-A form results from *in vitro* proteolysis. Journal of Molecular Endocrinology. 2001; 27:309–319. [PubMed: 11719283]

He WW, Sciavolino PJ, Wing J, Augustus M, Hudson P, Meissner PS, Curtis RT, Shell BK, Bostwick DG, Tindall DJ, et al. A novel human prostate-specific, androgen-regulated homeobox gene (NKX3.1) that maps to 8p21, a region frequently deleted in prostate cancer. Genomics. 1997; 43:69–77. [PubMed: 9226374]

Heemers HV, Regan KM, Schmidt LJ, Anderson SK, Ballman KV, Tindall DJ. Androgen modulation of coregulator expression in prostate cancer cells. Molecular Endocrinology. 2009; 23:572–583. [PubMed: 19164447]

Hosack DA, Dennis G Jr, Sherman BT, Lane HC, Lempicki RA. Identifying biological themes within lists of genes with EASE. Genome Biology. 2003; 4:P4.

Huggins C, Hodges CV. The effects of castration, of estrogen and of androgen injection on the serum phosphatases in metastatic carcinoma of the prostate. Cancer Research. 1941; 1:293–297.

Ji H, Wong WH. TileMap: create chromosomal map of tiling array hybridizations. Bioinformatics. 2005; 21:3629–3636. [PubMed: 16046496]

Ji H, Jiang H, Ma W, Johnson DS, Myers RM, Wong WH. An integrated software system for analyzing ChIP-chip and ChIP-seq data. Nature Biotechnology. 2008; 26:1293–1300.

Jia L, Berman BP, Jariwala U, Yan X, Cogan JP, Walters A, Chen T, Buchanan G, Frenkel B, Coetzee GA. Genomic androgen receptor-occupied regions with different functions, defined by histone acetylation, coregulators and transcriptional capacity. PLoS ONE. 2008; 3:e3645. [PubMed: 18997859]

Jia L, Landan G, Pomerantz M, Jaschek R, Herman P, Reich D, Yan C, Khalid O, Kantoff P, Oh W, et al. Functional enhancers at the gene-poor 8q24 cancer-linked locus. PLoS Genetics. 2009; 5 e1000597.

Jiang F, Wang Z. Identification and characterization of PLZF as a prostatic androgen-responsive gene. Prostate. 2004; 59:426–435. [PubMed: 15065091]

Ko CY, Hsu HC, Shen MR, Chang WC, Wang JM. Epigenetic silencing of CCAAT/enhancer-binding protein delta activity by YY1/polycomb group/DNA methyltransferase complex. Journal of Biological Chemistry. 2008; 283:30919–30932. [PubMed: 18753137]

Landers KA, Samaratunga H, Teng L, Buck M, Burger MJ, Scells B, Lavin MF, Gardiner RA. Identification of claudin-4 as a marker highly overexpressed in both primary and metastatic prostate cancer. British Journal of Cancer. 2008; 99:491–501. [PubMed: 18648369]

Li P, Yu X, Ge K, Melamed J, Roeder RG, Wang Z. Heterogeneous expression and functions of androgen receptor co-factors in primary prostate cancer. American Journal of Pathology. 2002; 161:1467–1474. [PubMed: 12368219]

Lin B, Ferguson C, White JT, Wang S, Vessella R, True LD, Hood L, Nelson PS. Prostate-localized and androgen-regulated expression of the membrane-bound serine protease TMPRSS2. Cancer Research. 1999; 59:4180–4184. [PubMed: 10485450]

Lin B, Wang J, Hong X, Yan X, Hwang D, Cho JH, Yi D, Utleg AG, Fang X, Schones DE, et al. Integrated expression profiling and ChIP-seq analyses of the growth inhibition response program of the androgen receptor. PLoS ONE. 2009; 4:e6589. [PubMed: 19668381]

Liu AY, Roudier MP, True LD. Heterogeneity in primary and metastatic prostate cancer as defined by cell surface CD profile. American Journal of Pathology. 2004; 165:1543–1556. [PubMed: 15509525]

Louie MC, Yang HQ, Ma AH, Xu W, Zou JX, Kung HJ, Chen HW. Androgen-induced recruitment of RNA polymerase II to a nuclear receptor-p160 coactivator complex. PNAS. 2003; 100:2226–2230. [PubMed: 12589022]

Lu S, Jenster G, Epner DE. Androgen induction of cyclin-dependent kinase inhibitor p21 gene: role of androgen receptor and transcription factor Sp1 complex. Molecular Endocrinology. 2000; 14:753–760. [PubMed: 10809237]

Lupien M, Eeckhoute J, Meyer CA, Wang Q, Zhang Y, Li W, Carroll JS, Liu XS, Brown M. FoxA1 translates epigenetic signatures into enhancer-driven lineage-specific transcription. Cell. 2008; 132:958–970. [PubMed: 18358809]

Nagabhushan M, Miller CM, Pretlow TP, Giaconia JM, Edgehouse NL, Schwartz S, Kung HJ, de Vere White RW, Gumerlock PH, Resnick MI, et al. CWR22: the first human prostate cancer xenograft with strongly androgen-dependent and relapsed strains both *in vivo* and in soft agar. Cancer Research. 1996; 56:3042–3046. [PubMed: 8674060]

Nelson PS, Clegg N, Arnold H, Ferguson C, Bonham M, White J, Hood L, Lin B. The program of androgen-responsive genes in neoplastic prostate epithelium. PNAS. 2002; 99:11890–11895. [PubMed: 12185249]

Nwosu V, Carpten J, Trent JM, Sheridan R. Heterogeneity of genetic alterations in prostate cancer: evidence of the complex nature of the disease. Human Molecular Genetics. 2001; 10:2313–2318. [PubMed: 11673416]

Riegman PH, Vlietstra RJ, van der Korput JA, Brinkmann AO, Trapman J. The promoter of the prostate-specific antigen gene contains a functional androgen responsive element. Molecular Endocrinology. 1991; 5:1921–1930. [PubMed: 1724287]

Ruizeveld de Winter JA, Janssen PJ, Sleddens HM, Verleun-Mooijman MC, Trapman J, Brinkmann AO, Santerse AB, Schroder FH, van der Kwast TH. Androgen receptor status in localized and locally progressive hormone refractory human prostate cancer. American Journal of Pathology. 1994; 144:735–746. [PubMed: 7512791]

Shah RB, Mehra R, Chinnaiyan AM, Shen R, Ghosh D, Zhou M, Macvicar GR, Varambally S, Harwood J, Bismar TA, et al. Androgen-independent prostate cancer is a heterogeneous group of diseases: lessons from a rapid autopsy program. Cancer Research. 2004; 64:9209–9216. [PubMed: 15604294]

Takayama K, Kaneshiro K, Tsutsumi S, Horie-Inoue K, Ikeda K, Urano T, Ijichi N, Ouchi Y, Shirahige K, Aburatani H, et al. Identification of novel androgen response genes in prostate cancer cells by coupling chromatin immunoprecipitation and genomic microarray analysis. Oncogene. 2007; 26:4453–4463. [PubMed: 17297473]

Takayama K, Tsutsumi S, Suzuki T, Horie-Inoue K, Ikeda K, Kaneshiro K, Fujimura T, Kumagai J, Urano T, Sakaki Y, et al. Amyloid precursor protein is a primary androgen target gene that promotes prostate cancer growth. Cancer Research. 2009; 69:137–142. [PubMed: 19117996]

Tan J, Sharief Y, Hamil KG, Gregory CW, Zang DY, Sar M, Gumerlock PH, deVere White RW, Pretlow TG, Harris SE, et al. Dehydroepiandrosterone activates mutant androgen receptors expressed in the androgen-dependent human prostate cancer xenograft CWR22 and LNCaP cells. Molecular Endocrinology. 1997; 11:450–459. [PubMed: 9092797]

Tepper CG, Boucher DL, Ryan PE, Ma AH, Xia L, Lee LF, Pretlow TG, Kung HJ. Characterization of a novel androgen receptor mutation in a relapsed CWR22 prostate cancer xenograft and cell line. Cancer Research. 2002; 62:6606–6614. [PubMed: 12438256]

Thomas MA, Preece DM, Bentel JM. Androgen regulation of the prostatic tumour suppressor NKX3.1 is mediated by its 3′ untranslated region. Biochemical Journal. 2010; 425:575–583. [PubMed: 19886863]

Tomlins SA, Rhodes DR, Perner S, Dhanasekaran SM, Mehra R, Sun XW, Varambally S, Cao X, Tchinda J, Kuefer R, et al. Recurrent fusion of TMPRSS2 and ETS transcription factor genes in prostate cancer. Science. 2005; 310:644–648. [PubMed: 16254181]

Viger RS, Guittot SM, Anttonen M, Wilson DB, Heikinheimo M. Role of the GATA family of transcription factors in endocrine development, function, and disease. Molecular Endocrinology. 2008; 22:781–798. [PubMed: 18174356]

Wainstein MA, He F, Robinson D, Kung HJ, Schwartz S, Giaconia JM, Edgehouse NL, Pretlow TP, Bodner DR, Kursh ED, et al. CWR22: androgen-dependent xenograft model derived from a primary human prostatic carcinoma. Cancer Research. 1994; 54:6049–6052. [PubMed: 7525052]

Wang Q, Li W, Liu XS, Carroll JS, Janne OA, Keeton EK, Chinnaiyan AM, Pienta KJ, Brown M. A hierarchical network of transcription factors governs androgen receptor-dependent prostate cancer growth. Molecular Cell. 2007; 27:380–392. [PubMed: 17679089]

Wang Q, Li W, Zhang Y, Yuan X, Xu K, Yu J, Chen Z, Beroukhim R, Wang H, Lupien M, et al. Androgen receptor regulates a distinct transcription program in androgen-independent prostate cancer. Cell. 2009; 138:245–256. [PubMed: 19632176]

Whitbread AK, Veveris-Lowe TL, Lawrence MG, Nicol DL, Clements JA. The role of kallikrein-related peptidases in prostate cancer: potential involvement in an epithelial to mesenchymal transition. Biological Chemistry. 2006; 387:707–714. [PubMed: 16800731]

Xu LL, Shi Y, Petrovics G, Sun C, Makarem M, Zhang W, Sesterhenn IA, McLeod DG, Sun L, Moul JW, et al. PMEPA1, an androgen-regulated NEDD4-binding protein, exhibits cell growth inhibitory function and decreased expression during prostate cancer progression. Cancer Research. 2003; 63:4299–4304. [PubMed: 12907594]

Yang G, Gregory CW, Shang Q, O'Brien DA, Zhang YL. Differential expression of CCAAT/enhancer-binding protein-delta (c/EBPdelta) in rat androgen-dependent tissues and human prostate cancer. Journal of Andrology. 2001; 22:471–480. [PubMed: 11330648]

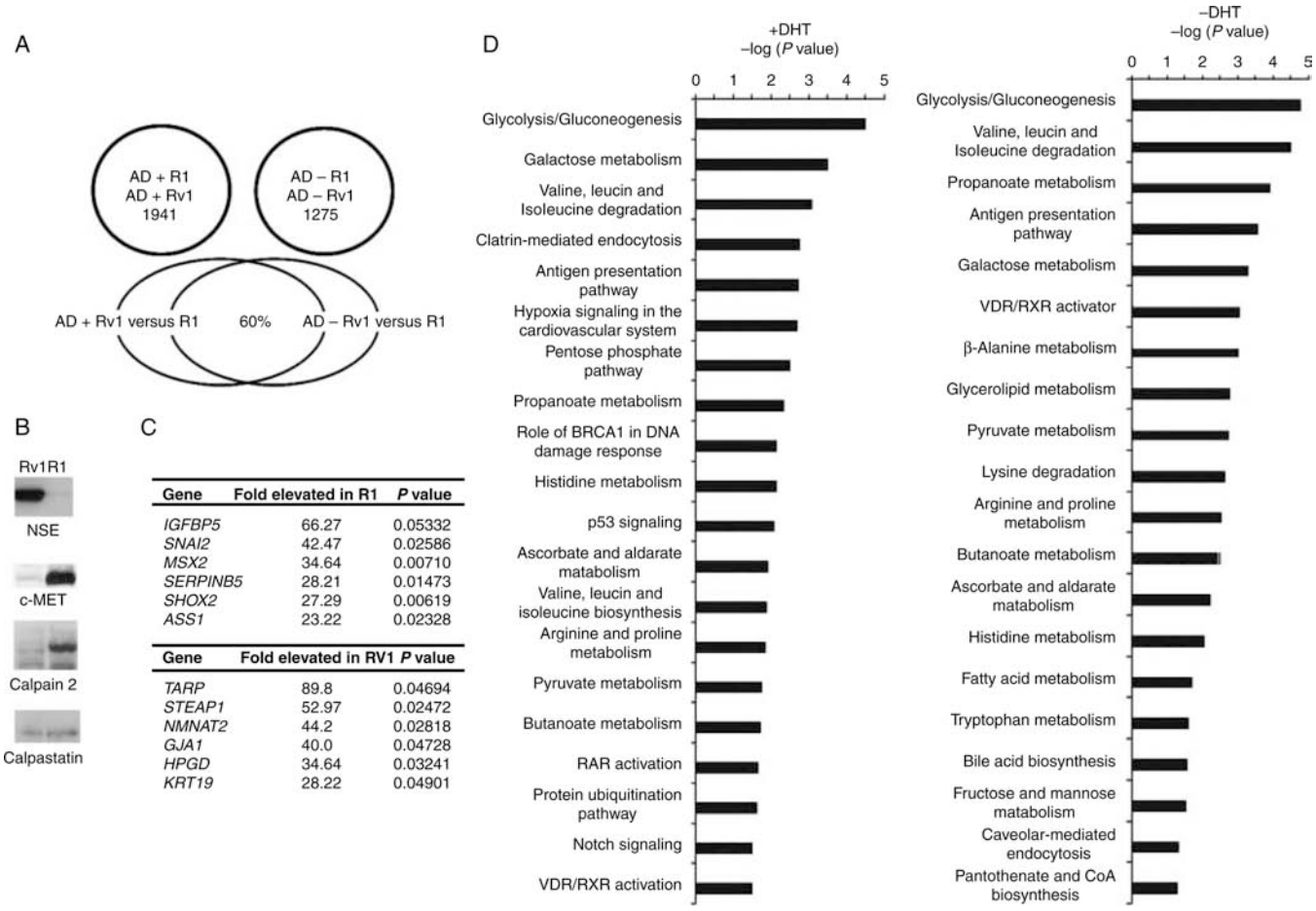

Figure 1.

Differences in gene expression of R1 and Rv1 cells in the presence and absence of a DHT. (A) Venn diagram of the number of genes differentially expressed in R1 and Rv1 cells in castrate levels of androgen and after a 2 h treatment with 10 nM DHT. The lower venn diagram shows the cohort of genes differentially expressed in the absence and presence of androgen. (B) Western blot analysis verification of several differentially expressed proteins that were identified by the expression array study. (C) The most differentially expressed transcripts in R1 and Rv1 cells treated with 10 nM DHT. (D) The IPA was used to identify the pathways that differed in the two cell lines in the presence and absence of androgen. The Fisher's exact test was used to determine the probability that the association between the dataset and a given pathway is due to chance alone. The most significant pathway differences in the presence and absence of androgen involved metabolic pathways.

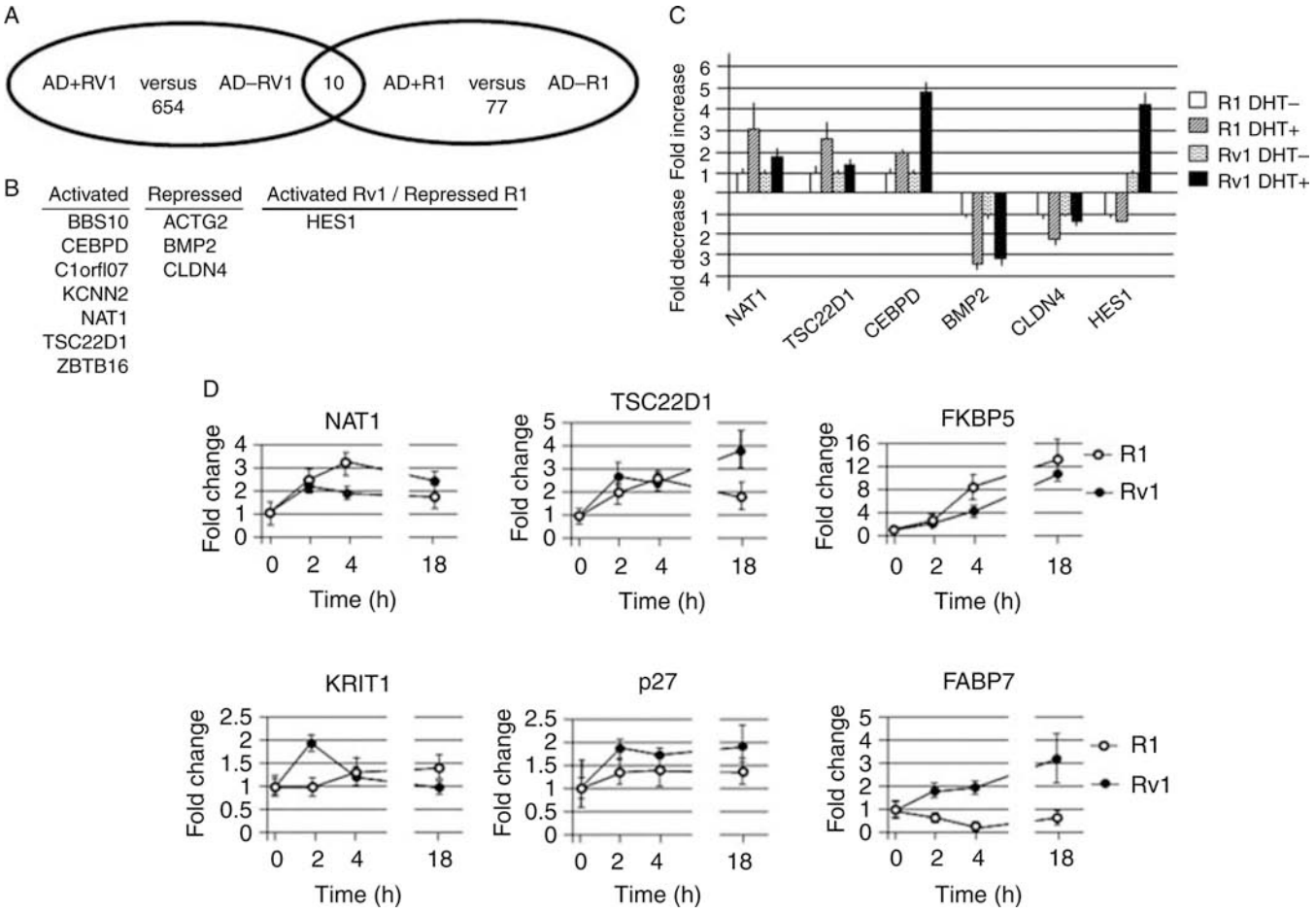

Figure 2.

Differences in AR-dependent gene expression of R1 and Rv1 cells. (A) Venn diagram of AR-regulated transcripts in R1 and Rv1 cells. (B) Transcripts that are commonly regulated in the two cell lines. Note that although HES1 is androgen regulated in both cell lines, HES1 expression is elevated in Rv1 cells, but repressed in R1 cells. (C) Real-time PCR verification of several AR-regulated transcripts. (D) Time course of DHT-inducible gene expression in R1 and Rv1 cells.

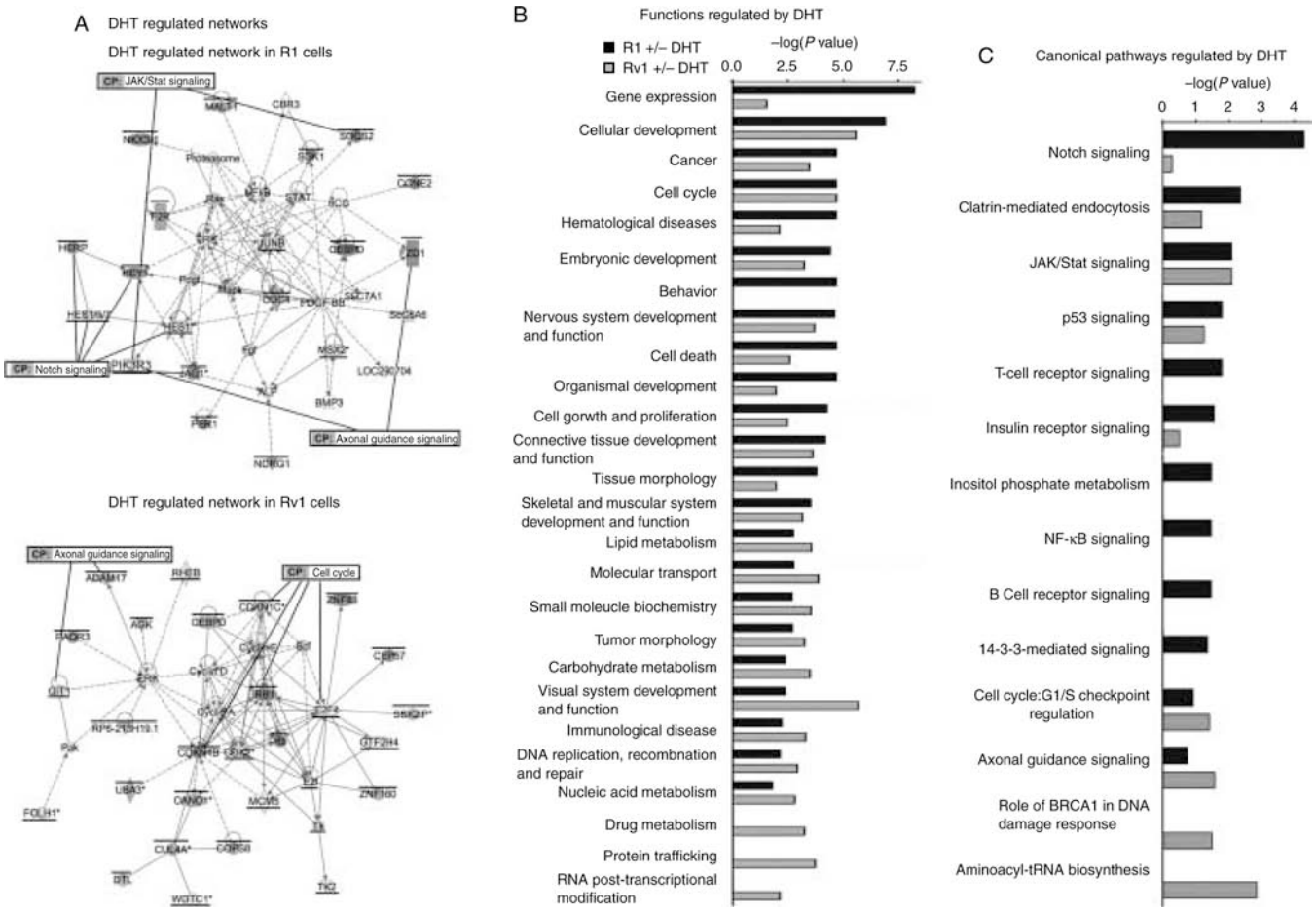

Figure 3.

Comparison of biological networks, pathways, and function of R1 and Rv1 DHT-regulated transcripts. (A) The most prominent DHT-regulated network in R1 and Rv1 cells. A bar above the gene denotes transcripts that are DHT transactivated, and an underscore denotes transcripts that are DHT repressed. Several components of the Notch signaling pathway are DHT regulated in R1 cells, whereas components of cell cycle are DHT regulated in Rv1 cells. (B) The most common functions of transcripts regulated by DHT in R1 and Rv1 cells. (C) The most common DHT-regulated canonical pathways in R1 and Rv1 cells.

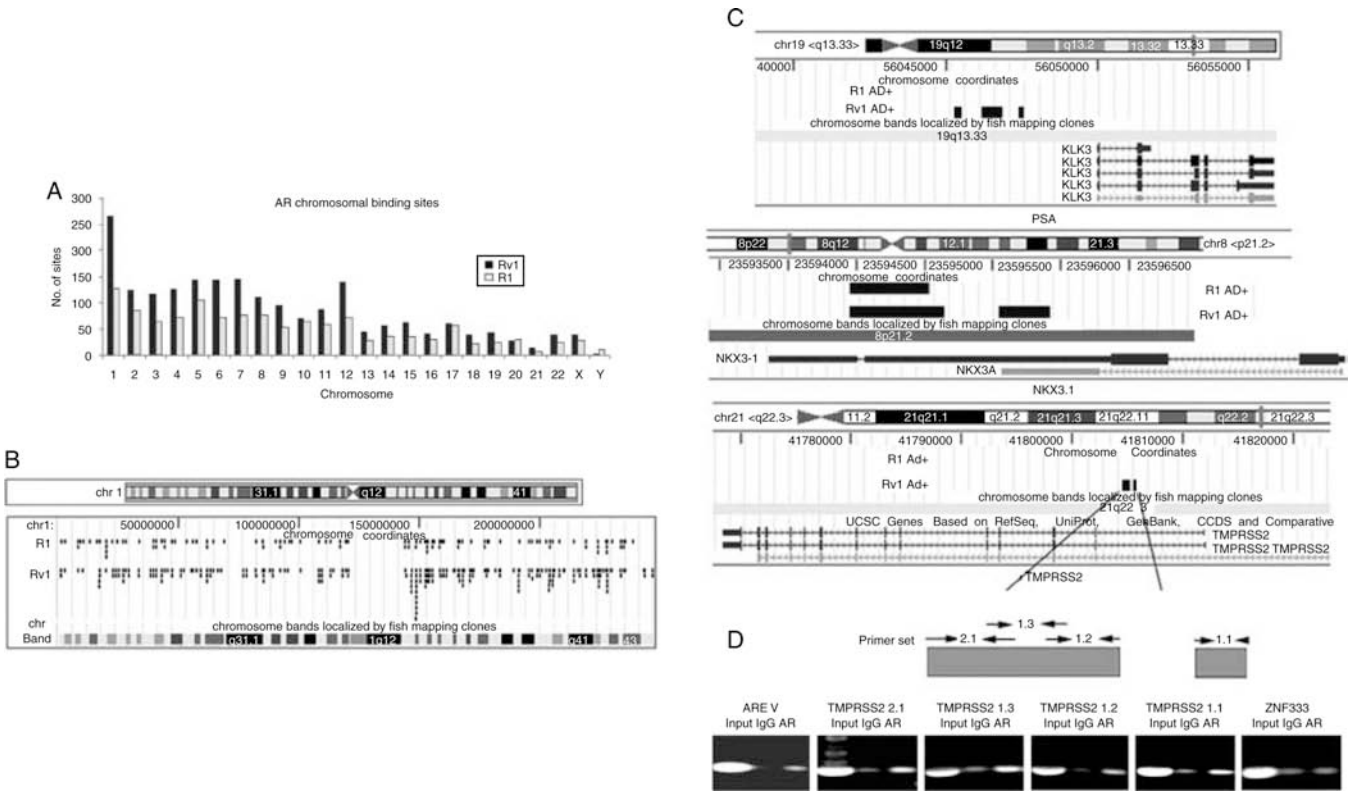

Figure 4.

Distribution of AR-binding sites in R1 and Rv1 cells. (A) The number of AR-binding sites detected on individual chromosomes after a 2 h DHT treatment is lower in R1 than in Rv1 cells. (B) More detailed mapping of AR binding on chromosome 1 in R1 and Rv1 cells. Few AR-binding sites are unique in R1 cells. (C) Precise location of AR binding to *PSA*, *NKX3.1*, and *TMPRSS2* genes in R1 and Rv1 cells. AR bound to common sequences of the *NKX3.1* gene, but AR binding to the *PSA* and *TMPRSS2* genes was detected only in Rv1 cells. (D) ChIP analysis of AR binding to sites in the *TMPRSS2* gene in Rv1 cells. The upper panel notes the location of the promoter sequences. ARE V contains an AR-binding site ~14 kb upstream of the *TMPRSS2* TSS. Sequences in the ZNF333 promoter served as a negative control.

A

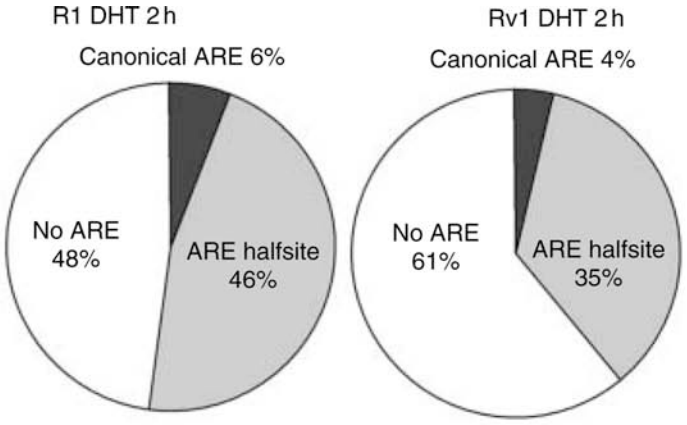

B

AR bound and DHT regulated genes

	R1	Rv1
No. of DHT regulated gene bound by AR	32	53
Percent of DHT regulated gene bound by AR	42	6
Location of ARE		
Intron	12.5%	28%
Exon	0	3.7%
5'-UTR	9.4%	17%
3'-UTR	6.25%	5.6%
within 5 kb of TSS	25%	47%
over 10 kb form TSS	68%	9.4%

C Most significant functions regulated by direct AR target genes

Function	No. of genes R1	Rv1
Transcriptional regulation	9 (28%)	11 (20%)
Cell cycle		5 (9.4)
Metabolic process	4 (12.5%)	3 (5.7)

Figure 5.

Characteristics of AR-binding sites and direct AR transcriptional target genes. (A) The half ARE is present in many AR-binding sites, whereas the canonical ARE is not. (B) AR binding was more prevalent in intronic sequences that are present in the 5′-UTR. (C) The most significant function of transcripts that are near an AR-binding site and are androgen regulated in R1 and Rv1 is transcriptional regulation.

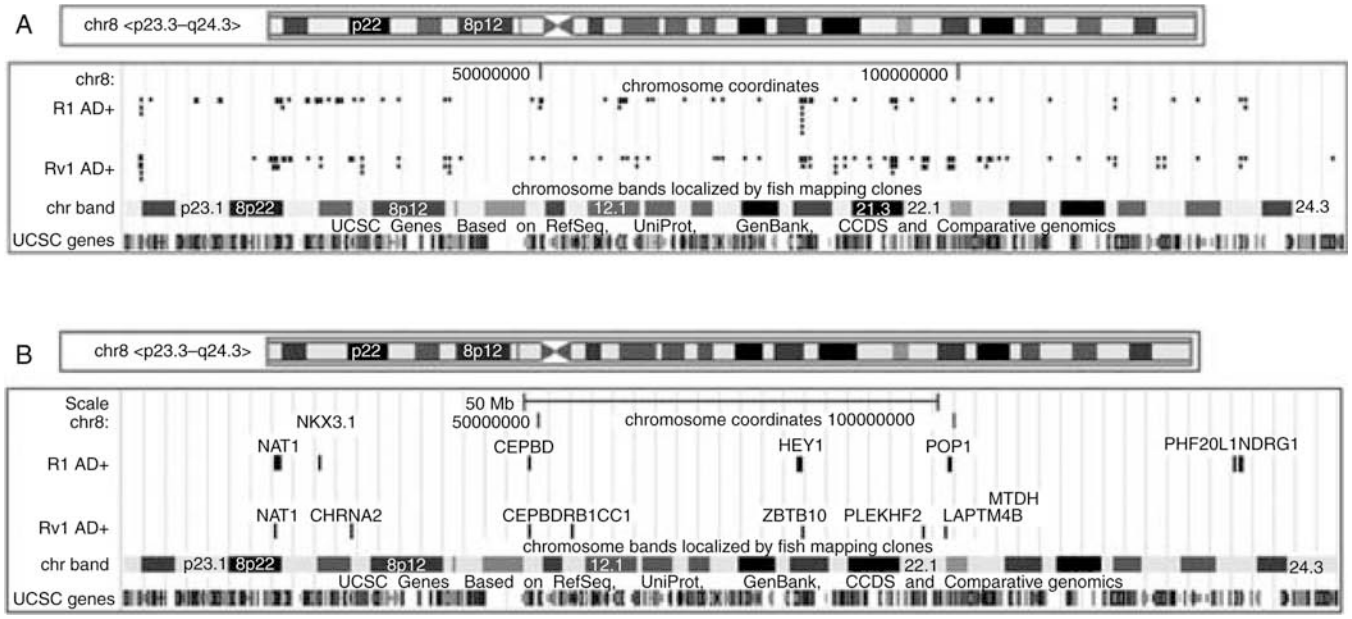

Figure 6.

AR-binding pattern on chromosome 8 in R1 and Rv1 cells. (A) AR-binding sites in R1 and Rv1 cells detected after DHT addition. (B) AR sites associated with transcripts that are AR regulated in R1 and Rv1 cells. Most androgen-responsive genes are transactivated, since only the expression of CHRNA2 in Rv1 cells is repressed.

Table 1

Androgen receptor (AR) co-regulators differentially expressed in R1 and Rv1 cells

Elevated in R1					Elevated in Rv1				
Symbol	**Act./Rep.**	**−DHT**	**+DHT**	**DHT reg.**	**Symbol**	**Act./Rep.**	**−DHT**	**+DHT**	**DHT reg.**
BRCA2	Act.		✓	Repressed in Rv1 *	ARID1A	Act.	✓	✓	
CARM1	Act.	✓		Induced in Rv1 *	CREBBP	Act.		✓	Induced in Rv1 *
CDK7	Act.	✓	✓		DDC	Act.	✓	✓	
COPS5	Act.	✓		Induced in Rv1	HMGB2	Act.	✓	✓	
FHL2	Act.		✓	Repressed in Rv1	HTATIP2	Act.	✓	✓	
GSN	Act.	✓	✓		IDE	Act.	✓	✓	
HIPK3	Act.		✓	Repressed in Rv1	IQWD1	Act.		✓	Induced in Rv1
HRMT1L2	Act.		✓		PLAGL1	Act.		✓	Induced in Rv1
HTATIP	Act.		✓	Repressed in Rv1	PRKDC	Act.		✓	Induced in Rv1
NCOA1	Act.	✓	✓		RB1	Act.	✓	✓	Induced in Rv1
NCOA2	Act.	✓	✓	Repressed in Rv1	RNF14	Act.		✓	Induced in Rv1
NONO	Act.	✓	✓		TMF1	Act.		✓	Induced in Rv1
PIAS2	Act.		✓	Repressed in Rv1	TRIM24	Act.		✓	Induced in Rv1
PNRC1	Act.	✓	✓		APPL	Rep.	✓	✓	
PXN	Act.	✓	✓	Repressed in Rv1	DNAJA1	Rep.		✓	Induced in Rv1
RAN	Act.	✓	✓		HDAC1	Rep.		✓	Induced in Rv1
SMARCA2	Act.	✓	✓		NCOR1	Rep.		✓	Induced in Rv1
SMARCC1	Act.		✓	Repressed in Rv1	PA2G4	Rep.		✓	Induced in Rv1
STAT3	Act.	✓			PAK6	Rep.	✓	✓	
TSC2	Act.	✓*	✓		ZNF278/PATZ1	Rep.	✓	✓	
ZMIZ1	Act.	✓	✓*						
AES	Rep.	✓	✓						
APPBP2	Rep.		✓	Repressed in Rv1					
CALR	Rep.		✓	Repressed in Rv1					
FLNA	Rep.	✓	✓						
HEY1	Rep.	✓	✓	Induced in R1					

Elevated in R1					Elevated in Rv1				
Symbol	**Act./Rep.**	**−DHT**	**+DHT**	**DHT reg.**	**Symbol**	**Act./Rep.**	**−DHT**	**+DHT**	**DHT reg.**
PTEN	Rep.	✓	✓						
TGIF	Rep.	✓	✓						
TLE1	Rep.	✓	✓						
FKBP5	Act.	Elevated in R1 in the presence of DHT, elevated in Rv1 in absence of DHT; DHT induced in R1 cells							

Act., activator; Rep., repressor; −DHT, castrate levels of androgen; +DHT, following addition of 10 nM DHT for 2 h; DHT reg., DHT regulated.

* indicates that the *P* value is slightly above 0.1 (up to o.12).

✓ indicates overexpression.

Published in final edited form as:
Horm Cancer. 2011 August ; 2(4): 224–238. doi:10.1007/s12672-011-0076-4.

Dual Blockade Of PKA And NFκB Inhibits H2 Relaxin-Mediated Castrate Resistant Growth Of Prostate Cancer Sublines And Induces Apoptosis

R.L. Vinall[1], **C.M. Mahaffey**[2], **R.R. Davis**[3], **Z. Luo**[4], **R. Gandour-Edwards**[5], **P.M. Ghosh**[1], **C.G. Tepper**[3], and **R. W. de Vere White**[1,6]

[1]Department of Urology, University of California, Davis School of Medicine and Cancer Center, Sacramento, CA 95817.

[2]Department of Hematology and Oncology, University of California, Davis School of Medicine and Cancer Center, Sacramento, CA 95817.

[3]Department of Biochemistry and Molecular Medicine, University of California, Davis School of Medicine and Cancer Center, Sacramento, CA 95817.

[4]Imperial College London (London, UK).

[5]Department of Pathology and Laboratory Medicine, University of California, Davis School of Medicine and Cancer Center, Sacramento, CA 95817.

Abstract

We previously demonstrated H2 relaxin (RLN2) facilitates castrate resistant (CR) growth of prostate cancer (CaP) cells through PI3K/Akt/β-catenin-mediated activation of the androgen receptor (AR) pathway. As inhibition of this pathway caused only ~50% reduction in CR growth, the goal of the current study was to identify additional RLN2-activated pathways that contribute to CR growth. Next-generation sequencing (NGS)-based transcriptome and gene ontology (GO) analyses comparing LNCaP stably transfected with RLN2 (LNCaP-RLN2) versus LNCaP-vector identified differential expression of genes associated with cell proliferation (12.7% of differentially expressed genes), including genes associated with the cAMP/PKA and NFκB pathways. Subsequent molecular analyses confirmed that the cAMP/PKA and NFκB pathways play a role in facilitating H2 relaxin-mediated CR growth of CaP cells. Inhibition of PKA attenuated RLN2-mediated AR activity, inhibited proliferation and caused a small but significant increase in apoptosis. Combined inhibition of the PKA and NFκB signaling pathways via inhibition of PKA and Akt induced significant apoptosis and dramatically reduced clonogenic potential, outperforming docetaxel, the standard of care treatment for CR CaP. Immunohistochemical (IHC) analysis of tissue microarrays (TMA) in combination with multispectral quantitative imaging comparing RLN2 levels in patients with BPH, PIN and CaP determined that RLN2 is significantly upregulated in CaP vs BPH (p=0.002). The combined data indicate RLN2 overexpression is frequent in CaP patients and provides a growth advantage to CaP cells. A near complete inhibition of RLN2-induced CR growth can be achieved by simultaneous blockade of both pathways.

[6]To whom requests for reprints should be addressed: Department of Urology, University of California, Davis, School of Medicine, 4860 Y Street, Suite 3500, Sacramento, CA 95817. Phone: (916) 734-2824, FAX: (916) 734-8094, rwdeverewhite@ucdavis.edu.

Conflicts of Interest

The authors declare no conflicts of interest.

Keywords

H2 relaxin; castrate resistant prostate cancer; androgen receptor; cyclic AMP; protein kinase A; NF kappaB

Introduction

Androgen ablation is the standard therapy for disseminated prostate cancer (CaP), however, patients develop resistance to this treatment regimen within 18–24 months [13]. Patients with castration resistant (CR) CaP are offered limited options, usually chemotherapy treatment with docetaxel, and more recently, the cancer vaccine "Provenge", whose effect is to increase patient survival time by a median of 3 or 4 months, respectively [18, 42, 30]. The identification and elucidation of pathways that promote CR CaP is critical for the development of successful new therapies to treat this disease.

H2 relaxin (RLN2) is a peptide hormone that is a member of the insulin-like superfamily. Several groups, including ours, have demonstrated that H2 relaxin plays a role in prostate carcinogenesis. Overexpression of RLN2 can induce tumor growth in a mouse model of CaP [37], and stimulation with RLN2 increases cell proliferation, invasiveness, and adhesion of CaP cells *in vitro* [7, 8]. Inhibition of RLN2 using an inhibitory analog [38], or suppression of its receptor LGR7 (also called RXFP1) [9] blocks RLN2-mediated CaP growth. Studies in human CaP have demonstrated that RLN2 expression is increased in radical prostatectomy specimens after 6 months of androgen ablation and in CR CaP, and that expression is highest in bone metastases [44]. Our group has demonstrated RLN2 mediates CR growth of CaP cells by a mechanism that involves PI3K-dependent co-translocation of the androgen receptor (AR) and β-catenin to the nucleus and transactivation of the PSA promoter [21, 46]. Based on our studies, others have also shown that RLN2-induced β-catenin stabilization is mediated by ProtocadherinY [43]. While it is clear β-catenin plays an important role in mediating the effects of RLN2 in CaP cells, inhibition of β-catenin stabilization or of Akt activation only partially inhibits RLN2-mediated growth of LNCaP, while blocking the RLN2 receptor, RXFP1, causes near complete inhibition. Thus the goal of the current study was to further elucidate the mechanism(s) by which RLN2 contributes to AR activation and CaP progression.

In the current study, we confirm that H2 relaxin expression is elevated in CaP patient specimens and in addition demonstrate that RLN2 is expressed at low levels in BPH relative to CaP specimens ($p=0.002$). This finding has not previously been reported. We have used next-generation sequencing (NGS)-based transcriptome and gene ontology (GO) analyses to identify additional downstream effectors of RLN2 in CaP cells. These data, combined with molecular and inhibitor studies, have identified the NF-κB and protein kinase A (PKA) signaling pathways as being activated by RLN2. Most importantly, when both pathways were simultaneously attenuated by the use of the PKA inhibitor H-89 as well as perifosine, which is an upstream inhibitor of NF-κB, RLN2-induced cell growth and survival were effectively down-regulated.

Materials and Methods

Cell Lines and Culture

LNCaP, PC-3 and Rwpe1 cells were purchased from the American Type Culture Collection (ATCC, Manassas, VA). CWR22Rv1 and PC346C (an androgen dependent cell line [22]) were kindly provided to us by Drs. Hsing-Jien Kung and Van Weerden respectively. All cell lines were maintained as previously described [46].

Generation of Stable Cell Lines

The RLN2 LNCaP sublines (LNCaP-rlx3 and LNCaP-rlx5) were generated in house. Briefly, the RLN2 allele was cloned into the pCR3.1 vector (Invitrogen, Carlsbad, CA) downstream of the cytomegalovirus promoter. Plasmids containing the RLN2 allele or empty pCR3.1 plasmid (LNCaP-vector) were stably transfected into LNCaP cells using Effectene (Qiagen, Valencia, CA). After 48 h, cells were grown under G418 (500 μg/ml) selection for 2–3 weeks until isolated colonies appeared. Colonies were selected and expanded in 24-well plates before being transferred to culture flasks.

Reagents

Antibodies: Total and phospho IκB-alpha, and Bcl-xL (Cell Signaling Technology, Beverly, MA), B-actin (Sigma-Aldrich Corporation, St. Louis, MO), NFκB (Santa Cruz BioTechnologies, Santa Cruz, CA), H2 relaxin (ALPCO, Salem, NH). *Inhibitors:* IKK inhibitor (a 14-amino acid peptide corresponding to the active IκB phosphorylation recognition sequence fused to the hydrophobic region of the fibroblast growth factor signal peptide, Calbiochem, Gibbstown, NJ), PKA inhibitors, H89 and PKI, (Calbiochem, Gibbstown, NJ).

SiRNA

Pre-validated siRNA specific for beta-catenin was purchased from Dharmacon (Lafayette, CO). To achieve knockdown, cells were transfected with either 20nM or 50nM siRNA using Lipofectamine 2000 as previously described [21].

Clonogenic Assay

Single cells (12,000) were seeded into 60-mm culture dishes containing FBS media on day 0 and allowed to attach for 24 h at 37°C. After 24 hours, FBS media was replaced with charcoal stripped serum (CSS) media and cultured for 14 days. Colonies were fixed in 1.0% crystal violet and 0.5% glacial acetic acid in ethanol, and visible colonies containing approximately 50 or more cells were counted.

Flow Cytometry

Cell cycle analysis: Analyses were performed as previously described [45]. *Apoptosis analysis:* The TACS annexin V-FITC kit (R&D Systems) was used to quantitate both early and late apoptosis. The analysis was performed using a Coulter Epics XL flow cytometer (Beckman Coulter), compensation was performed using FlowJo software (FlowJo, Ashland, OR). The assay was performed in accordance with the protocol described by the manufacturer. All samples were run in triplicate, all experiments were performed at least 3 times.

Immunoblot Analysis

Analyses were performed as previously described [46].

Cell culture IHC

Cells (50,000 per chamber) were seeded in chamber slides (BD Falcon, Two Oak Park, MA) in FBS media and allowed to adhere for 24 hours. After 24 hours, FBS media was replaced with CSS media. After 3 days, cells were washed with PBS (pH7.4) then fixed in ice-cold methanol for 7 minutes. After further washing, cells were incubated with 0.5% BSA for 20 minutes prior to the NFκB antibody (see reagents section for details) being added at a dilution of 1:250. After 60 minutes, cells were washed and then incubated with a FITC labeled secondary antibody (Sigma-Aldrich), 1:500. Cells were again washed and then

mounted using DAPI-containing mountant (Vector labs, Burlingame, CA). Staining was visualized by fluorescence microscopy using an Olympus BX61 microscope equipped with SlideBook digital imaging software.

cAMP and PKA kinase assays

cAMP; The cAMP Biotrak competitive enzyme immunoassay (Amersham-Pharmacia, RPN225) was used to determine cAMP activity levels 10 minutes after treatment of parental LNCaP with recombinant human (rh) H2 relaxin. Forskolin (Calbiochem) was used as a positive control. LNCaP were serum starved for 24 hours prior to the addition of rh H2 relaxin or forskolin. The assay was performed in accordance with the Protocol 3 described by the manufacturer. *PKA;* The PKA kinase activity assay (Stressgen, EKS-390A) was used to determine PKA activity levels 5, 15 and 30 minutes after treatment of parental LNCaP with rh H2 relaxin or rh H2 relaxin and H89. LNCaP were serum starved for 24 hours prior to the addition of rh H2 relaxin or H89. The assay was performed in accordance with the protocol described by the manufacturer. All samples were run in triplicate, all experiments were performed at least 3 times.

NFκB DNA binding assay

The NFκB p65 EZ-TFA Transcription Factor assay (Millipore) was used to determine whether H2 relaxin is able to mediate binding of NFκB to its DNA consensus sequence. This assay was performed using protein extracted from both LNCaP-vector treated with 100ng/ml rh H2 relaxin for 60 minutes and from the LNCaP-RLN2/C1 and LNCaP-RLN2/C2 sublines cultured in CSS media. The Whole Cell Extraction kit (Millipore) was used to prepare the protein extracts used in this assay. The assay was performed in accordance with the protocol described by the manufacturer. All samples were run in triplicate, all experiments were performed at least 3 times.

Tissue microarray (TMA) and TMA IHC

The tissue microarrays were constructed using a Semi-Automated Tissue Arrayer, TMAarrayer (Pathology Devices, Inc., Westminster, MD). Cores from 49 CaP (with known grade), 15 PIN and 24 BPH patients (4 core replicates of each) were analyzed. The protocol described by Thompson et al. was used to stain the CaP TMAs for H2 relaxin [44].

Multi-Spectral Imaging and Quantification of Staining

Images were obtained using an Olympus BX51 microscope with an attached Nuance CRI multispectral imaging system version 2.10.0 (Cambridge Research and Instrumentation, Woburn, MA). This imaging system is able to separate signals generated by different chromatogens and thereby improve quantitative accuracy (review; [20]). Isolation of background tissue and hematoxylin wavelengths was acheived by spectral analysis of hematoxylin only stained cores and slide mounted pure liquid hematoxylin. The 3,3'-Diaminobenzidine (DAB) wavelength was isolated by positive control core samples and slide mounted pure liquid DAB. Multispectral analysis was then used to assess the ratio of DAB level to TMA core area for each individual TMA core. Images were converted to a false fluorescence format.

RNA extraction and qRT-PCR

RNA extraction methods have previously been described [46]. RLN2 and GAPDH expression was assessed using pre-designed TaqMan primer/probes sets in combination with the TaqMan Reverse Transcription and Universal PCR Master Mix kits as per manufacturer's protocol (Applied Biosystems, Foster City, CA). Samples were run on an ABI 7900HT and data analyzed using the corresponding software. Triplicate samples were

run for each experimental group. Care was taken to ensure that the resulting Ct values for each group were within 0.5 Ct of each other.

Cell proliferation assay

Described by Vinall et al. [46].

PSA ELISA

LNCaP were seeded into 24 well plates (50,000 cells/well) in FBS media and allowed to attach for 24 hours. After 24 hours the FBS media was replaced with CSS media and the relevant inhibitors added (see reagents section for details. The level of PSA present in culture supernatants was measured using a PSA ELISA kit (MEDICORP, Montre´al, Que´bec, Canada) according to the manufacturer's protocol. Absorbance was measured at OD 450 using a Benchmark Plus Microplate Spectrophotometer (Bio-Rad Labs, Hercules, CA).

Sequencing-based transcriptome analysis

Next-generation sequencing (NGS) was utilized for whole transcriptome analysis of LNCaP-vector and the LNCaP-RLN2 and LNCaP-p53/R273H sublines. For this, RNA-Sequencing (RNA-Seq) libraries were prepared from 1 ug total RNA using the mRNA-Seq Sample Prep Kit (Illumina, San Diego, CA) according to the manufacturer's protocol. The libraries were then loaded on paired-end flow cells for cluster generation (cBot) followed by sequencing (2 × 40-bp) with the Genome Analyzer IIx (Illumina, Inc.) using kitted reagents (Illumina) and according to the manufacturer's protocols [4]. Data and bioinformatics analysis: Image processing, base calling, and quality scoring (Phred) were executed by SCS 2.6/RTA 1.6 software (Illumina, Inc.). CASAVA 1.7 (Illumina) was used for read alignment to the reference human genome sequence (GRCh37/hg19) using ELANDv2 and allowing for a maximum of two mismatches. Normalized transcript levels were quantified by calculation for RPKM (reads per kilobase of exon model per million mapped reads) [25]. Comparison analysis was performed in order to identify genes differentially expressed in the LNCaP-RLN2 clones as compared to the LNCaP-vector control. For this, genes up- or down-regulated in LNCaP-RLN2 were filtered based upon having RPKM values ≥25 (*i.e.*, moderate expression) in either the LNCaP-RLN2 or LNCaP-vector cell lines, respectively, exhibiting the same trend in regulation in both LNCaP-RLN2 clones, and having ≥1.5-fold change in expression (RLN2/Vector). Subsequently, Gene Ontology (GO) analysis [2] was performed in order to classify the genes according to biological process and molecular function.

Statistical analysis

At least three independent experiments were completed for each analysis described in this article. Data are shown as mean ± SD. Multiple group comparison was performed by one-way ANOVA followed by the Scheffe procedure for comparison of means using STATA software (College Station, TX). $p < 0.05$ was considered statistically significant (* signifies $p < 0.05$).

Results

RLN2 is elevated in CaP patient specimens relative to benign prostatic hyperplasia (BPH)

To determine the significance of RLN2 in human prostate cancer (CaP) patients, we conducted IHC analysis of 49 CaP, 15 PIN and 24 BPH specimens taken from patients with primary CaP undergoing prostatectomy (for PIN and CaP specimens) or TURP (for BPH) as initial treatment for the disease (Figure 1A). Note that RLN2 stained the epithelial cells strongly while some staining could also be seen for the stromal cells. However, the nuclei

did not stain for this peptide hormone at all, demonstrating the specificity of the staining. Specifically, the staining level increased from BPH<PIN=CaP indicating the increased accumulation of RLN2 during initiation of CaP. Quantification of staining using the Nuance multi-spectral imaging system demonstrated that RLN2 expression is significantly higher in CaP specimens relative to the BPH specimens (Figure 1B, 0.119+/−0.032 versus 0.95+/−0.021, p=0.002), a finding that has not previously been reported. The increase of RLN2 in CaP compared to BPH is of clinical relevance because in patients the serum levels of PSA increase in both cases. Since RLN2 can be detected in the serum [37], this means that the serum levels of this peptide could potentially be used as an independent marker of CaP as opposed to BPH. Further studies are required to test this hypothesis. A significant difference in RLN2 expression was not observed between the PIN and CaP specimens (p=0.475) and RLN2 expression did not correlate with Gleason grade (Figure 1C). Specimens from CaP patients with CR disease were not assessed due to lack of availability, however, other studies have observed very high H2 relaxin expression levels in bone metastases specimens from CR CaP patients [44]. Quantitative RT-PCR (qRT-PCR) analysis and RLN2 IHC was used to assess relative expression of RLN2 in “normal-like” RWPE-1 and multiple CaP cell lines (Figure 1D, E). Note that triplicate samples were run for each experimental group and the resulting Ct values for each group were within 0.5 Ct of each other. Excluding PC3, the aggressive tumors C4-2 and CWR22Rv1 expressed significantly higher levels of RLN2 compared to the RWPE-1 cells ($p<0.05$) derived from a normal human prostate and compared to the PC-346C cells ($p<0.05$) derived from an androgen-dependent CaP thereby supporting our hypothesis that RLN2 plays a role in progression to CR CaP.

Generation of LNCaP sublines that stably overexpress H2 relaxin

To understand the functional significance of increased RLN2 expression in CaP, we stably transfected LNCaP with plasmid expressing the RLN2 gene. LNCaP are an androgen dependent CaP cell line, and are the cell line that was used for all our previous RLN2-related studies [21, 46]. Two clones (LNCaP-RLN2/C1 and LNCaP-RLN2/C2) were chosen for further investigation of the role played by RLN2 in CaP. These sublines expressed ~20-fold higher levels of RLN2 mRNA relative to LNCaP stably transfected with the vector control (LNCaP-vector) (Figure 2A), $p<0.005$ for both LNCaP-RLN2/C1 and /C2 versus LNCaP-vector. LNCaP-R273H, an androgen independent LNCaP subline that stably expresses a $p53^{R273H}$ mutant allele, expressed the highest level of RLN2 mRNA, ~60-fold higher than the androgen dependent LNCaP-vector subline ($p<0.0005$), and was used as a positive control. Note that triplicate samples were run for each experimental group and the resulting Ct values for each group were within 0.5 Ct of each other. We have previously demonstrated that the $p53^{R273H}$ mutant, which is a hotspot mutation in CaP patients, can bind to the RLN2 promoter and drive RLN2 expression [44]. In the present study, the increase in RLN2 expression was observed at both the mRNA level (as determined by qRT-PCR) and at the protein level (as determined by immunocytochemistry in the same cell lines) (Figure 2B). It is noteworthy that the LNCaP-RLN2 sublines appear to be good models of CR CaP as they behave similarly to the CaP cells found in CR CaP patient tumors; they are able to grow in the absence of androgens and express normal levels of AR but high levels of PSA even in the absence of androgen, i.e. the AR pathway can be activated in a ligand independent manner.

Identification of downstream effectors of RLN2 using Next-Generation Sequencing (NGS) analysis

To help identify downstream effectors of RLN2 and to further elucidate the role played by RLN2 in CaP, we conducted next-generation DNA sequencing (NGS) analysis (i.e. RNA-Seq) followed by GO analysis using LNCaP-RLN2/C1 and LNCaP-RLN2/C2 vs LNCaP-vector sublines. Comparison of gene sequence analysis (Figure 2C) revealed 12.7% of genes

with >1.5-fold increased expression in the LNCaP-RLN2 sublines relative to the LNCaP-vector were related to proliferation. Other key processes associated with increased RLN2 expression were transcription (18.6%), metabolism (16.4%), signal transduction (11.7%) and proteolysis (6.2%) (Figure 2C). As expected, NGS analysis determined that the LNCaP-RLN2 sublines express high levels of RLN2 compared to the LNCaP-vector subline (350-fold and 582-fold increased expression in the LNCaP-RLN2/C1 and –RLN2/C2 sublines respectively). Table 1 lists the top 10 differentially expressed genes in the RLN2 versus vector control sublines. It is of note that H1 relaxin (RLN1) is also expressed at high levels in the RLN2 sublines. While the RLN1 isoform has been shown to be expressed in the prostate at the mRNA level, only the RLN2 is translated and secreted [16, 35, 31, 12, 17, 47] indicating that upregulation of RLN1 expression in the RLN2 sublines likely has no functional consequence. Expression of PSA (KLK3, 8-fold and 22-fold increased expression in LNCaP-RLN2/C1 and –RLN2/C2 respectively), a downstream target of the AR, and Cyclin D1 (CCND1, 1.44-fold and 1.2-fold increased expression), an important cell cycle regulator, was increased in the RLN2 sublines. Expression of TRAF1 and C-IAP1, which can be driven by NFκB, were also overexpressed (TRAF1, 2.01-fold and 3.08-fold increased expression, C-IAP1, 1.47-fold and 1.5-fold increased expression) (Table 1). Both of these molecules have been shown to promote cell survival.

To verify the observations made with the NGS/GO analysis, we demonstrated that stable expression of RLN2 increased PSA levels, but not AR expression, in LNCaP cells, confirming that RLN2 affects AR transcriptional activity but not expression (Figure 2D). These results thereby validate the use of these clones as a model for determining RLN2 function in CaP. Increased expression of RLN2 has been observed during neuroendocrine differentiation (NED) of CaP cells [10], a process that is associated with the development of CR CaP in CaP patients [48]. Our data also indicate that H2 relaxin is associated with NED, and thereby further support a role for H2 relaxin in progression to CR CaP. The LNCaP-RLN2/C1 and –RLN2/C2 sublines express increased levels of NSE and decreased levels of NEP compared to LNCaP-vector (Figure 2C). Neuron specific enolase (NSE) is a key marker of NED (review; [33]) and increased expression is associated with CaP progression [19]. Neural endopeptidase (NEP) is an enzyme that is expressed at high levels by normal CaP cells and is responsible for degrading neuropeptides such as bombesin, ET-1 and neurotensin that promote NED [26, 27]. NGS analysis revealed that mRNA levels of NSE and NEP were also altered in the LNCaP-RLN2 sublines, 9.532-fold and 18.796-fold increase in NSE in LNCaP-RLN2/C1 and –RLN2/C2 respectively, and a 2.544-fold and 1.668-fold decrease in NEP expression. Since cyclin D1 and several survival-related genes appeared to be upregulated in H2-relaxin overexpressing cells (Table 1), we determined whether RLN2 overexpression stimulated cell numbers. MTT assay verified that RLN2 overexpressing sublines have a significantly increased rate of cell growth in culture medium containing charcoal stripped serum (containing castrate levels of androgens) compared to vector transfected LNCaP cells (Figure 2E, statistical analysis compared the day 5 data for each subline and revealed a significant difference between the LNCaP-vector compared to all LNCaP-RLN2/C1 and /C2 as well as LNCaP-R273H, $p<0.005$). These observations are supported by our previous observations indicating ligand independent activation of the AR by RLN2 [46]. It should be noted that increased AR activity and increase cell proliferation are not characteristics that associated with NED. Our data indicate that the LNCaP-RLN2 sublines have some NED-like characteristics they are clearly not NE cells. While this is somewhat unusual, other groups have reported similar findings. For example, Snail induces NSE and chromogranin A expression in LNCaP as well as mediating nuclear translocation of AR and increased PSA expression [23].

RLN2 promotes activation of an NF-κB-dependent cell survival pathway in LNCaP prostate cancer cells

Since the NGS/GO analysis demonstrated an increase in TRAF1 and C-IAP1, which can be driven by NFκB, in LNCaP sublines overexpressing RLN2, we also investigated the activation of NFκB in these cells. The NF-κB subunits (p65, p50) remain bound to IκB-α in the cytoplasm; upon stimulation, IκB-α is degraded and p65/p50 released, which then translocates to the nucleus, and helps transcribe anti-apoptotic genes such as Bcl-xL [49]. To determine whether the NFκB pathway is active in the RLN2 LNCaP sublines we assessed IκB-α expression levels and phosphorylation state, NFκB localization, and binding of NFκB to its DNA consensus sequence. IκB-α levels were significantly lower in the RLN2 LNCaP sublines and IκB-α was phosphorylated indicating active degradation of IκB-α occurs in these cells (Figure 3A). Increased expression of Bcl-xL, a downstream effector of NFκB, was also observed in the LNCaP sublines overexpressing RLN2. Immunofluorescence analysis of the LNCaP-rlx sublines revealed a significant increase in levels of nuclear NFκB compared to LNCaP-vector (Figure 3B). LNCaP treated with TNF-α were used as a positive control for nuclear staining. We also demonstrate that RLN2 is able to facilitate binding of the NFκB p65 subunit to its DNA consensus sequence (Figure 3C). Significantly increased binding was observed in both LNCaP-vector treated with recombinant human (rh) RLN2 and in the RLN2 LNCaP sublines relative to the LNCaP-vector only control ($p<0.05$ for all 3 LNCaP sublines compared to LNCaP-vector). These studies indicate that activation of NF-κB is an important mediator of RLN2-mediated cell survival, and points to a mechanism by which RLN2 may induce CR CaP.

It is known that RLN2 signals via the G protein-coupled receptor (GPCR) RXFP1 in CaP cells. To determine whether the effects of RLN2 on NF-κB are mediated by RXFP1, we investigated the effect of RXFP1 knockdown on NF-κB activity. RXFP1-mediated activation of NF-κB could be inhibited using siRNA specific to RXFP1, the RLN2 receptor (Figure 3D), indicating that the effects of RLN2 on NF-κB are indeed mediated by RXFP1.

RLN2 stimulates cAMP production and PKA activation independent of NF-κB

Activation of the H2 relaxin receptor RXFP1 by RLN2 activates the G_s class of G-proteins ($G_{s\alpha}$), resulting in cyclic AMP (cAMP) dependent PKA activation. Hence, we investigated whether RLN2s effects are mediated by the PKA pathway in CaP cells. Previous studies performed in other cell types have demonstrated that RLN2 causes activation of the adenylate cyclase/AMP/PKA pathway [3, 15]. Our results validate these findings in CaP cells. Treatment of parental LNCaP with 10, 50 and 100 ng/ml recombinant human RLN2 (rhRLN2) induced a significant increase ($p<0.005$), ~2.2 and 2.1-fold increase in cAMP activity respectively compared to a 3.2-fold forskolin-induced response (positive control, $p<0.005$) (Figure 4A). However, this increase was transient as shown by the decrease in cAMP levels after 30 minutes of treatment. Similarly, treatment of parental LNCaP with 50 ng/ml RLN2 induced a ~3.3-fold increase in PKA activity ($p<0.005$) compared to a ~4.9-fold forskolin-induced increase (positive control, $p<0.005$) (Figure 4B). On the other hand, co-treatment with the PKA inhibitor H89 was able to completely inhibit this response to RLN2 indicating the assay is PKA specific (Figure 4B). Inhibition of PKA using H89 also caused a decrease in growth rate in both LNCaP-RLN2/C1 and –RLN2/C2 cultured in CSS media - in LNCaP-RLN2/C1 a ~1.8-fold decrease in growth rate was observed ($p<0.05$), and in LNCaP-RLN2/C2 a ~2.1-fold decrease ensued (Figure 4C, $p<0.05$). Inhibition of the PKA pathway did not directly affect the activation of NF-κB (data not shown), indicating that the PKA and the NF-κB pathways represent two different arms of the signaling mechanisms downstream of RLN2 (Figure 4F). Inhibition of PKA had a more dramatic effect on PSA expression (Figure 4D, E). Treatment with H89 caused a ~7-fold decrease in PSA levels in LNCaP-RLN2/C1 ($p<0.005$) and a ~5.6-fold decrease in LNCaP-RLN2/C2

($p<0.05$). It is of note that the RLN2 LNCaP sublines express very high levels of PSA even when cultured in castrate conditions. These data indicate that H2 relaxin induces the activation of the AR signaling pathway and cell growth in a ligand independent manner by a mechanism mediated by the activation of the cAMP/PKA pathway.

RLN2 overexpression confers resistance to treatment with therapeutic agents

Activation of the NF-κB pathway has been frequently associated with drug resistance. Since RLN2 induces an increase in NF-κB activity, we investigated whether RLN2 expression is also associated with resistance to various therapeutic drugs. Annexin V/propidium iodide (PI) labeling followed by flow cytometry analysis to investigate the effects on apoptosis showed that LNCaP cells transfected with vector only are highly susceptible to induction of apoptosis by various inhibitors including LY294002 (PI3K inhibitor), perifosine (Akt inhibitor), rapamycin (mTOR inhibitor) and docetaxel (anti-mitotic), whereas the LNCaP-RLN2/C1 and –RLN2/C2 sublines are more resistant to treatment with the same drugs (Figure 5A). Perifosine, rapamycin and docetaxel are all clinical agents. Perifosine has been shown to reduce PSA levels in 20% CaP patients with recurrent disease [5]. Several on-going clinical trials are testing the efficacy of rapamycin, and analogs of rapamycin alone and in combination with other agents (review; [11]). Docetaxel is the standard of care treatment for CaP patients with castrate resistant CaP (review; [39]). For LNCaP-vector, treatment with vehicle control, LY294002, perifosine, rapamycin and docetaxel induced ~10, 38, 22, 37, 29% apoptosis respectively (Figure 5A), but was reduced in LNCaP-RLN2/C1 (4, 20, 12, 13, 9%) and LNCaP-RLN2/C2 (1, 4, 10, 2, 1.5%). The levels of apoptosis in LNCaP-vector were statistically higher compared to those observed in the LNCaP RLN2 sublines regardless of the type of drug treatment ($p<0.05$). These data indicate that there is a link between RLN2 expression and chemoresistance in LNCaP cells, and provide rationale for combining targeted inhibition of the RLN2 pathway with conventional chemotherapy.

Combined treatment with perifosine and a PKA inhibitor in CaP cells overexpressing RLN2 promotes apoptosis

IKK causes phosphorylation of IκB-α and subsequent proteasome-mediated degradation. This degradation allows NFκB to translocate to the nucleus. Hence an IKK inhibitor would inhibit the activation of the NF-κB pathway. Perifosine is known to be an Akt inhibitor; however, it inhibits NF-κB activation to the same extent as the IKK inhibitor (Figure 5B). As perifosine has been FDA approved and is currently in clinical trials for the treatment of CaP, we investigated whether its effects on NF-κB would be of significance in the treatment of patients who overexpress RLN2 and may have developed resistance to commonly used drugs as a result. Hence we compared the effects of perifosine to that of the IKK inhibitor (Figure 5B,C). Inhibition of IKK in the LNCaP-RLN2/C1 and –RLN2/C2 sublines did not cause a significant increase in apoptosis or decrease in clonogenic potential (Figure 5C), whereas perifosine alone caused only a moderate increase in apoptosis and decrease in clonogenic potential (~2-fold increase and ~40% decrease respectively, Figure 5C). Similarly, simultaneous blockade of IKK and Akt resulted in only a modest increase in apoptosis and decrease in clonogenic potential compared to treatment with perifosine alone (Figure 5C). We concluded that the lack of a clinically relevant increase with dual blockade is due to the fact that both the IKK inhibitor and perifosine are acting on the same target, either directly or indirectly (see scheme in Figure 4F) resulting in decreased binding of NFκB to its DNA consensus sequence (Figure 5B).

We hypothesized that simultaneous blockade of pathways leading to PKA and NF-κB would therefore be the only way to completely block signaling downstream of RLN2-induced cell proliferation and survival (based on scheme in Figure 4F). H-89 alone had little or no effect on the RLN2 overexpressing clones (Figure 5D); in addition, inhibition of either IKK or

PKA caused only a moderate increase in the sensitivity of the RLN2 LNCaP sublines to treatment with docetaxel (Figure 5C,D). However, dual inhibition of both arms of the RLN2/RXFP1 pathway, with H-89 and perifosine, resulted in a larger and significant increase in apoptosis compared to blockade of either individual pathway (~2–3-fold increase in apoptosis compared to treatment with perifosine alone, ~15–18% apoptosis in the combination treatment, Figure 5D), and compared to treatment with docetaxel (docetaxel induced only ~2–3% apoptosis in the LNCaP-RLN2 sublines, Figure 5D). It is of note that this dual inhibition induced a similar level of apoptosis in the LNCaP-RLN2 sublines (15–18%) as docetaxel treatment in the LNCaP-vector subline (~25%). A significant decrease in clonogenic potential was also observed (~20–30% decrease compared to treatment with either the IKK inhibitor or perifosine alone (Figure 5D). Taken together, these results indicate that overexpression of RLN2, which is commonly seen in tumors from patients with CaP (Figure 1A), provides a growth advantage to CaP cells by causing activation of both the NF-κB and PKA pathways. A near complete inhibition of this growth advantage can be achieved only by simultaneous blockade of both pathways.

Discussion

The key finding of this study is that dual blockade of the PKA and NF-κB signaling pathways inhibits H2 relaxin-mediated castrate resistant growth of prostate cancer cells. This finding is of clinical relevance as our group and others have determined H2 relaxin is expressed at increased levels in CaP patients and increases in CaP patients following androgen ablation [44]. In addition, H2 relaxin has been demonstrated to play an important role in mediating CR CaP growth [37, 7, 8, 21, 46]. Focus was placed on determining the importance of the NF-κB and PKA pathways in facilitating H2 relaxin-mediated CR CaP growth because 1. NGS analyses identified the differential expression of several PKA and NF-κB-related genes in the LNCaP-RLN2 sublines, 2. These pathways are known to be dysregulated in CaP and are linked to CaP progression, 3. Both pathways have been demonstrated to be activated by H2 relaxin in other cell types.

Several groups have demonstrated a link between PKA activity and CaP progression (review; [24]). PKA can mediate ligand-independent activation of AR and can therefore play an important role in facilitating both androgen dependent and independent CaP. We have previously demonstrated that H2 relaxin mediates PI3K-dependent co-translocation of the androgen receptor (AR) and β-catenin to the nucleus and causes transactivation of the PSA promoter [21, 46]. Our current data indicate that H2 relaxin can also activate AR via PKA. H2 relaxin has been demonstrated to cause activation of PKA in other cell types [34, 14]. H2 relaxin signals via RXFP1 and 2, both of which are GPCRs that activate the G_s class of G-proteins ($G_{s\alpha}$) resulting in cAMP dependent PKA activation. Only RXFP1 is expressed in CaP cells [44]. Our data demonstrate AR activity is very high in the LNCaP-RLN2 sublines relative to LNCaP-vector, and that inhibition of PKA in the LNCaP-RLN2 sublines causes a significant inhibition of this elevated AR activity. These data indicate that PKA-mediated activation of AR is very important in a setting of elevated H2 relaxin expression.

NF-κB is a transcription factor which controls expression of genes associated with both cell proliferation and apoptosis [36]. NF-κB has been demonstrated to be constitutively active in several CaP cell lines and expressed at high levels in both PIN and CaP patient samples [1, 6, 19, 28, 40]. Usually NF-κB is sequestered in the cytoplasm through interaction of its p65 and p50 subunits with IkBα. Growth and survival stimuli induce phosphorylation of IkBα by IKKα resulting in IkBα degradation, followed by p65 phosphorylation and NF-κB translocation to the nucleus. We demonstrate that H2 relaxin is one of these growth stimuli; forced overexpression of H2 relaxin caused IkBα degradation, nuclear translocation of NF-κB and binding to the NF-κB DNA binding consensus sequence. Relaxin has previously

been shown to activate NF-κB in other organs but this is the first time it has been shown to activate NF-κB in CaP. While it has been shown that Akt phosphorylation such as that induced by H2 relaxin can phosphorylate the p65 subunit of NF-κB [41], we show that H2 relaxin promotes NF-κB activity by degrading IkBα.

There is sound rationale to simultaneously block both the PKA and NF-κB pathways in CaP cells that express elevated levels of H2 relaxin; both pathways are activated by H2 relaxin yet mediate proliferation by different mechanisms, and both pathways have been shown to be active in CaP patients. While inhibition of either pathway alone resulted in growth inhibition and/or a small increase in apoptosis, it was only when both pathways were inhibited simultaneously that a clinically relevant increase in apoptosis occurred. As inhibition of both IKK and Akt caused similar levels of NF-κB inhibition, we chose to use perifosine, an Akt inhibitor, for the drug combination studies as it has been FDA approved and tried in CaP clinical trials. In contrast, common IKK inhibitors such as Bay11-7082 have not and are therefore of limited relevance for translational studies. It is possible that our future studies may employ other inhibitors such as Bortezomib, a proteasome inhibitor that is currently in clinical use and has been found to inhibit NF-κB [32]. Currently, PKA inhibitors are not in clinical use in CaP patients. For future translational studies, we may employ drugs that lower cAMP levels such as beta-blockers, which are in clinical use, to determine if these have an effect on H2 relaxin signaling. It is of note that beta-blockers have been found to have a small effect on prevention of CaP [29]. It is also of note that the simultaneous blockade of the PKA and NF-κB pathways outperformed docetaxel, the standard of care treatment for advanced CR CaP.

In summary, our data indicate that simultaneous inhibition of PKA and NF-κB would prevent RLN2 mediated cell survival in CaP, and that in a setting of elevated RLN2 expression this combined inhibition is superior to docetaxel. The number of patients who would potentially benefit from this study is likely to be extensive since a significant portion of CaP patients overexpress RLN2.

Acknowledgments

The authors would like to thank Stephanie Soares for the construction of the TMA.

Financial Support:

DoD PC074103 (RLV, RGE, DVW)

The UC Davis Cancer Center Genomics Shared Resource is supported by Cancer Center Support Grant P30 CA93373-01 (R.W. dV.W.) from the NCI.

REFERENCES

1. Arlt A, Schafer H. NFkappaB-dependent chemoresistance in solid tumors. Int J Clin Pharmacol Ther. 2002; 40(8):336–347. [PubMed: 12467302]
2. Ashburner M, Ball CA, Blake JA, Botstein D, Butler H, Cherry JM, Davis AP, et al. Gene ontology: tool for the unification of biology. The Gene Ontology Consortium. Nat Genet. 2000; 25(1):25–29. [PubMed: 10802651]
3. Bathgate RA, Samuel CS, Burazin TC, Gundlach AL, Tregear GW. Relaxin: new peptides, receptors and novel actions. Trends Endocrinol Metab. 2003; 14(5):207–213. [PubMed: 12826326]
4. Bentley DR, Balasubramanian S, Swerdlow HP, Smith GP, Milton J, Brown CG, Hall KP, et al. Accurate whole human genome sequencing using reversible terminator chemistry. Nature. 2008; 456(7218):53–59. [PubMed: 18987734]

5. Chee KG, Longmate J, Quinn DI, Chatta G, Pinski J, Twardowski P, Pan CX, et al. The AKT inhibitor perifosine in biochemically recurrent prostate cancer: a phase II California/Pittsburgh cancer consortium trial. Clin Genitourin Cancer. 2007; 5(7):433–437. [PubMed: 18272025]
6. Domingo-Domenech J, Mellado B, Ferrer B, Truan D, Codony-Servat J, Sauleda S, Alcover J, et al. Activation of nuclear factor-kappaB in human prostate carcinogenesis and association to biochemical relapse. Br J Cancer. 2005; 93(11):1285–1294. [PubMed: 16278667]
7. Feng S, Agoulnik IU, Bogatcheva NV, Kamat AA, Kwabi-Addo B, Li R, Ayala G, Ittmann MM, Agoulnik AI. Relaxin promotes prostate cancer progression. Clin Cancer Res. 2007; 13(6):1695–1702. [PubMed: 17363522]
8. Feng S, Agoulnik IU, Li Z, Han HD, Lopez-Berestein G, Sood A, Ittmann MM, Agoulnik AI. Relaxin/RXFP1 signaling in prostate cancer progression. Ann N Y Acad Sci. 2009; 1160:379–380. [PubMed: 19416223]
9. Feng S, Agoulnik IU, Truong A, Li Z, Creighton CJ, Kaftanovskaya EM, Pereira R, et al. Suppression of relaxin receptor RXFP1 decreases prostate cancer growth and metastasis. Endocr Relat Cancer. 2010; 17(4):1021–1033. [PubMed: 20861284]
10. Figueiredo KA, Palmer JB, Mui AL, Nelson CC, Cox ME. Demonstration of upregulated H2 relaxin mRNA expression during neuroendocrine differentiation of LNCaP prostate cancer cells and production of biologically active mammalian recombinant 6 histidine-tagged H2 relaxin. Ann N Y Acad Sci. 2005; 1041:320–327. [PubMed: 15956728]
11. Garcia JA, Danielpour D. Mammalian target of rapamycin inhibition as a therapeutic strategy in the management of urologic malignancies. Mol Cancer Ther. 2008; 7(6):1347–1354. [PubMed: 18566209]
12. Garibay-Tupas JL, Bao S, Kim MT, Tashima LS, Bryant-Greenwood GD. Isolation and analysis of the 3'-untranslated regions of the human relaxin H1 and H2 genes. J Mol Endocrinol. 2000; 24(2):241–252. [PubMed: 10750025]
13. Gittes RF. Carcinoma of the prostate. N Engl J Med. 1991; 324(4):236–245. [PubMed: 1985245]
14. Halls ML, Bathgate RA, Roche PJ, Summers RJ. Signaling pathways of the LGR7 and LGR8 receptors determined by reporter genes. Ann N Y Acad Sci. 2005; 1041:292–295. [PubMed: 15956720]
15. Hsu SY, Kudo M, Chen T, Nakabayashi K, Bhalla A, van der Spek PJ, van Duin M, Hsueh AJ. The three subfamilies of leucine-rich repeat-containing G protein-coupled receptors (LGR): identification of LGR6 and LGR7 and the signaling mechanism for LGR7. Mol Endocrinol. 2000; 14(8):1257–1271. [PubMed: 10935549]
16. Ivell R, Einspanier A. Relaxin peptides are new global players. Trends Endocrinol Metab. 2002; 13(8):343–348. [PubMed: 12217491]
17. Ivell R, Hunt N, Khan-Dawood F, Dawood MY. Expression of the human relaxin gene in the corpus luteum of the menstrual cycle and in the prostate. Mol Cell Endocrinol. 1989; 66(2):251–255. [PubMed: 2612734]
18. Kasamon KM, Dawson NA. Update on hormone-refractory prostate cancer. Curr Opin Urol. 2004; 14(3):185–193. [PubMed: 15069310]
19. Lessard L, Karakiewicz PI, Bellon-Gagnon P, Alam-Fahmy M, Ismail HA, Mes-Masson AM, Saad F. Nuclear localization of nuclear factor-kappaB p65 in primary prostate tumors is highly predictive of pelvic lymph node metastases. Clin Cancer Res. 2006; 12(19):5741–5745. [PubMed: 17020979]
20. Levenson RM, Mansfield JR. Multispectral imaging in biology and medicine: slices of life. Cytometry A. 2006; 69(8):748–758. [PubMed: 16969820]
21. Liu S, Vinall RL, Tepper C, Shi XB, Xue LR, Ma AH, Wang LY, et al. Inappropriate activation of androgen receptor by relaxin via beta-catenin pathway. Oncogene. 2008; 27(4):499–505. [PubMed: 17653089]
22. Marques RB, Erkens-Schulze S, de Ridder CM, Hermans KG, Waltering K, Visakorpi T, Trapman J, Romijn JC, van Weerden WM, Jenster G. Androgen receptor modifications in prostate cancer cells upon long-termandrogen ablation and antiandrogen treatment. Int J Cancer. 2005; 117(2):221–229. [PubMed: 15900601]

23. McKeithen D, Graham T, Chung LW, Odero-Marah V. Snail transcription factor regulates neuroendocrine differentiation in LNCaP prostate cancer cells. Prostate. 70(9):982–992. [PubMed: 20166136]
24. Merkle D, Hoffmann R. Roles of cAMP and cAMP-dependent protein kinase in the progression of prostate cancer: cross-talk with the androgen receptor. Cell Signal. 23(3):507–515. [PubMed: 20813184]
25. Mortazavi A, Williams BA, McCue K, Schaeffer L, Wold B. Mapping and quantifying mammalian transcriptomes by RNA-Seq. Nat Methods. 2008; 5(7):621–628. [PubMed: 18516045]
26. Osman I, Dai J, Mikhail M, Navarro D, Taneja SS, Lee P, Christos P, Shen R, Nanus DM. Loss of neutral endopeptidase and activation of protein kinase B (Akt) is associated with prostate cancer progression. Cancer. 2006; 107(11):2628–2636. [PubMed: 17083125]
27. Osman I, Yee H, Taneja SS, Levinson B, Zeleniuch-Jacquotte A, Chang C, Nobert C, Nanus DM. Neutral endopeptidase protein expression and prognosis in localized prostate cancer. Clin Cancer Res. 2004; 10(12 Pt 1):4096–4100. [PubMed: 15217945]
28. Palayoor ST, Youmell MY, Calderwood SK, Coleman CN, Price BD. Constitutive activation of IkappaB kinase alpha and NF-kappaB in prostate cancer cells is inhibited by ibuprofen. Oncogene. 1999; 18(51):7389–7394. [PubMed: 10602496]
29. Perron L, Bairati I, Harel F, Meyer F. Antihypertensive drug use and the risk of prostate cancer (Canada). Cancer Causes Control. 2004; 15(6):535–541. [PubMed: 15280632]
30. Petrylak DP, Tangen CM, Hussain MH, Lara PN Jr, Jones JA, Taplin ME, Burch PA, et al. Docetaxel and estramustine compared with mitoxantrone and prednisone for advanced refractory prostate cancer. N Engl J Med. 2004; 351(15):1513–1520. [PubMed: 15470214]
31. Samuel CS, Tian H, Zhao L, Amento EP. Relaxin is a key mediator of prostate growth and male reproductive tract development. Lab Invest. 2003; 83(7):1055–1067. [PubMed: 12861045]
32. Sartore-Bianchi A, Gasparri F, Galvani A, Nici L, Darnowski JW, Barbone D, Fennell DA, Gaudino G, Porta C, Mutti L. Bortezomib inhibits nuclear factor-kappaB dependent survival and has potent in vivo activity in mesothelioma. Clin Cancer Res. 2007; 13(19):5942–5951. [PubMed: 17908991]
33. Shariff AH, Ather MH. Neuroendocrine differentiation in prostate cancer. Urology. 2006; 68(1):2–8. [PubMed: 16844446]
34. Shaw EE, Wood P, Kulpa J, Yang FH, Summerlee AJ, Pyle WG. Relaxin alters cardiac myofilament function through a PKC-dependent pathway. Am J Physiol Heart Circ Physiol. 2009; 297(1):H29–H36. [PubMed: 19429819]
35. Sherwood OD. Relaxin's physiological roles and other diverse actions. Endocr Rev. 2004; 25(2): 205–234. [PubMed: 15082520]
36. Shih VF, Tsui R, Caldwell A, Hoffmann A. A single NFkappaB system for both canonical and non-canonical signaling. Cell Res. 21(1):86–102. [PubMed: 21102550]
37. Silvertown JD, Ng J, Sato T, Summerlee AJ, Medin JA. H2 relaxin overexpression increases in vivo prostate xenograft tumor growth and angiogenesis. Int J Cancer. 2006; 118(1):62–73. [PubMed: 16049981]
38. Silvertown JD, Symes JC, Neschadim A, Nonaka T, Kao JC, Summerlee AJ, Medin JA. Analog of H2 relaxin exhibits antagonistic properties and impairs prostate tumor growth. Faseb J. 2007; 21(3):754–765. [PubMed: 17197386]
39. Singh P, Yam M, Russell PJ, Khatri A. Molecular and traditional chemotherapy: a united front against prostate cancer. Cancer Lett. 293(1):1–14. [PubMed: 20117879]
40. Sweeney C, Li L, Shanmugam R, Bhat-Nakshatri P, Jayaprakasan V, Baldridge LA, Gardner T, Smith M, Nakshatri H, Cheng L. Nuclear factor-kappaB is constitutively activated in prostate cancer in vitro and is overexpressed in prostatic intraepithelial neoplasia and adenocarcinoma of the prostate. Clin Cancer Res. 2004; 10(16):5501–5507. [PubMed: 15328189]
41. Takeshima E, Tomimori K, Kawakami H, Ishikawa C, Sawada S, Tomita M, Senba M, et al. NF-kappaB activation by Helicobacter pylori requires Akt-mediated phosphorylation of p65. BMC Microbiol. 2009; 9:36. [PubMed: 19216748]

42. Tannock IF, de Wit R, Berry WR, Horti J, Pluzanska A, Chi KN, Oudard S, et al. Docetaxel plus prednisone or mitoxantrone plus prednisone for advanced prostate cancer. N Engl J Med. 2004; 351(15):1502–1512. [PubMed: 15470213]
43. Thompson VC, Hurtado-Coll A, Turbin D, Fazli L, Lehman ML, Gleave ME, Nelson CC. Relaxin drives Wnt signaling through upregulation of PCDHY in prostate cancer. Prostate. 2010; 70(10): 1134–1145. [PubMed: 20503398]
44. Thompson VC, Morris TG, Cochrane DR, Cavanagh J, Wafa LA, Hamilton T, Wang S, Fazli L, Gleave ME, Nelson CC. Relaxin becomes upregulated during prostate cancer progression to androgen independence and is negatively regulated by androgens. Prostate. 2006; 66(16):1698–1709. [PubMed: 16998820]
45. Vinall RL, Hwa K, Ghosh P, Pan CX, Lara PN Jr, de Vere White RW. Combination treatment of prostate cancer cell lines with bioactive soy isoflavones and perifosine causes increased growth arrest and/or apoptosis. Clin Cancer Res. 2007; 13(20):6204–6216. [PubMed: 17947488]
46. Vinall RL, Tepper CG, Shi XB, Xue LA, Gandour-Edwards R, de Vere White RW. The R273H p53 mutation can facilitate the androgen-independent growth of LNCaP by a mechanism that involves H2 relaxin and its cognate receptor LGR7. Oncogene. 2006; 25(14):2082–2093. [PubMed: 16434975]
47. Welsh JB, Sapinoso LM, Kern SG, Brown DA, Liu T, Bauskin AR, Ward RL, et al. Large-scale delineation of secreted protein biomarkers overexpressed in cancer tissue and serum. Proc Natl Acad Sci U S A. 2003; 100(6):3410–3415. [PubMed: 12624183]
48. Wu JT, Astill ME, Liu GH, Stephenson RA. Serum chromogranin A: early detection of hormonal resistance in prostate cancer patients. J Clin Lab Anal. 1998; 12(1):20–25. [PubMed: 9484665]
49. Yardy GW, Brewster SF. Wnt signalling and prostate cancer. Prostate Cancer Prostatic Dis. 2005; 8(2):119–126. [PubMed: 15809669]

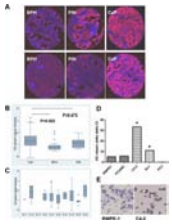

Figure 1. RLN2 expression is elevated in CaP patients

(A) Representative images from cores of BPH, PIN and CaP were obtained from patients with BPH (who underwent TURP) or CaP (who underwent prostatectomy) with IRB consent and assembled as a TMA. The cores were immunostained with an antibody to RLN2 and counterstained with hematoxylin. Multispectral imaging technologies were utilized to convert the brown staining (representing RLN2 localization) and the blue hematoxylin counterstain to false fluorescent imaging for better visualization and staining quantitation. Here shown are two representative cores from each group. **(B)** Box plot comparing median H2 relaxin expression values and interquartile ranges between the patient groups. Statistical analysis of RLN2 expression based on quantitation of multi-spectral imaging determined that RLN2 expression is higher in CaP patients compared to patients with BPH ($p=0.002$), while the difference in staining between BPH and PIN or PIN and CaP was not significant. All patient cores were assessed based on their DAB level to area score. **(C).** RLN2 expression did not correlate with Gleason grade. **(D)** Quantitative RT-PCR (qRT-PCR) analysis of RWPE-1 cells (derived from a normal prostate) vs several CaP cell lines demonstrated that, excluding PC3 cells, RLN2 expression is elevated in CaP cell lines. Triplicate samples were run for each experimental group and the resulting Ct values for each group were within 0.5 Ct of each other. **(E)** Immunocytochemical analysis in RWPE-1 vs C4-2 with RLN2 antibody (brown stainig) cells confirmed this trend. The cells were counterstained with hematoxylin (blue) which allows visualization of unstained cells.

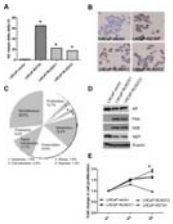

Figure 2. Effect of increased expression of RLN2 in LNCaP prostate cancer cells

(A) LNCaP sublines LNCaP-RLN2/C1 and LNCaP-RLN2/C2, which express elevated levels of RLN2, were generated by stable transfection of RLN2 in LNCaP cells. Quantitative RT-PCR (qRT-PCR) analysis for RLN2 mRNA levels in these sublines compared to vector-transfected LNCaP cells and LNCaP-R273H, a subline previously shown to express extremely high levels of this peptide hormone, demonstrated that the two RLN2 LNCaP sublines expressed RLN2 at significantly higher levels compared to LNCaP, but not as high as in $p53^{R273H}$-transfected cells. Triplicate samples were run for each experimental group and the resulting Ct values for each group were within 0.5 Ct of each other. **(B)** Immunocytochemical analysis of the cell lines confirmed this trend. **(C)** Next generation sequencing (NGS) followed by Gene Ontology (GO) analysis revealed 12.7% of genes that are differentially expressed between the RLN2 LNCaP and LNCaP-vector sublines are linked to proliferation. Other key processes associated with increased RLN2 expression were transcription (18.6%), metabolism (16.4%), signal transduction (11.7%) and proteolysis (6.2%). **(D)** The RLN2 LNCaP sublines express high levels of NSE and low levels of NEP, suggesting a neuroendocrine-like phenotype. While lower levels of AR were observed in the RLN2 LNCaP sublines, assessment of PSA levels indicates that the AR pathway is much more active. **(E)** MTT proliferation assay determined that the RLN2 LNCaP sublines are able to grow in the absence of androgen, as was the LNCaP-R273H subline, and that the difference in proliferation at the day 5 time point was statistically significant when comparing the LNCaP-vector and all 3 LNCaP sublines. (* signifies $p < 0.05$).

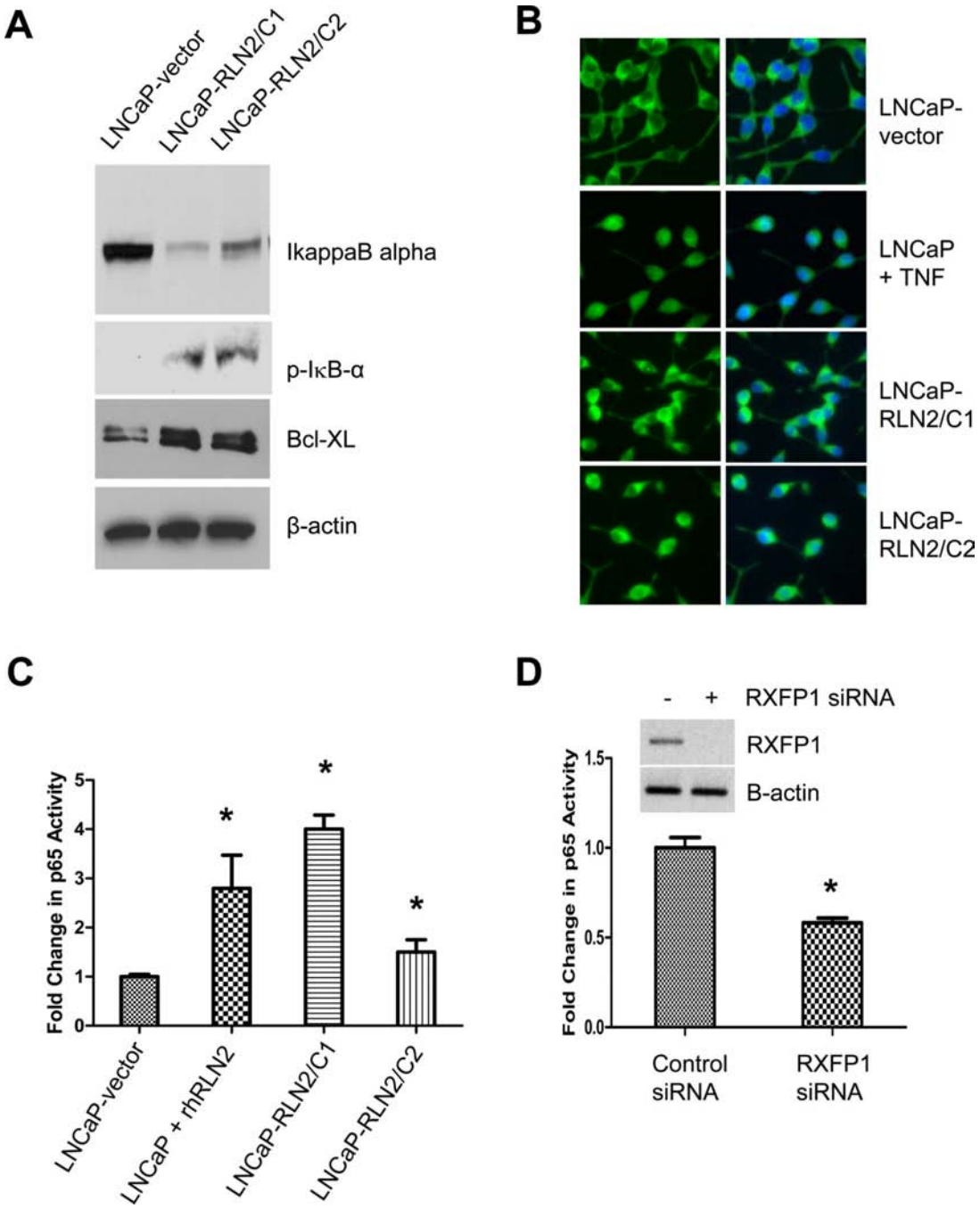

Figure 3. RLN2 induces activation of the NFκB pathway

(A) The RLN2 LNCaP sublines expressed decreased levels of IκB-α and increased levels of P-IκB-α, indicating RLN2 expression causes IκB-α degradation. Increased levels of Bcl-xL, a downstream effector of NFκB was also observed. **(B)** Increased nuclear translocation of NFκB is observed in RLN2 LNCaP sublines. LNCaP cells or the RLN2 overexpressing sublines were immunostained with anti-p65 antibody (green) or with DAPI to detect the nuclei (blue). Merger of the two stains indicated NF-κB nuclear localization. LNCaP cells treated with TNF-α (10 ng/ml) were used as positive control. Note that in LNCaP cells NF-κB remained in the cytoplasm whereas in the RLN2-overexpressing sublines, the complex is localized to the nucleus. **(C)** NF-κB transcriptional activity as determined by reporter assay

was significantly elevated in RLN2 LNCaP sublines and in parental LNCaP treated with rhRLN2 (human recombinant). Nuclear localization of functional NFκB was confirmed by assessment of the ability of NFκB to bind to its DNA binding consensus sequence. **(D) (upper panels)**. Knockdown of RXFP1, the RLN2 receptor, inhibited the ability of NFκB to bind to its DNA consensus sequence in the RLN2 LNCaP sublines **(lower panels)**. (* signifies $p < 0.05$).

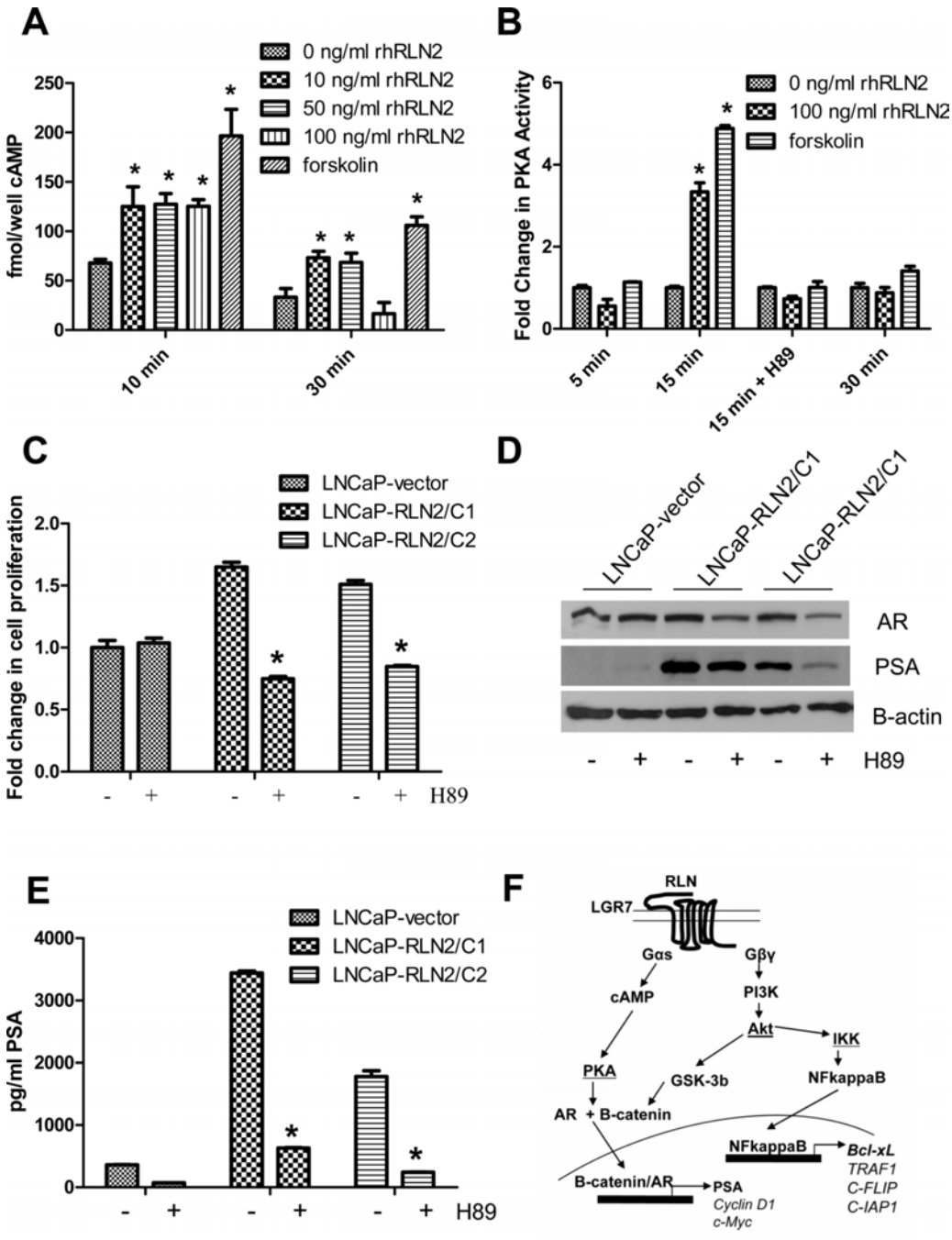

Figure 4. RLN2 stimulates cAMP production and PKA activation

(A) LNCaP cells were treated with 0, 10, 50, 100 ng/ml rhRLN2 (human recombinant) and cAMP levels measured by ELISA. 50 μM Forskolin, which directly stimulates cAMP production, is used as a positive control. **(B).** 100 ng/ml rhRLN2 induced PKA activation comparable to the positive control Forskolin as measured by the phosphorylation of Kemptide, a phosphate group acceptor synthetic peptide. Activation of PKA was observed 15 minutes post-treatment upon treatment with 100 ng/ml rhRLN2. This activation could be inhibited using H89, a PKA inhibitor. **(C, D)** Inhibition of PKA activity in LNCaP-RLN2/C1 and LNCaP-RLN2/C2 cells resulted in inhibition of **(C)** cell growth as measured by MTT assay and **(D, E)** PSA levels, as measured by both Western blotting as well as PSA

ELISA. Figure **4F** shows a schematic representation of RLN2 signaling in CaP cells based on data obtained from this and other studies of the RLN2 pathway in CaP cells. RLN2 is able to cause activation of both the cAMP/PKA and NF-κB signaling pathways by two independent mechanisms. Note that LGR7 is an alternate name for RXFP1. (* signifies $p < 0.05$).

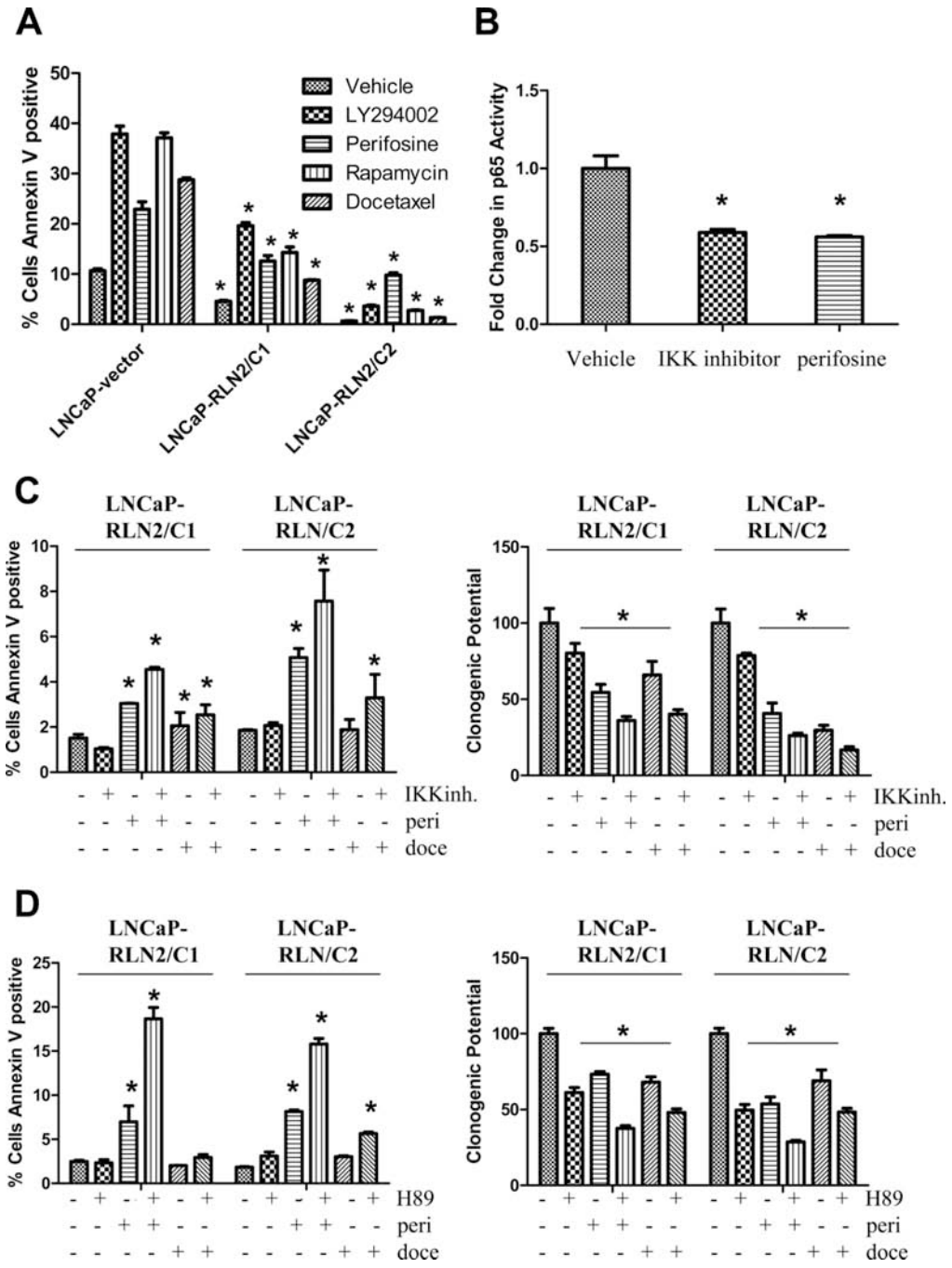

Figure 5. Combined blockade of the PKA and PI3K/Akt signaling pathways that are activated by RLN2 promotes apoptosis

(A) The RLN2 LNCaP sublines are resistant to apoptosis by several drugs, including LY294002, perifosine, rapamycin and docetaxel. The levels of apoptosis in LNCaP-vector were statistically higher compared to those observed in the LNCaP RLN2 sublines regardless of the type of drug treatment **(B)** Perifosine, similar to the IKK inhibitor decrease binding of NFκB to its DNA consensus sequence. **(C)** Inhibition of IKK in the LNCaP-RLN2/C1 and –RLN2/C2 sublines did not cause an increase in apoptosis, while perifosine alone caused only a moderate increase in apoptosis (~2-fold increase). Simultaneous blockade of IKK and Akt resulted in only a minimal increase in apoptosis compared to

treatment with perifosine alone **(left panel)**. A similar trend was observed by clonogenic assay **(right panel)**. **(D)** On the other hand, simultaneous blockade of PKA with H-89 together with perifosine resulted in a significant increase in apoptosis compared to blockade of either individual pathway (~2–3-fold increase in apoptosis compared to treatment with perifosine alone, ~15–18% apoptosis in the combination treatment) **(left panel)**, an increase that was far greater than that observed with docetaxel treatment (~2–3% apoptosis). Clonogenic assay showed this same trend **(right panel)**. (* signifies $p < 0.05$).

TABLE 1

Genes that are differentially expressed by LNCaP-RLN2 versus LNCaP-vector sublines

NGS was performed on mRNA-Seq libraries prepared from total RNA isolated from LNCaP-RLN2 and vector control cell lines. Data analysis was performed as described in *Materials and Methods*. Normalized transcript expression (RPKM values) was used for calculation of fold expression changes in the RLN2 LNCaP sublines relative to the vector control. The numbers listed in the LNCaP-RLN2/C1 and –RLN2/C2 columns of the table are fold change in gene expression relative to LNCaP-vector. This table also lists the relative expression of genes that have been shown to be driven by either the beta-catenin/AR complex or by NFκB and those involved in neuroendocrine differentiation (in grey). Both PSA (KLK3) and cyclin D1 (CCND1) have increased expression in the LNCaP-RLN2 sublines, as does TRAF1 and C-IAP1 (CIAPIN1). C-Myc and Bcl-xL were not differentially expressed.

Gene symbol	LNCaP-RLN2/C1 (fold-change relative to LNCaP-vector)	LNCaP-RLN2/C2 (fold-change relative to LNCaP-vector)	GO Function
SALL2	932	1827	transcription
CCL20	701	166	chemotaxis
KLHL13	693	187	catabolism
TCEA3	498	705	transcription
RLN1	419	241	signal transduction
TUSC3	413	264	glycosylation
PEG3	401	231	transcription
RLN2	350	582	female pregnancy
S100A10	267	165	signal transduction
MEST	196	106	mesoderm development
KLK3	8	22	catalytic activity
MYC	1.18	0.94	survival
CCND1	1.44	1.20	cell cycle
BCL2L1	0.83	0.93	survival
TRAF1	2.01	3.08	survival
CIAPIN1	1.47	1.50	survival
NSE	9.532	18.796	NED
NEP	2.544	1.668	NED

Published in final edited form as:
Immunol Endocr Metab Agents Med Chem. 2011 June ; 11(2): 131–149. doi: 10.2174/187152211795495643.

Targeting ErbB3: the New RTK(id) on the Prostate Cancer Block

Maitreyee K. Jathal[†,1], **Liqun Chen**[‡,1], **Maria Mudryj**[2,4], and **Paramita M. Ghosh**[*,1,3,4]

[1] Department of Urology, University of California Davis, CA. USA

[2] Department of Microbiology, University of California Davis, CA. USA

[3] Department of Biochemistry and Molecular Medicine, University of California Davis, CA. USA

[4] VA Northern California Health Care System, Mather, CA. USA

Abstract

Most prostate cancers (PCa) are critically reliant on functional androgen receptor (AR) signaling. At its onset, PCa is androgen-dependent and although temporarily halted by surgically or pharmacologically blocking the AR (androgen ablation), the disease ultimately recurs as an aggressive, fatal castration resistant prostate cancer (CRPC). FDA-approved treatments like docetaxel, a chemotherapeutic agent, and Provenge, a cancer vaccine, extend survival by a scant 3 and 4 months, respectively. It is clear that more effective drugs targeting CRPC are urgently needed. The ErbB family (EGFR/ErbB1, ErbB2/HER2/neu, ErbB3/HER3 and ErbB4/HER4) of receptor tyrosine kinases (RTKs) have long been implicated in PCa initiation and progression, but inhibitors of ErbB1 and ErbB2 (prototypic family members) fared poorly in PCa clinical trials. Recent research suggests that another family member ErbB3 abets emergence of the castration-resistant phenotype. Considerable efforts are being directed towards understanding ErbB3-mediated molecular mechanisms of castration resistance and searching for novel ways of inhibiting ErbB3 activity via rational drug design. Antibody-based therapy that prevents ligand binding to ErbB3 appears promising and fully-humanized antibodies that inhibit ligand-induced phosphorylation of ErbB3 are currently in early development. Small molecule tyrosine kinase inhibitors are also being vigorously pursued, as are siRNA-based approaches and combination treatment strategies- the simultaneous suppression of ErbB3 and its signaling partners or downstream effectors – with the primary purpose of undermining the resiliency of ErbB3-mediated signal transduction. This review summarizes the existing literature and reinforces the importance of ErbB3 as a therapeutic target in the clinical management of prostate cancer.

Keywords

ErbB3; Androgen Receptor; prostate cancer; castration resistance; EGFR; ErbB2; HER2; HER3; lapatinib; erlotinib; trastuzumab

1. INTRODUCTION

The prostate was first described in 1536 but prostate cancer (PCa) was not identified until 1853 [1]. At that time, it was considered a rare disease, likely due to shorter survival, since

[*]Address correspondence to this authors at the Department of Urology, University of California Davis School of Medicine, 4860 Y Street, Suite 3500, Sacramento, CA 95817, USA; Tel: (916)843-9336; Fax: (916)364-0306; Paramita.Ghosh@ucdmc.ucdavis.edu.
[‡]Current Address: Department of Medicine, University of California at San Francisco and Veterans Affairs Medical Center, 4150 Clement Street, Building 2, Room 589, San Francisco, CA 94121, USA
[†]Both Authors contributed equally.

PCa does not affect men until they are older. At the present time, however, it is the most common type of cancer afflicting men in the Western world, with over 2 million currently living with the disease. It is the second leading cause of cancer death in American men after lung cancer. In 2010, at least 217,730 men were diagnosed with prostate cancer and 32,050 were expected to die from the disease (American Cancer Society – Facts and Figures, 2010).

The occurrence and progression of PCa have been linked to the age, race and family history of the patient. 65% of all PCa are diagnosed in men older than 65 [2]. African-American men are three times as likely as Caucasian men are to die from PCa, while Asian-American men are at the lowest risk of developing the disease [2, 3]. Men with a single first-degree relative with a history of prostate cancer are twice as likely to develop PCa, while those with two or more relatives are nearly four times as likely to be diagnosed. The risk increases if the affected family members were diagnosed at a young age and the most susceptible men are those whose family members were diagnosed before age 60.

Patients diagnosed with localized PCa undergo watchful waiting if they are at low-risk or undergo surgery or radiation therapy if they are considered high risk. Prostatectomy, or surgery to remove the prostate, is one of the most common treatments for localized prostate cancer [4]. Radiation therapy is also a common form of treatment for prostate cancer patients. External beam radiotherapy (EBT), co-administered with androgen-ablative treatment, results in improved relapse-free and survival rates and has become the standard-of-care for locally-advanced PCa. In recent years, brachytherapy has also become common in treating subsets of patients with localized PCa [5]. Seeds of radioactive material are implanted in the prostate gland and deliver radiation over a short distance, thereby minimizing damage to normal, non-cancerous tissues.

The majority of patients undergoing treatment for localized prostate cancer respond to these therapies. A small fraction of these patients (15~30%), however, experience tumor recurrence within 5 years following localized treatment, indicating the presence of disseminated disease. These patients are then treated by androgen withdrawal therapy (AW). In the early 1970s, Huggins and Hodges made the seminal observation that androgens played a key role in PCa development and that orchiectomy (removal of the testes) induced cancer regression [6]. Based on their observations, androgen withdrawal continues to be the therapeutic mainstay for disseminated PCa to date; although the majority of patients with metastatic PCa currently are treated with drugs that reduce testicular androgen production, rather than surgery to remove the testes [7].

Androgen withdrawal therapy (AW) is currently the primary, first line, and therapeutic intervention for recurrent prostate cancer [7]. Essentially, AW therapy blocks AR signaling and inhibits the receptor's transcriptional activity. Pharmacological ablation includes gonadotrophin-releasing hormone (GnRH) super-agonists luteinizing-hormone (LH)-releasing hormone (LHRH) analogues, which downregulate the GnRH receptor in pituitary gonadotropes, thus suppressing LH release and inhibiting testicular testosterone secretion [8]. Synthetic GnRH agonists include leuprolide (Lupron), goserelin (Zoladex), buserelin and nafarelin. GnRH antagonists, which inhibit hormone binding to the GnRH receptor, have also been developed as PCa treatments. Several of these antagonists, such as cetrorelix (Cetrotide), abarelix and orgalutran (Ganirelix) are as effective as GnRH agonists in lowering serum testosterone, without causing a testosterone flare associated with GnRH-agonist therapy [9].

The effect of the first line therapy, however, remains in the patient for only about 18-24 months on an average, after which they develop resistance to this therapy. Non-steroidal anti-androgens competitively inhibit the binding of DHT or testosterones to the AR.

Examples within this category are flutamide, nilutamide and bicalutamide (Casodex). This method of treatment constitutes second line therapy and may be used upon failure of first line therapy, either alone, or together with LHRH modulators. Complete androgen blockade (CAB) combines an anti-androgen with a GnRH agonist [10]. This approach benefits about 25-35% of patients initially but does not confer any significant advantage in terms of survival for the majority of PCa sufferers.

Virtually all patients on AW or CAB eventually develop castration-resistant prostate cancer (CRPC) that is refractory to these treatments [7]. The current standard-of-care for CRPC is docetaxel-based chemotherapy, which offers a survival benefit of ~3 months [11], whereas the recently-FDA-approved PCa vaccine Sipuleucel-T (Provenge; Dendreon) extends patients' lifespans by 4.1 months [12]. Hence neither treatment is permanently curative. Patients eventually succumb to the disease [7] and it is clear that more effective therapies are urgently required. A large number of clinical trials have been conducted to identify potential treatments that cure CRPC, but to no avail. Our laboratory has therefore taken the stand that it is more advantageous and feasible to prevent the progression of prostate cancer to CRPC than to cure CRPC after it has already developed. In this review, therefore, we will examine known causes for the development of CRPC and methods by which it could be prevented.

2. FACTORS AFFECTING THE DEVELOPMENT OF CASTRATION RESISTANCE

2.1. Cell Proliferation and Apoptosis in CRPC

In the normal prostate of a mature male, the rate of cellular proliferation (1–2% rate of growth) is balanced by the rate of apoptosis (1–2% per day). This is dependent upon an adequate supply of androgens which ensure that neither involution nor overgrowth of the glands occurs. In contrast, the cancerous prostate suffers from rampant cell growth and/or decreased apoptosis [13, 14]. As described above, PCa cells are initially dependent upon androgens for their sustenance and AW results in tumor regression. It was initially assumed that AW resulted in the apoptotic death of the majority of PCa cells, and that the few that remained were resistant and eventually returned as castration resistant tumors. The number of studies determining proliferation or apoptotic indices in human patients following AW treatment is limited since the majority of patients undergo prostatectomy prior to start of treatment. However in a few reported studies, the results differed widely. Some groups reported increased levels of apoptosis 3 months after AW [15-17], but other investigators found no increase in apoptotic indices in the majority of patients either shortly [18] or 3 months after AW [19]. The authors of the latter study observed that androgen-deprivation was not associated with degeneration or necrosis of neoplastic glands and surmised that AW 'may be related more to suppression of tumor growth than to obliteration of tumor cells'. A similar concept had been put forth earlier [13], that both androgen-dependent and castration resistant human PCa tumors and cells altered their kinetic parameters (i.e., cell cycling status), rendering androgen ablative drugs utterly useless.

Attempts to test this hypothesis in animal models of prostate cancer have also yielded differing results. In the PC-82 and LuCaP xenograft models, increased apoptotic indices were observed following AW [20, 21], whereas in the Dunning R3327PAP rat model tumor growth and mitotic indices were reduced soon after AW but there were no signs of increased apoptosis and tumor cell numbers remained fairly constant throughout the study period [22, 23]. Earlier studies had determined that >80% of non-malignant rat ventral prostatic cells (taken from Sprague-Dawley or Copenhagen males) were lost within 10 days of castration [14, 24], and thus suggested that normal prostatic epithelial cell proliferation and death were differently controlled post-castration when compared to that in prostate tumors. Another

study demonstrated that AW in mice bearing the androgen-dependent CWR22 human prostate tumor xenograft was associated with a decrease in the proliferative index [25], but cellular changes indicative of apoptosis were notably absent. The authors inferred that the tumor cells were growth-arrested in a G0/early G1 state. Later results from the same group corroborated that hypothesis, revealing that the emergence of a castrate-resistant phenotype was associated with release from cell cycle arrest [26].

2.2. AR Signaling and Molecular Mechanisms of Resistance in CRPC

PCa cells rely on the androgen receptor (AR) for proliferation and survival. The AR is activated by ligand-binding and nuclear translocation, dimerization of two AR molecules, and binding to specific androgen-responsive elements (AREs) of androgen-responsive genes and modulating their transcription [27]. The AR is expressed in the majority of prostate tumors, both before and after AW therapy, regardless of their hormone sensitivity [28]. High levels of phosphorylated AR are associated with aggressive clinicopathological features; while increases in AR mRNA and protein levels are necessary and sufficient for progression to CRPC. This in turn is dependent upon a functional AR DNA-binding domain, implying that AR activity and levels are the driving forces for CRPC [27, 28]. The prostate-specific antigen (PSA) gene is an androgen-responsive gene and PSA protein levels are detected in the majority of CRPC, indicating a functional AR-signaling pathway.

Various authors have concluded that there are multiple mechanisms responsible for castration resistance. Overall, there are five principal mechanisms which ultimately increase the AR's cell-growth-promoting functions (Fig. **1**) (for a detailed review see [28] and references therein). (i) The androgen receptor is amplified in 25-30% of castrate resistant tumors. Increased AR levels result in increased sensitivity to residual low levels of androgens that are produced by the adrenal gland. (ii) Additionally, in some cases, there is evidence of enhanced rate of T (testosterone)→DHT (dihydrotestostereone) conversion by the enzyme 5α reductase. (iii) Further, the AR gene itself may be mutated, giving rise to a mutant protein which may be “promiscuous”, i.e. can be activated by other circulating steroid hormones (e.g. cortisol) and their metabolic by-products as well as by androgen antagonists like flutamide. These include expression of low molecular weight AR isoforms that are missing the ligand binding domain and are constitutively active allow for AR function in the absence of androgens. (iv) Co-regulator over-expression or co-repressor loss may also facilitate the conversion of anti-androgens into androgen agonists, or allow constitutive activation of the AR, despite the absence of significant levels of androgens in circulation. (v) Constitutive activation of the AR may also result from phosphorylation of the AR by various effectors which allow a configuration change in the AR, resulting in its enhanced transcriptional activity and transcription of target genes in CRPC cells at altered rates compared to castration sensitive cells. Further, altered co-repressor expression and binding and/or AR phosphorylation, also allows altered binding patterns of the AR in CRPC cells compared to its binding in castration sensitive cells [28].

It is of interest to note that most castrate resistant PCa cells, nevertheless, are still androgen sensitive. Although these cells would not cease growth when treated with anti-androgens, they would proliferate at an enhanced rate when challenged by additional doses of androgens [29]. The expression of the AR, is also responsible for cell survival, and in multiple cases, it has been shown that loss of AR expression results in cell death, even in CRPC cells [30-32]. It is likely; therefore, that ligand-dependent AR transcriptional activity is mainly responsible for regulating cell cycle proliferation, while ligand-independent AR activity may additionally regulate cell survival. Hence, androgen withdrawal may result in cell cycle arrest but even in the absence of ligands, the AR may be activated by mechanisms that are independent of ligand binding, which keeps the cells alive. When alternate pathways

that regulate cell cycle progression are activated in CRPC cells, this may result in a release from growth arrest and re-growth of the tumor.

2.3. Activation of Cell Signaling Pathways that Bypass AR Function in CRPC Cells

Studies from different laboratories indicate the existence of alternate pathways in CRPC cells that obviate the need for the AR in regulating the cell cycle pathways. Thus, the AR may be active and functional but cell survival may be regulated by parallel proliferation pathways, mediated, for example, by the serine/threonine kinase Akt [33]. Alternately the growth of the tumor may be facilitated by cancer stem or progenitor cells which do not express the AR but are selected by androgen-ablation therapy as the primary tumor cell type [34]. Alternately, the AR may be activated by a multitude of pathways that confer to it ligand-independent activation resulting in an ability to regulate cell survival, even in the absence of ligands. One of the major causes of re-activation of the cancer promoting pathways in cells that have undergone AW therapy is the phosphatidylinositol 3-kinase (PI3K) pathway. This pathway triggers a number of downstream targets such as Akt (reviewed by us earlier [35, 36]), which promotes cell survival pathways. The stimulation of these pathways prevents cell death during AW treatment [33, 37]. Since receptor tyrosine kinases (RTKs) of the ErbB family are known to turn on the PI3K pathway and regulate AR transcriptional activity in a ligand-independent manner, we will review in the following pages how ErbB receptors, regulate the progression to CRPC.

3. OVERVIEW OF ErbB RECEPTORS; STRUCTURE AND RECEPTOR ACTIVATION

The ErbB family consists of four closely related type 1 transmembrane tyrosine kinase receptors: the epidermal growth factor receptor (EGFR/HER1/ErbB1), ErbB2 (HER2/neu), ErbB3 (HER3) and ErbB4 (HER4). Signaling by the ErbB family regulates many cellular activities important for cell survival and function including cell division, migration, adhesion, differentiation and apoptosis. EGFR and ErbB2 have been described in many excellent reviews [38, 39] and hence will be described here only briefly.

3.1. ErbB Receptors are Activated by Ligand Binding, Dimerization and Phosphorylation

The ErbB receptors are activated by mesen chymal ligands – including heregulins (HRG, human) and neuregulins (NRG, esp. mice) and other epidermal growth factor (EGF)-like ligands [40] (Fig. **2**). The 4 ErbBs share an overall structure of two cysteine-rich domains in their extracellular region and an intracellular kinase domain, flanked by a carboxy-terminal tail with tyrosine autophosphorylation sites (Fig. **3**). Although they have essentially the same domain structure, the functional activity of each varies. ErbB-1, -2 and -4 have active tyrosine kinase domains and ErbB-1, -3 and -4 possess known ligands. ErbB-2 has no known ligand but is constitutively available for dimerization [40]. ErbB-3 can bind several growth factors but until recently was thought to lack intrinsic tyrosine kinase ability (being devoid of the requisite ATP-binding amino acid residues). Recent work has disproved this notion and will be discussed later in this article.

Receptor homo- or hetero-dimerization is imperative for ErbB function and signaling activity. ErbB receptors normally exist as inactive monomers with the homodimerization domains folded to prevent dimerization. Binding of a specific ligand induces a conformational change in the ErbB monomer and readies it for dimerization with a second, active ErbB monomer [40, 41]. The exception may be ErbB2, which is thought to be constitutively activated and readied for heterodimerization. Several different homodimer and heterodimer pairings are possible between the four receptors, with homodimers only weakly perpetuating signals compared to heterodimers (Fig. **2**). This ligand-induced dimerization

activates the intrinsic receptor tyrosine kinase activity and leads to trans-autophosphorylation of the monomeric partners [42]. Adapter proteins are recruited to these newly phosphorylated docking sites and a signaling cascade is initiated. It is important to note that ErbB2 and ErbB3 must heterodimerize with the other ErbBs if they are to transmit signals. ErbB2-containing heterodimers are the most potent complexes and the ErbB2-ErbB3 heterodimer is the most mitogenic and transforming of them all.

3.2. ErbB Function in Normal Tissue and in Tumorigenesis

The ErbB kinases are essential for development and tissue maintenance. Although these studies were conducted mostly in EGFR and ErbB2, it gives a broad overview of the functions of ErbB kinases in general. ErbB1 knockout mice die soon after birth, suffering defects in a large number of organs including skin, lung, the GI tract and the brain (reviewed in [43]). Basically, there is immature development in several epithelial organs. In normal mice, the ErbB2/ErbB4 heterodimer acts principally in the heart, whereas ErbB2/ErbB3 function is required for the development of the peripheral nervous system [43]. ErbB2 or ErbB3 knockout mice experience hypoplasia of the sympathetic ganglion chain, loss of cranial sensory ganglia and defective Schwann cell development, due to a loss of migratory ability of cells arising from the neural crest [44]. To circumvent the early lethality of ErbB2 knockout mice, conditional ErbB2 knockout mice have also been developed [45, 46]. Conditional knockdown of ErbB2 in various stages in the life of these mice demonstrated that lack of ErbB2 caused a development of cardiomyopathy, a lack of muscle spindles, defects in muscle regeneration, in effective neuromuscular synapses, abnormally thin myelin sheaths, movement abnormalities and a loss of motoneurons (reviewed in [43]). In the development of the mammary gland, the importance of ErbB1 in ductal growth and the contribution of ErbB2 and ErbB4 for lobulo-aveolar development and lactation has been demonstrated (reviewed in [47]). Based on these reports, it is fairly obvious that ErbB1 has major roles in epithelial cell development whereas ErbB2 plays an important role in cell migration and movement. While these receptors are essential in development, their malfunction later on in life may result in cancer development as well.

In the adult tissue, these receptors and their ligands are still present, but their function may be mainly to maintain the homeostasis of the organ. In cancer, on the other hand, the receptors are inappropriately activated resulting in increased proliferation, decreased survival and increased motility. Based on the existing literature to date, there are three main causes for the role of the ErbB receptors in tumorigenesis: (i) Increased receptor expression and/or gene amplification, (ii) increased ligand expression and (iii) activating mutation of the receptor. Increased expression of ErbB2 has been found to be a common cause for breast cancer [48]. ErbB2 overexpression in breast cancer is associated with poor prognosis, and resistance to hormonal therapy. ErbB2 overexpression has also been associated with metastasis in patients with breast and prostate cancer, especially to the bone [49]. On the other hand, the majority of tumors studied, not only those that are hormonally related, but also other solid tumors, do not exhibit any mutations in ErbB2, or for that matter, in ErbB3 or ErbB4. ErbB3 and ErbB4, when abnormally activated, is more likely to be due to increased availability of their ligands. The same is also true for ErbB1. In the normal prostate, the ligands for these receptors are produced in the stromal tissue, with receptor being expressed in the epithelial cells. In tumors, the epithelial cells themselves may start to produce the ligands, thereby maintaining the receptors in a constant state of activation. ErbB1 receptors, at least in some tumors, especially lung and head and neck, are also prone to mutations that keep these receptors in a constant state of activation [50, 51]. Comparison of the functions of EGFR and ErbB2 in normal development and in cancer indicates that these receptors continue to perform in cancer the tasks that they conducted in development,

which is tissue generation and cell migration, expect that now these tasks are conducted to the detriment of the patient.

In prostate cancer, mutations of any of the erbB receptors have not been seen; however, a large number of studies indicate that EGFR (ErbB1) and ErbB2 (HER2) interact with the AR in the absence of AR ligand binding and stimulate cell survival. The AR was found to both regulate [52] and be regulated by ErbB1 and ErbB2 [53] in castration sensitive, but not in CRPC, human cell lines. In particular, AR expression was suppressed by the activation of ErbB1 [53]; while ectopic expression of ErbB2 was shown to stimulate ligand independent activation of the AR [54]. ErbB2 overexpression in an androgen dependent prostate cancer cell line enhanced AR activity and hormone-independent cell growth [55], whereas small interfering RNA (siRNA)–mediated ErbB2 knockdown impaired prostate cancer cell growth and AR activity [56]. Nevertheless, a large number of ErbB1 and ErbB2 inhibitors were identified which inhibited cell proliferation and survival and also prevented AR transcriptional activity (discussed below). Based on these reports, as well as the fact that ErbB2 regulated PI3K/Akt activation, which made them successful targets of therapy in a number of other solid cancers, ErbB1 and ErbB2 inhibitors were assumed to be the panacea that would kill prostate cancer cells, and prevent castrate resistant prostate cancer.

3.3. ErbB1 (EGFR) and ErbB2 (HER2) Inhibitors in Cancer Therapy

The ErbB family is an established therapeutic target for many human cancers. Anti-ErbB drugs include monoclonal antibodies (MAbs) that target the extracellular regions of the receptor (for example, Trastuzumab, which targets ErbB2), as well as small-molecule tyrosine kinase inhibitors (TKIs) that prevent signal transduction through the receptor's tyrosine kinase domain (for example, erlotinib, which targets ErbB1) (reviewed in [38]). ErbB1 and ErbB2 have been the major recipients of attention with much less consideration given to ErbB3 as a consequence of its impaired kinase activity and previously perceived subservient status compared to ErbB2, which was considered to be the “master positive regulator of the ErbB network” [57]. The anti-ErbB2 monoclonal antibody Trastuzumab was the first inhibitor of the ErbB family to be approved by the US Food and Drug Administration (FDA) in 1998 for the treatment of HER-2 positive breast cancer. Today it is in regular clinical use for the treatment of breast cancer alongside hormone-based therapy. The monoclonal antibody Cetuximab and the small molecule TKIs Gefitinib and Erlotinib target ErbB1 in several types of epithelial cancers and have also received regulatory approval – cetuximab (Erbitux) for metastatic colorectal cancer and squamous cell carcinoma of the head and neck, erlotinib (Tarceva) for metastatic pancreatic cancer and non-small-cell lung cancer (NSCLC) and gefitinib (Iressa) for advanced NSCLC [38]. A second-generation, irreversible, pan-ErbB inhibitor presently undergoing clinical trials in patients with advanced lung cancer is PF00299804 [58, 59]. This molecule is a potent inhibitor of ErbB1-activating mutations as well as the ErbB1 T790M resistance mutation both *in vitro* and *in vivo*. The drug also effectively inhibits wild-type ErbB2 and insertion ErbB2 mutations which are observed in the 20-30% of lung cancers that fail gefinitib or erlotinib therapy [58].

3.4. The Failure of ErbB1 and ErbB2 Inhibitors in Prostate Cancer

PCa cells express ErbB1, ErbB2, and ErbB3 receptors [60] so Trastuzumab, Gefitinib and Erlotinib were tested for single-agent therapeutic efficacy in clinical trials in patients with CRPC. No agent, however, displayed any meaningful activity in Phase II trials of men with PCa [61-65]. Preclinical studies had also used Pertuzumab (2C4) - a monoclonal antibody directed against ErbB2 but differed from Trastuzumab in that it prevented ErbB2 heterodimerization with other ErbB family members rather than obstructing ErbB2's ligand-binding domain [38]. Pertuzumab was used to inhibit the growth of CRPC xenografts, while

Trastuzumab used in the same study showed minimal effectiveness in preventing CRPC xenograft growth [66].

In sharp contrast to the preclinical studies, phase II trials of Pertuzumab in patients with CRPC were wholly unsatisfactory - no patient achieved the primary endpoint of >50% decline in PSA [67]. The dual kinase inhibitor lapatinib fared somewhat better in phase II single-agent clinical trials, being fairly well-tolerated and resulting in stable disease for 12 weeks but evidencing no PSA responses [68]. These results challenged the significance of the ErbB1/ErbB2 axis in PCa.

3.5. ErbB3 Activation May Prevent ErbB1 and ErbB2 Inhibitors in PCa

It had been known that while ErbB kinase signals were required for optimal AR function at low levels of androgen, this signaling was mediated not by ErbB1 but by the heterodimerization of ErbB2 with ErbB3 [56]. Sergina *et al.* later demonstrated that ErbB3 was upregulated and provided compensatory signaling precisely in response to ErbB1/ErbB2-directed TKI treatment [69]. ErbB3 activity was characterized by increased membrane localization and phosphorylation. Indeed, ErbB3-directed siRNA duly restored the pro-apoptotic effects of TKIs [69]. These reports suggested that the failure of EGFR and ErbB2 inhibitors may be due to the activation of ErbB3 in these tumors.

Primary PCa cells frequently overexpress ErbB3, which is unaccompanied by increases in ErbB1 or ErbB2 protein [70]. In fact, a surge in the levels – and activation – of ErbB3 is seen when relatively small amounts of ErbB2 are present [71]. Recent work by Soler *et al.* demonstrates that ErbB3 is required for and promotes the invasive capacity of prostate epithelial cells [72]. It achieves this objective by ligand-specific transactivation with either ErbB1 or ErbB2. Castration resistant DU-145 PCa cells were reliant upon ErbB3 expression for optimal motility and clonogenicity *in vitro* and tumorigenicity *in vivo* in response to the NRG-1, EGF and fetal bovine serum [72]. Although MCF-7 breast cancer cells appeared to require ErbB3 as part of an autocrine response induced by EGF and FBS, the response of DU-145 prostate cancer cells to these stimuli, while requiring ErbB3, did not appear to involve autocrine stimulation of the receptor. In both cell types, clonogenicity and tumorigenicity were severely compromised after ErbB3 knockdown with siRNA [72].

ErbB3 has six binding sites for the p85 regulatory subunit of PI3K, as well as for activators of the Ras/mitogen activated protein kinase (MAPK) pathway, and ErbB3-mediated signaling may be responsible for oncogenic cell survival and the promotion of CRPC. As described earlier, AW results in cell cycle arrest whereas CRPC occurs because of release from that arrest. Recent work from our lab shows that in both castration sensitive and CRPC human PCa cell lines and xenografts, AW brought about a visible increase in the protein levels of ErbB3 [73]. This in turn augmented AR transcriptional activity and cell proliferation, signaling the reentry of growth-arrested tumor cells into an actively cycling state. Conversely, ErbB3 downregulation via siRNA suppressed cell viability and impeded CRPC growth [73]. These studies reveal the significant cross-talk between ErbB3 and the AR and indicate a mechanism by which cells may develop resistance to ErbB1 or ErbB2 inhibitors.

4. ErbB3 IN PROSTATE CANCER

4.1. Cellular Localization

The high expression of ErbB3 in certain human cancers suggested that it might be involved in tumor development and, if so, could be marked as a therapeutic target. The cancerous prostate, in comparison to its normal counterpart, overexpresses ErbB3 protein (by IHC visualization [73] and microarray analyses [70]), which indicate poor prognosis. A secreted

isoform of ErbB3 – p45 sErbB3 - was found in PCa bone metastases, activated osteoblasts and new bone matrices but not in the epithelial cells of primary PCa [74]. This isoform stimulated the expression of osteonectin from bone cells which in turn enhanced the invasiveness of PCa cells [75]. It may be mentioned that a secreted, truncated form of ErbB3 – p85 sErbB3 - that acts as a negative regulator of ligand-stimulated ErbB-2, -3 and -4, was found to naturally occur in patients with metastatic breast cancer [76], but has not been studied in PCa patients.

Along with its plasma membranous and cytoplasmic locations, ErbB3, which has a nuclear localization sequence (NLS) near its C-terminal, has been observed in the nuclei of PCa tissues and cell lines. In human PCa tissues, nuclear levels of ErbB3 were low or absent in the benign prostate but increased as the cancer progressed to hormone resistance [77]. Surprisingly, in PCa cell lines, the trend was reversed, with nuclear ErbB3 levels being higher in hormone-sensitive rather than in CRPC cases [77]. As a result, the authors of that study initially associated nuclear ErbB3 staining with risk of disease progression, but in later work discovered that low nuclear localization of ErbB3 was a predictor of biochemical recurrence in patients with PCa and positive surgical margins after radical prostatectomy [78]. ErbB3 expression was also upregulated in the nuclei of PCa cells taken from lymph nodes and bone metastases of patients who had undergone AW therapy [79]. In subcutaneous xenograft tumors of MDA-PCa-2b and PC-3 cell lines, ErbB-3 was predominantly in the membrane/cytoplasm; however, it was present in the nuclei of the xenograft tumor cells implanted in the femur. Castration of mice bearing subcutaneous MDA PCa 2b tumors induced a transient nuclear translocation of ErbB-3, with relocalization to the membrane/cytoplasm upon tumor recurrence [79]. Based on these results, the authors speculate that nuclear localization of ErbB-3 may aid prostate cancer cell survival during androgen ablation and progression of prostate cancer in bone. Based on these results, one can conclude that nuclear localization of ErbB3 may reflect a response to cellular stress (in this case the blocking of AR signaling using an anti-androgen), regulation of RNA synthesis during growth arrest and release from nuclear sequestration in response to proliferation (i.e. when the anti-androgen is removed).

4.2. Ligand-Induced Activation of ErbB3

ErbB3 overexpression does not indicate its activation, since activation requires ligands, dimerization partners, the availability of phosphorylation sites and a variety of intracellular partners to enable signaling. *In vitro* studies suggest that overexpression of a normal receptor leads to transformation only when its appropriate ligand is present; therefore ErbB overexpression has to be accompanied by ligand upregulation (reviewed in [28]). For example, poor prognosis in CRPC directly correlates with overexpressed EGFR, ErbB2, and ErbB3 receptors (at mRNA and/or protein levels) and upregulation of ErbB ligands such as TGF-alpha, ARG, HB-EGF and EPG. mRNA levels for these ligands were increased 10-100 fold in CRPC as compared to castration sensitive PCa cells [80].

As mentioned earlier, the primary ligands for ErbB3 are members of the NRG family, a large group of isoforms possessing an EGF-like C-terminal and a variable N-terminal region [40]. NRG binding to ErbB3 is followed by ErbB3 heterodimerization, especially with ErbB2. ErbB3/ErbB2 dimerization is favored also by ErbB2 overexpression, which biases heterodimerization towards itself [40]. In the absence of ligand binding, ErbB3 exists in a self-associated, oligomeric, catalytically-inactive state, whereas NRG-bound ErbB3 undergoes a conformational change such that it is stabilized and it's extended form exposes the dimerization interface for interaction with ErbB2 [81] (Fig. **4**). The extracellular domain of ErbB3 retains NRG-binding ability even at low acidic pH (owing to the absence of a critical, pH-sensitive histidine residue in domain III) indicating a mechanism of survival in the low pH tumor microenvironment [82]. Analysis of PCa cells reveals the existence of a

paracrine loop involving NRG1 and the ErbB3-ErbB2 dimer [60]. The effects of ErbB3 activation by NRG likely depend upon the ratios of NRG isoforms present, their status as secreted (i.e. expressed but unprocessed or sequestered, hence inactive), and the relative amounts of other ErbB receptors.

NRG1 too is overexpressed in PCa and elicits different ErbB3/ErbB2 activation profiles depending upon the hormone-sensitivity of the cells [60]. For example, androgen-dependent LNCaP cells displayed ErbB3/ErbB2 activation, triggering several downstream cascades including PI3K in response to NRG addition [66]. In contrast, CRPC cell lines demonstrated highly variable outcomes – the AR-negative DU145 and PC-3 were unaffected by NRG, CWR22Rv1 demonstrated ErbB3/ErbB2 dimer formation and cell proliferation, and the recurrent PCa cell line CWR-R1 activated an autocrine pathway between NRG and low-level, constitutively-active ErbB3/ErbB2 that led to AR transactivation via the MAPK and PI3K/Akt routes [66, 83]. Significantly, the growth factors EGF and betacellulin, which are not canonical ErbB3 ligands (see Fig. **2**), also showed increased binding to ErbB3 co-expressed with ErbB2 but other ErbB family ligands TGF-alpha, ARG and HB-EGF did not [84]. These reports indicate the ability of the cancerous cell to activate non-specific binding in ErbB3 although the mechanism of action in these cases is not fully known. Ligand-induced activation of ErbB3 is followed by physical association with other ErbB receptors **(**Fig. **4)**. It may be noted that ErbB4 expression is lost in most PCa patients, leaving only ErbB1 and ErbB2 available for heterodimerization with ErbB3 [60] (Fig. **5**).

4.3. ErbB3 Phosphorylation and Downstream Signaling Partners

ErbB3 heterodimerization is followed by autophosphorylation on tyrosine residues and each receptor thus activates its partner (Fig. **4**). Kinases other than ErbB family members can also phosphorylate ErbB3 and notable among these are Src and MET [85, 86]. Both kinases bind to ErbB3, increase its phosphorylation and enhance oncogenic signaling via the ErbB3/ErbB2 heterodimer. Additionally, ErbB3 is activated by the non-receptor Tec family tyrosine kinase Bmx/Etk [87]. In response to ligand stimulation, Bmx/Etk is activated by tyrosine phosphorylation downstream of Src and PI3K in PTEN-deficient PCa cells. Etk downregulation by siRNA markedly decreases PCa cell growth, implying potential validity as a therapeutic target. Other kinase activators of ErbB3 include CDK5 [88], the breast cancer associated BRK/PTK6 [89], transactivation by cellular stress and cytokines like TNF-alpha and Interferon-alpha [90, 91]. Janus tyrosine kinases JAK1 and TYK2 have also been implicated as ErbB3 interactors, though neither demonstrated physical association with ErbB3 [92]. The transphosphorylation events resulting from kinase activity create docking sites for adaptor protein binding. These phosphotyrosine binding proteins associate with the tail of each ErbB molecule after engagement into dimeric complexes and determine the specificity and potency of the ensuing intra-cellular signal.

An invariable target of activated ErbB3 heterodimeric complexes is the PI3K/AKT pathway. While ErbB1 and ErbB2 interact with and activate PI3K via adaptor proteins, ErbB3 possesses six binding sites for the p85 regulatory subunit of PI3K, enabling its direct activation [40]. Each of these p85 sites cooperatively contributed to ErbB3 signaling, as was demonstrated by sequential mutation and restoration. Indeed, ErbB3 seems to be the preferred partner when signaling occurs through the PI3K pathway [93]. Activated PI3K phosphorylates AKT which sets in motion the phosphorylation and activation of numerous downstream proteins, resulting in processes that represses apoptosis and promote survival. ErbB3/PI3K/AKT-induced survival and proliferation pathways have been implicated in numerous human cancers and AKT has been singled out for its regulation of CRPC cell proliferation by activating additional signal transduction pathways and stimulating ligand-independent AR activation [29, 35, 36]. Indeed, it has long been known that Akt phosphorylation increases during AW treatment of castration sensitive cells and remains

high in CRPC, but for long, it was not known what factors contributed to this elevation. Our recent work implicates ErbB3 as a possible cause for the increase in Akt phosphorylation since ErbB3 also increased during AW and remained high in CRPC [73]. Therefore the increase in ErbB3 is likely a major cause for the inability of AW to induce cell death.

4.4. Interaction Between ErbB3 and the AR is Mediated by Ebp1

As mentioned in section 2.2, above, the AR is known to remain active in CRPC and continues to regulate signaling pathways that allow them to proliferate and differentiate. There is some evidence suggesting that ErbB3 may be responsible for this ligand-independent AR activation. It was observed that ErbB2/ErbB3 heterodimers, but not ErbB2/ErbB1 units, modulated AR transcriptional activity by stabilizing AR protein and enhancing binding to its cognate AREs [56]. Phosphorylated AR was correlated with activated ErbB3 in animal models and AR-mediated transactivation of reporter genes in human CWR-R1 PCa cells [83].

An intriguing mediator of AR-ErbB3 interaction is the ErbB3 binding protein-1 (Ebp1) [94]. First discovered in a yeast two-hybrid assay, it interacted with the first 15 amino acids of the juxtamembrane domain of unphosphorylated ErbB3, binding directly to ErbB3 only if that RTK was constitutively phosphorylated by PKC [95]. Ebp1 exists as two isoforms that differ in their abilities to bind ErbB3, localize intracellularly and affect cell survival and differentiation [96]. Ebp1 is also recognized as a nucleolar growth regulating factor and an inhibitor of eIF2α phosphorylation, an initiator of protein translation. Ebp1 is phosphorylated upon NRG stimulation, dissociates itself from ErbB3 and travels to the nucleus. There it interacts directly with the cell cycle regulator pRB, inhibiting transcription of E2F regulated genes by recruiting, among other factors, SIN3A and histone deacetylase (reviewed in [97]).

Ebp1 contains an LXXLL motif that allows it to interact with the AR. It is an AR corepressor which inhibits transcription from AR-responsive gene promoters, including transcription of the AR itself [98, 99]. Ebp1 mRNA and protein levels, therefore, decrease in PCa versus normal prostate tissue [100]. *In vitro* and *in vivo* data demonstrated that Ebp1 overexpression resulted in reduced incidence of LNCaP tumors and slower growth of remaining tumors while siRNA-mediated Ebp1 downregulation in LNCaP cells activated the AR despite absence of androgen [101]. Combined Ebp1 upregulation and cyclin D1 downregulation ($Ebp1^{+}/D1^{-}$) predicted PSA relapse, establishing Ebp1's correlation to PCa progression [102].

4.5. Regulation of ErbB3 Levels by the AR is Mediated by Nrdp1

Early work on the regulation of ErbB3 degradation by Nrdp1 was conducted in mammary tumor models and has only recently been applied to PCa. The proteasomal degradation of ErbB3 is regulated by the RING finger E3 ubiquitin ligase Nrdp1 (neuregulin receptor degradation protein 1), also known as RNF41 or FLRF. Like Ebp1, described above, Nrdp1 too was discovered as an ErbB3-interacting protein by yeast two-hybrid analyses and stimulated ErbB3 ubiquitination and degradation in a ligand-independent manner [103]. Thus it regulated the RTK's steady-state levels. Corepressor experiments indicated that Nrdp1 specifically bound to ErbB3 and ErbB4 but not to ErbB1 or ErbB2. The C-terminal domain (CTD) of Nrdp1 directly binds to ErbB3's cytoplasmic tail while the N-terminal RING finger domain is responsible for ErbB3 ubiquitination and turnover. Nrdp1 is itself highly labile, undergoing self-ubiquitination and proteasomal degradation via the deubiquitinating enzyme USP8 [104]. Both proteins – Nrdp1 and USP8 - thus contribute to the efficiency of ErbB3 downregulation by steering it away from the recycling pathway and towards the degradation route. Proteins th at target recep tors towards ligand-independent

degradation potentially play a significant role in stifling tumor growth properties by suppressing receptor levels. In a transgenic murine model of ErbB2-induced mammary carcinogenesis, the ErbB2 transgene product is highly expressed in tumors but is scarcely detected in non-tumor tissue [105]. Similarly, ErbB3 protein is overexpressed only in tumors and not in uninvolved mammary tissues in these animals. This is not attributed to differences in transcript levels [105]. The same group reported the interesting observation that Nrdp1 protein was present in healthy mammary tissue from the ErbB2-transgenic mice but was completely lost in tumors [105], suggesting that Nrdp1 played the role of tumor suppressant by keeping ErbB3 levels – and signaling - in check.

Little however is known about the expression and function of Nrdp1 in PCa. Recent work from our lab has offered novel insight into one potential mechanism of Nrdp1-mediated CRPC development. We show that ErbB3 protein is negatively regulated by the AR in androgen dependent cells, but not in CRPC cells [73]. AW caused a sharp drop in AR protein levels and transcriptional activity, resulting in the growth arrest of castration sensitive cells. A simultaneous increase in ErbB3 levels was observed in the castration sensitive cells, persisting even after the cessation of AW treatment, which likely drove, at least partly, the eventual growth of the CRPC cells. Continued probe of the AR-ErbB3 relationship uncovered the involvement of Nrdp1, which was found to be under the positive transcriptional control of the AR in castration sensitive cells, and AR-mediated Nrdp1 expression resulted in the ubiquitination and degradation of ErbB3 in these cells. Significantly, CRPC cells, unlike castration sensitive ones, appeared to experience a proliferative advantage because the AR was no longer able to direct the transcription of Nrdp1 in CRPC. The differential regulation of ErbB receptors by the AR in castration sensitive, but not in CRPC cells have also been reported for EGFR and ErbB2 by two separate groups who demonstrated that the AR regulated and was regulated by ErbB1 and ErbB2 in castration sensitive, but not in CRPC, human cell lines [52, 53]. Steroid receptor control of the ErbB receptors likely indicates a mechanism by which the AR suppressed cell growth regulated by the ErbB receptors in castration sensitive cells, and loss of this control with PCa progression may be an important aspect of why and how castration resistance develops.

5. ErbB3 AND TKI RESISTANCE

It is apparent from the above discussion that ErbB3 is intimately involved in the transformative pathways that drive PCa from a castration sensitive to a castration resistant phenotype. Several experimental approaches are being developed using ErbB3 as a therapeutic target. Strategies to target this RTK can broadly be divided into two categories – targeting only the ErbB3 receptor or preventing the formation of ErbB2/ErbB3 oncogenic unit (see below). Among the classes of agents being developed, small molecule tyrosine kinase inhibitors (TKIs) and monoclonal antibodies (MAbs) have gone the farthest. The majority of small molecule TKIs interferes with ATP binding within the receptor's catalytic domain and obstructs trans-autophosphorylation whereas MAbs are raised such that they target the receptor's extracellular region and limit ligand binding. The exception is Pertuzumab which was developed to prevent the dimerization of ErbB2 with ErbB3 (discussed earlier). The end result is that ErbB signaling is inhibited. While we describe a myriad of methods, we note that not all of them have been applied specifically to a PCa model.

The principal signaling function of ErbB3 in cancers was thought to be its role as a binding partner of ErbB1 or ErbB2 and a scaffold for the recruitment of cytosolic signaling proteins. Targeting scaffold functions is difficult for currently available pharmaceutical technologies, and for a long time, ErbB3 lacked a specific inhibitor, particularly since ErbB3 was thought

to lack kinase activity [106]. However, recent data from Shi *et al*. provide surprising evidence of ErbB3's ability to bind to ATP and promote autophosphorylation of the receptor's intracellular domain when clustered at a membrane surface [107]. While ErbB3's tyrosine kinase activity was ~1000-fold lower than that of ErbB1, this small amount of activity was clearly sufficient for the initial autophosphorylation steps. Full kinase activation – or activity that is 150-1000-fold greater – is required only for the receptor to phosphorylate downstream signaling or docking molecules [107]. The weakly-catalytic ErbB3 thus efficiently phosphorylates ErbB2 whose vastly superior kinase activity then takes up the task of phosphorylating downstream substrates, propagating the pro-survival signal in a rapid and robust manner. ErbB3 autophosphorylation *in vitro* is uninhibited by single inhibitors of ErbB1 or ErbB2, displaying the probable culpability of residual ErbB3 kinase signaling in promoting TKI resistance [107].

Despite the current finding of weak intrinsic kinase function in ErbB3, it is still difficult to target the function of this RTK because the overall role of the kinase function is relatively low-grade compared to its function in heterodimer formation and in scaffolding. To overcome this drawback, and yet recognizing the importance of ErbB3 in different cancers, pharmaceutical companies and other investigators have taken innovative approaches to inhibit this RTK. Below, we will discuss possible methods of inhibiting ErbB3 signaling, some intentional and some fortuitous (see Table **1**).

5.1. Monoclonal Humanized Anti-ErbB3 Antibodies

ErbB3's signaling functions depend upon ligand binding to its extracellular domain and inhibitors are generated to disrupt this interaction. A recently-characterized, ErbB3-specific humanized antibody MM-121 blocked ligand-dependent ErbB3 activation induced by the ErbB1, ErbB2 or MET receptors [108]. This MAb was tested in a variety of human cancer cell lines and tumor xenograft models (lung, renal, gastric, breast and ovarian) and worked most efficiently in those cancers that overexpressed the ErbB3-specific ligand heregulin. The aggressive human prostate cancer cell line DU-145 also fell into this category, for it harbors a strongly-activating, ErbB3-heregulin autocrine loop. In contrast, the Ab fared poorly in cells with an amplified ErbB2 gene because their growth was likely driven by ligand-independent and not ligand-dependent mechanisms. MM-121 is currently in clinical development as a therapy against a variety of cancers [108].

Another ErbB3-targeted MAb is AMG-888 (U3-1287, NCT00730470) - *in vitro* studies showed that AMG-888 was able to inhibit the growth of multiple tumor cell lines (breast, lung, colorectal) that were resistant to other ErbB family inhibitors[1]. Additionally, AMG-888 demonstrated statistically significant growth inhibition of established xenograft tumors as a single agent and in combination with other ErbB family inhibitors. This fully-humanized MAb is currently in Phase I trials in patients with advanced solid tumors that have become refractory to standard therapy or for which no acceptable treatment currently exists. AMG-888 prevents ligand-induced phosphorylation of ErbB3, ErbB2, and downstream effector molecules including Akt, ERK1 and ERK2. *In vivo* studies show that colony formation in pancreatic cancer cells and tumor growth in pancreatic, non-small cell lung cancer, and colorectal xenograft models are both significantly decreased following treatment with this drug (see also [109]).

[1]Freeman, D., S. Ogbagabriel, M. Rothe, R. Radinsky, and M. Treder. Fully human anti-HER3 mAb U3-1287 (AMG 888) demonstrates unique *in vitro* and *in vivo* activities 309 versus other HER family inhibitors in NSCLC models. Proceedings of the 99th Annual Meeting of the American Association for Cancer Research. 2008. San Diego, CA, USA.

5.2. Dual- or Multi-ErbB Inhibitory Approach

It should be clear by now that the ErbB receptors cooperate with each other in driving signal transduction towards malignant transformation. The mutual interactions that exist between these receptors tend to compromise the success of drugs that target individual receptors in cancer treatment. Preclinical studies show that tumor cells can rescue themselves, in more ways than one, from the inhibitory effects of an agent directed toward one ErbB receptor. They may alter their activation ability by relying on the ligand for a different ErbB receptor [110], shifting their signaling profiles such that an untargeted receptor is made to drive cellular growth [69, 111] or co-opting an entirely different RTK into a pro-survival, heterotrimeric supercomplex [112]. In all cases, signaling is but temporarily halted, only to inevitably return stronger than before. On the other hand, both *in vitro* and *in vivo* models have shown that employing a dual- or multi-ErbB inhibitory approach demonstrates greater anti-tumor activity than agents targeting an individual ErbB receptor [113-117]. Strategies involve putting together two types of MAbs, combining TKIs with MAbs or administering single molecules that inhibit one or more ErbBs simultaneously (discussed later). In the case of ErbB3, MM-121 combined with the anti-ErbB1 MAb cetuximab led to prolonged RTK inhibition in a mouse lung cancer model when compared to MM-121 alone [108]. As an ErbB-targeted approach, the combination of a MAb and TKI uses two agents with different sites of action. For example, trastuzumab plus the dual ErbB1/ErbB2 inhibitor lapatinib given to patients with metastatic breast cancer increased progression-free survival rate [118]. Among the reasons proposed for their therapeutic synergy was the ability of lapatinib (but inability of trastuzumab) to bind to truncated ErbB2 [93], often overexpressed in metastatic breast cancer.

Multi-ErbB inhibitors are being pursued most vigorously and antagonize the actions of ErbB heterodimers or inhibit, at one time, more than one individual ErbB receptor. Implicit in the inhibition of the ErbB1/ErbB2 heterodimer is the notion that ErbB3 too will be deactivated for lack of available ErbB dimerisation partners, especially in diseases like PCa where the fourth member of this family, ErbB4, is lost [60] (Fig. **6**). Of note is the fact that the newer pan-ErbB inhibitors also aim at directly disrupting ErbB3 activity.

The first-generation, irreversible, pan-ErbB inhibitor canertinib (Cl-1033) inhibited TK activity of all the ErbB family members without affecting other RTKs (PDGFR, FGFR, IGFR) even when administered at high concentrations to a variety of human cancer cell lines, including PCa cell lines [119]. It is interesting to note that canertinib also induced G1 cell cycle arrest and apoptosis in an ErbB-independent manner in cell lines derived from human pre-myelocytes and histiocytic lymphomas [120]. While transcripts for all ErbBs were readily detected in these cell lines, protein expression was absent. This raises the possibility of canertinib exerting an off-target effect through an as-yet undetermined molecular mechanism, possibly involving the inhibition of mRNA translation of the ErbB receptors [120]. Canertinib is currently in Phase II clinical trials for the treatment of patients with advanced-stage non-small cell lung cancer (NSCLC) [121].

The pan-TKI MP470 was designed using a structure-based approach and inhibited cell proliferation in human castration resistant and CRPC cell lines [122]. When co-administered with erlotinib in the context of an LNCaP mouse xenograft model, the drugs not only completely abrogated ErbB1, ErbB2 and ErbB3 phosphorylation, but also prevented ErbB3 binding to PI3K and inhibited downstream Akt activity, even in androgen-depleted conditions. The safety and efficacy of the MP470-erlotinib combination is currently being evaluated in Phase 1 clinical trials for refractory solid tumors [122].

One of the most recently-documented pan-ErbB inhibitors is AstraZeneca's AZD8931 [123], shown to have activity as an equipotent TKI against ErbB1, ErbB2 and ErbB3 signaling in a

variety of human head and neck, non-small-cell lung and breast cancer cell lines and murine xenograft models. The drug displayed greater inhibitory activity towards the ErbB3/ErbB2 oncodimer and was expected to be of particular use in solid tumors that did not contain amplified ErbB2 or mutated ErbB1 genes.

Another pan-ErbB inhibitor mentioned above is PF00299804, a potent inhibitor of EGFR-activating mutations as well as the EGFR T790M resistance mutation both *in vitro* and *in vivo* [58]. PF00299804 also inhibits both wild-type and gefitinib-resistant mutated ErbB2 identified in lung cancers [58]. Increased expression of ErbB3 was shown to induce resistance to PF00299804 [124]. This drug is an irreversible inhibitor of ErbB1 [58], which has been shown to inhibit the growth of various cell lines overexpressing ErbB3 [59].

One of the most successful pan-ErbB inhibitors have been lapatinib (GW275016) which has been mentioned throughout in this review. Tyrosine phosphorylation of ErbB2 and ErbB3, AR transactivation, and cell proliferation induced by heregulin were more potently inhibited by lapatinib than the EGFR-specific inhibitor gefitinib [83]. Basal proliferation in the absence of growth factors was also inhibited by lapatinib to a greater extent than gefitinib, suggesting that low level HER2/H ER3 activ ation perhaps by an autocrine pathway contributes to the proliferation signal [83, 125]. As mentioned earlier, a Phase II multicenter clinical trial to evaluate Lapatinib in early stage, hormonally untreated recurrent or metastatic prostate cancer was unsuccessful [68], but will be discussed further in the section below.

5.3. Effectiveness of Dual ErbB1/ErbB2 Inhibitors in Combination with AW Therapy

As mentioned earlier in this article, activation of the ErbB2/ErbB3 signaling cascade can lead to constitutive, ligand-independent activation of the AR and render PCa cells indifferent to AR inhibition [55, 56]. In fact, activation of the ErbB receptors, leading to stimulation of parallel signaling pathways that bypass the AR and regulate cell signaling and survival independent of the AR, is a major cause of the development of CRPC (see section 2.2). On the other hand, merely inhibiting ErbB2, or dual ErbB1/ErbB2 or even pan-ErbB inhibitors were insufficient to inhibit cell growth completely in patients with CRPC [67], given that this disease is associated with a large number of aberrations, many of which are associated with increased activation of the AR. Therefore, it is more reasonable to utilize the ErbB inhibitiors at an earlier stage in order to prevent the progression of the disease. Rather than apply these drugs to patients with CRPC, they may be better used in hormone-sensitive patients when combined with anti-androgens.

Indeed, applying an ErbB inhibitor alongside an AR inhibitor appears to be more efficacious, at least in initial studies. For example, in MDA PCa 2a prostate cancer cells, the AR antagonist hydroxyflutamide proved more efficacious when combined with cetuximab and trastuzumab [126]. Significantly, in androgen-dependent PCa cell lines, co-administration of gefitinib and bicalutamide resulted in concurrent inhibition of AR and ErbB1/ErbB2 pathways, causing a significant delay in the onset of ErbB-driven castration resistance [127]. The same principle has been suggested for PCa patients who have undergone radical prostatectomy and radiation therapy - lapatinib plus an anti-androgen appear to offer a better therapeutic option than lapatinib alone[2].

The problem with anti-androgens is that the patients acquire resistant to this treatment fairly quickly. Acquisition of resistance employs multiple mechanisms including the failure of the drug to bind to its target. In that case, alternate mechanisms of action to decrease AR

[2]Chen, Y., G. Wilding, J. Gee, R.P. DiPaola, M. Pins, M.A. Carducci, M.N. Stein, G. Bubley, and G. Liu; A phase II trial of lapatinib (GW572016) in patients with recurrent prostate cancer as evident by a rising PSA. *J Clin Oncol*, **2008**. *26* (15), 5170-5170.

transcriptional activity are needed. Clinical resistance to TKI therapy is also associated with re-activation of PI3K signaling [69]. The combination of anti-ErbB/anti-PI3K therapeutics is effective in animal models and is undergoing extensive clinical testing [128]. There has been emphasis on the use of PI3K inhibitors in tumors that are resistant to the ErbB1 or ErbB2 inhibitors Erlotinib, Lapatinib, and Trastuzumab because the resurgence of PI3K signaling is largely due to the direct activation of upregulated ErbB3 [129-131].

6. CONCLUSIONS AND FUTURE DIRECTIONS

The preponderance of literature leads to the conclusion that CRPC arises because a few (or more) tumor cells survive first line AW therapy and then recur with an altered phenotype that no longer respond to this therapy. Hence, if the existing tumor cells are all eliminated completely, then the chances of the tumor recurring are reduced to a large extent, regardless of whether the tumor arises by alterations in existing tumor cells or whether cancer stem cells give rise to new tumors that are castration resistant. Activation of the PI3K pathway appears to be a major factor in the ability of the cells to survive, whether by apoptosis or by the triggering of autophagy. Therefore, disruption of the cell survival mechanism during AW seems to be a promising method by which CRPC can be prevented to a large extent.

Disruption of the PI3K/Akt pathway directly is of course possible, but Akt is such an important mechanism in the survival of all the cells in the body, that systemic inhibition of Akt phosphorylation is bound to have a tremendous impact on the survival of normal cells as well. Indeed, in Phase II clinical trials, the Akt inhibitor perifosine was shown to cause Grade 1-2 fatigue and gastrointestinal toxicities [132], and Grade 3 dose-limiting toxicities resulting in hyponatremia, arthritis, hyperuricemia, and photophobia [133]. Indeed, since the ErbB receptors are major activators of the PI3K/Akt pathway, it may be advantageous to inhibit the ErbB receptors directly. However, as has been shown above, inhibition of EGFR or ErbB2 individually did not seem to have a significant impact in clinical trials. We also offer proof that the failure of these single EGFR and ErbB2 inhibitors may result from the activation of ErbB3, and that dual inhibition of EGFR and ErbB2 may fare better, especially in patients undergoing AW therapy[2]. This observation is all the more significant because we have shown that AW therapy at the cellular level induces an increase in ErbB3 levels that may contribute to the induction of the CRPC phenotype [73].

Fig. (**6**) summarizes how the presence of ErbB3 prevents the effect of individual inhibitors of EGFR and ErbB2 on cell survival. Most prostate cancer cells do not express ErbB4 [60, 134], indeed, expression of ErbB4 appeared to disrupt the growth of prostate cancer cells [135, 136]. Therefore, the only possible ErbB dimers in PCa are EGFR homodimers and ErbB1-ErbB2, ErbB2-ErbB3, and ErbB1-ErbB3 heterodimers. Individual inhibition of EGFR using specific and selective inhibitors would disrupt the functioning of EGFR homodimers and ErbB1-ErbB2 and ErbB1-ErbB3 homodimers, but signaling would still continue through the ErbB2-ErbB3 heterodimers. Similarly, individual inhibition of ErbB2 would prevent signaling downstream of ErbB1-ErbB2 and ErbB2-ErbB3 heterodimers but allow signaling downstream of EGFR homodimers and ErbB1-ErbB3 heterodimers. However, dual inhibition of both EGFR and ErbB2 would inhibit all 4 dimers, thereby completely stopping the abnormal activation of downstream targets through the ErbB receptors.

Since it has become clear that ErbB3 occupies a prominent role in regulating cellular processes that promote CRPC future studies that explore in greater detail previously un-characterized aspects of ErbB3 biology are warrented. What roles do the truncated isoforms of ErbB3 play, given their opposing functions? Recent clinical findings indicate that p45 sErbB3 could be involved in the bone-forming pheno-type typical of bone metastases in PCa

[137]. The novel ErbB3 isoform p85 sErbB3 may be an ideal candidate for cancer drug development, given its effectiveness at blocking HRG-induced cell growth [76]. What is the importance of ErbB3's nuclear and nucleolar localization? Recent work has revealed a vast array of interesting proteins - for example, Ras regulatory molecules and proteins involved in cell motility - that might bind to ErbB3 and promote ErbB3-mediated tumorigenesis [84]. The molecular basis of these interactions, as well as those involving ErbB3 regulation by the non-ErbB tyrosine kinases Src, MET and CDK5 (among others) remain unknown and merit further investigation. The widely-expressed Ebp1 has presented itself as a viable therapeutic target in CRPC and it would be interesting to learn of studies that advanced this premise. However, Fig. (**6**) also shows the limitations of single therapy using ErbB3 inhibitors. We conclude that ErbB3 inhibitors in combination with other related inhibitors may be of interest in the prevention of prostate cancer progression to CRPC.

ABBREVIATIONS

AR	Androgen Receptor
ARE	Androgen Response Element
ARG	Ampiregulin
AW	Androgen withdrawal
BRK/PTK6	Breast tumour kinase/Tyrosine-protein kinase-6
CAB	Complete androgen blockade
CDK5	Cyclin-dependent kinase-5
CRPC	Castration Resistant Prostate Cancer
CTD	C-terminal domain
DHT	Dihydrotestostereone
Ebp1	ErbB3 binding protein-1
EBT	External beam radiotherapy
EGF	Epidermal Growth Factor
EGFR	Epidermal Growth Factor Receptor
eIF2α	Eukaryotic translation initiation factor 2
EPG	Epiregulin
ErbB	Erythroblastic Leukemia Viral Oncogene Homolog
ERK	Extracellular signal-regulated kinase
FDA	Food and Drug Admininstration
FGFR	Fibroblast growth factor receptor
FLRF	Fetal Liver Related Factor
GnRH	Gonadotrophin-releasing hormone
HB-EGF	Heparin-Binding Epidermal Growth Factor
HER	Human Epidermal growth factor Receptor
HRG	Heregulins
IGFR	Insulin-like growth factor receptor

IHC	Immunohistochemistry
JAK	Janus kinase (“just another kinase”)
LHRH	Luteinizing-hormone-releasing hormone
MAb	Monoclonal antibody
MAPK	Mitogen activated protein kinase
MET	MNNG HOS Transforming gene
NLS	Nuclear localization sequence
Nrdp1	Neuregulin receptor degradation protein 1
NRG	Neuregulin
NSCLC	Non-small-cell lung cancer
PCa	Prostate Cancer
PDGFR	Platelet-derived growth factor receptor
PI3K	Phosphatidylinositol 3-kinase
PKC	Protein Kinase C
pRB	Retinoblastoma gene product
PSA	Prostate-specific antigen
PTEN	Phosphatase with tensin homogy
RING	Really interesting new gene
RTK	Receptor tyrosine kinase
siRNA	Small Interfering RNA
TGF	Transforming Growth Factor
TK	Tyrosine Kinase
TKI	Tyrosine kinase inhibitor
TNF	Tumor Necrosis Factor
TYK2	Tyrosine kinase-2

REFERENCES

1. Adams J. The case of scirrhous of the prostate gland with corresponding affliction of the lymphatic glands in the lumbar region and in the pelvis. Lancet. 1853; 1(1):393–393.
2. Pisu M, Oliver JS, Kim YI, Elder K, Martin M, Richardson LC. Treatment for older prostate cancer patients: disparities in a southern state. Med. Care. 2010; 48(10):915–922. [PubMed: 20733530]
3. Williams H, Powell IJ. Epidemiology, pathology, and genetics of prostate cancer among African Americans compared with other ethnicities. Methods Mol. Biol. 2009; 472:439–453. [PubMed: 19107447]
4. Galvin DJ, Eastham JA. Critical appraisal of outcomes following open radical prostatectomy. Curr. Opin. Urol. 2009; 19(3):297–302. [PubMed: 19365894]
5. Marcus DM, Jani AB, Godette K, Rossi PJ. A review of low-dose-rate prostate brachytherapy--techniques and outcomes. J. Natl. Med. Assoc. 2010; 102(6):500–510. [PubMed: 20575216]
6. Huggins C, Hodges CV. Studies on prostatic cancer. I. The effect of castration, of estrogen and androgen injection on serum phosphatases in metastatic carcinoma of the prostate. CA Cancer J. Clin. 1972; 22(4):232–240. [PubMed: 4625049]

7. Diaz M, Patterson SG. Management of androgen-independent prostate cancer. Cancer Control. 2004; 11(6):364–373. [PubMed: 15625524]
8. Labrie F, Belanger A, Cusan L, Labrie C, Simard J, Luu-The V, Diamond P, Gomez J-L, Candas B. History of LHRH agonist and combination therapy in prostate cancer. Endocr. Relat. Cancer. 1996; 3(3):243–278.
9. Thompson IM. Flare associated with LHRH-agonist therapy. Rev. Urol. 2001; 3(Suppl. 3):S10–14. [PubMed: 16986003]
10. Akaza H. Combined androgen blockade for prostate cancer: review of efficacy, safety and cost-effectiveness. Cancer Sci. 2011; 102(1):51–56. [PubMed: 21091846]
11. Petrylak D. Therapeutic options in androgen-independent prostate cancer: building on docetaxel. BJU Int. 2005; 96(Suppl. 2):41–46. [PubMed: 16359438]
12. Higano CS, Small EJ, Schellhammer P, Yasothan U, Gubernick S, Kirkpatrick P, Kantoff PW. Sipuleucel-T. Nat. Rev. Drug Discov. 2010; 9(7):513–514. [PubMed: 20592741]
13. Berges RR, Vukanovic J, Epstein JI, CarMichel M, Cisek L, Johnson DE, Veltri RW, Walsh PC, Isaacs JT. Implication of cell kinetic changes during the progression of human prostatic cancer. Clin. Cancer Res. 1995; 1(5):473–480. [PubMed: 9816006]
14. Isaacs JT. Antagonistic effect of androgen on prostatic cell death. Prostate. 1984; 5(5):545–557. [PubMed: 6483690]
15. Armas OA, Aprikian AG, Melamed J, Cordon-Cardo C, Cohen DW, Erlandson R, Fair WR, Reuter VE. Clinical and pathobiological effects of neoadjuvant total androgen ablation therapy on clinically localized prostatic adenocarcinoma. Am. J. Surg. Pathol. 1994; 18(10):979–991. [PubMed: 7522415]
16. Matsushima H, Goto T, Hosaka Y, Kitamura T, Kawabe K. Correlation between proliferation, apoptosis, and angiogenesis in prostate carcinoma and their relation to androgen ablation. Cancer. 1999; 85(8):1822–1827. [PubMed: 10223578]
17. Reuter VE. Pathological changes in benign and malignant prostatic tissue following androgen deprivation therapy. Urology. 1997; 49(3A Suppl):16–22. [PubMed: 9123731]
18. Westin P, Stattin P, Damber JE, Bergh A. Castration therapy rapidly induces apoptosis in a minority and decreases cell proliferation in a majority of human prostatic tumors. Am. J. Pathol. 1995; 146(6):1368–1375. [PubMed: 7778676]
19. Murphy WM, Soloway MS, Barrows GH. Pathologic changes associated with androgen deprivation therapy for prostate cancer. Cancer. 1991; 68(4):821–828. [PubMed: 1906775]
20. Bladou F, Vessella RL, Buhler KR, Ellis WJ, True LD, Lange PH. Cell proliferation and apoptosis during prostatic tumor xenograft involution and regrowth after castration. Int. J. Cancer. 1996; 67(6):785–790. [PubMed: 8824549]
21. van Weerden WM, van Kreuningen A, Elissen NM, Vermeij M, de Jong FH, van Steenbrugge GJ, Schröder FH. Castration-induced changes in morphology, androgen levels, and proliferative activity of human prostate cancer tissue grown in athymic nude mice. Prostate. 1993; 23(2):149–164. [PubMed: 8378188]
22. Brändström A, Westin P, Bergh A, Cajander S, Damber JE. Castration induces apoptosis in the ventral prostate but not in an androgen-sensitive prostatic adenocarcinoma in the rat. Cancer Res. 1994; 54(13):3594–3601. [PubMed: 8012987]
23. Westin P, Bergh A, Damber JE. Castration rapidly results in a major reduction in epithelial cell numbers in the rat prostate, but not in the highly differentiated Dunning R3327 prostatic adenocarcinoma. Prostate. 1993; 22(1):65–74. [PubMed: 8426839]
24. English HF, Kyprianou N, Isaacs JT. Relationship between DNA fragmentation and apoptosis in the programmed cell death in the rat prostate following castration. Prostate. 1989; 15(3):233–250. [PubMed: 2555799]
25. Agus DB, Golde DW, Sgouros G, Ballangrud A, Cordon-Cardo C, Scher HI. Positron emission tomography of a human prostate cancer xenograft: association of changes in deoxyglucose accumulation with other measures of outcome following androgen withdrawal. Cancer Res. 1998; 58(14):3009–3014. [PubMed: 9679964]

26. Agus DB, Cordon-Cardo C, Fox W, Drobnjak M, Koff A, Golde DW, Scher HI. Prostate cancer cell cycle regulators: response to androgen withdrawal and development of androgen independence. J. Natl. Cancer Inst. 1999; 91(21):1869–1876. [PubMed: 10547394]
27. Edwards J, Bartlett JM. The androgen receptor and signal-transduction pathways in hormone-refractory prostate cancer. Part 1: Modifications to the androgen receptor. BJU Int. 2005; 95(9): 1320–1326. [PubMed: 15892825]
28. Feldman BJ, Feldman D. The development of androgen-independent prostate cancer. Nat. Rev. Cancer. 2001; 1(1):34–45. [PubMed: 11900250]
29. Ghosh PM, Malik SN, Bedolla RG, Wang Y, Mikhailova M, Prihoda TJ, Troyer DA, Kreisberg JI. Signal transduction pathways in androgen-dependent and -independent prostate cancer cell proliferation. Endocr. Relat. Cancer. 2005; 12(1):119–134. [PubMed: 15788644]
30. Liao X, Tang S, Thrasher JB, Griebling TL, Li B. Small-interfering RNA-induced androgen receptor silencing leads to apoptotic cell death in prostate cancer. Mol. Cancer Ther. 2005; 4(4): 505–515. [PubMed: 15827323]
31. Snoek R, Cheng H, Margiotti K, Wafa LA, Wong CA, Wong EC, Fazli L, Nelson CC, Gleave ME, Rennie PS. *In vivo* knockdown of the androgen receptor results in growth inhibition and regression of well-established, castration-resistant prostate tumors. Clin. Cancer Res. 2009; 15(1):39–47. [PubMed: 19118031]
32. Cheng H, Snoek R, Ghaidi F, Cox ME, Rennie PS. Short hairpin RNA knockdown of the androgen receptor attenuates ligand-independent activation and delays tumor progression. Cancer Res. 2006; 66(21):10613–10620. [PubMed: 17079486]
33. Wen Y, Hu MC, Makino K, Spohn B, Bartholomeusz G, Yan DH, Hung MC. HER-2/neu promotes androgen-independent survival and growth of prostate cancer cells through the Akt pathway. Cancer Res. 2000; 60(24):6841–6845. [PubMed: 11156376]
34. Lukacs RU, Lawson DA, Xin L, Zong Y, Garraway I, Goldstein AS, Memarzadeh S, Witte ON. Epithelial stem cells of the prostate and their role in cancer progression. Cold Spring Harb Symp. Quant. Biol. 2008; 73:491–502. [PubMed: 19022743]
35. Ghosh PM, Malik S, Bedolla R, Kreisberg JI. Akt in prostate cancer: possible role in androgen-independence. Curr. Drug Metab. 2003; 4(6):487–496. [PubMed: 14683476]
36. Wang Y, Kreisberg JI, Ghosh PM. Cross-talk between the androgen receptor and the phosphatidylinositol 3-kinase/Akt pathway in prostate cancer. Curr. Cancer Drug Targets. 2007; 7(6):591–604. [PubMed: 17896924]
37. Cinar B, De Benedetti A, Freeman MR. Post-transcriptional regulation of the androgen receptor by Mammalian target of rapamycin. Cancer Res. 2005; 65(7):2547–2553. [PubMed: 15805247]
38. Gross ME, Jo S, Agus DB. Update on HER-kinase-directed therapy in prostate cancer. Clin. Adv. Hematol. Oncol. 2004; 2(1):53–56. 64. [PubMed: 16163160]
39. Lorenzo GD, Bianco R, Tortora G, Ciardiello F. Involvement of growth factor receptors of the epidermal growth factor receptor family in prostate cancer development and progression to androgen independence. Clin. Prost Cancer. 2003; 2(1):50–57.
40. Olayioye MA, Neve RM, Lane HA, Hynes NE. The ErbB signaling network: receptor heterodimerization in development and cancer. EMBO. J. 2000; 19(13):3159–3167. [PubMed: 10880430]
41. Hynes NE, Lane HA. ERBB receptors and cancer: the complexity of targeted inhibitors. Nat. Rev. Cancer. 2005; 5(5):341–354. [PubMed: 15864276]
42. Yarden Y, Sliwkowski MX. Untangling the ErbB signalling network. Nat. Rev. Mol. Cell Biol. 2001; 2(2):127–137. [PubMed: 11252954]
43. Holbro T, Hynes NE. ErbB receptors: directing key signaling networks throughout life. Annu. Rev. Pharmacol. Toxicol. 2004; 44:195–217. [PubMed: 14744244]
44. Riethmacher D, Sonnenberg-Riethmacher E, Brinkmann V, Yamaai T, Lewin GR, Birchmeier C. Severe neuropathies in mice with targeted mutations in the ErbB3 receptor. Nature. 1997; 389(6652):725–730. [PubMed: 9338783]
45. Crone SA, Zhao YY, Fan L, Gu Y, Minamisawa S, Liu Y, Peterson KL, Chen J, Kahn R, Condorelli G, Ross J Jr. Chien KR, Lee KFS. ErbB2 is essential in the prevention of dilated cardiomyopathy. Nat. Med. 2002; 8(5):459–465. [PubMed: 11984589]

46. Ozcelik C, Erdmann B, Pilz B, Wettschureck N, Britsch S, Hubner N, Chien KR, Birchmeier C, Garratt AN. Conditional mutation of the ErbB2 (HER2) receptor in cardiomyocytes leads to dilated cardiomyopathy. Proc. Natl. Acad. Sci. USA. 2002; 99(13):8880–8885. [PubMed: 12072561]
47. Stern DF. ErbBs in mammary development. Exp. Cell Res. 2003; 284(1):89–98. [PubMed: 12648468]
48. Ross JS, Fletcher JA. The HER-2/neu oncogene in breast cancer: prognostic factor, predictive factor, and target for therapy. Stem Cells. 1998; 16(6):413–428. [PubMed: 9831867]
49. Lu X, Kang Y. Epidermal growth factor signalling and bone metastasis. Br. J. Cancer. 2010; 102(3):457–461. [PubMed: 20010942]
50. Bronte G, Rizzo S, La Paglia L, Adamo V, Siragusa S, Ficorella C, Santini D, Bazan V, Colucci G, Gebbia N, Russo A. Driver mutations and differential sensitivity to targeted therapies: a new approach to the treatment of lung adenocarcinoma. Cancer Treat. Rev. 2010; 36(Suppl. 3):S21–29. [PubMed: 21129606]
51. Laurent-Puig P, Lievre A, Blons H. Mutations and response to epidermal growth factor receptor inhibitors. Clin. Cancer Res. 2009; 15(4):1133–1139. [PubMed: 19228718]
52. Pignon J-C, Koopmansch B, Nolens G, Delacroix L, Waltregny D, Winkler R. Androgen receptor controls EGFR and ERBB2 gene expression at different levels in prostate cancer cell lines. Cancer Res. 2009; 69(7):2941–2949. [PubMed: 19318561]
53. Cai C, Portnoy DC, Wang H, Jiang X, Chen S, Balk SP. Androgen receptor expression in prostate cancer cells is suppressed by activation of epidermal growth factor receptor and ErbB2. Cancer Res. 2009; 69(12):5202–5209. [PubMed: 19491261]
54. Di Lorenzo G, Autorino R, De Laurentiis M, Cindolo L, D'Armiento M, Bianco AR, De Placido S. HER-2/neu receptor in prostate cancer development and progression to androgen independence. Tumori. 2004; 90(2):163–170. [PubMed: 15237576]
55. Craft N, Shostak Y, Carey M, Sawyers CL. A mechanism for hormone-independent prostate cancer through modulation of androgen receptor signaling by the HER-2/neu tyrosine kinase. Nat. Med. 1999; 5(3):280–285. [PubMed: 10086382]
56. Mellinghoff IK, Vivanco I, Kwon A, Tran C, Wongvipat J, Sawyers CL. HER2/neu kinase-dependent modulation of androgen receptor function through effects on DNA binding and stability. Cancer Cell. 2004; 6(5):517–527. [PubMed: 15542435]
57. Citri A, Yarden Y. EGF-ERBB signalling: towards the systems level. Nat. Rev. Mol. Cell Biol. 2006; 7(7):505–516. [PubMed: 16829981]
58. Engelman JA, Zejnullahu K, Gale C-M, Lifshits E, Gonzales AJ, Shimamura T, Zhao F, Vincent PW, Naumov GN, Bradner JE, Althaus IW, Gandhi L, Shapiro GI, Nelson JM, Heymach JV, Meyerson M, Wong K-K, Jänne PA. PF00299804, an irreversible pan-ERBB inhibitor, is effective in lung cancer models with EGFR and ERBB2 mutations that are resistant to gefitinib. Cancer Res. 2007; 67(24):11924–11932. [PubMed: 18089823]
59. Gonzales AJ, Hook KE, Althaus IW, Ellis PA, Trachet E, Delaney AM, Harvey PJ, Ellis TA, Amato DM, Nelson JM, Fry DW, Zhu T, Loi C-M, Fakhoury SA, Schlosser KM, Sexton KE, Winters RT, Reed JE, Bridges AJ, Lettiere DJ, Baker DA, Yang J, Lee HT, Tecle H, Vincent PW. Antitumor activity and pharmacokinetic properties of PF-00299804, a second-generation irreversible pan-erbB receptor tyrosine kinase inhibitor. Mol. Cancer Ther. 2008; 7(7):1880–1889. [PubMed: 18606718]
60. Grasso AW, Wen D, Miller CM, Rhim JS, Pretlow TG, Kung HJ. ErbB kinases and NDF signaling in human prostate cancer cells. Oncogene. 1997; 15(22):2705–2716. [PubMed: 9400997]
61. Salzberg M, Rochlitz C, Morant R, Thalmann G, Pedrazzini A, Roggero E, Schonenberger A, Knuth A, Borner M. An open-label, noncomparative phase II trial to evaluate the efficacy and safety of docetaxel in combination with gefitinib in patients with hormone-refractory metastatic prostate cancer. Onkologie. 2007; 30(7):355–360. [PubMed: 17596743]
62. Gross M, Higano C, Pantuck A, Castellanos O, Green E, Nguyen K, Agus DB. A phase II trial of docetaxel and erlotinib as first-line therapy for elderly patients with androgen-independent prostate cancer. BMC Cancer. 2007; 7:142. [PubMed: 17662137]

63. Morris MJ, Reuter VE, Kelly WK, Slovin SF, Kenneson K, Verbel D, Osman I, Scher HI. HER-2 profiling and targeting in prostate carcinoma. Cancer. 2002; 94(4):980–986. [PubMed: 11920466]
64. Ziada A, Barqawi A, Glode LM, Varella-Garcia M, Crighton F, Majeski S, Rosenblum M, Kane M, Chen L, Crawford ED. The use of trastuzumab in the treatment of hormone refractory prostate cancer; phase II trial. Prostate. 2004; 60(4):332–337. [PubMed: 15264245]
65. Lara PN Jr. Chee KG, Longmate J, Ruel C, Meyers FJ, Gray CR, Edwards RG, Gumerlock PH, Twardowski P, Doroshow JH, Gandara DR. Trastuzumab plus docetaxel in HER-2/neu-positive prostate carcinoma: final results from the California Cancer Consortium Screening and Phase II Trial. Cancer. 2004; 100(10):2125–2131. [PubMed: 15139054]
66. Agus DB, Akita RW, Fox WD, Lewis GD, Higgins B, Pisacane PI, Lofgren JA, Tindell C, Evans DP, Maiese K, Scher HI, Sliwkowski MX. Targeting ligand-activated ErbB2 signaling inhibits breast and prostate tumor growth. Cancer Cell. 2002; 2(2):127–137. [PubMed: 12204533]
67. de Bono JS, Bellmunt J, Attard G, Droz JP, Miller K, Flechon A, Sternberg C, Parker C, Zugmaier G, Hersberger-Gimenez V, Cockey L, Mason M, Graham J. Open-label phase II study evaluating the efficacy and safety of two doses of pertuzumab in castrate chemotherapy-naive patients with hormone-Refractory prostate cancer. J. Clin. Oncol. 2007; 25(3):257–262. [PubMed: 17235043]
68. Sridhar SS, Hotte SJ, Chin JL, Hudes GR, Gregg R, Trachtenberg J, Wang L, Tran-Thanh D, Pham N-A, Tsao M-S, Hedley D, Dancey JE, Moore MJ. A Multicenter phase II clinical trial of lapatinib (GW572016) in hormonally untreated advanced prostate cancer. Am. J. Clin. Oncol. 2009:1–1. [PubMed: 19194115]
69. Sergina NV, Rausch M, Wang D, Blair J, Hann B, Shokat KM, Moasser MM. Escape from HER-family tyrosine kinase inhibitor therapy by the kinase-inactive HER3. Nature. 2007; 445(7126): 437–441. [PubMed: 17206155]
70. Lozano JJ, Soler M, Bermudo R, Abia D, Fernandez PL, Thomson TM, Ortiz AR. Dual activation of pathways regulated by steroid receptors and peptide growth factors in primary prostate cancer revealed by factor analysis of microarray data. BMC Genomics. 2005; 6:109–109. [PubMed: 16107210]
71. Smith BL, Chin D, Maltzman W, Crosby K, Hortobagyi GN, Bacus SS. The efficacy of Herceptin therapies is influenced by the expression of other erbB receptors, their ligands and the activation of downstream signalling proteins. Br. J. Cancer. 2004; 91(6):1190–1194. [PubMed: 15305194]
72. Soler M, Mancini F, Meca-Cortés O, Sánchez-Cid L, Rubio N, López-Fernández S, Lozano JJ, Blanco J, Fernández PL, Thomson TM. HER3 is required for the maintenance of neuregulin-dependent and -independent attributes of malignant progression in prostate cancer cells. Int. J. Cancer. 2009; 125(11):2565–2575. [PubMed: 19530240]
73. Chen L, Siddiqui S, Bose S, Mooso B, Asuncion A, Bedolla RG, Vinall R, Tepper CG, Gandour-Edwards R, Shi X, Lu X-H, Siddiqui J, Chinnaiyan AM, Mehra R, deVere White R, Carraway KL, Ghosh PM. Nrdp1-mediated regulation of ErbB3 expression by the androgen receptor in androgen-dependent but not castrate-resistant prostate cancer cells. Cancer Res. 2010; 70(14): 5994–6003. [PubMed: 20587519]
74. Vakar-Lopez F, Cheng C-J, Kim J, Shi GG, Troncoso P, Tu S-M, Yu-Lee L-Y, Lin S-H. Up-regulation of MDA-BF-1, a secreted isoform of ErbB3, in metastatic prostate cancer cells and activated osteoblasts in bone marrow. J. Pathol. 2004; 203(2):688–695. [PubMed: 15141384]
75. Chen N, Ye X-C, Chu K, Navone NM, Sage EH, Yu-Lee L-Y, Logothetis CJ, Lin S-H. A secreted isoform of ErbB3 promotes osteonectin expression in bone and enhances the invasiveness of prostate cancer cells. Cancer Res. 2007; 67(14):6544–6548. [PubMed: 17638862]
76. Lee H, Akita RW, Sliwkowski MX, Maihle NJ. A Naturally Occurring Secreted Human ErbB3 Receptor Isoform Inhibits Heregulin-stimulated Activation of ErbB2, ErbB3, and ErbB4. Cancer Res. 2001; 61(11):4467–4473. [PubMed: 11389077]
77. Koumakpayi IH, Diallo J-S, Le Page C, Lessard L, Gleave M, Bégin LR, Mes-Masson A-M, Saad F. Expression and nuclear localization of ErbB3 in prostate cancer. Clin. Cancer Res. 2006; 12(9): 2730–2737. [PubMed: 16675564]
78. Koumakpayi IH, Diallo J-S, Le Page C, Lessard L, Filali-Mouhim A, Bégin LR, Mes-Masson A-M, Saad F. Low nuclear ErbB3 predicts biochemical recurrence in patients with prostate cancer. BJU Int. 2007; 100(2):303–309. [PubMed: 17532856]

79. Cheng C-J, Ye X-C, Vakar-Lopez F, Kim J, Tu S-M, Chen D-T, Navone NM, Yu-Lee L-Y, Lin S-H, Hu MCT. Bone microenvironment and androgen status modulate subcellular localization of ErbB3 in prostate cancer cells. Mol. Cancer Res. 2007; 5(7):675–684. [PubMed: 17634423]
80. Tørring N, Jørgensen PE, Sørensen BS, Nexø E. Increased expression of heparin binding EGF (HB-EGF), amphiregulin, TGF alpha and epiregulin in androgen-independent prostate cancer cell lines. Anticancer Res. 2000; 20(1A):91–95. [PubMed: 10769639]
81. Kani K, Warren CM, Kaddis CS, Loo JA, Landgraf R. Oligomers of ERBB3 have two distinct interfaces that differ in their sensitivity to disruption by heregulin. J. Biol. Chem. 2005; 280(9): 8238–8247. [PubMed: 15611073]
82. Kani K, Park E, Landgraf R. The extracellular domains of ErbB3 retain high ligand binding affinity at endosome pH and in the locked conformation. Biochemistry. 2005; 44(48):15842–15857. [PubMed: 16313187]
83. Gregory CW, Whang YE, McCall W, Fei X, Liu Y, Ponguta LA, French FS, Wilson EM, Earp HS. Heregulin-induced activation of HER2 and HER3 increases androgen receptor transactivation and CWR-R1 human recurrent prostate cancer cell growth. Clin. Cancer Res. 2005; 11(5):1704–1712. [PubMed: 15755991]
84. Jones JT, Akita RW, Sliwkowski MX. Binding specificities and affinities of egf domains for ErbB receptors. FEBS Lett. 1999; 447(2-3):227–231. [PubMed: 10214951]
85. Engelman JA, Zejnullahu K, Mitsudomi T, Song Y, Hyland C, Park JO, Lindeman N, Gale C-M, Zhao X, Christensen J, Kosaka T, Holmes AJ, Rogers AM, Cappuzzo F, Mok T, Lee C, Johnson BE, Cantley LC, Jänne PA. MET amplification leads to gefitinib resistance in lung cancer by activating ERBB3 signaling. Science. 2007; 316(5827):1039–1043. [PubMed: 17463250]
86. Ishizawar RC, Miyake T, Parsons SJ. c-Src modulates ErbB2 and ErbB3 heterocomplex formation and function. Oncogene. 2007; 26(24):3503–3510. [PubMed: 17173075]
87. Jiang X, Borgesi RA, McKnight NC, Kaur R, Carpenter CL, Balk SP. Activation of nonreceptor tyrosine kinase Bmx/Etk mediated by phosphoinositide 3-kinase, epidermal growth factor receptor, and ErbB3 in prostate cancer cells. J. Biol. Chem. 2007; 282(45):32689–32698. [PubMed: 17823122]
88. Fu AK, Fu WY, Cheung J, Tsim KW, Ip FC, Wang JH, Ip NY. Cdk5 is involved in neuregulin-induced AChR expression at the neuromuscular junction. Nat, Neurosci. 2001; 4(4):374–381. [PubMed: 11276227]
89. Kamalati T, Jolin HE, Fry MJ, Crompton MR. Expression of the BRK tyrosine kinase in mammary epithelial cells enhances the coupling of EGF signalling to PI 3-kinase and Akt, via erbB3 phosphorylation. Oncogene. 2000; 19(48):5471–5476. [PubMed: 11114724]
90. Hemi R, Paz K, Wertheim N, Karasik A, Zick Y, Kanety H. Transactivation of ErbB2 and ErbB3 by tumor necrosis factor-alpha and anisomycin leads to impaired insulin signaling through serine/threonine phosphorylation of IRS proteins. J. Biol. Chem. 2002; 277(11):8961–8969. [PubMed: 11779863]
91. Walters DK, French JD, Arendt BK, Jelinek DF. Atypical expression of ErbB3 in myeloma cells: cross-talk between ErbB3 and the interferon-alpha signaling complex. Oncogene. 2003; 22(23): 3598–3607. [PubMed: 12789268]
92. Walters DK, Jelinek DF. A role for Janus kinases in crosstalk between ErbB3 and the interferon-alpha signaling complex in myeloma cells. Oncogene. 2004; 23(6):1197–1205. [PubMed: 14647450]
93. Baselga J, Swain SM. Novel anticancer targets: revisiting ERBB2 and discovering ERBB3. Nat. Rev. Cancer. 2009; 9(7):463–475. [PubMed: 19536107]
94. Yoo JY, Wang XW, Rishi AK, Lessor T, Xia XM, Gustafson TA, Hamburger AW. Interaction of the PA2G4 (EBP1) protein with ErbB-3 and regulation of this binding by heregulin. Br. J. Cancer. 2000; 82(3):683–690. [PubMed: 10682683]
95. Lessor TJ, Hamburger AW. Regulation of the ErbB3 binding protein Ebp1 by protein kinase C. Mol. Cell. Endocrinol. 2001; 175(1-2):185–191. [PubMed: 11325528]
96. Liu Z, Ahn J-Y, Liu X, Ye K. Ebp1 isoforms distinctively regulate cell survival and differentiation. Proc. Natl. Acad. Sci. USA. 2006; 103(29):10917–10922. [PubMed: 16832058]

97. Sithanandam G, Anderson LM. The ERBB3 receptor in cancer and cancer gene therapy. Cancer Gene Ther. 2008; 15(7):413–448. [PubMed: 18404164]

98. Zhang Y, Fondell JD, Wang Q, Xia X, Cheng A, Lu ML, Hamburger AW. Repression of androgen receptor mediated transcription by the ErbB-3 binding protein, Ebp1. Oncogene. 2002; 21(36): 5609–5618. [PubMed: 12165860]

99. Zhang Y, Hamburger AW. Specificity and heregulin regulation of Ebp1 (ErbB3 binding protein 1) mediated repression of androgen receptor signalling. Br. J. Cancer. 2005; 92(1):140–146. [PubMed: 15583694]

100. Zhang Y, Linn D, Liu Z, Melamed J, Tavora F, Young CY, Burger AM, Hamburger AW. EBP1, an ErbB3-binding protein, is decreased in prostate cancer and implicated in hormone resistance. Mol. Cancer Ther. 2008; 7(10):3176–3186. [PubMed: 18852121]

101. Zhang Y, Wang X-W, Jelovac D, Nakanishi T, Yu M-H, Akinmade D, Goloubeva O, Ross DD, Brodie A, Hamburger AW. The ErbB3-binding protein Ebp1 suppresses androgen receptor-mediated gene transcription and tumorigenesis of prostate cancer cells. Proc. Natl. Acad. Sci. USA. 2005; 102(28):9890–9895. [PubMed: 15994225]

102. Gannon PO, Koumakpayi IH, Le Page C, Karakiewicz PI, Mes-Masson A-M, Saad F. Ebp1 expression in benign and malignant prostate. Cancer Cell Int. 2008; 8:18–18. [PubMed: 19025630]

103. Diamonti AJ, Guy PM, Ivanof C, Wong K, Sweeney C, Carraway KL. An RBCC protein implicated in maintenance of steady-state neuregulin receptor levels. Proc. Nat. Acad. Sci. USA. 2002; 99(5):2866–2871. [PubMed: 11867753]

104. Wu X, Yen L, Irwin L, Sweeney C, Carraway KL. Stabilization of the E3 ubiquitin ligase Nrdp1 by the deubiquitinating enzyme USP8. Mol. Cell. Biol. 2004; 24(17):7748–7757. [PubMed: 15314180]

105. Yen L, Cao Z, Wu X, Ingalla ERQ, Baron C, Young LJT, Gregg JP, Cardiff RD, Borowsky AD, Sweeney C, Carraway KL. Loss of Nrdp1 enhances ErbB2/ErbB3-dependent breast tumor cell growth. Cancer Res. 2006; 66(23):11279–11286. [PubMed: 17145873]

106. Hsieh AC, Moasser MM. Targeting HER proteins in cancer therapy and the role of the non-target HER3. Br. J. Cancer. 2007; 97(4):453–457. [PubMed: 17667926]

107. Shi F, Telesco SE, Liu Y, Radhakrishnan R, Lemmon MA. ErbB3/HER3 intracellular domain is competent to bind ATP and catalyze autophosphorylation. Proc. Natl. Acad. Sci. USA. 2010; 107(17):7692–7697. [PubMed: 20351256]

108. Schoeberl B, Faber AC, Li D, Liang MC, Crosby K, Onsum M, Burenkova O, Pace E, Walton Z, Nie L, Fulgham A, Song Y, Nielsen UB, Engelman JA, Wong KK. An ErbB3 antibody, MM-121, is active in cancers with ligand-dependent activation. Cancer Res. 2010; 70(6):2485–2494. [PubMed: 20215504]

109. van der Horst EH, Murgia M, Treder M, Ullrich A. Anti-HER-3 MAbs inhibit HER-3-mediated signaling in breast cancer cell lines resistant to anti-HER-2 antibodies. Int. J. Cancer. 2005; 115(4):519–527. [PubMed: 15704104]

110. Motoyama AB, Hynes NE, Lane HA. The efficacy of ErbB receptor-targeted anticancer therapeutics is influenced by the availability of epidermal growth factor-related peptides. Cancer Res. 2002; 62(11):3151–3158. [PubMed: 12036928]

111. Garrett J, Olivares M, Rinehart C, Dave B, Cook R, Chang J, Arteaga C. Transcriptional and post-translational upregulation of HER3 (ErbB3) counteracts antitumor effect of HER2 tyrosine kinase inhibitors. Cancer Res. 2009; 69(24 Supplement):63–63.

112. Huang X, Gao L, Wang S, McManaman JL, Thor AD, Yang X, Esteva FJ, Liu B. Heterotrimerization of the Growth Factor Receptors erbB2, erbB3, and Insulin-like Growth Factor-I Receptor in Breast Cancer Cells Resistant to Herceptin. Cancer Res. 2010; 70(3):1204–1214. [PubMed: 20103628]

113. Konecny G, Finn R, Venkatesan N, Rusnak D, Gilmer T, Berger M, Chen J, Slamon DJ, Pegram M. The novel dual kinase inhibitor GW572016 is particularly active in HER2-positive and trastuzumab-conditioned breast cancer cells. Breast Cancer Res. Treat. 2003; 82:S171–S171.

114. Konecny GE, Pegram MD, Venkatesan N, Finn R, Yang G, Rahmeh M, Untch M, Rusnak DW, Spehar G, Mullin RJ, Keith BR, Gilmer TM, Berger M, Podratz KC, Slamon DJ. Activity of the

dual kinase inhibitor lapatinib (GW572016) against HER-2-overexpressing and trastuzumab-treated breast cancer cells. Cancer Res. 2006; 66(3):1630–1639. [PubMed: 16452222]

115. Normanno N, Campiglio M, De Luca A, Somenzi G, Maiello M, Ciardiello F, Gianni L, Salomon DS, Menard S. Cooperative inhibitory effect of ZD1839 (Iressa) in combination with trastuzumab (Herceptin) on human breast cancer cell growth. Ann. Oncol. 2002; 13(1):65–72. [PubMed: 11863114]
116. Scaltriti M, Verma C, Guzman M, Jimenez J, Parra JL, Pedersen K, Smith DJ, Landolfi S, Ramon y Cajal S, Arribas J, Baselga J. Lapatinib, a HER2 tyrosine kinase inhibitor, induces stabilization and accumulation of HER2 and potentiates trastuzumab-dependent cell cytotoxicity. Oncogene. 2009; 28(6):803–814. [PubMed: 19060928]
117. Ye D, Mendelsohn J, Fan Z. Augmentation of a humanized anti-HER2 mAb 4D5 induced growth inhibition by a human-mouse chimeric anti-EGF receptor mAb C225. Oncogene. 1999; 18(3): 731–738. [PubMed: 9989823]
118. Blackwell KL, Burstein HJ, Storniolo AM, Rugo H, Sledge G, Koehler M, Ellis C, Casey M, Vukelja S, Bischoff J, Baselga J, O'Shaughnessy J. Randomized study of Lapatinib alone or in combination with trastuzumab in women with ErbB2-positive, trastuzumab-refractory metastatic breast cancer. J. Clin. Oncol. 2010; 28(7):1124–1130. [PubMed: 20124187]
119. Slichenmyer WJ, Elliott WL, Fry DW. CI-1033, a pan-erbB tyrosine kinase inhibitor. Semin. Oncol. 2001; 28(5 Suppl. 16):80–85. [PubMed: 11706399]
120. Trinks C, Djerf EA, Hallbeck A-L, Jönsson J-I, Walz TM. The pan-ErbB receptor tyrosine kinase inhibitor canertinib induces ErbB-independent apoptosis in human leukemia (HL-60 and U-937) cells. Biochem. Biophys. Res. Commun. 2010; 393(1):6–10. [PubMed: 20096663]
121. Dewji MR. Early phase I data on an irreversible pan-erb inhibitor: CI-1033. What did we learn? J. Chemother. 2004; (16 Suppl. 4):44–48. [PubMed: 15688609]
122. Qi W, Cooke LS, Stejskal A, Riley C, Croce KD, Saldanha JW, Bearss D, Mahadevan D. MP470, a novel receptor tyrosine kinase inhibitor, in combination with Erlotinib inhibits the HER family/PI3K/Akt pathway and tumor growth in prostate cancer. BMC Cancer. 2009; 9:142–142. [PubMed: 19432987]
123. Hickinson DM, Klinowska T, Speake G, Vincent J, Trigwell C, Anderton J, Beck S, Marshall G, Davenport S, Callis R, Mills E, Grosios K, Smith P, Barlaam B, Wilkinson RW, Ogilvie D. AZD8931, an Equipotent, Reversible Inhibitor of Signaling by Epidermal Growth Factor Receptor, ERBB2 (HER2), and ERBB3: A Unique Agent for Simultaneous ERBB Receptor Blockade in Cancer. Clin Cancer Res. 2010; 16(4):1159–1169. [PubMed: 20145185]
124. Turke AB, Zejnullahu K, Wu YL, Song Y, Dias-Santagata D, Lifshits E, Toschi L, Rogers A, Mok T, Sequist L, Lindeman NI, Murphy C, Akhavanfard S, Yeap BY, Xiao Y, Capelletti M, Iafrate AJ, Lee C, Christensen JG, Engelman JA, Janne PA. Preexistence and clonal selection of MET amplification in EGFR mutant NSCLC. Cancer Cell. 2010; 17(1):77–88. [PubMed: 20129249]
125. Liu Y, Majumder S, McCall W, Sartor CI, Mohler JL, Gregory CW, Earp HS, Whang YE. Inhibition of HER-2/neu kinase impairs androgen receptor recruitment to the androgen responsive enhancer. Cancer Res. 2005; 65(8):3404–3409. [PubMed: 15833875]
126. Ye D, Mendelsohn J, Fan Z. Androgen and epidermal growth factor down-regulate cyclin-dependent kinase inhibitor p27Kip1 and costimulate proliferation of MDA PCa 2a and MDA PCa 2b prostate cancer cells. Clin. Cancer Res. 1999; 5(8):2171–2177. [PubMed: 10473102]
127. Festuccia C, Gravina GL, Muzi P, Biordi L, Ronchi P, Martella O, Vicentini C, Bologna M. Gefitinib and bicalutamide show synergistic effects in primary cultures of prostate cancer derived from androgen-dependent naive patients. Oncol. Rep. 2007; 18(5):1321–1327. [PubMed: 17914592]
128. Knight ZA, Lin H, Shokat KM. Targeting the cancer kinome through polypharmacology. Nat. Rev. Cancer. 2010; 10(2):130–137. [PubMed: 20094047]
129. Eichhorn PJA, Gili M, Scaltriti M, Serra V, Guzman M, Nijkamp W, Beijersbergen RL, Valero V, Seoane J, Bernards R, Baselga J. Phosphatidylinositol 3-kinase hyperactivation results in lapatinib resistance that is reversed by the mTOR/phosphatidylinositol 3-kinase inhibitor NVP-BEZ235. Cancer Res. 2008; 68(22):9221–9230. [PubMed: 19010894]

130. Fan Q-W, Cheng CK, Nicolaides TP, Hackett CS, Knight ZA, Shokat KM, Weiss WA. A dual phosphoinositide-3-kinase alpha/mTOR inhibitor cooperates with blockade of epidermal growth factor receptor in PTEN-mutant glioma. Cancer Res. 2007; 67(17):7960–7965. [PubMed: 17804702]

131. Junttila TT, Akita RW, Parsons K, Fields C, Lewis Phillips GD, Friedman LS, Sampath D, Sliwkowski MX. Ligand-independent HER2/HER3/PI3K complex is disrupted by trastuzumab and is effectively inhibited by the PI3K inhibitor GDC-0941. Cancer Cell. 2009; 15(5):429–440. [PubMed: 19411071]

132. Posadas EM, Gulley J, Arlen PM, Trout A, Parnes HL, Wright J, Lee MJ, Chung EJ, Trepel JB, Sparreboom A, Chen C, Jones E, Steinberg SM, Daniels A, Figg WD, Dahut WL. A phase II study of perifosine in androgen independent prostate cancer. Cancer Biol. Ther. 2005; 4(10): 1133–1137. [PubMed: 16138006]

133. Chee KG, Longmate J, Quinn DI, Chatta G, Pinski J, Twardowski P, Pan CX, Cambio A, Evans CP, Gandara DR, Lara PN Jr. The AKT inhibitor perifosine in biochemically recurrent prostate cancer: a phase II California/Pittsburgh cancer consortium trial. Clin. Genitourin. Cancer. 2007; 5(7):433–437. [PubMed: 18272025]

134. Robinson D, He F, Pretlow T, Kung HJ. A tyrosine kinase profile of prostate carcinoma. Proc. Natl. Acad. Sci. USA. 1996; 93(12):5958–5962. [PubMed: 8650201]

135. Vidal GA, Clark DE, Marrero L, Jones FE. A constitutively active ERBB4/HER4 allele with enhanced transcriptional coactivation and cell-killing activities. Oncogene. 2007; 26(3):462–466. [PubMed: 16832345]

136. Williams EE, Trout LJ, Gallo RM, Pitfield SE, Bryant I, Penington DJ, Riese DJ 2nd. A constitutively active ErbB4 mutant inhibits drug-resistant colony formation by the DU-145 and PC-3 human prostate tumor cell lines. Cancer Lett. 2003; 192(1):67–74. [PubMed: 12637154]

137. Lin S-H, Lee Y-C, Choueiri MB, Wen S, Mathew P, Ye X, Do K-A, Navone NM, Kim J, Tu S-M, Yu-Lee L-Y, Logothetis CJ. Soluble ErbB3 levels in bone marrow and plasma of men with prostate cancer. Clin. Cancer Res. 2008; 14(12):3729–3736. [PubMed: 18559590]

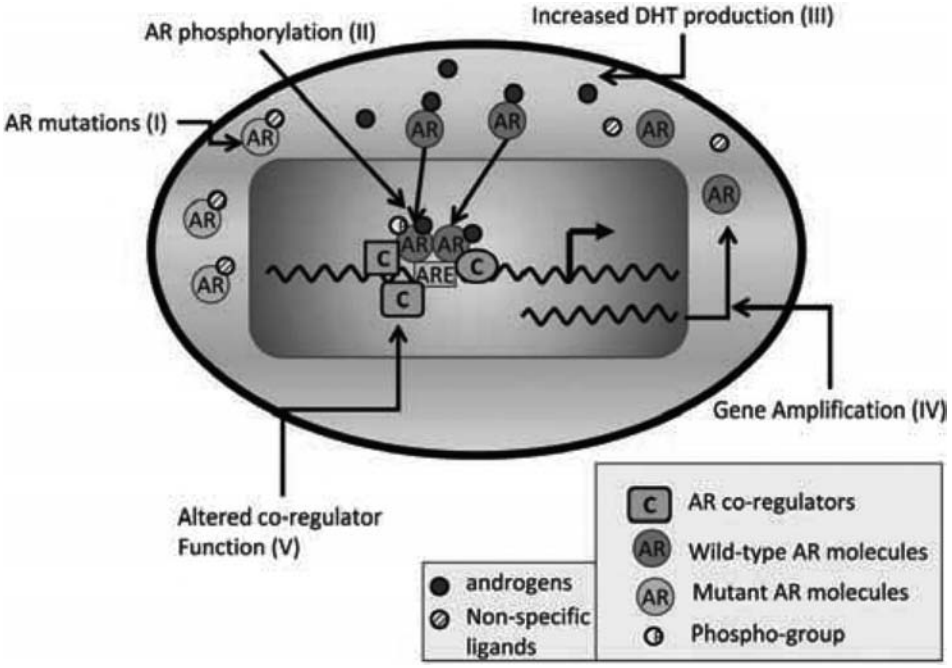

Fig. (1). Molecular mechanisms of castration resistance

Normal prostate and ADPCa cells are dependent on ligand-driven AR activity for their growth and survival. The AR is activated by binding to its ligands, translocating to the nucleus, homodimer formation and binding to specific androgen-responsive elements (AREs) of androgen-responsive genes and modulating their transcription. On the other hand, CRPC cells activate mechanisms that enable their survival in an environment with castrate levels of androgen. These include (i) mutations in the AR, (ii) ligand-independent AR phosphorylation and activation, (iii) increased AR ligand production, (iv) AR gene amplification and (v) altered functions of AR co-regulatory proteins. Different shapes of the co-regulators (C) represent different types of coregulators that bind to the AR.

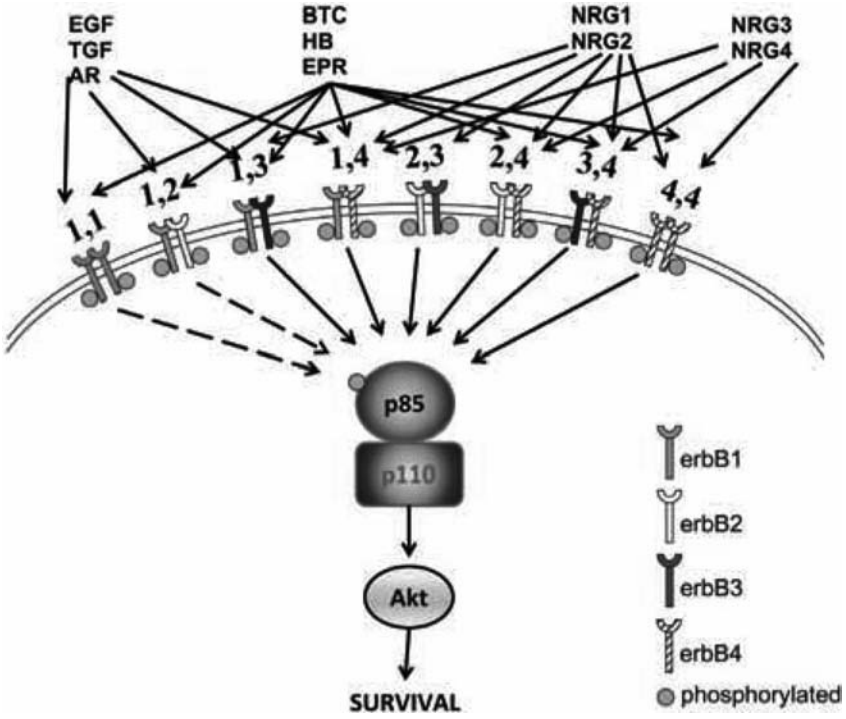

Fig. (2). ErbB family signaling

Three groups of ligands bind to ErbB family receptors. EGF (epidermal growth factor), ARG (amphiregulin) and TGF-α (transforming growth factor alpha) bind to ErbB1; BTC (betacellulin), HB-EGF (heparin-binding EGF-like factor) and EPR (epiregulin) bind to ErbB1 and ErbB4; NRG-1 and NRG-2 (neuregulins 1, 2) bind to ErbB3 and ErbB4; NRG-3 and NRG-4 (neuregulins 3,4) bind only to ErbB4. Possible receptor pairings are shown (note that ErbB3 cannot homodimerize owing to its weak kinase activity and ErbB4 is absent in prostate cancer). ErbB dimers activate pro-survival pathways mediated by Akt (shown here) as well as other pathways not shown. ErbB3 is unique because it binds directly to PI3K which in turn associates directly with and activates Akt, which is directly known to stimulate cell survival.

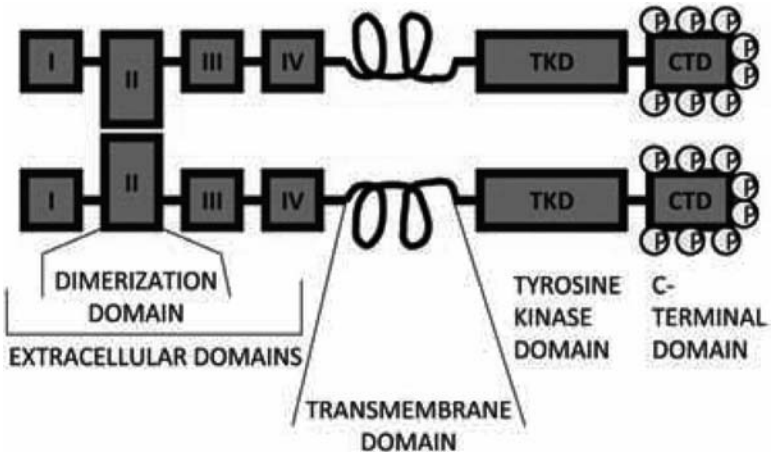

Fig. (3). Schematic of ErbB structure

All members have a large extracellular ligand-binding region (consisting of subdomains I-IV), a single, small intracellular transmembrane-spanning region (which precedes the cytoplasmic tyrosine kinase domain) and a C-terminal tail, which houses the docking (ie phosphorylation) sites for phosphotyrosine-binding effector molecules. Subdomains I and III are leucine-rich repeats that function in ligand binding (also called L1 and L2), whereas subdomains II and IV are laminin-like, cysteine-rich domains (also called CR1 and CR2). The monomeric ErbB receptor is autoinhibited by the interaction of domain II with domain IV. This keeps subdomains I and III apart and prevents ligand binding by disrupting the ligand-binding pocket and burying the dimerization loop of domain II. Ligand binding relieves these inhibitory interactions and encourages dimerization by allowing the loop from domain II of one monomer to access the docking site on domain II of a second, ligand-bound monomer. The receptor dimer is thus stabilized, the kinase domain is activated and specific tyrosine residues within the cytoplasmic tail are phosphorylated. These phosphorylated residues serve as docking sites for a range of proteins and the subsequent activation of intracellular signalling pathways.

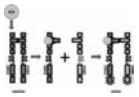

Fig. (4). NRG activation of ErbB3

ErbB3 has a high affinity for NRG and this is greatly increased by dimerization with ERBB2. As with the other ErbBs, in the absence of ligand, a direct intramolecular interaction between domains II and IV keeps ErbB3 in a closed (locked or tethered) conformation that prevents interaction between domains I and III. This conformation disrupts the ligand-binding pocket and buries the dimerization arm of domain II. ErbB2 is inherently unable to dimerize because of a strong interaction between domains I and III which leads to a constitutively extended dimerization arm. ErbB2 is therefore constantly primed for interactions with ligand-bound receptors of the ErbB family. In the presence of NRG, the dimerization loop from domain II of ErbB3 extends to interact intramolecularly with a ligandless, primed ErbB2 monomer to form the oncogenic ErbB2-ErbB3 heterodimer.

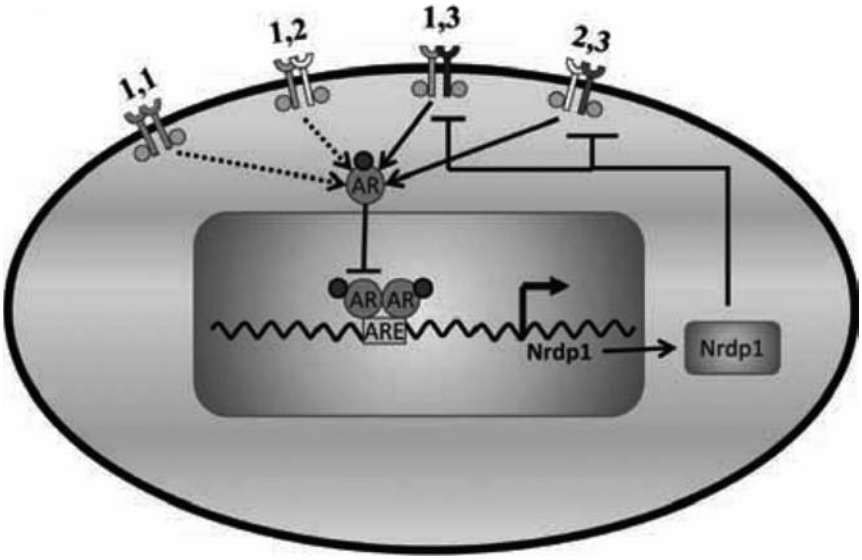

Fig. (5). AR controls ErbB3 levels via transcriptional control of the E3 ubiquitin ligase Nrdp1

Activated AR enters the nucleus and binds to androgen response elements (ARE) in the Nrdp1 promoter region, initiating transcription of that molecule. Nrdp1 thus produced attaches ubiquitin to ErbB3 and marks it for proteasomal degradation, thereby regulating receptor levels. This regulation occurs in castration-sensitive PCa but is lost en route to castration-resistance. As a result, ErbB3 levels remain sufficiently high and continue to drive tumorigenic growth.

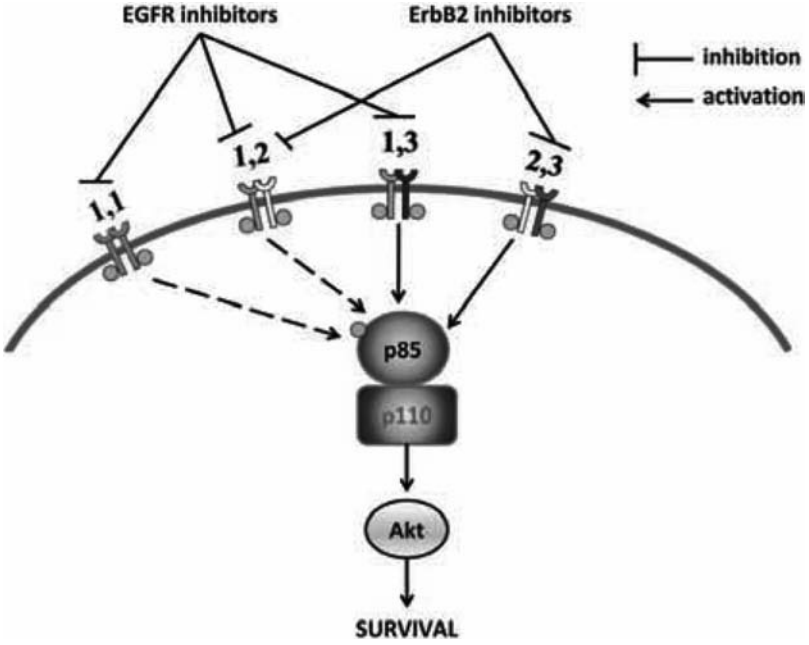

Fig. (6). Inhibition of ErbB3 signaling using a multi-receptor targeting approach

The simultaneous inhibition of ErbB1 and ErbB2 in PCa will leave no dimerization partner for ErbB3 and halt its oncogenic signaling. The only possible ErbB dimers in PCa are EGFR homodimers and ErbB1-ErbB2, ErbB2-ErbB3, and ErbB1-ErbB3 heterodimers (see text). All these dimers would stimulate cell survival, for example, though the PI3K/Akt pathway (shown) as well as by other pathways (not shown). ErbB1 inhibitors would disrupt ErbB homodimers and ErbB1-ErbB2 and ErbB1-ErbB3 homodimers, but signaling would still continue through the ErbB2-ErbB3 heterodimers. Similarly, ErbB2 inhibitors would prevent signaling downstream of ErbB1-ErbB2 and ErbB2-ErbB3 heterodimers but allow signaling downstream of EGFR homodimers and ErbB1-ErbB3 heterodimers. However, dual inhibition of both EGFR and ErbB2 would inhibit all 4 dimers, thereby eliminating cell survival downstream of the ErbB receptors.

Table 1

List of ErbB Inhibitors Described in this Review

Name of Drug	Class	Target	Current Status
MM-121	Monoclonal humanized ErbB3 antibody	ligand-dependent ErbB3 activation	Phase II for triple-negative breast cancer, Phase I/II for advanced NSCLC, Phase I for gynaecological cancers
AMG-888 (U3-1287)	Monoclonal humanized ErbB3 antibody	ligand-induced phosphorylation of ErbB3	Phase I for advanced NSCLC and advanced solid tumors
Canertinib (Cl-1033)	irreversible pan-ErbB TKI	ErbB tyrosine kinase domain	Phase II for refractory metastatic breast cancer and advanced NSCLC
MP-470	pan-ErbB inhibitor (ErbB1, 2, 3)	ErbB phosphorylation	Phase I for advanced solid tumors
AZD8931	reversible pan-ErbB inhibitor (ErbB1, 2, 3)	ErbB phosphorylation	Phase I for advanced solid tumors, Phase II for breast cancer
Trastuzumab (Herceptin)	monoclonal humanized ErbB2/ ErbB3 antibody	ligand-dependent ErbB3 activation (prevents ErbB3/ErbB2 dimerisation)	FDA-approved for metastatic breast cancer
Erlotinib (Tarceva)	reversible ErbB 1 TKI	Prevents ATP binding to ErbB 1 TK domain	FDA-approved for metastatic NSCLC
Cetuximab (Erbitux)	monoclonal humanized ErbB1 antibody	ligand-dependent ErbB1 activation (prevents ErbB3/ErbB1 dimerisation)	FDA-approved for irinotecan-refractory colon cancer and advanced head-and-neck cancers
Lapatinib (Tykerb)	Dual TKI inhibitor (ErbB1, 2)	ErbB tyrosine kinase domain	FDA-approved for breast cancer (triple-positive)
PF00299804	pan-ErbB inhibitor (ErbB1, 2, 4)	ErbB tyrosine kinase domain	Phase II for advanced NSCLC
Pertuzumab (Omnitarg/2C-4)	monoclonal humanized ErbB2 antibody	ligand-dependent ErbB2 activation (prevents ErbB3/ErbB2 dimerisation)	Phase II for advanced solid tumors
Gefitinib (Iressa)	reversible ErbB1 TKI	Prevents ATP binding to ErbB1 TK domain	FDA-approved for metastatic NSCLC

Published in final edited form as:
Clin Cancer Res. 2011 October 1; 17(19): 6218–6228. doi:10.1158/1078-0432.CCR-11-1548.

Dual EGFR/HER2 inhibition sensitizes prostate cancer cells to androgen withdrawal by suppressing ErbB3

Liqun Chen[1,2], **Benjamin A. Mooso**[1,2], **Maitreyee K. Jathal**[1,2], **Anisha Madhav**[1,2], **Sherra D. Johnson**[1,2], **Elyse van Spyk**[1,2], **Margarita Mikhailova**[3], **Alexandra Zierenberg Ripoll**[2], **Lingru Xue**[2], **Ruth L. Vinall**[2], **Ralph W deVere White**[2], and **Paramita M. Ghosh**[1,2]

[1]VA Northern California Health Care System, Mather, CA

[2]University of California Davis, Sacramento, CA

[3]University of Texas Health Science Center at San Antonio, San Antonio, TX

Abstract

Purpose—Patients with recurrent prostate cancer (PCa) are commonly treated with androgen withdrawal therapy (AWT); however, almost all patients eventually progress to castration resistant prostate cancer (CRPC), indicating failure of AWT to eliminate androgen-sensitive PCa. The overall goal of these studies is to determine whether dual inhibition of the receptor tyrosine kinases EGFR and HER2 would prolong the effectiveness of this treatment in PCa.

Experimental Design—We used androgen-dependent LNCaP cells and its CRPC sublines LNCaP-AI and C4-2. Additional data were collected in pRNS-1-1 cells stably expressing a mutant androgen receptor (AR-T877A), and in nude mice harboring CWR22 tumors. Studies utilized EGFR inhibitors erlotinib and AG1478, and HER2 inhibitors trastuzumab and AG879.

Results—Dual EGFR/HER2 inhibition induced apoptosis selectively in androgen-sensitive PCa cells undergoing AWT, but not in the presence of androgens, or in CRPC cells. We show that AWT alone failed to induce significant apoptosis in androgen-dependent cells, due to AWT-induced increase in HER2 and ErbB3, which promoted survival by increasing Akt phosphorylation. AWT-induced ErbB3 stabilized the AR and stimulated PSA, while it was inactivated only by inhibition of both its dimerization partners EGFR and HER2 (PCa cells do not express ErbB4); but not the inhibition of any one receptor alone, explaining the success of dual EGFR/HER2 inhibition in sensitizing androgen-dependent cells to AWT. The effectiveness of the inhibitors in suppressing growth correlated with its ability to prevent Akt phosphorylation.

Conclusions—These studies indicate that dual EGFR/HER2 inhibition, administered together with AWT; sensitize PCa cells to apoptosis during AWT.

Keywords

HER1; ErbB2; HER3; PKB; Androgen Receptor

INTRODUCTION

Androgen withdrawal therapy (AWT) is currently the standard of care for men with advanced prostate cancer (PCa) (1); however, it was found that in most patients its effects

Corresponding Author: Paramita M. Ghosh, Ph.D., Department of Urology, University of California Davis School of Medicine, 4860 Y Street, Suite 3500, Sacramento, CA 95817, Phone: (916)843-9336, Fax: (916)364-0306, Paramita.Ghosh@ucdmc.ucdavis.edu.

typically last 18–24 months, after which the patient developed resistance to such therapy (castration resistant prostate cancer; CRPC). Although some groups reported increased apoptosis in prostatic tissue following AWT (2, 3), others found no increase in apoptotic indices in the majority of tumors (4, 5), although proliferation indices were consistently suppressed (2, 4). These studies, therefore, concluded that "*androgen deprivation may act through suppression rather than ablation of prostatic cancers*" (5, 6). These reports indicate that failure to undergo apoptosis during AWT maybe a major cause of resistance of PCa cells to this therapy. Surviving cells likely undergo growth arrest and lie dormant following AWT, but will revive when an alternate growth stimulant comes to release it from this growth arrest, as was demonstrated in a CWR22 xenograft model (7, 8). Therefore, adjuvant therapy that causes apoptosis during AWT would impede the onset of CRPC.

Here we investigate the role of ErbB inhibitors in this effect. The ErbB family of four closely related type 1 transmembrane tyrosine kinase receptors include the epidermal growth factor receptor (EGFR/HER1/ErbB1), and related family members ErbB2 (HER2/neu), ErbB3 (HER3) and ErbB4 (HER4) (9). The ErbB receptors are activated by ligand binding, dimerization and phosphorylation. EGFR, ErbB3, ErbB4, but not HER2, have specific ligands, such as EGF for EGFR and heregulins (HRG1-4) for ErbB3 and ErbB4 (9). However, ErbB3 lacks significant kinase activity; hence both HER2 and ErbB3 require heterodimerization, with each other or the other ErbB receptors, for phosphorylation and activation. Significantly, PCa cells typically lack ErbB4 expression, but express high levels of ErbB3 (10, 11).

EGFR and HER2 are known to regulate cell proliferation, differentiation, angiogenesis and survival (12); however, in clinical trials for patients with CRPC, studies using selective and specific inhibitors of individual receptors did not show any significant effect (13–17). In recent times, a number of dual EGFR/HER2 inhibitors have been developed, and were found to be more effective against PCa cells and animal models compared to the single inhibitors (18, 19). Tyrosine phosphorylation of HER2 and ErbB3, transactivation of the androgen receptor (AR), and cell proliferation induced by heregulin were more potently inhibited by the EGFR/HER2 dual tyrosine kinase inhibitor GW572016 (lapatinib) than the EGFR-specific inhibitor gefitinib (20, 21). Despite the success of the pre-clinical studies, in phase II single-agent clinical trials, lapatinib was fairly well-tolerated and resulted in stable disease for 12 weeks but evidenced no decrease in prostate specific antigen (PSA), an AR transcriptional target, in patients with hormone sensitive PCa (22) or in unselected patients with CRPC, as measured by PSA (23).

Here, we concentrate on the effects of dual EGFR/HER2 inhibitors and the conditions under which they are effective. It is known that AR function at low levels of androgen is mediated not by EGFR, but by the heterodimerization of HER2 with ErbB3 (18). Sergina et al demonstrated that ErbB3 was upregulated and provided compensatory signaling precisely in response to EGFR/HER2-directed tyrosine kinase inhibitor (TKI) treatment (24). Indeed, ErbB3-directed RNA inhibition duly restored the pro-apoptotic effects of TKIs (24). These reports suggested that the failure of EGFR and HER2 inhibitors may be due to the activation of ErbB3 in these tumors. Studies conducted *in vitro* (25, 26), in animal models (6), and in clinical specimens (27) indicate an increase in Akt phosphorylation during AWT which promotes cell survival. Based on these reports we investigated whether dual EGFR/HER2 inhibitors were effective when they downregulated ErbB3 and/or Akt phosphorylation, and whether they impede PCa progression to CRPC by inducing cell death during AWT.

MATERIALS AND METHODS

Cell Culture and Pharmacological Treatments

Androgen-dependent LNCaP prostate cancer cells were purchased from American Type Culture Collection (ATCC, Manassas, VA), and C4-2 cells were obtained from UroCor (Oklahoma City, OK). Castration resistant clones of LNCaP cells (LNCaP-AI cells) have been described by us elsewhere (11, 25). pRNS-1-1 cells were also described earlier (11, 28). Recombinant human epidermal growth factor (EGF) and insulin-like growth factor 1 (IGF-1) were obtained from Invitrogen, (Carlsbad, CA), recombinant human heregulin 1 (HRG1) was from PeproTech INC. (Rochy Hill, NJ). AG1478 and AG879 were from Calbiochem, EMD Chemicals, Inc. (Gibbstown, NJ). Erlotinib (Tarceva) was provided by OSI Pharmaceuticals, Inc. (Melville, NY), and also was obtained from LC Laboratories (Woburn, MA), while trastuzumab (Herceptin) was a gift from Genentech, Inc. (South San Francisco, CA). Bicalutamide (Casodex) was kindly provided by AstraZeneca (Cheshire, UK), while lapatinib was purchased from LC Laboratories (Woburn, MA). Rabbit polyclonal EGFR, HER2, ErbB3, β-actin and AR antibodies were from Santa Cruz Biotechnology (Santa Cruz, CA). Rabbit polyclonal anti-phospho-Akt (Ser 473), anti-phospho-EGFR (Y1068), anti-phospho-HER2 (Y1248), phospho-ErbB3 (Y1289), α-tubulin and Akt antibodies were from Cell Signaling Technology (Beverly, MA). Transfections and plasmids used have been described earlier (11). Human Akt1 siRNA was obtained from Santa Cruz Biotechnology, Santa Cruz, CA against the sequence: 5'-ACGAGGGGAGUACAUCAAGAC-3'.

Mouse Studies—4–5-week old Balb/c athymic nude-Foxn1nu (nu/nu) male mice were obtained from Harlan Sprague Dawley, Inc. (Indianapolis, IN). Suspensions of CWR22 cells were mixed in 50% Matrigel solubilized basement membrane (BD Biosciences, Bedford, MA) and xenografts were established by subcutaneous injections of 2.5×10^6 cells/site into the flanks. When palpable tumors were observed, animals were treated with (i) vehicle or (ii) a combination of erlotinib (0.8 mg/Kg, 100 μl per dose, 5 times per week by oral gavage) and trastuzumab (20 mg/Kg, 90 μl per dose, 2 times per week by i.p. injection), dissolved in a solution of phosphate buffered saline (PBS) and 0.5% Tween 20. 3 days after start of drug regimen, the animals were castrated by bilateral scrotal excision, following isoflurone-anesthetization. Control animals were sham-operated by opening the animals surgically, but no tissues were removed. Drug administration was continued post-surgery, but after 8 days, the mice were euthanized, tumors were collected and divided into sections for paraffin-embedding and snap-freezing in liquid nitrogen. Mice were weighed and blood was collected periodically and PSA levels measured by a standard ELISA kit (Fitzgerald Industries Intnl., Acton, MA).

Immunohistochemistry and Statistical Analysis—We used rabbit polyclonal anti-ErbB3 (C-17) (1:100 dilution) antibodies from Santa Cruz Biotechnology, Santa Cruz, CA, Ki67 was from DAKO (Carpinteria, CA), while TUNEL kit was from Millipore (Billerica, MA). For negative controls we used a Universal Rabbit IgG control (DAKO) in place of the primary antibody. Diaminobenzidine (DAB) was used as a chromogen, and counterstaining was with hematoxylin. Only the epithelial cells were scored. The extent of staining was scored 0–3, where 0 represented no staining, +0.5 represents low (<20% staining), +1 represent intermediate (30–50%), +1.5 (50–70%) and +2 represent high staining (>80%). To evaluate the differences in staining expression in the three diagnostic groups, we used t-tests with a Welch approximation. Columns represent the mean ± standard deviation of samples from each group.

Flow cytometry and MTT assay—MTT and flow cytometric analysis was carried out as described earlier (11, 29, 30). Proliferation was estimated in propidium iodide stained ethanol-fixed cells by MODFIT (Verity software, Topsham, ME), while the rate of apoptosis induction was estimated in live cells staining with Annexin V by CellQuest V3.1 (Becton-Dickinson, Franklin Lanes, NJ).

RESULTS

Dual EGFR/HER2 inhibition sensitized androgen-dependent prostate cancer cells, but not castration resistant lines, to apoptosis by androgen withdrawal

We first compared the individual effects of the HER2 inhibitor trastuzumab (21 μg/ml), and the EGFR inhibitor erlotinib (10 μM), to dual inhibition with both drugs in androgen dependent LNCaP PCa cells. The drug combination caused cell cycle arrest in LNCaP cells following 48 hours of treatment in FBS medium (Figure 1A, **upper**). Culture in CSS, where androgen levels are significantly lower, also induced cell cycle arrest, but very little apoptosis, in these cells. However, the combination of trastuzumab and erlotinib, but not the individual drugs, induced 10-fold higher apoptosis in LNCaP cells in CSS-containing media (Figure 1A, **lower**). The overall effect is that, in FBS, dual EGFR/HER2 inhibition prevented cell number increase, whereas upon culture in CSS, additionally, there was a decrease in cell numbers indicating cell death (Supplemental Figure 1A). Unlike LNCaP cells, however, its CRPC sublines C4-2 (Figure 1A, **lower**) or LNCaP-AI (Supplementary Figure 1B), which have higher AR transcriptional activity (25), did not respond to dual inhibition of EGFR and HER2 even in CSS. Similarly, LNCaP cells underwent apoptosis in response to the dual EGFR/HER2 inhibitor lapatinib in CSS, but not in FBS, while its CRPC subline C4-2 cells were resistant to apoptosis by this drug (Supplementary Figure 2). Dual EGFR/HER2 inhibition prevented cell growth in FBS in AR-negative pRNS-1-1 cells stably transfected with vector only, but not those expressing AR(T877A), an androgen-sensitive active mutation found in LNCaP cells (Figure 1B). However, in CSS, where AR was inactive, this treatment inhibited growth, despite the presence of the AR(T877A) mutant (Figure 1B). These results indicate that AR activity suppresses the effects of ErbB inhibitors.

Androgen withdrawal stimulates, while dual EGFR/HER2 inhibition suppresses, ErbB3 levels

48 hour treatment with erlotinib (10 μM), but not trastuzumab (21 μg/ml) inhibited EGF-stimulated EGFR phosphorylation, whereas trastuzumab, but not erlotinib, affected the expression of HER2 (Figure 2A, **left**). On the other hand, the combination, but not the individual drugs, inhibited ErbB3 phosphorylation, and reduced ErbB3 levels (Figure 2A, **right**) also (Supplementary Figure 3A). Since PCa cells do not express ErbB4 (Supplementary Figure 3B) (10), we examined the effects of AWT on the levels of the other ErbB receptors. There was no significant change in EGFR levels upon culture in CSS, however, both HER2 and ErbB3 levels increased significantly as AR levels declined (Figure 2B, **upper panels**) (also Supplementary Figure 3C). Consistent with previous findings (6, 26), we saw a concomitant increase in Akt phosphorylation (Ser 473) in LNCaP (Figure 2B, **upper**). However, AWT caused no change in ErbB3 in LNCaP-AI cells, which expressed both higher AR (11) and ErbB3 (Figure 2B, **lower panels**). Comparison of LNCaP vs LNCaP-AI showed that the latter expressed higher levels of HER2 and ErbB3, and also higher ErbB3 phosphorylation (Figure 2C). Taken together, these results indicate that in LNCaP cells, but not its CRPC subline, ErbB3 levels increase during AWT whereas it is suppressed by dual EGFR/HER2 inhibition.

Dual EGFR/HER2 inhibition suppresses ErbB3 and PSA levels in CWR22 xenografts in nude mice

CWR22 xenografts were established in 4–5 month old male nude mice, and when the tumors were palpable, the animals were treated with vehicle only or with erlotinib (0.8 mg/Kg, 5 times per week) and trastuzumab (20 mg/Kg, 2 times per week) in combination. The animals were castrated, or sham operated, 3 days after the drugs were started, but drug treatments were continued until the end. The animals were divided as: (a) vehicle only, sham operated (n=6), (b) vehicle only, castrated (n=6) and (c) drug-treated, castrated (n=6). CWR22 tumors shrink rapidly following castration, hence to obtain sizable tumors that can be analyzed; the animals were sacrificed 8 days after the procedure. Serum levels of prostate specific antigen (PSA), a clinical indicator of AR activity in the prostate, were analyzed in blood drawn (i) at the beginning of the study, (ii) on the day of castration/sham operation, and (iii) at the end of the study (Figure 3A, **upper**). In vehicle-treated, sham operated animals, PSA levels increased significantly with time ($p=0.049$), whereas in castrated animals, the change in PSA was not significant. In those treated with the drug combination, PSA levels decreased three-fold. At the end of the study, the difference between PSA levels from castrated animals that were vehicle treated (16.3 ± 8.3 ng/ml) vs drug treated (4.3 ± 3.2 ng/ml) was significant ($p=0.02$), whereas the difference between sham-operated (29.8 ± 7.9 ng/ml) vs control animals were not ($p>0.05$).

Staining for ErbB3 in the formalin-fixed and paraffin-embedded (FFPE) sections showed weak staining in the sham operated mice (n=6) whereas the castrated and vehicle treated mice showed strong staining (n=6), which was eliminated in the castrated mice treated with the drug combination (n=5; one of the tumors was too small for analysis) (Figure 3B). Quantitation of the staining levels showed a significant increase in ErbB3 levels from sham operated, vehicle treated (0.63 ± 0.43) to castrated, vehicle treated tumors (1.33 ± 0.26) ($p=0.009$), which was reduced 40% in tumors treated with the drugs in castrated animals (0.8 ± 0.45) ($p=0.05$) (Figure 3C). Castration suppressed proliferation and induced apoptosis in these animals, as indicated by Ki67 and TUNEL staining (Supplementary Figure 4), respectively, whereas both effects were enhanced by treatment with the drug combination (Figure 3D). These results confirm that dual EGFR/HER2 inhibition reduce ErbB3 levels and reduces serum PSA levels.

ErbB3 overexpression stabilizes androgen receptor levels and promotes castration resistant cell growth mediated by Akt

LNCaP cells overexpressing ErbB3 grew at a much faster rate compared to parental LNCaP cells (Figure 4A, **upper**) and were not growth inhibited by the AR antagonist bicalutamide (Casodex) even at 10 μM (Figure 4A, **middle**) indicating androgen-independent cell growth. Flow cytometric analysis revealed this to be due to an increase in the percentage of cells entering the cell cycle (increased S-phase) which was not impeded by bicalutamide (Figure 4A, **lower**). Although culture in CSS-containing medium causes a decrease in the levels of the AR in LNCaP cells, increased expression of ErbB3 in the same cells maintained AR levels (Figure 4B). Since ErbB3 is a known inducer of Akt phosphorylation (29), we examined the role of Akt in ErbB3-mediated cell growth. Increased ErbB3 stimulated Akt phosphorylation (Figure 4C), while downregulation of Akt expression by siRNA suppressed ErbB3-induced proliferation in LNCaP cells (Figure 4D), thereby indicating that Akt phosphorylation mediated the regulation of LNCaP cell growth by ErbB3.

Resistance to growth inhibition by dual EGFR/HER2 inhibition correlates with the ability of the inhibitors to suppress Akt phosphorylation

LNCaP-AI cells expressed higher levels of Akt phosphorylation compared to parental LNCaP cells (Figure 5A, **upper**). Treatment with the combination of trastuzumab and

erlotinib, but not the individual drugs, significantly inhibited heregulin 1β (HRG1)-induced Akt phosphorylation in LNCaP cells, but not in LNCaP-AI (Figure 5A, **lower**). Similarly, the same combination inhibited Akt phosphorylation in parental pRNS-1-1 cells which lack a functional AR, whereas in cells that express AR(T877A), the drug combination failed to inhibit Akt activity (Supplementary Figure 5A). These results correlate Akt phosphorylation with the growth inhibitory effects of the combination of trastuzumab and erlotinib. In addition, the tyrphostins AG1478 (EGFR inhibitor) and AG879 (HER2 inhibitor) (Figure 5B, **upper**), in combination, inhibited Akt phosphorylation in CSS-, but not in FBS-containing medium (Figure 5B, **lower**). Similar to trastuzumab and erlotinib, the combination of AG1478 and AG879, but not the individual drugs, suppressed growth of pRNS-1-1(ART877A) cells in CSS-containing medium, whereas they had little or no effect on cell growth in FBS-containing medium (Figure 5C). On the other hand, LNCaP-AI cells were not growth arrested by the latter combination (Supplementary Figure 5B). These results indicate that suppression of cell growth by the drug combination correlates with inhibition of Akt phosphorylation.

Suppression of Akt phosphorylation sensitizes castration resistant prostate cancer cells to dual EGFR/HER2 inhibition

Finally, we investigated methods of overcoming the resistance of PCa cells to ErbB inhibitors. Since LNCaP-AI are not sensitive to dual inhibition of EGFR and HER2, and expressed higher ErbB3 compared to LNCaP, we investigated whether the increase in ErbB3 contributed to this resistance. Similar to the effects of a combination of erlotinib and trastuzumab, the combination of AG1478 and AG879 impeded the increase in cell numbers but did not reduce them below initial levels in LNCaP cells cultured in FBS (Figure 6A, **upper**), indicating growth arrest but not cell death. However, when the same cells were cultured in CSS, there was a 50% decrease in cell numbers indicating cell death (Figure 6A, **lower**). On the other hand, culture in CSS failed to have a similar effect in LNCaP cells overexpressing ErbB3 (Figure 6B), indicating that ErbB3 increase induced resistance to this drug combination. In support of a role for Akt phosphorylation in this process, LNCaP cells cultured in CSS experienced increasing Akt phosphorylation over a period of 5 days when exposed to vehicle alone whereas when they were exposed to the combination of AG1478 and AG879, Akt phosphorylation was significantly impeded (Figure 6C, **upper**). On the other hand, in LNCaP-AI cells resistant to this drug combination (Supplementary Figure 5B), the increase in Akt phosphorylation in response to CSS exposure was not affected (Figure 6C, **lower**). The fact that Akt phosphorylation increased upon CSS treatment in LNCaP-AI cells whereas ErbB3 levels did not (Figure 2B) indicates that other factors also contribute to Akt phosphorylaiton in CRPC. Our results indicated that, failure of dual EGFR/HER2 inhibition to induce apoptosis resulted from a failure of the same drugs to downregulate Akt phosphorylation. In support, AG1478 and AG879 in combination was not effective in inducing apoptosis in LNCaP-AI cells in the presence of control siRNA (9.89% in control siRNA vs 13.25% in control siRNA + AG1478 + AG879), whereas Akt siRNA alone induced a significant increase in Annexin V staining (28.28%) which was further increased in the presence of the drugs (44.65%) (Figure 6D).

DISCUSSION

Previous studies showed that the dual EGFR/HER2 inhibitor lapatinib evidenced no decrease in PSA in patients with hormone sensitive PCa (22) or in unselected patients with CRPC (23). The goal of this study was to determine whether dual EGFR/HER2 inhibition has any role in the prevention of disease progression in PCa. We demonstrate that androgen-dependent PCa cells with low ErbB activity do not show substantial response to ErbB inhibitors, whereas during AWT, ErbB2 and ErbB3 levels increase, which regulates Akt

phosphorylation and also cell survival. Hence, during this period, if the increase in these receptors is inhibited by dual EGFR/ErbB2 inhibition, which also inhibits ErbB3 phosphorylation, the increase in Akt phosphorylation and survival can be prevented. However, once ErbB3 levels have increased, the same drugs fail to affect the levels of Akt phosphorylation, thereby indicating that they can inhibit *de novo* activation of ErbB3 but cannot dephosphorylate the receptor after it is activated.

Although individual EGFR and HER2 inhibitors had differential effects on PCa cells, the overall effect of dual inhibition was similar. The difference between various inhibitors of the same receptor may be attributed to the strength of the binding of these inhibitors to the receptor. We see that in both cases, the drug combinations resulted in a decrease in Akt phosphorylation. Since ErbB4 is lost in PCa, the ErbB dimers formed in this disease include EGFR homodimers and EGFR-HER2, HER2-ErbB3 and EGFR-ErbB3 heterodimers (discussed in details in (31)). All contribute to survival of PCa cells; hence inhibition of only one receptor will not prevent downstream signaling. Our data shows that inhibition of both EGFR and HER2 is required to prevent ErbB3 signaling, likely by preventing its dimerization. Since only ErbB3 but not EGFR or HER2 have p85 PI3K binding sites (9), the majority of the Akt signaling may be downstream of ErbB3 dimerization with EGFR or HER2, which will be inhibited only upon dual inhibition. ErbB3 monoclonal antibodies such as MM-121 are currently in development (32), and are also likely to succeed in combination with other ErbB inhibitors such as lapatinib.

We show that in cells expressing high AR, either hormone-naïve cells never exposed to AWT, or in CRPC cells that have high AR transcriptional activity, dual ErbB inhibition is unable to inhibit Akt phosphorylation and cell survival. In a previous study, we had shown that in hormone-naïve cells, the AR suppresses ErbB3 levels by transcriptionally regulating the ErbB3 inhibitor Nrdp1 (11). Since ErbB3 is capable of inducing AR-independent cell growth, this is likely an attempt by the AR to suppress AR-independent signaling. Hence, in androgen-dependent cells growing in the presence of high androgen levels, cell-survival is AR-dependent and not ErbB3-dependent. Therefore, inhibition of ErbB3 or its binding partners will not affect cell growth or survival. On the other hand, when AR levels decreased during AWT, ErbB3 levels rebound and cell growth becomes dependent on signal transduction downstream of this receptor. Therefore, if at this time, ErbB3 signaling is suppressed, cell survival is impacted.

ErbB3 increase during AWT likely as an attempt to prevent AR decrease. In this study, we show that ErbB3 stabilize AR levels; thereby preventing its decrease in low-androgen medium. Further studies are required to see whether this is the mechanism by which ErbB3 promotes androgen-independent cell growth, but if so, it will explain why, in some CRPC cells, growth is still AR dependent, but not androgen dependent, as has been demonstrated by other labs (33, 34). Despite this, it appears that the ErbB3-stabilized AR is incapable of downregulating ErbB3 (which is reasonable, if it requires that ErbB3 to stabilize it), as we previously showed (11). Furthermore, once the cell progresses to a CRPC phenotype, it is no longer capable of responding to dual EGFR/HER2 inhibition to downregulate Akt phosphorylation downstream of ErbB3. Hence, dual EGFR/HER2 inhibition does not affect cell survival or even cell growth in CRPC cells.

In CRPC cells, the effects of ErbB receptors and the AR are compounded by high Akt phosphorylation (29). Akt is induced by other factors including IGF, hence in CRPC cells, which are associated with multiple changes in cell signaling pathways (see (35) and references within), it is likely that the cells have become adept at kinase switching, resulting in activation of multiple cell survival pathways. As a result, in these cells, dual EGFR/HER2 inhibition will not prevent all aberrant Akt phosphorylation. Therefore, our goal is to prevent

the increase in aberrant Akt phosphorylation, and PSA progression, indicative of relapse, following AWT, by using the dual inhibitors during and not after this treatment. The clinical and therapeutic consequences of such a treatment could be quite profound. A 2009 study of 1,078 patients with hormone-sensitive PCa enrolled in SWOG trial 9346, where PSA progression (PSA-P) was defined as an increase of ≥25% over nadir, median subsequent overall survival was shown to be 10 months in patients experiencing PSA-P within 7 months of hormone treatment, vs 44 months for those who did not have PSA-P during this period (36). Therefore, it is likely that if co-administration of dual EGFR/HER2 inhibitors delays PSA-P beyond 7 months, we would see a significant increase in PSA progression.

In conclusion, our data indicate that dual EGFR/HER2 inhibition is an effective tool for sensitizing androgen-dependent PCa cells to apoptosis during AWT, likely preventing PCa progression to CRPC following AWT treatment, but is not effective in CRPC cells expressing high Akt phosphorylation. However, this strategy may find utility with the advent of new therapeutic agents such as abiraterone acetate, a CYP17 inhibitor that blocks steroid biosynthesis (37), and MDV3100, a more potent AR inhibitor (38). In post-docetaxel patients, abiraterone increased survival by 3.9 months over controls (37) and it would be of interest to see whether this leads to an increase in ErbB3/HER2 as well, and whether prevention of this increase, if any, would further prolong survival. It is clear from the current study, that the window of opportunity for using ErbB inhibitors in PCa is when ErbB3 is rising and not when it is stable. The study also demonstrates that potentially effective drugs if utilized in the wrong clinical setting may be prematurely judged to be ineffective.

STATEMENT OF TRANSLATIONAL RELEVANCE

The goal of these studies is to identify therapeutic strategies that prolong the effectiveness of androgen withdrawal therapy (AWT) in patients with metastatic prostate cancer (PCa). Inhibitors of ErbB kinases such as erlotinib, lapatinib and trastuzumab have been tested in patients with castration resistant prostate cancer (CRPC) and in hormone-naïve patients, with little effect. Here we present novel data demonstrating that, instead, dual ErbB inhibitors sensitize PCa to AWT, and are thereby likely to prolong its effects. We show that during AWT, HER2 and ErbB3 levels increase, resulting in significant ErbB-dependent survival advantage that allows progression to CRPC. However, dual EGFR/HER2 inhibition, which inhibits their dimerization partner ErbB3 as well, induced apoptosis in cells undergoing AWT, despite ineffectiveness in hormone-naïve cells and in cells that have already progressed to CRPC. Our data indicate that administration of dual EGFR/HER2 inhibitors in PCa patients undergoing AWT may impede the onset of CRPC.

Supplementary Material

Refer to Web version on PubMed Central for supplementary material.

Acknowledgments

We thank Dr. Clifford G. Tepper, Department of Biochemistry and Molecular Medicine, UC Davis, for CWR22 cells; Dr. XuBao Shi, Department of Urology, UC Davis for the gift of pRNS-1-1 cells stably transfected with AR mutants, and Dr. John Koland for pCDNA3-ErbB3 plasmids. We also thank Xiao-Hua Lu and Yu Wang for technical assistance with some experiments, Astrazeneca for bicalutamide, OSI Pharmaceuticals for the gift of erlotinib and Genentech for the gift of trastuzumab for the completion of this project. This work was supported by Department of Defense, Idea Development Award PC081177 and by Awards# R21CA109057 and RO1CA133209 from the National Institutes of Health.

REFERENCES

1. Catalona WJ. Management of cancer of the prostate. N Engl J Med. 1994; 331:996–1004. [PubMed: 7880240]
2. Matsushima H, Goto T, Hosaka Y, Kitamura T, Kawabe K. Correlation between proliferation, apoptosis, and angiogenesis in prostate carcinoma and their relation to androgen ablation. Cancer. 1999; 85:1822–1827. [PubMed: 10223578]
3. Reuter VE. Pathological changes in benign and malignant prostatic tissue following androgen deprivation therapy. Urology. 1997; 49:16–22. [PubMed: 9123731]
4. Westin P, Stattin P, Damber JE, Bergh A. Castration therapy rapidly induces apoptosis in a minority and decreases cell proliferation in a majority of human prostatic tumors. Am J Pathol. 1995; 146:1368–1375. [PubMed: 7778676]
5. Murphy WM, Soloway MS, Barrows GH. Pathologic changes associated with androgen deprivation therapy for prostate cancer. Cancer. 1991; 68:821–828. [PubMed: 1906775]
6. Carver BS, Chapinski C, Wongvipat J, Hieronymus H, Chen Y, Chandarlapaty S, et al. Reciprocal Feedback Regulation of PI3K and Androgen Receptor Signaling in PTEN-Deficient Prostate Cancer. Cancer Cell. 2011; 19:575–586. [PubMed: 21575859]
7. Agus DB, Akita RW, Fox WD, Lewis GD, Higgins B, Pisacane PI, et al. Targeting ligand-activated ErbB2 signaling inhibits breast and prostate tumor growth. Cancer Cell. 2002; 2:127–137. [PubMed: 12204533]
8. Agus DB, Cordon-Cardo C, Fox W, Drobnjak M, Koff A, Golde DW, et al. Prostate cancer cell cycle regulators: response to androgen withdrawal and development of androgen independence. Journal of the National Cancer Institute. 1999; 91:1869–1876. [PubMed: 10547394]
9. Olayioye MA, Neve RM, Lane HA, Hynes NE. The ErbB signaling network: receptor heterodimerization in development and cancer. The EMBO journal. 2000; 19:3159–3167. [PubMed: 10880430]
10. Grasso AW, Wen D, Miller CM, Rhim JS, Pretlow TG, Kung HJ. ErbB kinases and NDF signaling in human prostate cancer cells. Oncogene. 1997; 15:2705–2716. [PubMed: 9400997]
11. Chen L, Siddiqui S, Bose S, Mooso B, Asuncion A, Bedolla RG, et al. Nrdp1-mediated regulation of ErbB3 expression by the androgen receptor in androgen-dependent but not castrate-resistant prostate cancer cells. Cancer Res. 2010; 70:5994–6003. [PubMed: 20587519]
12. Yarden Y, Sliwkowski MX. Untangling the ErbB signalling network. Nat Rev Mol Cell Biol. 2001; 2:127–137. [PubMed: 11252954]
13. Salzberg M, Rochlitz C, Morant R, Thalmann G, Pedrazzini A, Roggero E, et al. An open-label, noncomparative phase II trial to evaluate the efficacy and safety of docetaxel in combination with gefitinib in patients with hormone-refractory metastatic prostate cancer. Onkologie. 2007; 30:355–360. [PubMed: 17596743]
14. Gross M, Higano C, Pantuck A, Castellanos O, Green E, Nguyen K, et al. A phase II trial of docetaxel and erlotinib as first-line therapy for elderly patients with androgen-independent prostate cancer. BMC cancer. 2007; 7:142. [PubMed: 17662137]
15. Morris MJ, Reuter VE, Kelly WK, Slovin SF, Kenneson K, Verbel D, et al. HER-2 profiling and targeting in prostate carcinoma. Cancer. 2002; 94:980–986. [PubMed: 11920466]
16. Ziada A, Barqawi A, Glode LM, Varella-Garcia M, Crighton F, Majeski S, et al. The use of trastuzumab in the treatment of hormone refractory prostate cancer; phase II trial. The Prostate. 2004; 60:332–337. [PubMed: 15264245]
17. Lara PN Jr, Chee KG, Longmate J, Ruel C, Meyers FJ, Gray CR, et al. Trastuzumab plus docetaxel in HER-2/neu-positive prostate carcinoma: final results from the California Cancer Consortium Screening and Phase II Trial. Cancer. 2004; 100:2125–2131. [PubMed: 15139054]
18. Mellinghoff IK, Vivanco I, Kwon A, Tran C, Wongvipat J, Sawyers CL. HER2/neu kinase-dependent modulation of androgen receptor function through effects on DNA binding and stability. Cancer Cell. 2004; 6:517–527. [PubMed: 15542435]
19. Gravina GL, Marampon F, Piccolella M, Biordi L, Ficorella C, Motta M, et al. Antitumor effects of carnertinib in castration resistant prostate cancer models: A Comparative study with erlotinib. Prostate. 2011

20. Gregory CW, Whang YE, McCall W, Fei X, Liu Y, Ponguta LA, et al. Heregulin-induced activation of HER2 and HER3 increases androgen receptor transactivation and CWR-R1 human recurrent prostate cancer cell growth. Clin Cancer Res. 2005; 11:1704–1712. [PubMed: 15755991]
21. Liu Y, Majumder S, McCall W, Sartor CI, Mohler JL, Gregory CW, et al. Inhibition of HER-2/neu kinase impairs androgen receptor recruitment to the androgen responsive enhancer. Cancer research. 2005; 65:3404–3409. [PubMed: 15833875]
22. Sridhar SS, Hotte SJ, Chin JL, Hudes GR, Gregg R, Trachtenberg J, et al. A multicenter phase II clinical trial of lapatinib (GW572016) in hormonally untreated advanced prostate cancer. Am J Clin Oncol. 2010; 33:609–613. [PubMed: 20042973]
23. Whang YE, Moore CN, Armstrong AJ, Rathmell WK, Godley PA, Crane JM, et al. A phase II trial of lapatinib in hormone refractory prostate cancer. ASCO Annual Meeting Proceedings (Post-Meeting Edition); 2008 May 20. Journal of Clinical Oncology. 2008:16037.
24. Sergina NV, Rausch M, Wang D, Blair J, Hann B, Shokat KM, et al. Escape from HER-family tyrosine kinase inhibitor therapy by the kinase-inactive HER3. Nature. 2007; 445:437–441. [PubMed: 17206155]
25. Mikhailova M, Wang Y, Bedolla R, Lu XH, Kreisberg JI, Ghosh PM. AKT regulates androgen receptor-dependent growth and PSA expression in prostate cancer. Adv Exp Med Biol. 2008; 617:397–405. [PubMed: 18497063]
26. Murillo H, Huang H, Schmidt LJ, Smith DI, Tindall DJ. Role of PI3K signaling in survival and progression of LNCaP prostate cancer cells to the androgen refractory state. Endocrinology. 2001; 142:4795–4805. [PubMed: 11606446]
27. Festuccia C, Gravina GL, Muzi P, Pomante R, Ventura L, Vessella RL, et al. Bicalutamide increases phospho-Akt levels through Her2 in patients with prostate cancer. Endocr Relat Cancer. 2007; 14:601–611. [PubMed: 17914091]
28. Shi XB, Xue L, Tepper CG, Gandour-Edwards R, Ghosh P, Kung HJ, et al. The oncogenic potential of a prostate cancer-derived androgen receptor mutant. Prostate. 2007; 67:591–602. [PubMed: 17262801]
29. Ghosh PM, Malik SN, Bedolla RG, Wang Y, Mikhailova M, Prihoda TJ, et al. Signal transduction pathways in androgen-dependent and -independent prostate cancer cell proliferation. Endocr Relat Cancer. 2005; 12:119–134. [PubMed: 15788644]
30. Wang Y, Mikhailova M, Bose S, Pan CX, deVere White RW, Ghosh PM. Regulation of androgen receptor transcriptional activity by rapamycin in prostate cancer cell proliferation and survival. Oncogene. 2008; 27:7106–7117. [PubMed: 18776922]
31. Jathal MK, Chen L, Mudryj M, Ghosh PM. Targeting ErbB3: the New RTK(id) on the Prostate Cancer Block. Immunol Endocr Metab Agents Med Chem. 2011; 11:131–149. [PubMed: 21603064]
32. Schoeberl B, Faber AC, Li D, Liang MC, Crosby K, Onsum M, et al. An ErbB3 antibody, MM-121, is active in cancers with ligand-dependent activation. Cancer research. 2010; 70:2485–2494. [PubMed: 20215504]
33. Compagno D, Merle C, Morin A, Gilbert C, Mathieu JR, Bozec A, et al. SIRNA-directed in vivo silencing of androgen receptor inhibits the growth of castration-resistant prostate carcinomas. PLoS One. 2007; 2:e1006. [PubMed: 17925854]
34. Agoulnik IU, Vaid A, Bingman WE, Erdeme H 3rd, Frolov A, Smith CL, et al. Role of SRC-1 in the promotion of prostate cancer cell growth and tumor progression. Cancer Res. 2005; 65:7959–7967. [PubMed: 16140968]
35. Zhu ML, Kyprianou N. Androgen receptor and growth factor signaling cross-talk in prostate cancer cells. Endocr Relat Cancer. 2008; 15:841–849. [PubMed: 18667687]
36. Hussain M, Goldman B, Tangen C, Higano CS, Petrylak DP, Wilding G, et al. Prostate-specific antigen progression predicts overall survival in patients with metastatic prostate cancer: data from Southwest Oncology Group Trials 9346 (Intergroup Study 0162) and 9916. J Clin Oncol. 2009; 27:2450–2456. [PubMed: 19380444]
37. de Bono JS, Logothetis CJ, Molina A, Fizazi K, North S, Chu L, et al. Abiraterone and increased survival in metastatic prostate cancer. N Engl J Med. 2011; 364:1995–2005. [PubMed: 21612468]

38. Scher HI, Beer TM, Higano CS, Anand A, Taplin ME, Efstathiou E, et al. Antitumour activity of MDV3100 in castration-resistant prostate cancer: a phase 1–2 study. Lancet. 2010; 375:1437–1446. [PubMed: 20398925]

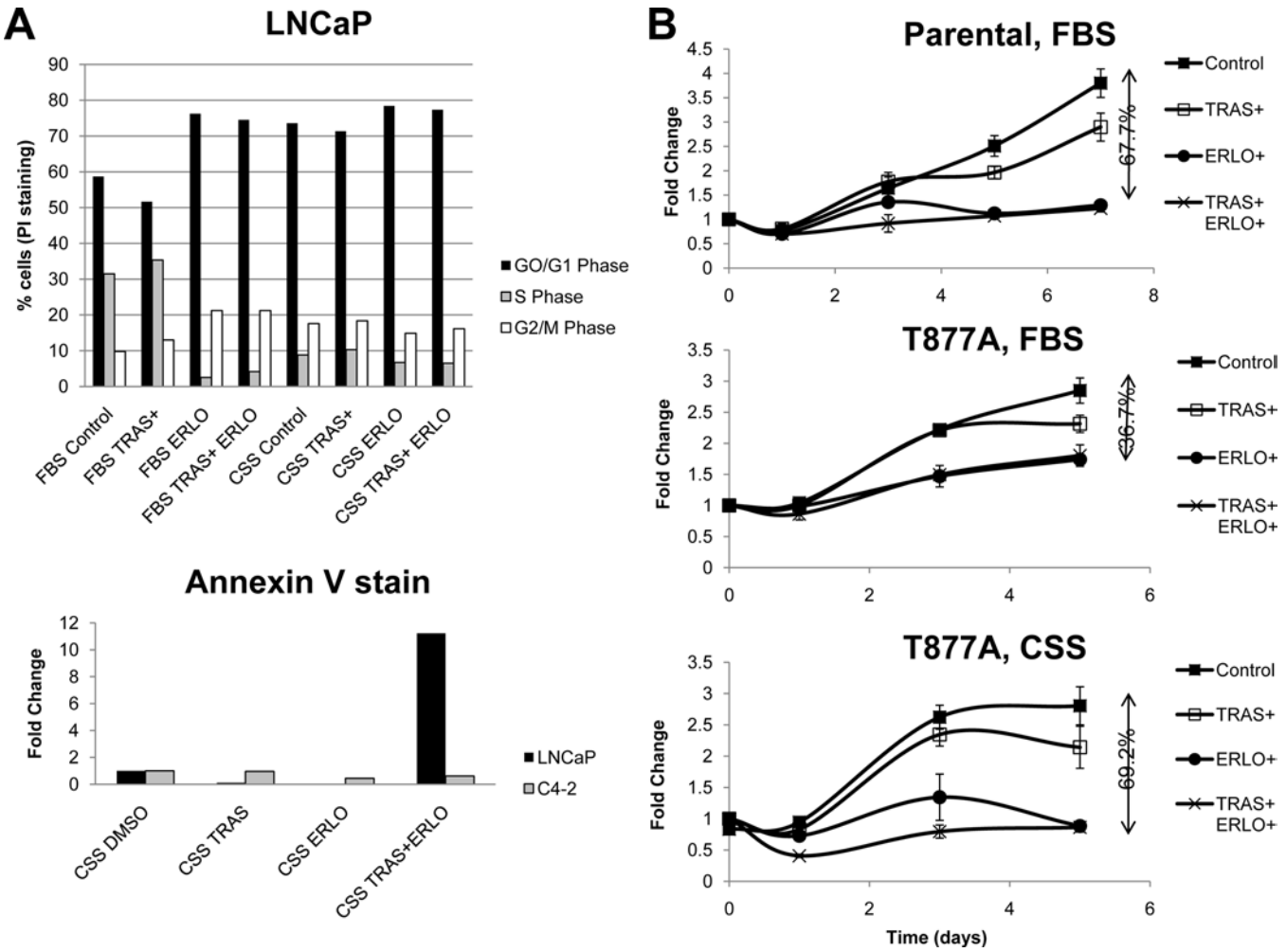

FIGURE 1. Androgen withdrawal sensitized prostate epithelial cells to apoptosis by the combination of trastuzumab and erlotinib

(A) LNCaP cells were cultured in the presence of FBS or CSS for 48 hours together with trastuzumab (21μg/ml), erlotinib (10μM), or combinations thereof. The cells were collected and analyzed by flow cytometry to determine **(upper)** the fraction of cells in S-phase (which indicates proliferation) and **(lower)** those undergoing apoptosis (data presented represent fold changes over control cells treated with DMSO alone, 1.1% in LNCaP 3.48% in C4-2 cells). **(B) (upper panel)** MTT assay was used to determine the cell growth rate of parental pRNS-1-1 cells with the combination of Erlotinib (10 μM) and/or Trastuzumab (21 μg/ml) for 24 hours. **(Lower panels)** MTT assay to determine the effect of Erlotinib and/or Trastuzumab in the presence of **(middle panel)** medium containing FBS **(lower panel)** or CSS in pRNS-1-1 cells transfected with mutant AR (T877A). Data represents mean ± S.D. for three independent experiments.

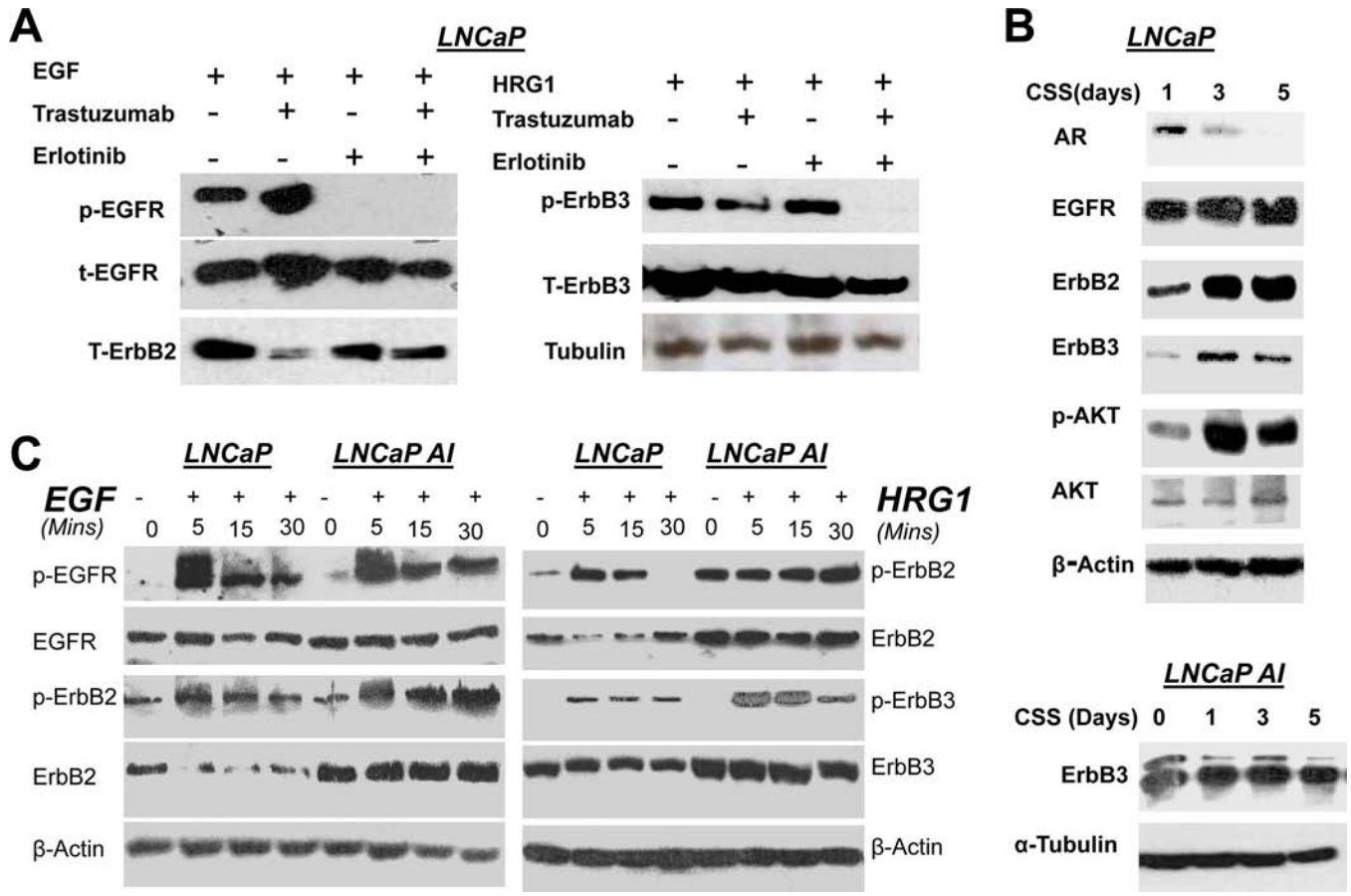

FIGURE 2. ErbB3 inhibition by the combination of erlotinib and Traztuzumab, and its stimulation by AWT, in LNCaP cells

(A) Western blots demonstrating the effect of erlotinib (10 μM) and Transtuzumab (21 μg/ml) on ErbB receptor tyrosine kinases. **(left)** LNCaP cells were serum starved in the presence of erlotinib and/or trastuzumab for 48 hours, followed by further treatment with 10 ng/ml EGF for 5 mins. Lysates were blotted with anti-phospho EGFR (Y1068) **(1st Panel)**, anti-EGFR **(2nd Panel)**, or anti-HER2 **(3rd Panel)** antibodies. **(right)** Alternately, the cells were stimulated with 50 ng/ml HRG1 to induce ErbB3 phosphorylation, and immunoblotted with anti-phospho ErbB3 **(1st panel)** and anti-ErbB3 **(2nd panel). (B)** Western blots demonstrating that AWT causes increased HER2 and ErbB3 expression and phosphorylation of Akt. LNCaP cells were cultured in FBS-containing medium up to 75% confluence and then switched to CSS-containing medium for the indicated period of time. Cell lysate was collected and immunoblotted with antibodies to anti-AR **(1st panel)**, anti-EGFR **(2nd Panel)**, anti-HER2 **(3rd panel)**, anti-ErbB3 **(4th Panel)**, anti-phospho Akt (Ser 473) **(5th panel)**, anti-Akt **(6th Panel)**, and anti-β-actin **(7th Panel)**. In contrast to LNCaP, it's CRPC subline LNCaP-AI did not experience a similar increase in ErbB3 following AWT **(8th panel). (C)** Comparison of the activation and expression of the ErbB receptors expressed in LNCaP cells and it's CRPC subline LNCaP-AI. The cells were serum starved for 48 hours and then EGF (10 ng/ml) **(left)**, or HRG (50 ng/ml) **(right)** were added for the times indicated.

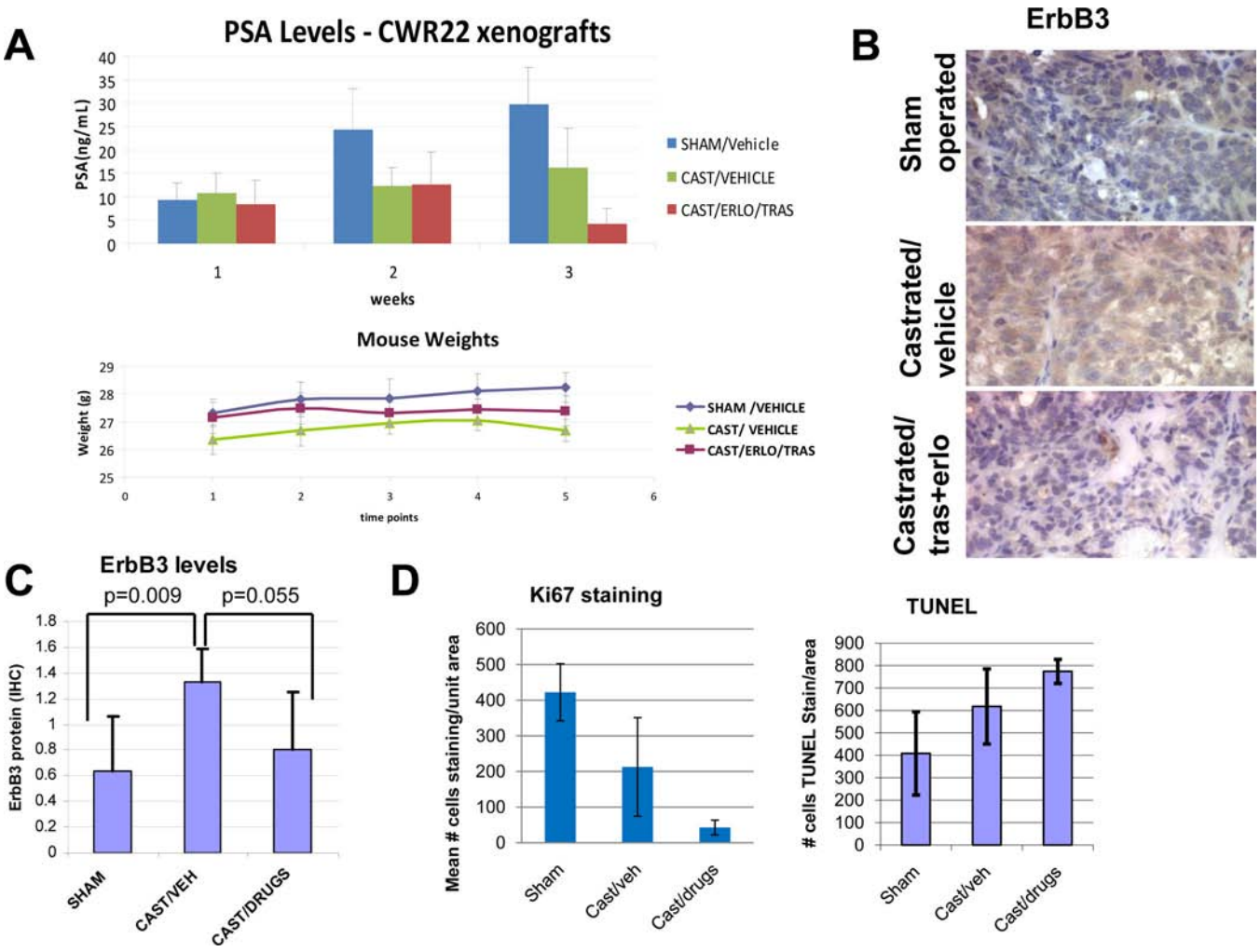

FIGURE 3. The combination of EGFR and HER2 inhibitors inhibited PSA and ErbB3 levels in CWR22 xenograft-bearing nude mice

(A) (upper panel) Serum PSA was measured in weekly blood draws from the three groups of animals: sham operated/vehicle treated (n=6), castrated/vehicle treated (n=6) and castrated/drug treated (n=5), **(lower panel)** while their body weight was monitored to determine overall health. **(B)** Representative ErbB3 stainings of tumors extracted from **(upper)** sham operated (this section was scored +1), **(middle)** castrated/vehicle treated (this section scored +2) and **(lower)** castrated/trastuzumab+erlotinib treated (this section scored +0.5) mice (20X). **(C)** The scores from each group were statistically analyzed to determine overall effects. Castrated/ vehicle treated mice had a significant overall increase in mean ErbB3 levels (1.33 ± 0.26, n=6) compared to sham operated animals (0.63 ± 0.43, n=6), p=0.009; which decreased again (0.8 ± 0.45, n=5) in castrated/ drug treated mice (p=0.05). **(D)** Ki67 and TUNEL staining to determine levels of proliferation and apoptosis in CWR22 xenograft tumors in the same three groups. There was a significant decrease in nuclear staining for both Ki67 (p=0.0027) and TUNEL (p=0.0037) in cells from tumors extracted from the castrated+trastuzumab+erlotinib group compared to the sham castrated (intact) group (n=6).

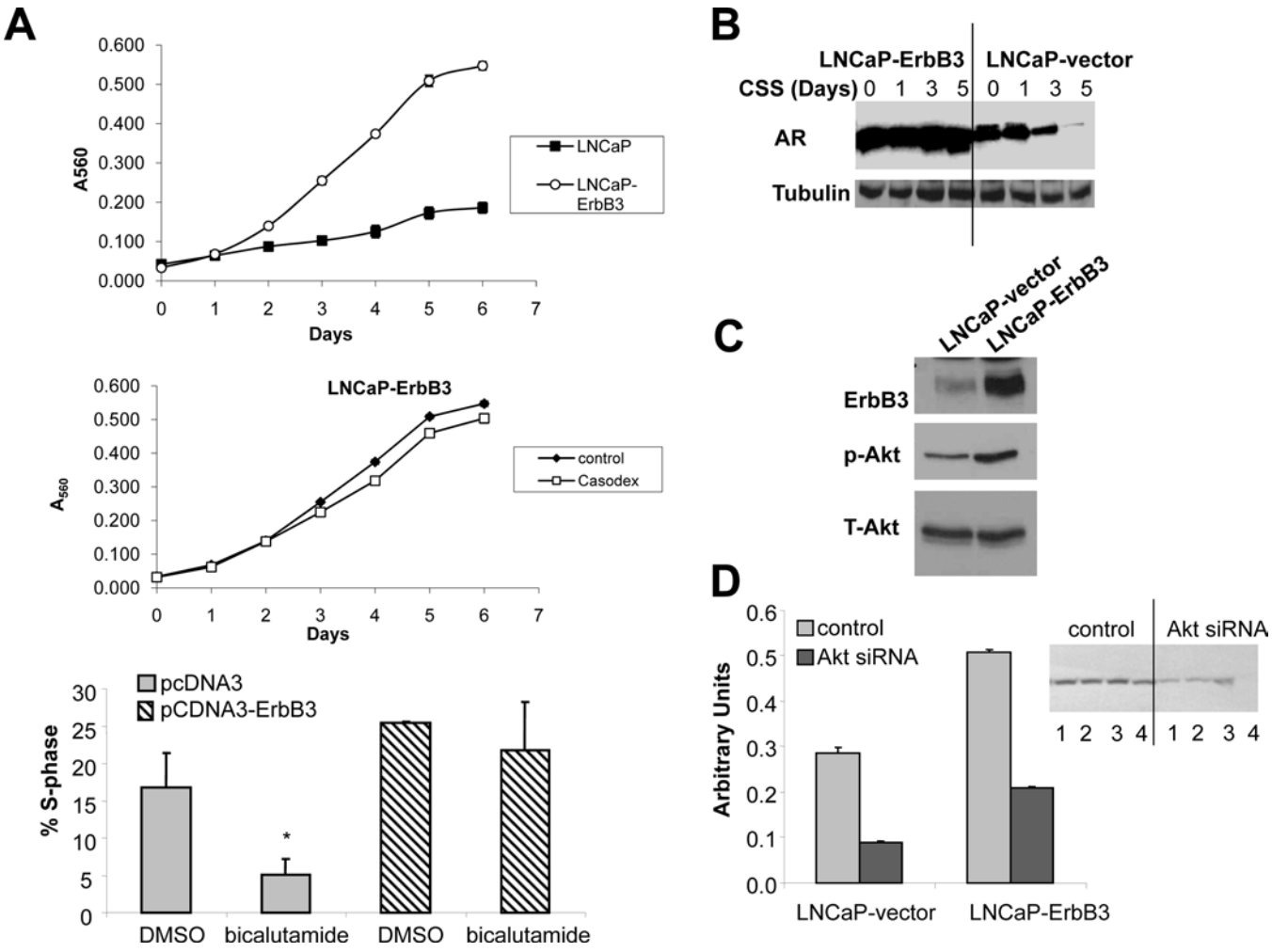

FIGURE 4. Increased ErbB3 levels induce castration resistant cell growth mediated by Akt and androgen receptor stabilization

(A) (upper) MTT assay showing the growth of LNCaP cells transfected with an empty vector or with pcDNA3-ErbB3 cultured in FBS over 6 days. **(middle)** MTT assay showing the growth rate of LNCaP-ErbB3 cells cultured with DMSO (control) or 10 μM bicalutamide (Casodex). All data in this series is representative of three independent experiments. **(lower)** Flow cytometric analysis showing that LNCaP cells expressing pcDNA3 alone were responsive to bicalutamide-induced growth arrest whereas those expressing high ErbB3 levels did not. "*": p=<0.05. **(B)** LNCaP cells transfected with vector (pCDNA3) or overexpressing ErbB3 were cultured in FBS-containing medium until 70% confluent, then switched to medium containing CSS and collected after the periods shown. AR and tubulin (loading control) levels were determined by Western blotting. **(C)** LNCaP cells were stably transfected with vector alone or with a plasmid expressing ErbB3, and demonstrates an increase in ErbB3 levels in the latter cells as well as an increase in Akt phosphorylation. **(D)** ErbB3 mediated cell growth was dependent on Akt activation. LNCaP cells transfected with vector alone or ErbB3 plasmid were subjected to treatment with control or Akt siRNA. The effect of Akt siRNA on Akt levels are shown in the inset. Growth rates were estimated after 4 days of treatment by MTT assay.

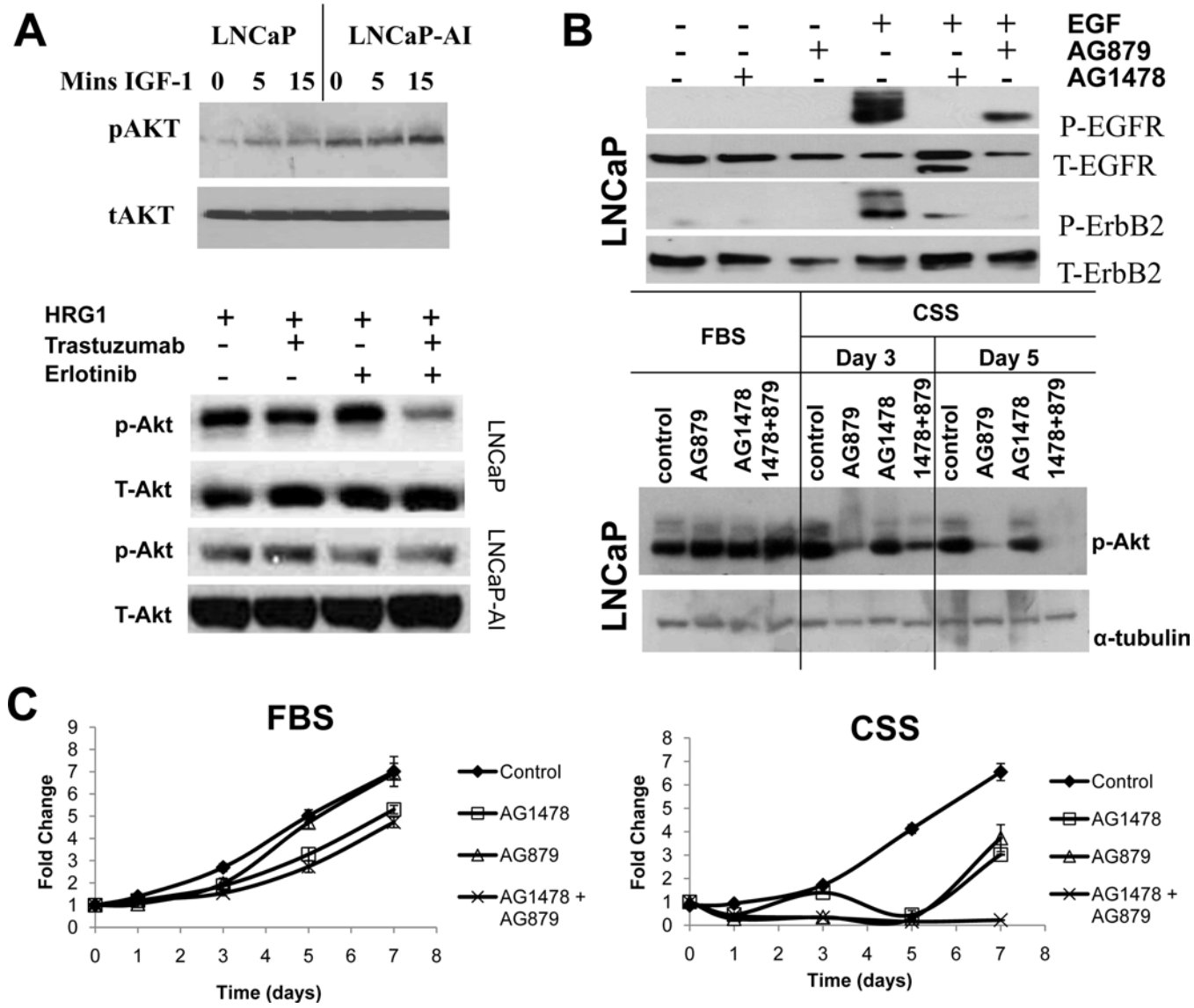

FIGURE 5. Akt phosphorylation at Ser 473 correlates with the ability of ErbB inhibitors to impede cell growth

(A) (upper) LNCaP-AI cells experience increased levels of Akt phosphorylation (Ser 473) compared to LNCaP. LNCaP-AI cells were serum starved and then treated with 10 ng/ml IGF-1 for various times as shown. Note the increase in Akt phosphorylation at Ser 473 with time. **(lower)** Western blots demonstrating the effect of erlotinib (10 μM) and trastuzumab (21 μg/ml) on LNCaP and LNCaP-AI cells. Cells were grown to 75% confluence, and then serum starved for 48 hours in the presence of erlotinib or trastuzumab or both. The cells were then further treated with 50 ng/ml HRG1 for 15 mins, to stimulate Akt phosphorylation downstream of ErbB3 activation, cell lysates collected and immunoblotted with antibodies to anti-phospho Akt (Ser 473) **(1st, 3rd Panels)**, and total Akt **(2nd, 4th Panels). (B) (upper)** Western blots demonstrating the specificity and selectivity of AG1478 and AG879 on the activation of EGFR and HER2 respectively. Serum starved LNCaP cells were treated with vehicle (DMSO), 5 μM AG1478 or 2 μM AG879 for 48 hours followed by further treatment with PBS or 10 ng/mls EGF for 5 mins. EGF induced the phosphorylation of both EGFR (Tyr1068) and HER2 (Tyr1248). **(lower)** LNCaP cells cultured in FBS or CSS were treated

with the two drugs for 3 or 5 days. Western blotting shows that in the presence of FBS, there was no effect of the drugs, alone or in combination, on Akt phosphorylation whereas in CSS, Akt phosphorylation at Ser 473 was significantly affected. **(C)** MTT assay was used to determine the cell growth rate with the combination of AG879 (2 μM) and AG1478 (5 μM) of pRNS1-1 cells stably transfected with a T877A mutant AR grown in medium containing FBS **(left panel)** or medium containing CSS **(right panel)**. Data represents mean ± S.D. of three independent experiments.

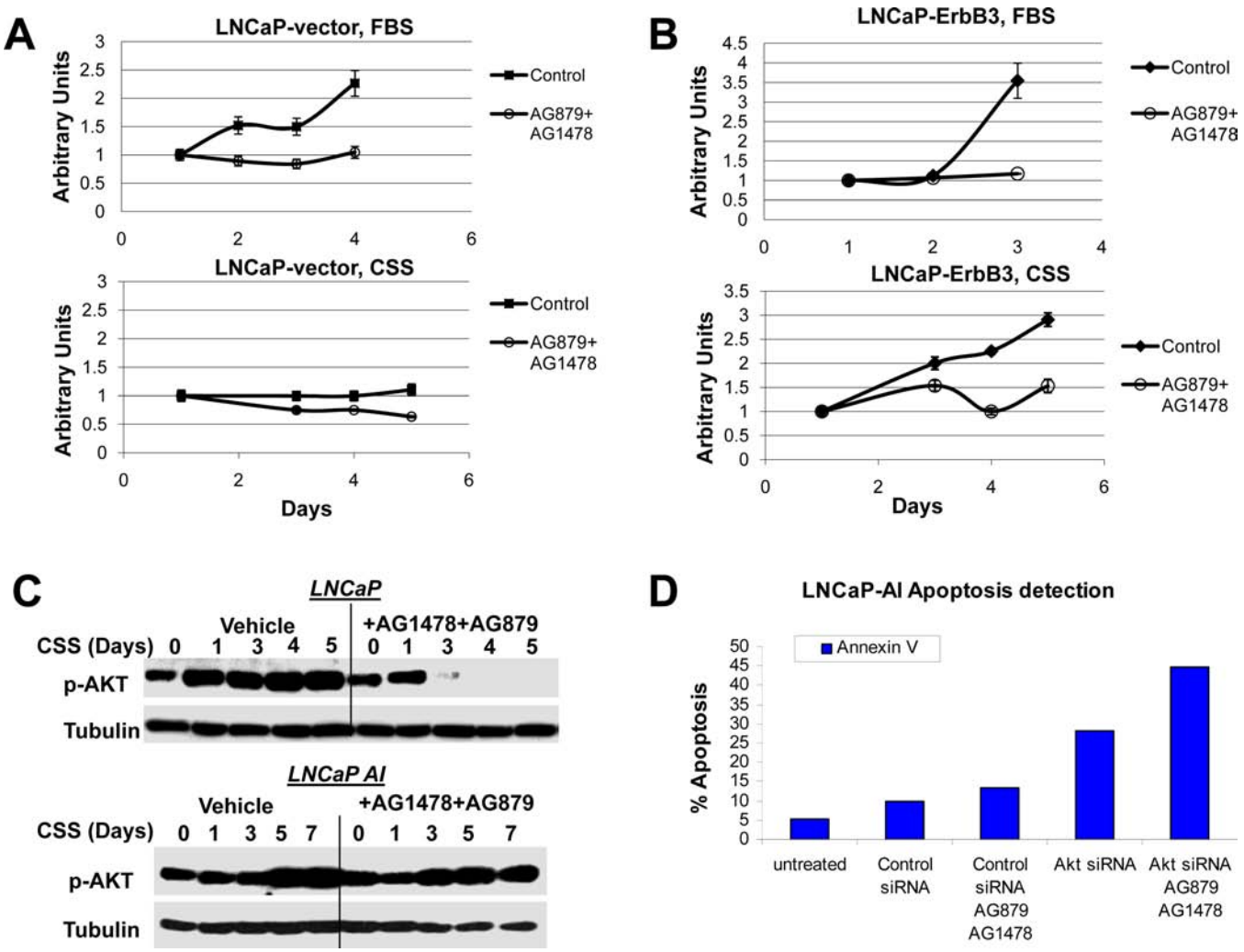

FIGURE 6. ErbB3 overexpression induces resistance to dual EGFR/HER2 inhibition in CRPC, which can be overcome by Akt downregulation

(A,B) LNCaP cells expressing vector alone, or overexpressing erbB3, were treated with 2 μM AG879, 5 μM AG1478, or both, were cultured in medium containing FBS or CSS. MTT assays were conducted to determine the effects of the drug combination on cell growth. **(A, upper)** In medium containing FBS, where control cells experienced a 2.25-fold increase in cell number after four days of treatment, those treated with a combination of AG1478 and AG879 failed to grow ($p<0.0001$), but showed no decrease in cell numbers. **(A, lower)** LNCaP cells transfected with vector only showed a decrease in cell numbers upon culture in CSS. **(B)** FBS- or CSS-cultured, ErbB3-transfected LNCaP cells demonstrated comparable increase in growth rates (2.5-fold increase in growth in 4 days), but dual treatment with AG1478 and AG879 prevented growth ($p=0.004$), but did not decrease cell numbers. Data represents mean ± S.D. of three independent experiments for each point. **(C)** LNCaP and LNCaP AI cells were cultured in FBS then switched to CSS-containing medium in the presence of vehicle (DMSO) or a combination of AG1478 and/or AG879. Cells were harvested after the indicated period of time, and cell lysates run on 10% SDS-PAGE, immunoblotted and the blots stained with rabbit polyclonal anti-phospho-Akt (Ser 473) antibody. **(D)** Flow cytometric analysis of LNCaP-AI cells following 48 hour treatment with siRNA duplexes against a scrambled sequence or Akt1 siRNA. Propidium iodide and

Annexin V-FITC stained cells were then analyzed by flow cytometry to determine the fraction of cells undergoing apoptosis.

Enhancing the effectiveness of androgen deprivation in prostate cancer by inducing Filamin A nuclear localization

Benjamin A Mooso[1,2], Ruth L Vinall[2,†], Clifford G Tepper[2], Rosalinda M Savoy[2], Jean P Cheung[2], Sheetal Singh[1,2], Salma Siddiqui[1], Yu Wang[2,‡], Roble G Bedolla[3], Anthony Martinez[2], Maria Mudryj[1,2], Hsing-Jien Kung[2], Ralph W deVere White[2] and Paramita M Ghosh[1,2]

[1]VA Northern California Health Care System, Mather, California, USA
[2]Department of Urology, University of California Davis School of Medicine, 4860 Y Street, Suite 3500, Sacramento, California 95817, USA
[3]University of Texas Health Science Center at San Antonio, San Antonio, Texas, USA

(Correspondence should be addressed to P M Ghosh at Department of Urology, University of California Davis School of Medicine; Email: paramita.ghosh@ucdmc.ucdavis.edu)

[†](R L Vinall is now at California Northstate College of Pharmacy, Rancho Cordova, California, USA)
[‡](Y Wang is now at Lerner Research Institute, Cleveland Clinic Foundation, Cleveland, Ohio, USA)

Abstract

As prostate cancer (CaP) is regulated by androgen receptor (AR) activity, metastatic CaP is treated with androgen deprivation therapy (ADT). Despite initial response, patients on ADT eventually progress to castration-resistant CaP (CRPC), which is currently incurable. We previously showed that cleavage of the 280 kDa structural protein Filamin A (FlnA) to a 90 kDa fragment, and nuclear localization of the cleaved product, sensitized CRPC cells to ADT. Hence, treatment promoting FlnA nuclear localization would enhance androgen responsiveness. Here, we show that FlnA nuclear localization induced apoptosis in CRPC cells during ADT, identifying it as a treatment tool in advanced CaP. Significantly, the natural product genistein combined polysaccharide (GCP) had a similar effect. Investigation of the mechanism of GCP-induced apoptosis showed that GCP induced FlnA cleavage and nuclear localization and that apoptosis resulting from GCP treatment was mediated by FlnA nuclear localization. Two main components of GCP are genistein and daidzein: the ability of GCP to induce G2 arrest was due to genistein whereas sensitivity to ADT stemmed from daidzein; hence, both were needed to mediate GCP's effects. FlnA cleavage is regulated by its phosphorylation; we show that ADT enhanced FlnA phosphorylation, which prevented its cleavage, whereas GCP inhibited FlnA phosphorylation, thereby sensitizing CaP cells to ADT. In a mouse model of CaP recurrence, GCP, but not vehicle, impeded relapse following castration, indicating that GCP, when administered with ADT, interrupted the development of CRPC. These results demonstrate the efficacy of GCP in promoting FlnA nuclear localization and enhancing androgen responsiveness in CaP.

Endocrine-Related Cancer (2012) **19** 759–777

Introduction

Prostate cancer (CaP), both localized and involving distant metastases, depends on the androgen receptor (AR) for growth and survival. Therefore, metastatic CaP is treated with androgen deprivation therapy (ADT; Catalona 1994); however, patients on this treatment eventually relapse, indicative of the development of castration-resistant CaP (CRPC). Although a number of FDA-approved treatments for CRPC are currently available, the condition remains essentially incurable, with high mortality rates. Response rate to ADT and time to progression, however, vary among

DOI: 10.1530/ERC-12-0171
1351–0088/12/019–759
Online version via http://www.endocrinology-journals.org

patients, and therefore, the goal of the present project was to conduct preclinical studies to identify therapy that ensures sensitivity to ADT in the majority of patients, in order to increase the survival rate in this population.

Previously, we demonstrated that the structural protein Filamin A (FlnA), which promotes actin stress fiber formation in the cytoplasm, is localized to the nucleus of androgen-dependent cells, where it impeded CRPC development (Wang *et al*. 2007, Bedolla *et al*. 2009). 88.4% of metastatic deposits from CRPC patients expressed cytoplasmic FlnA, whereas 75% of hormone-naïve localized tumors expressed nuclear FlnA (Bedolla *et al*. 2009). In support of these observations, *in vitro* studies showed that cytoplasmic localization of FlnA was associated with increased cell motility and invasion (Bedolla *et al*. 2009) whereas nuclear localization was associated with castration-sensitive growth (Wang *et al*. 2007). Our results indicated that therapies that promoted the induction of FlnA nuclear translocation would enhance the effectiveness of ADT. The overall goal of these studies was to identify a clinically safe drug that can promote FlnA localization to the nucleus.

Full-length FlnA (280 kDa) is mainly cytoplasmic and consists of an N-terminal actin-binding domain followed by 24 repeats, each 96-amino acids long, interrupted by two hinge domains H1 and H2 (van der Flier & Sonnenberg 2001). Proteolysis of FlnA by cleavage at H1 between repeats 15 and 16 created a 170 kDa N-terminal fragment and a 110 kDa C-terminal fragment, which was further cleaved at H2 between repeats 23 and 24, to yield a 90 kDa fragment, which can translocate to the nucleus. Surprisingly, FlnA was also found to localize to the nucleolus, where it inhibited rRNA production (Deng *et al*. 2012), but the mechanism of transportation to that organelle is currently unknown. The hinge domain of the AR binds to the C-terminal domain of FlnA at repeats 18–19 and co-localizes to the nucleus (Ozanne *et al*. 2000, Loy *et al*. 2003). Phosphorylation of FlnA at Ser 2152 prevented cleavage of the protein (Gorlin *et al*. 1990), whereas dephosphorylation of FlnA induced nuclear localization and promoted sensitivity to ADT (Wang *et al*. 2007, Bedolla *et al*. 2009). Despite the attractiveness of using FlnA to enhance androgen sensitivity, the translational potential of these studies, until now, was impeded by a lack of clinically safe drugs that prevent FlnA phosphorylation and promote its cleavage.

Here, for the first time, we show that genistein combined polysaccharide (GCP), a natural product, induces FlnA nuclear localization. GCP consists of 9% genistein, 6% daidzein, 2% glycetin, 3% equol, 15% lipid, 5% protein, and 60% carbohydrate (deVere White *et al*. 2010). An initial case study reported that 1.5 g GCP daily for 6 weeks caused tumor regression in a 63-year-old man presenting with T3, Gleason grade 6 (3+3) CaP, and reduced serum levels of prostate-specific antigen (PSA) from 19.4 to 10.2 ng/ml in 3 weeks, indicative of reduction in AR activity (Ghafar *et al*. 2002). Following this report, the effect of GCP in CaP was investigated in a number of laboratories. *In vitro* and *in vivo* studies revealed that GCP reduced cell growth in both androgen-dependent and -independent cells (Bemis *et al*. 2004, Vinall *et al*. 2007). GCP markedly suppressed mTOR-p70S6K signaling and attenuated excessive androgen signaling, which is a hallmark of advanced CaP (Tepper *et al*. 2007, Vinall *et al*. 2007).

Clinical studies from our institute in men with localized CaP demonstrated the safety of GCP and resulted in no change or decline in PSA (deVere White *et al*. 2004). In an additional study of GCP alone in men with a diagnosis of CaP but no prior treatment, participants showed no evidence of metastasis; however, serum genistein levels did not correlate with PSA (deVere White *et al*. 2010). These studies encouraged investigation of GCP in advanced disease. *In vitro* studies showed that GCP treatment in combination with AR knockdown (Vinall *et al*. 2007) or co-treatment with the AR antagonist bicalutamide (Burich *et al*. 2008) had enhanced efficacy. However, the mechanism of enhanced efficacy of GCP in the absence of androgens was unknown. Although GCP is known to inhibit the PI3K/Akt/mTOR pathway, its effect on AR suppression was independent of this pathway (Tepper *et al*. 2007). The lack of a mediator of GCP action on the AR severely impaired efforts to understand its role in CaP control, until now.

Collaboration between two independent teams investigating the actions of GCP and FlnA, as shown here, finally led to the demonstration that GCP targets FlnA and cleaves this molecule to the 90 kDa fragment, which can then translocate to the nucleus and impede relapse following ADT. Our results show that nuclear localization of FlnA promotes androgen dependence and that the cooperative effect of GCP and ADT in CaP results from simultaneous effects of these two treatments on this molecule both *in vitro* and *in vivo*. Our results therefore identify GCP-induced FlnA nuclear localization as a therapeutic module that enhances the efficacy of ADT.

Materials and methods

Cell culture and materials

LNCaP and CWR22Rv1 (ATCC, Manassas, VA, USA), C4-2 cells (Urocor, Oklahoma City, OK, USA), CWR-R1 cells (Dr Elizabeth Wilson, University of North Carolina), and PC-346C cells (Dr W M van Weerden, Josephine Nefkens Institute, Erasmus MC, Rotterdam, The Netherlands) were cultured in fetal bovine serum (FBS) or charcoal-stripped serum (CSS) as indicated. All cell lines used here were investigated for the presence of contaminants and their cellular origins were verified before use. The following plasmids were used in the transfections: pCMV-FlnA, FlnA(16–24), and FlnA(1–15) plasmids kindly provided by Dr E W Yong, National University of Singapore, Singapore; PSA-luciferase construct (hPSA-luc) kindly provided by Dr XuBao Shi, University of California Davis. Cells were transfected using Lipofectamine 2000 reagent (Invitrogen) according to the manufacturer's specifications based on established protocols.

Materials used

GCP and bicalutamide were kindly provided by AminoUp, Japan, and AstraZeneca, Cheshire, UK respectively. PKI(14–22) was from Calbiochem (Billerica, MA, USA), dihydrotestosterone (DHT) and genistein were from Sigma–Aldrich, and daidzein was from Fisher Scientific (Waltham, MA, USA). PKI, genistein, daidzein, and bicalutamide were dissolved in DMSO, while DHT was dissolved in ethanol. For *in vitro* studies, GCP was dissolved in a solution of 50% DMSO and 50% ethanol, whereas *in vivo*, it was provided as a suspension in peanut oil.

Subcellular fractionation

Cells were collected in 0.5 ml Buffer A (10 mM HEPES, pH 7.9, 10 mM KCl, 0.1 mM EDTA, and 0.5 mM dithiothreitol) containing 200 µl 10% IGEPAL and protease inhibitors (0.1 mM benzamidine, 1 mM phenylmethylsulfonyl fluoride (PMSF), and 10 µg/ml each phenanthroline, leupeptin, aprotinin, and pepstatin A). Following 10 min of incubation at room temperature, the lysates were transferred to ice and centrifuged at 4 °C at 250 ***g*** in a benchtop refrigerated centrifuge (Eppendorf 5417R) for 5 min and the supernatant collected as the cytosolic fraction. The pellet containing the nuclei was resuspended in 150 ml Buffer B (20 mM HEPES, pH 7.9, 0.4 M NaCl, 1 mM EDTA, and 10% glycerol) containing the same protease inhibitors and solubilized by vigorous shaking using a sonicator at 4 °C for 2 h. The suspension was then centrifuged at 4 °C as before for 5 min and the supernatant collected as the nuclear fraction.

Antibodies used

Rabbit polyclonal antibodies against β-actin, AR, cyclin A, cyclin B, and cyclin D1 were from Santa Cruz Biotechnology (Santa Cruz, CA, USA). Mouse MABs against Akt, GAPDH, and α-tubulin along with rabbit polyclonal antibodies against caspase 3, lamin A, poly (ADP-ribose) polymerase (PARP), and phospho-FlnA (S2152) were from Cell Signaling (Beverly, MA, USA). Mouse monoclonal anti-FlnA antibody (C-terminal) was from Millipore (Billerica, MA, USA), rabbit polyclonal anti-FlnA antibody (C-terminal) (for immunofluorescence) was from Abcam (Cambridge, MA, USA), and rabbit polyclonal anti-FlnA (N-terminal) was from Santa Cruz Biotechnology.

RNA inhibition

Anti-FlnA siRNA duplex with the following target sequence was purchased from Dharmacon Research, Inc., Lafayette, CO, USA: 5′-CAACGTTGGTAGTCATTGT-3′. A pool of four duplexes sold as AR siRNA (Santa Cruz Biotechnology) with the following sequences: Strand #1: 5′-CAGUCCCACUUGUGUCAAATT-3′, Strand #2: 5′-CCUGAUCUGUGGAGAUGAATT-3′, Strand #3: 5′-GUCGUCUUCGGAAAUGUUATT-3′, and Strand #4: 5′-GACAGUGUCACACAUUGAATT-3′. Control was a pool of four scrambled nonspecific siRNA duplex (si*CONTROL* Non-Targeting siRNA Pool, Dharmacon Research, Inc.).

Analysis of cell proliferation or apoptosis using flow cytometry

Cells were grown under desired conditions in 60 mm dishes at 1×10^6 cells/dish. Flow cytometry was conducted on FACSCalibur (Becton Dickinson Immunocytometry Systems, San Jose, CA, USA). Cells were illuminated with 200 mW of 488 nm light produced by an argon-ion laser and 635 nm light produced by a red-diode laser. Fluorescence was read through a 630/22 nm band-pass filter (for propidium iodide) or a 661/16 nm band-pass filter (for Annexin V-Alexa Fluor 647). Data were collected on 20 000 cells as determined by forward and right angle light scatter and stored as frequency histograms; data used for cell cycle analysis were further analyzed using MODFIT (Verity Software, Topsham, ME, USA).

3-[4,5-Dimethylthiazol-2yl]-2,5-diphenyl-tetrazolium bromide assay

Cells were cultured in 24-well plates and treated as indicated. Following treatment, each well was incubated with 25 µl of 5 mg/ml 3-[4,5-dimethylthiazol-2yl]-2,5-diphenyl-tetrazolium bromide (MTT; Sigma–Aldrich) for 1 h in a 5% CO_2 incubator at 37 °C, which converted the reactants to formazan in actively dividing cells. Proliferation rates were estimated by colorimetric assay reading formazan intensity in a plate reader at 562 nm.

Western blotting

Whole-cell extracts were prepared by lysing cells in 300 µl cell lysis buffer (50 mM Tris–HCl, pH 7.4, 150 mM NaCl, and 1% NP-40) containing the protease inhibitors 0.1 mM benzamidine, 1 mM PMSF, and 10 mg/ml each of phenanthroline, leupeptin, aprotinin, and pepstatin A and phosphatase inhibitors 20 mM β-glycerol phosphate, 1 mM Na-orthovanadate, and 10 mM NaF. Proteins were quantitated by BCA assay (Pierce, Rockford, IL, USA) and fractionated on 29:1 acrylamide-bis SDS–PAGE. Electrophoresis was performed at 150 V for 2 h using mini vertical electrophoresis cells (Mini-PROTEAN 3 Electrophoresis Cell, Bio-Rad). The gels were electroblotted for 2 h at 200 mA using Mini Trans-Blot Electrophoretic Transfer Cell (Bio-Rad) onto 0.2 µm polyvinylidene difluoride membrane (Osmonics, Westborough, MA, USA). The blots were stained overnight with primary antibodies at 4 °C and detected by enhanced chemiluminescence (Pierce) following incubation with a peroxidase-labeled secondary antibody (donkey anti-mouse IgG or goat anti-rabbit IgG, F_c specific, Jackson ImmunoResearch, West Grove, PA, USA).

Immunofluorescence

Cells were rinsed with PBST (PBS with 0.05% Tween 20) and fixed with ice-cold methanol for 15 min at room temperature. Fixed cells were washed three times with PBST and blocked with 10% BSA for 30 min at room temperature. Primary antibody, prepared in 1% BSA, was applied to the cells, which were incubated at 4 °C overnight. Cells were then washed three times with PBST and FITC-conjugated anti-rabbit secondary antibody (Jackson ImmunoResearch), diluted 1:1000 in 1% BSA, was added and incubated for 30 min at room temperature in the dark. After washing three times with PBST, slow fade mounting medium with DAPI (Invitrogen) was applied to the slides before mounting of the coverslips.

Quantitative real-time PCR

Total cellular RNA was prepared from cells using RNeasy mini kit (Qiagen, Inc.) based on the manufacturer's protocol. cDNA was synthesized from 1 µg RNA using QuantiTect reverse transcription kit based on manufacturer's protocol. cDNAs were diluted 1:4 in ddH_2O and 2 µl diluted cDNA were added to 5 µl EXPRESS SYBR GreenER qPCR SuperMix (Invitrogen) and 200 nM of each primer. GAPDH was used as the endogenous expression standard. PCR conditions were 20 s of initial denaturation step at 95 °C, 40 cycles at 95 °C for 3 s, and 60 °C for 30 s, followed by additional 95 cycles starting at 60 °C with 0.5 °C increase per cycle for melt curve analysis. GAPDH forward: 5′-TGCACCACCAACTGCTTA and reverse 5′-AGAGGCAGGGATGATGTTC; FlnA forward 5′-AAGTGACCGCCAATAACGAC and reverse 5′-GGCGTCACCCTGTGACTTAT.

Evaluation of mouse retrovirus

Cell lysates were prepared using RIPA Buffer containing protease and phosphatase inhibitors and normalized to 2 µg/µl using BCA Protein Assay (Pierce). Lysate (50 µg) was loaded per lane, run on a 12% SDS–PAGE gel, and transferred using semidry transfer unit (Bio-Rad) at 15 V for 70 min. Gag antibody (1:250) and β-actin antibody (1:10 000, Sigma A-1978) were diluted in 5% Milk Protein TBS Tween and incubated overnight with rocking at 4 °C. Membranes were washed 4× TBS Tween for 10 min at room temperature and then incubated with goat anti-mouse secondary antibody (1:5000, Santa Cruz SC-2005). Membranes were washed again 4× TBS Tween for 10 min at room temperature and incubated for 1 min in SuperSignal West Pico Chemiluminescent Substrate (Pierce 34080). Membranes were drained of excess fluid and images were taken using FluorChem E Imager and analyzed using AlphaView SA software (Protein Simple, Santa Clara, CA, USA).

Mouse xenograft studies

Four- to five-week-old athymic nude male mice ($n=24$, Harlan, Indianapolis, IN, USA) were implanted with 12.5 mg, 90-day release testosterone pellets (Innovative Research of America, Sarasota, FL, USA) before injection of CWR22 prostate tumor suspension s.c. in the right flank. These experiments were conducted under an IACUC approved protocol. Cells were mixed 1:1 with 50% Matrigel (BD Biosciences, San Jose, CA, USA) before s.c. injection (2.5×10^6 cells per injection). When palpable tumors were observed, their pellets were removed, and the

animals were left untreated ($n=6$) or treated with vehicle ($n=8$) or GCP (1.2 mg/kg per day) ($n=10$) as a suspension in water dispersed in peanut oil by esophageal gavage for 14 consecutive days, after which drug treatment was discontinued. Control animals were given water droplets dispersed in peanut oil only ($n=8$). Uniformity of the suspension was maintained by vigorous shaking before gavage for each animal. Twenty-one days after start of experiment, the animals were castrated ($n=22$) and/or left intact (sham operated, $n=2$). Sham-operated mice were opened up but then closed again without castration. Two mice from each group (sham castrated, castrated-untreated, castrated-vehicle treated, castrated-GCP treated) were killed 3 days post-castration for molecular analysis. Four others were killed due to large tumor size. The remaining 12 mice (six on GCP and six on vehicle) were used as described in the Results section. Tumor dimensions were measured twice a week using calipers. At the end of the study, tumor-bearing mice were killed using CO_2 gas followed by cervical dislocation.

Immunohistochemistry

Mouse tumors were fixed in 10% buffered formalin (Medical Industries, Richmond, IL, USA) at room temperature. The tumor was paraffin embedded and processed based on established protocols. Paraffin-embedded cell blocks were then sectioned and sections were heated to 60 °C, cleared, and rehydrated in xylene and graded alcohols. Antigen retrieval was performed with 10 mM citrate buffer at pH 6.0 for 10 min in a pressure chamber at 121 °C and 10 more minutes without pressure. Slides were allowed to cool for another 20 min, followed by sequential rinsing in TBS-T (50 mM Tris–HCl, pH 7.4, 150 mM NaCl, and Tween 20 (0.1%)). Endogenous peroxidase activity was quenched by incubation in TBS-T containing 3% hydrogen peroxide. Slides were then blocked with 10% BSA. Each incubation step was carried out at room temperature and was followed by three sequential washes (5 min each) in TBS-T. Sections were incubated in mouse monoclonal anti-FlnA antibody against the C-terminal (Millipore), diluted in TBS-T containing 1% BSA (1 h), followed by incubations with biotinylated secondary antibody for 15 min, peroxidase-labeled streptavidin for 15 min (LSAB-2 Dako Corp., Carpenteria, CA, USA), and diaminobenzidine and hydrogen peroxide chromogen substrate (Dako Corp.). Slides were counter-stained with hematoxylin and mounted. Negative controls were incubated with Universal Mouse Negative Control (Dako Corp.) in place of primary antibody.

Statistical analysis

Tumor volumes were calculated as $V=\text{length}\times\text{height}\times\pi/6$. The change in tumor volume was calculated as percentage of the volume of the tumor at the time of castration. Analyses using an unpaired, two-tailed Student's *t*-test were used to compare tumor sizes of the two study groups: untreated vs GCP treated $-P<0.05$ was considered statistically significant. All *in vitro* experiments using MTT or luciferase data were performed in triplicate. Data are presented as relative luciferase activity using means of untreated controls as standards, normalized to the corresponding reading for β-gal.

Results

Nuclear localization of a 90 kDa FlnA fragment induces apoptosis in CaP cells

We previously demonstrated that androgen-sensitive and -insensitive cell lines differentially expressed nuclear localization of FlnA, a structural protein (Wang *et al*. 2007, Bedolla *et al*. 2009). A castrate-resistant subline of LNCaP cells, C4-2, has been developed from tumors obtained by co-implantation of LNCaP cells with bone stromal cells in castrated nude mice (Thalmann *et al*. 1994). We previously showed that C4-2 cells express very high AR transcriptional activity compared with LNCaP cells (Ghosh *et al*. 2005). Unlike LNCaP, C4-2 cells were not growth arrested by the anti-androgen bicalutamide (Casodex) (Fig. 1A, left), a competitive inhibitor of AR ligand binding (Masiello *et al*. 2002). C4-2 cells expressed lower levels of 90 kDa FlnA compared with LNCaP (Fig. 1A, right) and lower levels of FlnA in the nucleoplasm (Fig. 1B), but not in the nucleolus. Transfection of a plasmid expressing C-terminal FlnA (FlnA 16–24), which resulted in the appearance of the 90 kDa FlnA fragment (Loy *et al*. 2003, Wang *et al*. 2007), restored nuclear expression of FlnA in C4-2 cells (Fig. 1B). This effect required the presence of the AR because it was not observed in AR null PC-3 cells (Wang *et al*. 2007), but in C4-2 cells expressing full-length AR as well as CWR22Rv1 cells expressing a truncated form of AR (Fig. 1C). Transfection of FlnA 16–24, but not full-length FlnA or FlnA 1–15 (N-terminal), induced apoptosis in cells treated with the AR antagonist bicalutamide (Fig. 1D). Taken together, these results demonstrate that nuclear localization of the 90 kDa fragment of FlnA induces apoptosis in CaP cells.

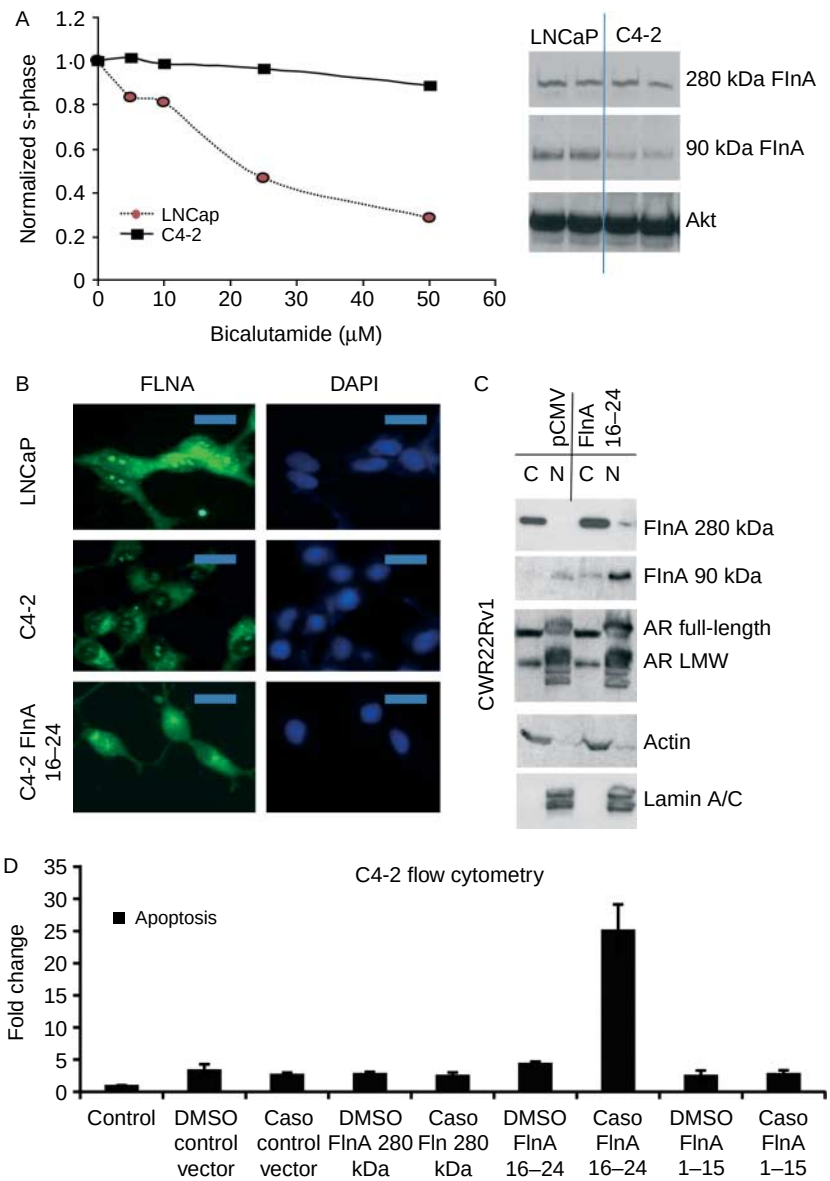

Figure 1 Nuclear localization of a 90 kDa FlnA fragment induces apoptosis in prostate cancer cells. (A) (Left) LNCaP and C4-2 cells were treated with increasing doses of the anti-androgen bicalutamide for 48 h and the percentage of cells in S-phase was analyzed by flow cytometry in PI-stained cells. (Right) Untreated LNCaP and C4-2 cells. Western blotting revealed that both cell lines expressed equal levels of 280 kDa FlnA, but LNCaP cells expressed higher levels of 90 kDa FlnA compared with C4-2. (B) LNCaP, C4-2, and C4-2 cells stably transfected with FlnA 16–24 (C4-2 16–24) were stained by immunofluorescence for FlnA with an antibody specific to the C-terminus of FlnA. Immunofluorescent staining shows nuclear localization of 90 kDa FlnA in LNCaP cells whereas in C4-2 cells FlnA was mainly localized to the cytoplasm but not in the nucleoplasm, although bright staining in the nucleolus was also detected. In contrast, C4-2 16–24 cells expressed this protein equally in the cytoplasm and the nucleus, while nucleolar staining could still be detected. Scale bar: 10 μm. (C) Subcellular fractionation of CWR22Rv1 cells transfected with 1 μg/ml cDNA expressing FlnA 16–24 showing that the 16–24 fragment goes into the nucleus. Some full-length FlnA enters the nucleus when transfected with FlnA 16–24 due to nucleolar localization. (D) Flow cytometric analysis in PI-stained, ethanol-fixed C4-2 cells to determine the % cells undergoing apoptosis. Apoptosis was considered to be the cells staining with Annexin V and showed that transfection with FlnA 16–24 induced apoptosis in C4-2 cells.

Treatment with GCP replicates the effects of FlnA nuclear localization

The above results indicated that restoration of FlnA nuclear localization likely restored hormone-sensitive behavior in CaP. Therefore, pharmaceutical approaches to FlnA cleavage were pursued. Castration-resistant CWR22Rv1 cells derived from a relapsed CWR22 tumor were chosen for these studies because they express multiple forms of AR – a 114 kDa full-length form containing a H874Y point mutation and an in-frame tandem duplication of exon 3, as well as truncated AR species lacking the ligand binding domain (LBD; Tepper *et al*. 2002). Hence, treatment that promotes hormone sensitivity in these cells would be widely applicable. Transfection of FlnA 16–24, but not full-length FlnA or FlnA 1–15, promoted expression of the 90 kDa fragment both in the nucleus and in the cytoplasm (Fig. 2A), sensitized these cells to bicalutamide (Fig. 2B), and induced apoptosis (Fig. 2C).

The physiological range of testosterone in FBS is 55.1–97.5 pM whereas that in CSS is 15.6–19.0 pM (Sedelaar & Isaacs 2009). Hence, culture in CSS results in ADT *in vitro*. GCP sensitized CWR22Rv1 cells to ADT, resulting in growth arrest and apoptosis (Fig. 2D), which was enhanced in low androgen levels. This was accompanied by increases in caspase 3 and PARP cleavage, indicative of apoptosis, especially in low-androgen medium (Fig. 2E). These results demonstrated that the effect of GCP was very similar to that induced by FlnA 16–24.

FlnA cleavage to the 90 kDa fragment mediates GCP-induced apoptosis

We previously showed that the AR activated similar pathways in CWR22Rv1 and CWR-R1, two cell lines established from two independent relapsed CWR22 tumors (Chen *et al*. 2010*a*). Similar to CWR22Rv1 (Tepper *et al*. 2002), CWR-R1 cells were refractory to hormonal treatment (Fig. 3A); significantly, these cells were also sensitized to cytostatic effects of GCP in low-androgen media (Fig. 3B). Investigation of the mechanism of this effect indicated that GCP induced G2/M arrest in CaP cells (Fig. 3C), similar to its main component genistein as has been demonstrated by other laboratories in various cell lines (Lian *et al*. 1998, Schmidt *et al*. 2008, Zhao *et al*. 2009, Han *et al*. 2010). Further, GCP suppressed the levels of 280 kDa FlnA while causing an increase in the levels of the cleaved FlnA levels (110 and 90 kDa) (Fig. 3D), thereby indicating that GCP causes FlnA cleavage.

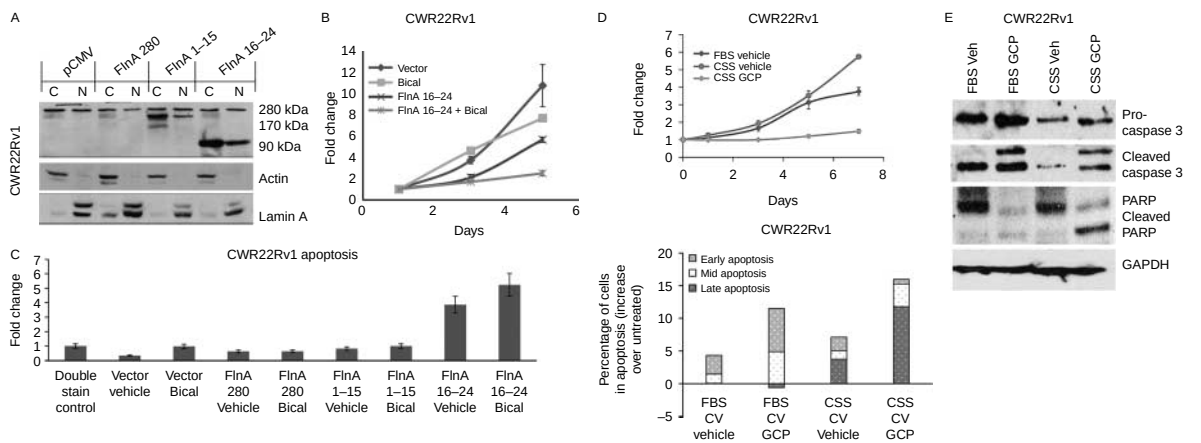

Figure 2 Treatment with genistein combined polysaccharide (GCP) replicates the effects of FlnA nuclear localization. (A) Expression of the transfected proteins when CWR22Rv1 cells were transiently transfected for 48 h with 2 μg/ml of an empty vector, full-length FlnA (280 kDa), FlnA 1–15 (170 kDa), or FlnA 16–24 (90 kDa). Actin and lamin A were used as markers of the cytoplasm and the nucleus respectively. (B) As estimated by MTT assay, neither 10 μM bicalutamide nor FlnA 16–24 individually had significant effects on the growth of CWR22Rv1 cells, but in combination, they prevented cell growth. Each point on the graph represents mean ± S.D. of three independent readings. (C) CWR22Rv1 cells underwent apoptosis when transfected with FlnA 16–24 but not when transfected with an empty vector, FlnA 280 or FlnA 1–15 as determined by flow cytometry after 48 h in Annexin V- and propidium iodide-stained cells. (D) (Upper) MTT assay showing effect of CWR22Rv1 cells with GCP or vehicle in FBS- and CSS-containing medium. Each point on the graph represents mean ± S.D. of three independent readings. (Lower) Analysis of apoptosis by flow cytometry in propidium iodide- and Annexin V-stained cells demonstrating that CWR22Rv1 cells treated with 100 μg/ml GCP for 48 h experienced more apoptosis than vehicle-treated cells. Early apoptosis: Annexin V staining, mid-apoptosis: Annexin V + PI staining, late apoptosis: PI staining. Results presented represent numbers after subtraction from untreated cells. Note the increase in apoptosis in cells cultured in CSS vs FBS containing medium. (E) Western blots demonstrating that 100 μg/ml GCP after 48 h increased apoptosis as demonstrated by cleaved caspase 3 and PARP levels.

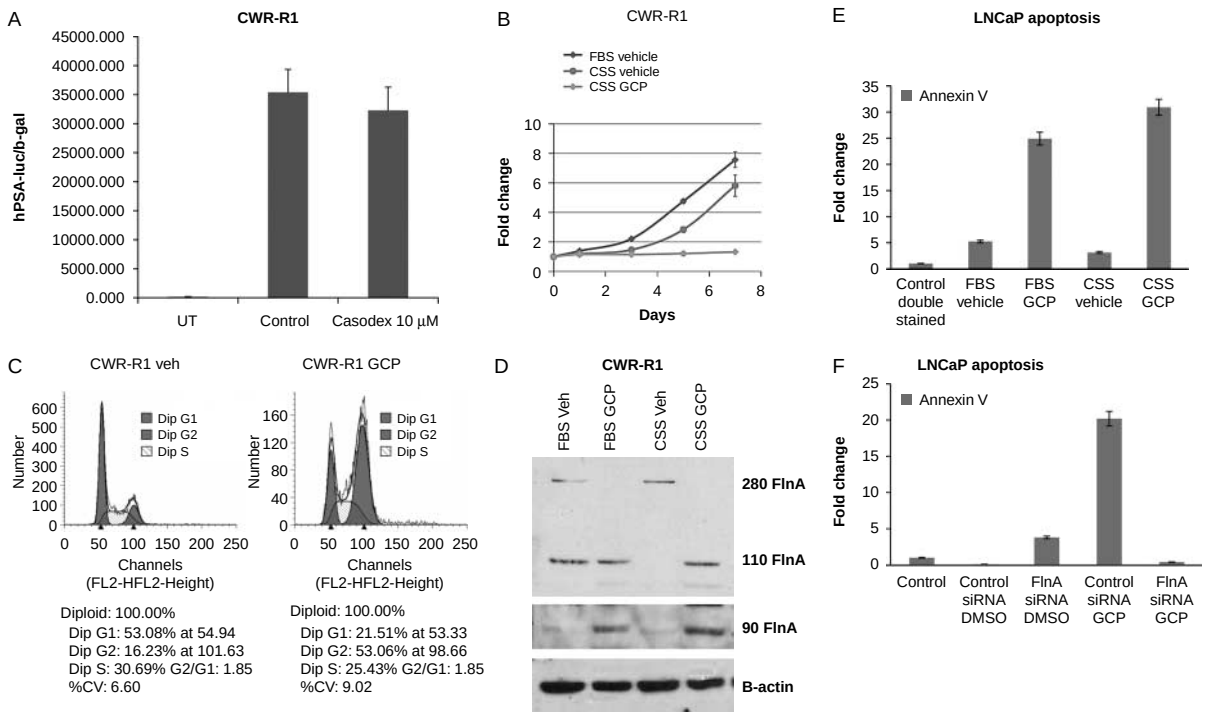

Figure 3 Treatment with GCP induces FlnA cleavage to the 90 kDa fragment that mediates GCP-induced apoptosis. (A) Luciferase assay to determine AR transcriptional activity on a PSA promoter to determine the effect of 10 μM bicalutamide or vehicle in CWR-R1 cells. Cells were cultured in FBS and collected after 48 h. Each point on the graph represents mean ± S.D. of three independent readings. (B) MTT assay showing effect of CWR-R1 cells with GCP or vehicle in FBS and CSS containing medium. Each point on the graph represents mean ± S.D. of three independent readings. (C) Cell cycle analysis by flow cytometry in PI-stained, ethanol-fixed cells demonstrating that CWR-R1 cells treated with 100 μg/ml GCP for 48 h undergo G2/M arrest. (D) Immunoblots to determine levels of various FlnA fragments in CWR-R1 cells cultured in FBS vs CSS and treated with either vehicle or 100 μg/ml GCP for 48 h. An antibody to the C-terminal end of FlnA that recognizes the 280, 110, and 90 kDa bands was used in this study. (E) Apoptosis in LNCaP cells determined by flow cytometry in Annexin V and PI stained in medium containing FBS or CSS in the presence of vehicle or 100 μg/ml GCP for 48 h. (F) Role of FlnA in GCP-induced apoptosis. LNCaP cells were subjected to control or FlnA siRNA and treated with vehicle or 100 μg/ml GCP for 48 h. Apoptosis was determined by flow cytometry in cells stained with propidium iodide and Annexin V.

CWR-R1 and CWR22Rv1 lines had been propagated in mice and were contaminated by mouse retrovirus (Paprotka *et al.* 2011). On the other hand, LNCaP cells were free from this virus (Sfanos *et al.* 2011). Similar to CWR22Rv1, GCP induced apoptosis in LNCaP cells, and this effect was more prominent in CSS-cultured cells (Fig. 3E). Therefore, we investigated whether GCP-induced apoptosis was mediated by FlnA. Significantly, FlnA siRNA, but not control siRNA, prevented GCP-induced apoptosis in LNCaP cells (Fig. 3F). These results show that GCP-induced apoptosis is enhanced with ADT and is mediated by FlnA.

GCP's effects reflect a combination of both genistein and daidzein

Next, we investigated which components of GCP are responsible for its effects. In human patients, the serum levels of genistein and daidzein were determined to be 43 and 51 μmol/l respectively (about 10 μg/ml each in an average adult male), following 6 months of GCP intake at 5 g/day (deVere White *et al.* 2010). At comparable doses, daidzein reduced proliferation in the absence, rather than the presence, of androgens (22.4% decrease in FBS, $P=0.039$, vs 69.5% decrease in CSS, $P<0.0001$) whereas the effect of genistein remained virtually unchanged in FBS (84.68% decrease, $P=0.002$) vs CSS (74% decrease, $P<0.0001$) (Fig. 4A). We verified these results in androgen-sensitive PC-346C CaP cells (Fig. 4B; van Weerden *et al.* 1996, Limpens *et al.* 2006) that did not express the mouse retrovirus (Fig. 4D). Genistein induced G2 arrest in PC-346C cells, while daidzein growth arrested them at G1 (Fig. 4B), while GCP resulted in growth arrest in both G1 and G2, with very few cells in S-phase. Significantly, genistein, but not daidzein, restored the levels of the 90 kDa FlnA

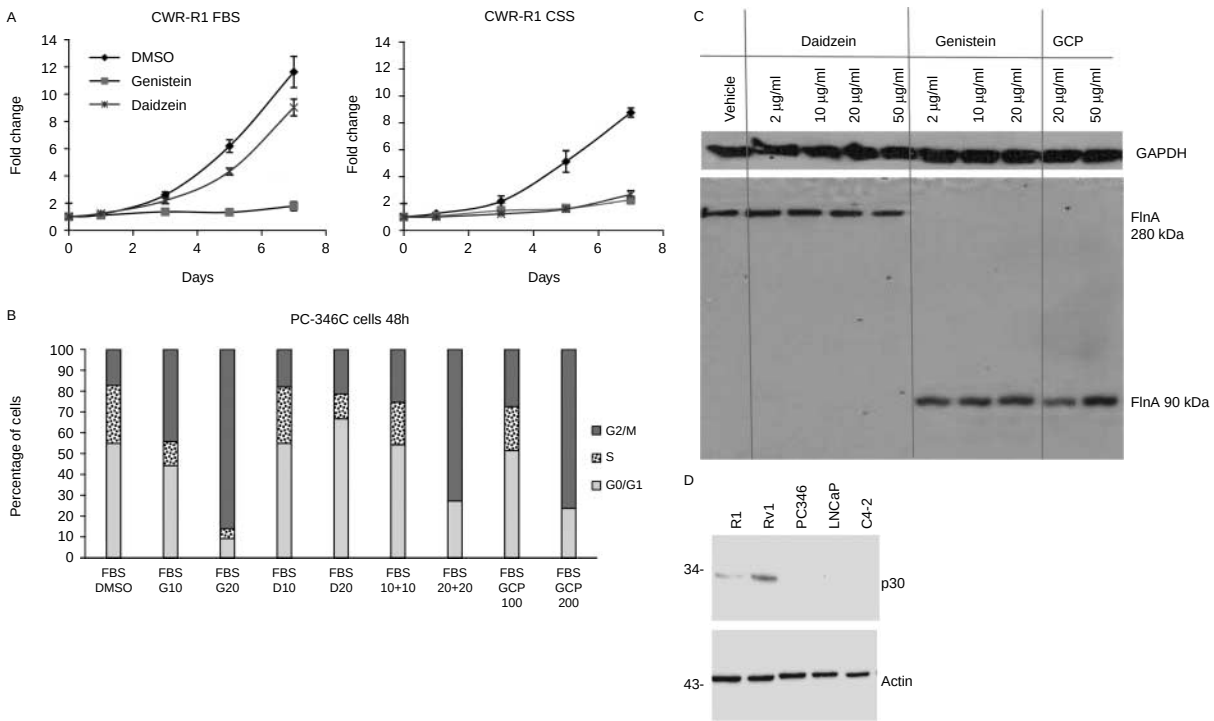

Figure 4 A combination of genistein and daidzein is required for rendering the effects of GCP. (A) MTT assay showing the effect of 10 μg/ml genistein or daidzein on CWR-R1 cells grown in either FBS- or CSS-containing medium. Each point on the graph represents mean ± S.D. of three independent readings. (B) Cell cycle analysis by flow cytometry in PI-stained, ethanol-fixed PC-346C cells demonstrating that treatment for 48 h with GCP and genistein undergo G2/M arrest while cells treated with daidzein do not. Note that the combination of daidzein (10 μg/ml) and genistein (10 μg/ml) is equivalent in effect to 100 μg/ml GCP, whereas the combination of daidzein (20 μg/ml) and genistein (20 μg/ml) is equivalent in effect to 200 μg/ml GCP. (C) Western blots demonstrating that 48-h treatment with genistein and GCP, but not daidzein, increases expression of the 90 kDa FlnA fragment in C4-2 cells. An antibody to the C-terminal end of FlnA, which recognizes the 280, 110, and 90 kDa bands, was used in this study. (D) To ensure that the cell lines we used (other than CWR22Rv1 and CWR22R1) do not carry murine retroviruses, we used a Gag antibody (Paprotka *et al.* 2011) that detects all murine retroviral gag proteins, thus offering a highly sensitive way of detecting viral infection. The cell lysates from the five cell lines were western blotted with Gag and β-actin antibodies. As expected, CWR22Rv1 and R1 express murine retroviral gag proteins, whereas others do not.

fragment (Fig. 4C). Therefore, both genistein and daidzein are needed to replicate the effects of GCP.

Castration-sensitive LNCaP cells exhibited greater sensitivity to GCP + ADT compared with CRPC C4-2 cells

LNCaP cells retain the ability to convert testosterone in FBS to effective levels of DHT, a stronger ligand for AR, whereas they are unable to do so in CSS. Culture in CSS induced 55% reduction in LNCaP cell growth ($P = 0.0014$) compared with culture in FBS. GCP treatment in FBS also reduced growth by 51% compared with vehicle ($P = 0.0006$); however, the combination of ADT and GCP decreased growth by 87% ($P = 0.0002$; Fig. 5A), demonstrating greater efficacy of GCP in lower levels of androgens. Flow cytometry showed that GCP induced G2 arrest in LNCaP cells in FBS, whereas in CSS, GCP also depleted cells in S-phase (Fig. 5B). Western blotting of lysates collected from GCP- and vehicle-treated cells in FBS and CSS showed that GCP treatment decreased cyclin D1 levels, completely suppressed cyclin A levels, but increased cyclin B levels, thereby supporting a G2 arrest (Fig. 5C). Further, GCP induced cleavage of PARP, especially in the presence of CSS, indicating the induction of apoptosis (Fig. 5C). Western blotting showed that GCP promoted the expression of the 90 kDa fragment of FlnA in LNCaP cells as well, both in FBS and in CSS, similar to our observation in CWR22Rv1 (Fig. 5C).

C4-2 cells do not express inherent levels of the 90 kDa fragment, yet GCP induced expression of the 90 kDa fragment in these cells as well (Fig. 5D). Culture in CSS did not affect the ability of these cells to grow, despite the addition of 100 μg/ml GCP (not shown), likely due to aberrant DHT production in C4-2 cells even from castrate levels of testosterone (Cai *et al.* 2011). In contrast, bicalutamide,

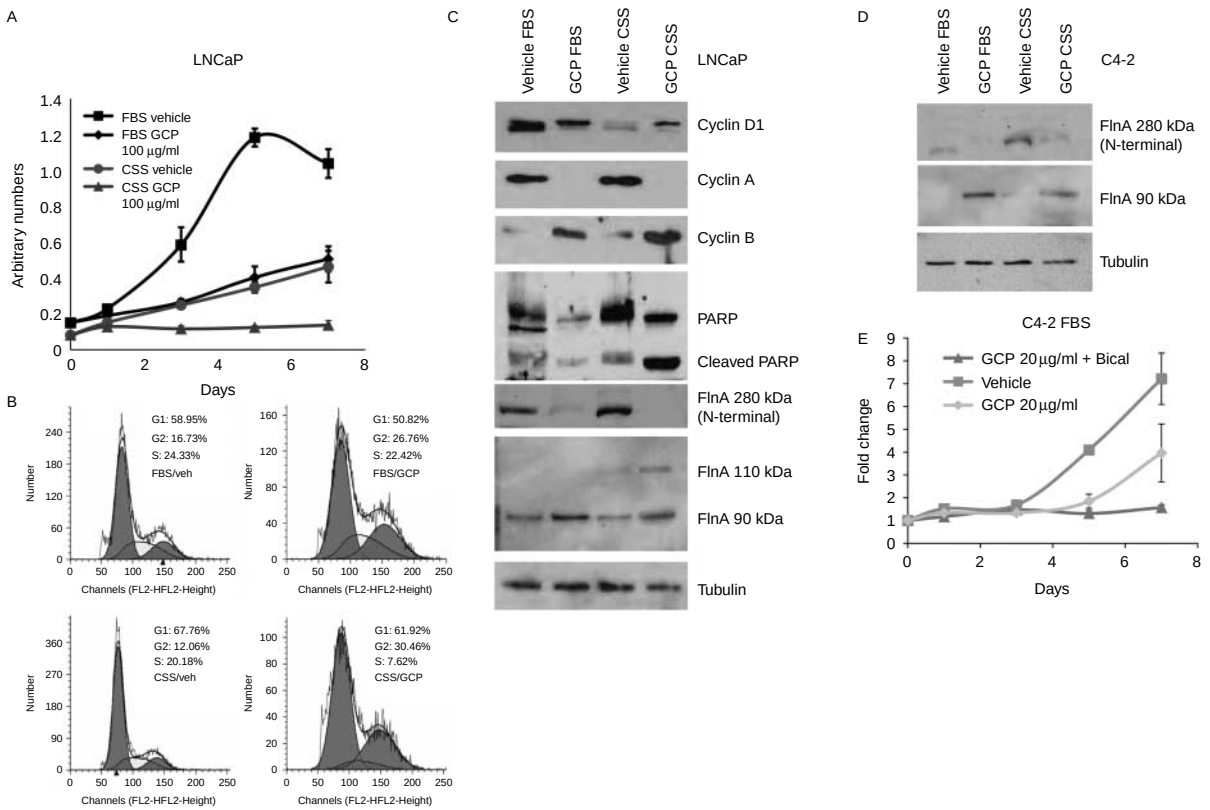

Figure 5 GCP treatment sensitized castration-sensitive LNCaP cells to androgen withdrawal induced apoptosis by increasing levels of 90 kDa FlnA. (A) MTT assay in LNCaP cells showing that GCP reduced cell numbers in low-androgen media. Cells were plated in medium containing either FBS (high androgen) or CSS (low androgen) in the presence of vehicle (50% DMSO and 50% ethanol) or 100 μg/ml GCP for up to 7 days. Each point on the graph represents mean ± S.D. of three independent readings. (B) Cell cycle analysis by flow cytometry in propidium iodide (PI)-stained ethanol-fixed cells demonstrating that 100 μg/ml GCP induced cell cycle arrest in LNCaP cells cultured for 48 h in medium with CSS, but not FBS. In the presence of FBS, GCP induced an increase in cells in G2, only, while in CSS additionally, there was a lack of cells in S-phase. (C and D) Immunoblots to determine levels of various proteins in (C) LNCaP and (D) C4-2 cells cultured in FBS vs CSS in vehicle or 100 μg/ml GCP for 48 h. Note that an antibody to the N-terminal end of FlnA was used to determine the 280 kDa band while an antibody to the C-terminal end of FlnA was used to determine the 110 and 90 kDa bands. (E) MTT assay showing growth arrest in C4-2 cells treated with 10 μM bicalutamide and 20 μg/ml GCP despite the continued growth in GCP alone. Each point on the graph represents mean ± S.D. of three independent readings.

a competitive inhibitor of AR ligand binding, induced growth arrest even in the presence of 20 μg/ml GCP in C4-2 cells (Fig. 5E). The differential effects in FBS and CSS in LNCaP cells, and CSS vs bicalutamide in C4-2, indicate that GCP is ineffective in the presence of ligands, but in the absence of ligands (with bicalutamide) is able to overcome castrate-resistant AR activation.

Androgen deprivation phosphorylates FlnA and prevents its cleavage to the 90 kDa fragment

Next, we investigated the molecular mechanism of the process by which GCP sensitized CaP cells to ADT. Prolonged culture in CSS reduced the levels of 90 kDa FlnA (Fig. 6A), whereas supplementation of cells in CSS with 1 nM DHT restored its levels (Fig. 6B). These results indicated that cleavage of full-length FlnA to the 90 kDa fragment is androgen regulated, consistent with the increase in 280 kDa FlnA with CSS seen in Figs 3D and 5C, D. This increase was not related to transcriptional control; levels of FlnA mRNA were decreased by AR siRNA, but not control siRNA (Fig. 6C), implicating the increase in 280 kDa FlnA levels to posttranscriptional modifications. Interestingly, FlnA levels decreased both from the nucleoplasm and the cytoplasm when LNCaP cells were cultured in CSS for prolonged periods (Fig. 6D), but in the nucleolus remained unchanged. Further studies are required to explain how nucleolar FlnA is protected.

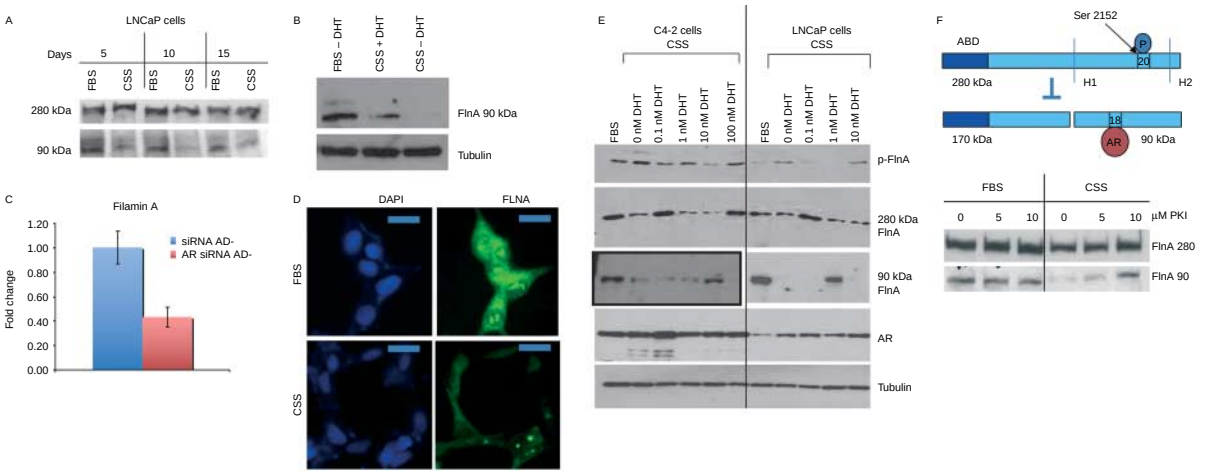

Figure 6 ADT prevents Filamin A cleavage to the 90 kDa fragment and phosphorylates FlnA at Ser 2152. (A) LNCaP cells were cultured for up to 15 days in FBS- or CSS-containing medium, and the levels of 90 and 280 kDa FlnA were determined by western blotting. (B) Western blot showing decreased expression of the 90 kDa FlnA fragment in LNCaP cells in CSS vs FBS, whereas its levels were restored by the addition of 1 nM DHT. (C) FlnA expression in CWR22Rv1 cells is regulated by the AR. AR siRNA decreased FlnA mRNA expression by ~60% as determined by qPCR in medium with CSS (AD-). (D) LNCaP cells were grown in either FBS or CSS containing medium, and FlnA protein expression was determined by immunofluorescence. Scale bar: 10 μm. Note that cells grown in FBS-containing medium show higher expression of FlnA compared with cells grown in CSS-containing medium. (E) LNCaP and C4-2 cells were cultured in FBS or CSS with increasing levels of DHT as indicated for 48 h. Western blots demonstrate the levels of expression of various proteins. Note that C4-2 cells actually have much lower levels of FlnA 90 kDa; therefore, the blot shown here for C4-2 was at a higher exposure. (F) (Upper) Scheme showing FlnA cleavage at H1 is regulated by phosphorylation at Ser 2152. When FlnA is phosphorylated, it does not undergo cleavage and remains in the cytoplasm, whereas upon dephosphorylation, FlnA is cleaved to the 90 kDa fragment, which translocates to the nucleus. (Lower) LNCaP cells were cultured in FBS or CSS with increasing levels of the PKA inhibitor PKI 14–22 (PKI) for 48 h. Western blotting demonstrated that culture in CSS depleted levels of the 90 kDa FlnA, but treatment with increasing doses of PKA inhibitor in CSS-containing medium restored its expression.

C4-2 cells expressed higher levels of FlnA phosphorylation at Ser 2152 compared with LNCaP (Fig. 6E). In both cell lines, culture in CSS stimulated FlnA phosphorylation, but treatment with low doses, but not high doses, of DHT prevented ADT-induced FlnA phosphorylation (Fig. 6E). These results are consistent with the observation that low doses of DHT stimulate whereas high doses inhibit cell growth (Hofman *et al*. 2001). Loss of 90 kDa FlnA coincided with an increase in FlnA phosphorylation or with an increase in 280 kDa FlnA, indicating that the level of 90 kDa FlnA results from cleavage of the 280 kDa form or is negatively regulated by FlnA phosphorylation. As a result, FlnA cleavage to the 90 kDa fragment was also regulated by androgens (Fig. 6E).

Additionally, we verified that FlnA phosphorylation regulates its cleavage, using a regulator of protein kinase A (PKA), known to phosphorylate FlnA (Jay *et al*. 2000, 2004). As we previously showed that a PKA inhibitor increased FlnA cleavage and nuclear translocation (Bedolla *et al*. 2009), we treated LNCaP cells cultured in FBS or CSS with increasing concentrations of the PKA inhibitor 14–22 (PKI). Significantly, the PKI had no effect in FBS, but in CSS medium, loss of expression of the 90 kDa fragment was prevented by treatment with the PKI (Fig. 6F). Taken together, the above data demonstrate that ADT suppresses cleavage to 90 kDa FlnA by enhancing phosphorylation at Ser 2152.

GCP dephosphorylates FlnA at Ser 2152 and promotes the formation of the 90 kDa fragment and FlnA nuclear localization

In support of data showing that ADT prevents FlnA cleavage to the 90 kDa fragment, 48 h treatment with bicalutamide depleted CWR22Rv1 cells of the 90 kDa FlnA fragment while the level of full-length FlnA increased. In contrast, GCP increased the levels of 90 kDa FlnA while reducing the levels of the full-length protein (Fig. 7A, upper). Comparison of LNCaP and C4-2 cells with vehicle or GCP showed that GCP treatment in C4-2 cells restored FlnA localization to the nucleus (Fig. 7A, lower). These results prompted us to examine the role of GCP on FlnA phosphorylation.

Androgen-dependent PC-346C and LNCaP cells expressed lower levels of phospho-FlnA compared

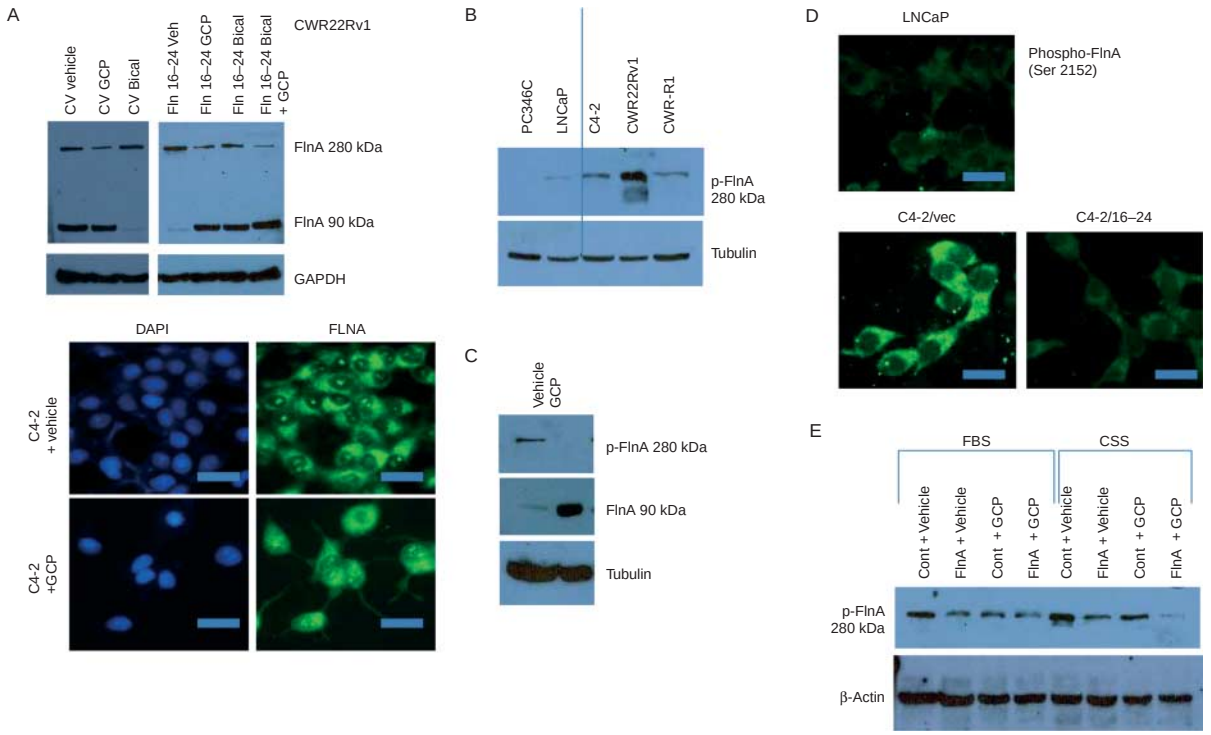

Figure 7 GCP prevents phosphorylation of full-length FlnA and promotes cleavage of FlnA to its 90 kDa fragment. (A) (Upper) Western blot showing expression of FlnA in CWR22Rv1 cells. Treatment with 10 μM bicalutamide depleted levels of 90 kDa FlnA while transfection with FlnA 16–24 and further treatment with 100 μg/ml GCP for 48 h rescued the expression of the 90 kDa FlnA fragment. Note higher exposure of left panel compared with right. (Lower) LNCaP and C4-2 cells treated with vehicle or 100 μg/ml GCP were stained with an antibody specific to the C-terminus FlnA to determine subcellular localization. LNCaP cells and C4-2 cells treated with GCP showed FlnA expression in the nucleus while C4-2 cells treated with vehicle showed expression only in the cytosol. Scale bar: 10 μm. (B) Western blot comparing levels of phosphorylated full-length FlnA (Ser 2152) in various cell lines. (C) Western blot demonstrating that GCP prevented phosphorylation of full-length FlnA and increased expression of 90 kDa FlnA. (D) LNCaP cells and C4-2 cells transfected with vector or FlnA 16–24 were stained with an antibody specific for phosphorylated FlnA (Ser 2152) and FlnA phosphorylation levels determined by immunofluorescence. Scale bar: 10 μm. (E) LNCaP cells were cultured in medium containing either FBS or CSS and treated as indicated. Growth in CSS-containing medium increased the phosphorylation of full-length FlnA while treatment with GCP reduced full-length FlnA phosphorylation.

with the CRPC lines C4-2, CWR22Rv1, and CWR-R1 (Fig. 7B). Hence, we investigated the effect of GCP in CRPC cells. GCP treatment of C4-2 cells prevented FlnA phosphorylation and cleaved the protein to the 90 kDa fragment (Fig. 7C). In support, by immunofluorescence, C4-2 cells expressed higher levels of phospho-FlnA (Ser 2152) compared with LNCaP (Fig. 7D). Incidentally, phosphorylated FlnA was localized in the cytoplasm, showing that FlnA phosphorylation prevented its nuclear translocation. Transfection with FlnA 16–24 in C4-2 cells prevented its phosphorylation, in support for a role of its effector GCP in suppressing FlnA phosphorylation. Culture in CSS increased the levels of FlnA phosphorylation at Ser 2152, which was suppressed by GCP treatment (Fig. 7E). These results show that GCP sensitizes CaP cells to ADT by preventing ADT-induced FlnA phosphorylation.

GCP treatment prevented relapse in the CWR22 xenograft mouse model following ADT

As GCP sensitized CaP cells to ADT, we investigated whether it impeded development of CRPC following ADT. Athymic nu/nu mice were s.c. implanted with CWR22 tumor extracts. When the tumors were palpable, mice were treated with GCP or vehicle as described in the Materials and methods section. Following 2 weeks of treatment, the animals underwent sham operation or were castrated; initial tumors from each group were collected 3 days post-surgery and showed strong Ki67 staining, indicative of proliferation, in sham-operated but not in castrated animals (Fig. 8A). Sham-operated, untreated tumors showed strong nuclear localization of FlnA, while castrated tumors, either untreated or treated with vehicle only, showed weak cytoplasmic, but no nuclear staining for FlnA (Fig. 8B). In contrast, castrated,

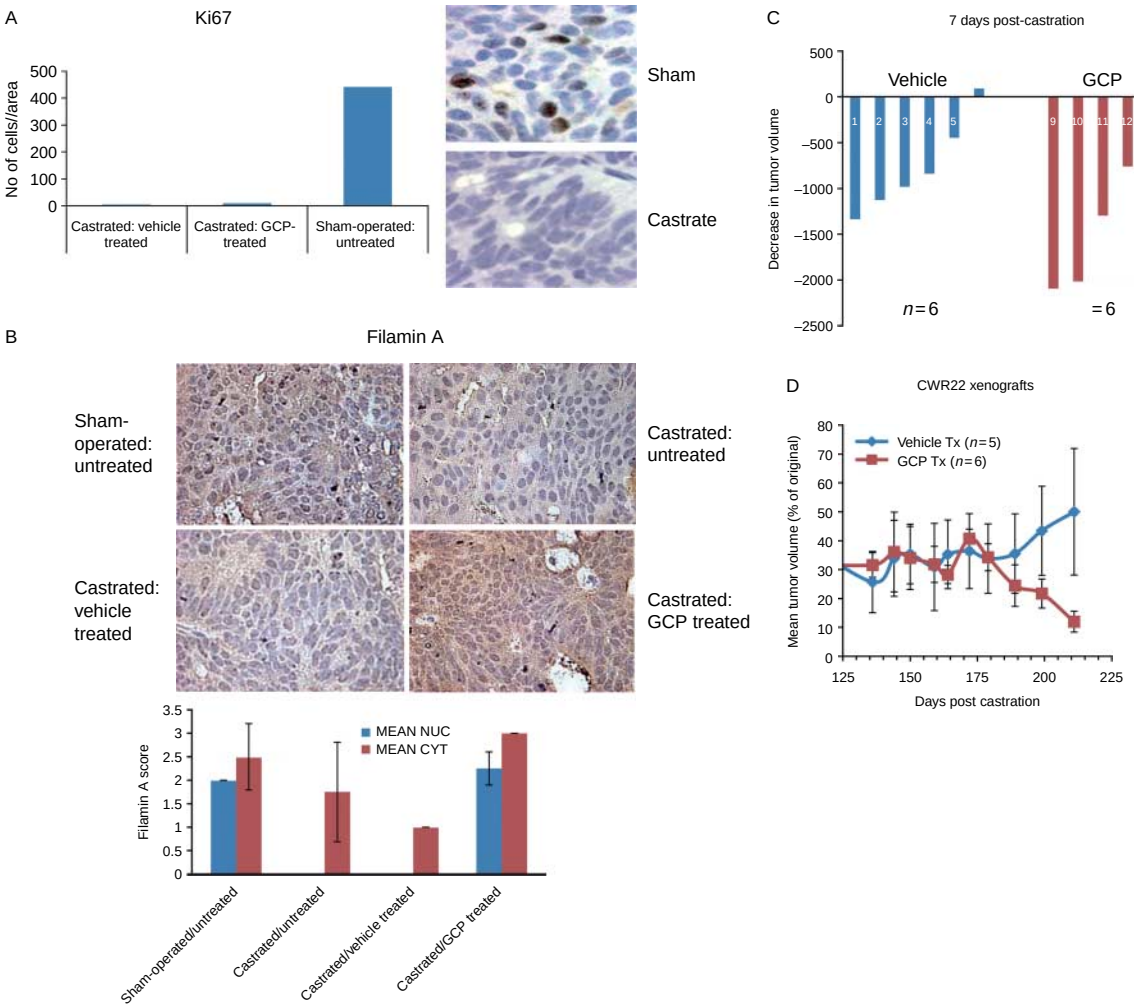

Figure 8 GCP treatment prevented relapse in the CWR22 xenograft mouse model. (A) The tumors were paraffin-embedded, sectioned, and stained with anti-Ki67 antibody to determine the effect of GCP and castration on proliferation. Note that tumors in sham-operated animals were positive for Ki67 staining whereas those that were castrated, either in the presence or in the absence of GCP lacked this staining. Tumors were collected 3 days after the operation. (B) FlnA and AR staining (brown) in tumors from animals who were i) sham operated, untreated, ii) castrated, untreated, iii) castrated, vehicle treated, and iv) castrated, GCP-treated. Note high FlnA staining in the latter group. (C) Both vehicle- and GCP-treated tumors rapidly underwent tumor regression within 7 days following castration. Waterfall plot showing tumor regression in the animals 7 days post-castration. Note that GCP-treated tumors underwent greater levels of regression compared with those in vehicle-fed mice. Red circle denotes one tumor that did not undergo significant change in volume. (D) After the initial regression (up to ~35 days), tumor volume remained essentially steady until 179 days post-castration after which GCP-treated tumors continued to regress while vehicle-treated tumors began to recover and were distinctly larger than the tumors in GCP-treated mice after 211 days.

GCP-treated tumors exhibited strong FlnA staining (brown) both in the nucleus and in the cytoplasm (Fig. 8B). Within the first 7 days following castration, the tumors in GCP-treated mice regressed (mean reduction 1148 mm^3, $n=6$) compared with vehicle-treated mice (mean reduction 772 mm^3, $n=6$) (Fig. 8C). The animals were monitored for up to 7 months (211 days) following castration. During this time, control CWR22 xenografts regressed approximately 38 days post-castration (mean reduction 40%, $P=0.0008$; $n=6$), after which the tumors stabilized for several months and then relapsed after 6 months post-castration (179 days, relapse was defined as two or more consecutive increases in tumor volume $>5\%$ each time) (one control animal had to be killed due to large tumor size). There was essentially no significant difference between the control ($n=5$) and GCP ($n=6$) groups until 6 months post-castration, after which, tumors in vehicle-treated mice remained steady relapsed ($P>0.05$), whereas GCP-treated tumors continued to regress ($P=0.0056$) (Fig. 8D). After 211 days (7 months post-castration), tumors in

vehicle-treated mice were distinctly larger (mean reduction 50% compared with initial tumor volumes; $P=0.25$) than the ones in GCP-treated mice (mean reduction 88% compared with initial volumes; $P=0.002$) (Fig. 8D). Taken together, these results indicated that GCP treatment prolonged the effects of castration (ADT) in this model.

Discussion

CaP patients with metastases, treated with ADT, frequently relapse, leading to CRPC, which essentially remains incurable. Studies found that although proliferation indices were consistently suppressed following ADT (Westin *et al*. 1995, Matsushima *et al*. 1999), apoptosis was only partially affected (Murphy *et al*. 1991, Westin *et al*. 1995). Surviving cells likely undergo growth arrest and lie dormant following ADT, but revive when androgen-independent stimulants release them from growth arrest (Agus *et al*. 1999, 2002). Hence, our goal was to develop treatments that promote apoptosis during ADT in CaP cells. Here, we show that proteolysis of FlnA to the 90 kDa fragment and its subsequent nuclear localization induces apoptosis and sensitizes AR-positive CaP cells to ADT.

Full-length FlnA is a well-known mediator of cell migration (Feng & Walsh 2004). FlnA proteolysis has two effects: i) it prevents cell migration mediated by full-length FlnA scaffolding interaction between actin on its N-terminal end and actin-binding proteins on its C-terminal end (Bedolla *et al*. 2009) and ii) the C-terminal FlnA in the nucleus suppresses AR activity (Loy *et al*. 2003). FlnA had no effect in AR-negative PC-3 cells but inhibited growth of not only LNCaP and C4-2 cells that express a full-length AR with a mutation in its LBD (T877A) but also CWR22Rv1 and CWR-R1 cells that express both full-length and a truncated AR lacking the LBD (Chen *et al*. 2010*a*,*b*). Hence, FlnA is a likely target that may serve to regulate the ability of CaP cells to respond to androgens, and the objective of these studies was to identify clinically safe pharmaceutical agents that regulate FlnA proteolysis.

We previously showed that FlnA cleavage to the 90 kDa fragment and subsequent nuclear translocation suppresses migration (Bedolla *et al*. 2009). The repeat structure of FlnA allows it to act as scaffold regulating co-localization of various cell migration regulators such as integrins (Ott *et al*. 1998, D'Addario *et al*. 2002, Robertson *et al*. 2003, Travis *et al*. 2004) and migfilin (Das *et al*. 2011). Various studies have reported that FlnA promotes cell migration (Nagano *et al*. 2002, Gawecka *et al*. 2010), whereas others show that it suppresses migration (Xu *et al*. 2010). It is likely that the differential effect is caused by a relative expression of intact vs cleaved FlnA. Surprisingly, a recent study indicated the presence of FlnA in the nucleolus where it inhibits rRNA production (Deng *et al*. 2012). FlnA expresses a nucleolar localization signal, and the C-terminal end of the molecule (FlnA 16–24) is needed to inhibit rRNA proteins (Deng *et al*. 2012). Our results reveal that despite the decrease in cytoplasmic and nuclear levels of FlnA with ADT, the expression of nucleolar FlnA remains unchanged, indicating that it is protected from degradation. It is important to note that nucleolar FlnA is not phosphorylated (Fig. 7D), hence reflects the cleaved product as well. Further studies are required to determine whether nucleolar FlnA plays a role in AR signaling.

The data presented show that the AR affects both FlnA levels and proteolysis. Androgens promote FlnA cleavage to the 90 kDa fragment; thus, ADT prevents FlnA cleavage and FlnA nuclear (but not nucleolar) localization. Androgens had a biphasic effect on FlnA expression and cleavage. At low androgen levels, there was very little FlnA cleavage whereas at physiological levels of DHT, FlnA cleavage was resumed, likely caused by decreased FlnA phosphorylation (Ohta & Hartwig 1995). However, at very high levels (100 nM DHT), FlnA was again phosphorylated. Therefore, FlnA is likely cleaved and as a result remains in the nucleus only at physiological levels of androgens and is dispersed when these levels are too high or too low. Loss of 90 kDa FlnA may be one cause for resistance to ADT in advanced CaP.

Interestingly, GCP-induced FlnA dephosphorylation promoted FlnA cleavage and nuclear localization. AR levels regulate FlnA expression, phosphorylation, cleavage, and nuclear localization, while FlnA in turn regulates AR transcriptional activity; hence, it is not surprising that the interaction between these factors play a role in the efficacy of ADT. We show that both genistein and daidzein are needed for effective regulation – neither component of GCP, by itself, could achieve this effect. Therefore, GCP-induced G2 arrest is mediated by genistein, while in CSS (but not in FBS), daidzein induced G1 arrest, explaining why GCP caused androgen responsiveness. Other studies had noted combination effects of genistein and daidzein that may contribute to other effects of GCP noted by us. While multiple reports noted that genistein inhibits metastasis in most cancers (Pavese *et al*. 2010, Zhang *et al*. 2010), including CaP (Lakshman *et al*. 2008), some reports noted that genistein promoted metastasis (Nakamura *et al*. 2011). Daidzein appears to

prevent genistein-induced metastasis in some models (Singh-Gupta *et al*. 2010), but not in others (Martinez-Montemayor *et al*. 2010). Our data indicate that the effect of dietary isoflavones on tumor promotion and metastasis may be related to the ability of the isoflavones to induce FlnA proteolysis.

The kinase mediating FlnA phosphorylation has not yet been identified. The Ser 2152 site on FlnA is a substrate for $p90^{RSK}$ (Woo *et al*. 2004), PKA (Jay *et al*. 2000, 2004), and PKCα (Tigges *et al*. 2003), which are likely candidates. We previously showed that ADT causes the upregulation of ErbB3, a member of the EGFR family (Chen *et al*. 2010*c*, 2011). This family stimulates not only PI3K but also the MAPK family, including JNK, which in turn activates $p90^{RSK}$ (Zhang *et al*. 2001). On the other hand, $p90^{RSK}$ is inhibited by genistein (Gwin *et al*. 2011) and by daidzein (Kang *et al*. 2007). Genistein also inhibits EGFR (Aggarwal & Shishodia 2006) and mTOR (Anastasius *et al*. 2009) and members of our group had demonstrated earlier that mTOR is one of the primary targets of GCP (Tepper *et al*. 2007). Previous studies have indicated that MAPK regulates mTOR activity via RSK (Roux *et al*. 2007, Carriere *et al*. 2008), which may indicate a prominent role for this kinase in GCP-mediated FlnA proteolysis.

Several lines of evidence indicate that GCP-induced FlnA cleavage prevents ligand-independent AR transcriptional activity. First of all, GCP inhibited growth of androgen-dependent LNCaP cells in CSS but had no effect on C4-2 cells in CSS, whereas in the presence of bicalutamide, GCP induced growth arrest in C4-2 cells. Upon ligand binding, the AR undergoes a conformational change that allows it to enter the nucleus and induce transcriptional activity (Kuil *et al*. 1995). In some CRPC cells, the AR can be activated by nonspecific ligands that allow the cells to propagate in CSS and also by ligand-independent AR conformational change, which induces resistance to antiandrogens such as bicalutamide (Feldman & Feldman 2001). Hence, GCP was able to prevent ligand-independent AR activity and overcome the effects of bicalutamide but was ineffective when aberrant ligands activated the AR. Second, GCP and FlnA 16–24 induced growth arrest in CWR22Rv1 cells expressing a truncated AR lacking the LBD. Our data indicate that this effect can be prevented by the presence of nuclear FlnA, but further studies are needed to elucidate the mechanism by which FlnA promotes this effect. In this respect, FlnA is distinct from other AR co-repressors such as NCoR and SMRT and likely explains results showing the inability of the latter to inhibit AR activity in CRPC lines (Laschak *et al*. 2011).

Finally, we show that in the CWR22 androgen-dependent xenograft model, relapsed tumors following castration were observed in vehicle-treated but not GCP-treated mice, although both tumors regressed at similar rates. This was accompanied by induction of FlnA in GCP. Our current and previous results (Wang *et al*. 2007) reveal that nuclear localization of the 90 kDa FlnA fragment sensitizes CaP cells to the effects of ADT. These results indicate that due to increased nuclear FlnA, co-administration of GCP together with ADT may be an important therapeutic strategy to prevent CRPC development.

Declaration of interest

The authors declare that there is no conflict of interest that could be perceived as prejudicing the impartiality of the research reported.

Funding

This work was supported by a Biomedical Laboratory Research and Development (BLRD) service Merit Award (I01BX000400) from the Department of Veterans Affairs and by R01CA133209 from the National Cancer Institute.

Acknowledgements

The authors wish to thank Christopher B Wee and Honglin Chen for their expert technical assistance in mouse xenograft and qPCR studies respectively. They also thank Dr E W Yong, National University of Singapore, Singapore, for pCMV-FlnA, FlnA(16–24), and FlnA(1–15). Human PSA-luciferase construct (hPSA-luc) was kindly provided by Dr XuBao Shi, University of California Davis, Dept of Urology. CWR-R1 cells were provided by Dr Elizabeth Wilson (University of North Carolina) while PC-346C cells were obtained from Dr W M van Weerden, Josephine Nefkens Institute. Casodex (bicalutamide) was kindly provided by AstraZeneca, Cheshire, UK, while GCP was generously provided by Amino Up, Shin-ei, Kiyota, Sapporo, Japan. The work reported here does not represent the views or opinions of the Department of Veteran Affairs or the United States Government.

References

Aggarwal BB & Shishodia S 2006 Molecular targets of dietary agents for prevention and therapy of cancer. *Biochemical Pharmacology* **71** 1397–1421. (doi:10.1016/j.bcp.2006.02.009)

Agus DB, Cordon-Cardo C, Fox W, Drobnjak M, Koff A, Golde DW & Scher HI 1999 Prostate cancer cell cycle regulators: response to androgen withdrawal and

development of androgen independence. *Journal of the National Cancer Institute* **91** 1869–1876. (doi:10.1093/jnci/91.21.1869)

Agus DB, Akita RW, Fox WD, Lewis GD, Higgins B, Pisacane PI, Lofgren JA, Tindell C, Evans DP, Maiese K *et al.* 2002 Targeting ligand-activated ErbB2 signaling inhibits breast and prostate tumor growth. *Cancer Cell* **2** 127–137. (doi:10.1016/S1535-6108(02)00097-1)

Anastasius N, Boston S, Lacey M, Storing N & Whitehead SA 2009 Evidence that low-dose, long-term genistein treatment inhibits oestradiol-stimulated growth in MCF-7 cells by down-regulation of the PI3-kinase/Akt signalling pathway. *Journal of Steroid Biochemistry and Molecular Biology* **116** 50–55. (doi:10.1016/j.jsbmb.2009.04.009)

Bedolla RG, Wang Y, Asuncion A, Chamie K, Siddiqui S, Mudryj MM, Prihoda TJ, Siddiqui J, Chinnaiyan AM, Mehra R *et al.* 2009 Nuclear versus cytoplasmic localization of filamin A in prostate cancer: immunohistochemical correlation with metastases. *Clinical Cancer Research* **15** 788–796. (doi:10.1158/1078-0432.CCR-08-1402)

Bemis DL, Capodice JL, Desai M, Buttyan R & Katz AE 2004 A concentrated aglycone isoflavone preparation (GCP) that demonstrates potent anti-prostate cancer activity *in vitro* and *in vivo*. *Clinical Cancer Research* **10** 5282–5292. (doi:10.1158/1078-0432.CCR-03-0828)

Burich RA, Holland WS, Vinall RL, Tepper C, White RW & Mack PC 2008 Genistein combined polysaccharide enhances activity of docetaxel, bicalutamide and Src kinase inhibition in androgen-dependent and independent prostate cancer cell lines. *BJU International* **102** 1458–1466. (doi:10.1111/j.1464-410X.2008.07826.x)

Cai C, Chen S, Ng P, Bubley GJ, Nelson PS, Mostaghel EA, Marck B, Matsumoto AM, Simon NI, Wang H *et al.* 2011 Intratumoral *de novo* steroid synthesis activates androgen receptor in castration-resistant prostate cancer and is upregulated by treatment with CYP17A1 inhibitors. *Cancer Research* **71** 6503–6513. (doi:10.1158/0008-5472.CAN-11-0532)

Carriere A, Cargnello M, Julien LA, Gao H, Bonneil E, Thibault P & Roux PP 2008 Oncogenic MAPK signaling stimulates mTORC1 activity by promoting RSK-mediated raptor phosphorylation. *Current Biology* **18** 1269–1277. (doi:10.1016/j.cub.2008.07.078)

Catalona WJ 1994 Management of cancer of the prostate. *New England Journal of Medicine* **331** 996–1004. (doi:10.1056/NEJM199410133311507)

Chen H, Libertini SJ, George M, Dandekar S, Tepper CG, Al-Bataina B, Kung HJ, Ghosh PM & Mudryj M 2010*a* Genome-wide analysis of androgen receptor binding and gene regulation in two CWR22-derived prostate cancer cell lines. *Endocrine-Related Cancer* **17** 857–873. (doi:10.1677/ERC-10-0081)

Chen H, Libertini SJ, Wang Y, Kung HJ, Ghosh P & Mudryj M 2010*b* ERK regulates calpain 2-induced androgen receptor proteolysis in CWR22 relapsed prostate tumor cell lines. *Journal of Biological Chemistry* **285** 2368–2374. (doi:10.1074/jbc.M109.049379)

Chen L, Siddiqui S, Bose S, Mooso B, Asuncion A, Bedolla RG, Vinall R, Tepper CG, Gandour-Edwards R, Shi X *et al.* 2010*c* Nrdp1-mediated regulation of ErbB3 expression by the androgen receptor in androgen-dependent but not castrate-resistant prostate cancer cells. *Cancer Research* **70** 5994–6003. (doi:10.1158/0008-5472.CAN-09-4440)

Chen L, Mooso BA, Jathal MK, Madhav A, Johnson SD, van Spyk E, Mikhailova M, Zierenberg-Ripoll A, Xue L, Vinall RL *et al.* 2011 Dual EGFR/HER2 inhibition sensitizes prostate cancer cells to androgen withdrawal by suppressing ErbB3. *Clinical Cancer Research* **17** 6218–6228. (doi:10.1158/1078-0432.CCR-11-1548)

D'Addario M, Arora PD, Ellen RP & McCulloch CA 2002 Interaction of p38 and Sp1 in a mechanical force-induced, β 1 integrin-mediated transcriptional circuit that regulates the actin-binding protein filamin-A. *Journal of Biological Chemistry* **277** 47541–47550. (doi:10.1074/jbc.M207681200)

Das M, Ithychanda SS, Qin J & Plow EF 2011 Migfilin and filamin as regulators of integrin activation in endothelial cells and neutrophils. *PLoS ONE* **6** e26355. (doi:10.1371/journal.pone.0026355)

Deng W, Lopez-Camacho C, Tang JY, Mendoza-Villanueva D, Maya-Mendoza A, Jackson DA & Shore P 2012 Cytoskeletal protein filamin A is a nucleolar protein that suppresses ribosomal RNA gene transcription. *PNAS* **109** 1524–1529. (doi:10.1073/pnas.1107879109)

Feldman BJ & Feldman D 2001 The development of androgen-independent prostate cancer. *Nature Reviews. Cancer* **1** 34–45. (doi:10.1038/35094009)

Feng Y & Walsh CA 2004 The many faces of filamin: a versatile molecular scaffold for cell motility and signalling. *Nature Cell Biology* **6** 1034–1038. (doi:10.1038/ncb1104-1034)

van der Flier A & Sonnenberg A 2001 Structural and functional aspects of filamins. *Biochimica et Biophysica Acta* **1538** 99–117. (doi:10.1016/S0167-4889(01)00072-6)

Gawecka JE, Griffiths GS, Ek-Rylander B, Ramos JW & Matter ML 2010 R-Ras regulates migration through an interaction with filamin A in melanoma cells. *PLoS ONE* **5** e11269. (doi:10.1371/journal.pone.0011269)

Ghafar MA, Golliday E, Bingham J, Mansukhani MM, Anastasiadis AG & Katz AE 2002 Regression of prostate cancer following administration of genistein combined polysaccharide (GCP), a nutritional supplement: a case report. *Journal of Alternative and Complementary Medicine* **8** 493–497. (doi:10.1089/107555302760253694)

Ghosh PM, Malik SN, Bedolla RG, Wang Y, Mikhailova M, Prihoda TJ, Troyer DA & Kreisberg JI 2005 Signal transduction pathways in androgen-dependent and -independent prostate cancer cell proliferation. *Endocrine-Related Cancer* **12** 119–134. (doi:10.1677/erc.1.00835)

Gorlin JB, Yamin R, Egan S, Stewart M, Stossel TP, Kwiatkowski DJ & Hartwig JH 1990 Human endothelial actin-binding protein (ABP-280, nonmuscle filamin): a molecular leaf spring. *Journal of Cell Biology* **111** 1089–1105. (doi:10.1083/jcb.111.3.1089)

Gwin J, Drews N, Ali S, Stamschror J, Sorenson M & Rajah TT 2011 Effect of genistein on p90RSK phosphorylation and cell proliferation in T47D breast cancer cells. *Anticancer Research* **31** 209–214.

Han H, Zhong C, Zhang X, Liu R, Pan M, Tan L, Li Y, Wu J, Zhu Y & Huang W 2010 Genistein induces growth inhibition and G2/M arrest in nasopharyngeal carcinoma cells. *Nutrition and Cancer* **62** 641–647. (doi:10.1080/01635581003605490)

Hofman K, Swinnen JV, Verhoeven G & Heyns W 2001 E2F activity is biphasically regulated by androgens in LNCaP cells. *Biochemical and Biophysical Research Communications* **283** 97–101. (doi:10.1006/bbrc.2001.4738)

Jay D, Garcia EJ, Lara JE, Medina MA & de la Luz Ibarra M 2000 Determination of a cAMP-dependent protein kinase phosphorylation site in the C-terminal region of human endothelial actin-binding protein. *Archives of Biochemistry and Biophysics* **377** 80–84. (doi:10.1006/abbi.2000.1762)

Jay D, Garcia EJ & de la Luz Ibarra M 2004 *In situ* determination of a PKA phosphorylation site in the C-terminal region of filamin. *Molecular and Cellular Biochemistry* **260** 49–53. (doi:10.1023/B:MCBI.0000026052.76418.55)

Kang NJ, Lee KW, Rogozin EA, Cho YY, Heo YS, Bode AM, Lee HJ & Dong Z 2007 Equol, a metabolite of the soybean isoflavone daidzein, inhibits neoplastic cell transformation by targeting the MEK/ERK/p90RSK/activator protein-1 pathway. *Journal of Biological Chemistry* **282** 32856–32866. (doi:10.1074/jbc.M701459200)

Kuil CW, Berrevoets CA & Mulder E 1995 Ligand-induced conformational alterations of the androgen receptor analyzed by limited trypsinization. Studies on the mechanism of antiandrogen action. *Journal of Biological Chemistry* **270** 27569–27576. (doi:10.1074/jbc.270.46.27569)

Lakshman M, Xu L, Ananthanarayanan V, Cooper J, Takimoto CH, Helenowski I, Pelling JC & Bergan RC 2008 Dietary genistein inhibits metastasis of human prostate cancer in mice. *Cancer Research* **68** 2024–2032. (doi:10.1158/0008-5472.CAN-07-1246)

Laschak M, Bechtel M, Spindler KD & Hessenauer A 2011 Inability of NCoR/SMRT to repress androgen receptor transcriptional activity in prostate cancer cell lines. *International Journal of Molecular Medicine* **28** 645–651. (doi:10.3892/ijmm.2011.735)

Lian F, Bhuiyan M, Li YW, Wall N, Kraut M & Sarkar FH 1998 Genistein-induced G2-M arrest, p21WAF1 upregulation, and apoptosis in a non-small-cell lung cancer cell line. *Nutrition and Cancer* **31** 184–191. (doi:10.1080/01635589809514701)

Limpens J, Schroder FH, de Ridder CM, Bolder CA, Wildhagen MF, Obermuller-Jevic UC, Kramer K & van Weerden WM 2006 Combined lycopene and vitamin E treatment suppresses the growth of PC-346C human prostate cancer cells in nude mice. *Journal of Nutrition* **136** 1287–1293.

Loy CJ, Sim KS & Yong EL 2003 Filamin-A fragment localizes to the nucleus to regulate androgen receptor and coactivator functions. *PNAS* **100** 4562–4567. (doi:10.1073/pnas.0736237100)

Martinez-Montemayor MM, Otero-Franqui E, Martinez J, De La Mota-Peynado A, Cubano LA & Dharmawardhane S 2010 Individual and combined soy isoflavones exert differential effects on metastatic cancer progression. *Clinical & Experimental Metastasis* **27** 465–480. (doi:10.1007/s10585-010-9336-x)

Masiello D, Cheng S, Bubley GJ, Lu ML & Balk SP 2002 Bicalutamide functions as an androgen receptor antagonist by assembly of a transcriptionally inactive receptor. *Journal of Biological Chemistry* **277** 26321–26326. (doi:10.1074/jbc.M203310200)

Matsushima H, Goto T, Hosaka Y, Kitamura T & Kawabe K 1999 Correlation between proliferation, apoptosis, and angiogenesis in prostate carcinoma and their relation to androgen ablation. *Cancer* **85** 1822–1827. (doi:10.1002/(SICI)1097-0142(19990415)85:8<1822::AID-CNCR24>3.0.CO;2-1)

Murphy WM, Soloway MS & Barrows GH 1991 Pathologic changes associated with androgen deprivation therapy for prostate cancer. *Cancer* **68** 821–828. (doi:10.1002/1097-0142(19910815)68:4<821::AID-CNCR2820680426>3.0.CO;2-S)

Nagano T, Yoneda T, Hatanaka Y, Kubota C, Murakami F & Sato M 2002 Filamin A-interacting protein (FILIP) regulates cortical cell migration out of the ventricular zone. *Nature Cell Biology* **4** 495–501. (doi:10.1038/ncb808)

Nakamura H, Wang Y, Kurita T, Adomat H & Cunha GR 2011 Genistein increases epidermal growth factor receptor signaling and promotes tumor progression in advanced human prostate cancer. *PLoS ONE* **6** e20034. (doi:10.1371/journal.pone.0020034)

Ohta Y & Hartwig JH 1995 Actin filament cross-linking by chicken gizzard filamin is regulated by phosphorylation *in vitro*. *Biochemistry* **34** 6745–6754. (doi:10.1021/bi00020a020)

Ott I, Fischer EG, Miyagi Y, Mueller BM & Ruf W 1998 A role for tissue factor in cell adhesion and migration mediated by interaction with actin-binding protein 280. *Journal of Cell Biology* **140** 1241–1253. (doi:10.1083/jcb.140.5.1241)

Ozanne DM, Brady ME, Cook S, Gaughan L, Neal DE & Robson CN 2000 Androgen receptor nuclear translocation is facilitated by the f-actin cross-linking protein filamin. *Molecular Endocrinology* **14** 1618–1626. (doi:10.1210/me.14.10.1618)

Paprotka T, Delviks-Frankenberry KA, Cingoz O, Martinez A, Kung HJ, Tepper CG, Hu WS, Fivash MJ Jr,

Coffin JM & Pathak VK 2011 Recombinant origin of the retrovirus XMRV. *Science* **333** 97–101. (doi:10.1126/science.1205292)

Pavese JM, Farmer RL & Bergan RC 2010 Inhibition of cancer cell invasion and metastasis by genistein. *Cancer Metastasis Reviews* **29** 465–482. (doi:10.1007/s10555-010-9238-z)

Robertson SP, Twigg SR, Sutherland-Smith AJ, Biancalana V, Gorlin RJ, Horn D, Kenwrick SJ, Kim CA, Morava E, Newbury-Ecob R *et al.* 2003 Localized mutations in the gene encoding the cytoskeletal protein filamin A cause diverse malformations in humans. *Nature Genetics* **33** 487–491. (doi:10.1038/ng1119)

Roux PP, Shahbazian D, Vu H, Holz MK, Cohen MS, Taunton J, Sonenberg N & Blenis J 2007 RAS/ERK signaling promotes site-specific ribosomal protein S6 phosphorylation via RSK and stimulates cap-dependent translation. *Journal of Biological Chemistry* **282** 14056–14064. (doi:10.1074/jbc.M700906200)

Schmidt F, Knobbe CB, Frank B, Wolburg H & Weller M 2008 The topoisomerase II inhibitor, genistein, induces G2/M arrest and apoptosis in human malignant glioma cell lines. *Oncology Reports* **19** 1061–1066.

Sedelaar JP & Isaacs JT 2009 Tissue culture media supplemented with 10% fetal calf serum contains a castrate level of testosterone. *Prostate* **69** 1724–1729. (doi:10.1002/pros.21028)

Sfanos KS, Aloia AL, Hicks JL, Esopi DM, Steranka JP, Shao W, Sanchez-Martinez S, Yegnasubramanian S, Burns KH, Rein A *et al.* 2011 Identification of replication competent murine gammaretroviruses in commonly used prostate cancer cell lines. *PLoS ONE* **6** e20874. (doi:10.1371/journal.pone.0020874)

Singh-Gupta V, Zhang H, Yunker CK, Ahmad Z, Zwier D, Sarkar FH & Hillman GG 2010 Daidzein effect on hormone refractory prostate cancer *in vitro* and *in vivo* compared to genistein and soy extract: potentiation of radiotherapy. *Pharmaceutical Research* **27** 1115–1127. (doi:10.1007/s11095-010-0107-9)

Tepper CG, Boucher DL, Ryan PE, Ma AH, Xia L, Lee LF, Pretlow TG & Kung HJ 2002 Characterization of a novel androgen receptor mutation in a relapsed CWR22 prostate cancer xenograft and cell line. *Cancer Research* **62** 6606–6614.

Tepper CG, Vinall RL, Wee CB, Xue L, Shi XB, Burich R, Mack PC & deVere White RW 2007 GCP-mediated growth inhibition and apoptosis of prostate cancer cells via androgen receptor-dependent and -independent mechanisms. *Prostate* **67** 521–535. (doi:10.1002/pros.20548)

Thalmann GN, Anezinis PE, Chang SM, Zhau HE, Kim EE, Hopwood VL, Pathak S, von Eschenbach AC & Chung LW 1994 Androgen-independent cancer progression and bone metastasis in the LNCaP model of human prostate cancer. *Cancer Research* **54** 2577–2581.

Tigges U, Koch B, Wissing J, Jockusch BM & Ziegler WH 2003 The F-actin cross-linking and focal adhesion protein filamin A is a ligand and *in vivo* substrate for protein kinase C α. *Journal of Biological Chemistry* **278** 23561–23569. (doi:10.1074/jbc.M302302200)

Travis MA, van der Flier A, Kammerer RA, Mould AP, Sonnenberg A & Humphries MJ 2004 Interaction of filamin A with the integrin β 7 cytoplasmic domain: role of alternative splicing and phosphorylation. *FEBS Letters* **569** 185–190. (doi:10.1016/j.febslet.2004.04.099)

Vinall RL, Hwa K, Ghosh P, Pan CX, Lara PN Jr & deVere White RW 2007 Combination treatment of prostate cancer cell lines with bioactive soy isoflavones and perifosine causes increased growth arrest and/or apoptosis. *Clinical Cancer Research* **13** 6204–6216. (doi:10.1158/1078-0432.CCR-07-0600)

Wang Y, Kreisberg JI, Bedolla RG, Mikhailova M, deVere White RW & Ghosh PM 2007 A 90 kDa fragment of filamin A promotes Casodex-induced growth inhibition in Casodex-resistant androgen receptor positive C4-2 prostate cancer cells. *Oncogene* **26** 6061–6070. (doi:10.1038/sj.onc.1210435)

van Weerden WM, de Ridder CM, Verdaasdonk CL, Romijn JC, van der Kwast TH, Schroder FH & van Steenbrugge GJ 1996 Development of seven new human prostate tumor xenograft models and their histopathological characterization. *American Journal of Pathology* **149** 1055–1062.

Westin P, Stattin P, Damber JE & Bergh A 1995 Castration therapy rapidly induces apoptosis in a minority and decreases cell proliferation in a majority of human prostatic tumors. *American Journal of Pathology* **146** 1368–1375.

deVere White RW, Hackman RM, Soares SE, Beckett LA, Li Y & Sun B 2004 Effects of a genistein-rich extract on PSA levels in men with a history of prostate cancer. *Urology* **63** 259–263. (doi:10.1016/j.urology.2003.09.061)

deVere White RW, Tsodikov A, Stapp EC, Soares SE, Fujii H & Hackman RM 2010 Effects of a high dose, aglycone-rich soy extract on prostate-specific antigen and serum isoflavone concentrations in men with localized prostate cancer. *Nutrition and Cancer* **62** 1036–1043. (doi:10.1080/01635581.2010.492085)

Woo MS, Ohta Y, Rabinovitz I, Stossel TP & Blenis J 2004 Ribosomal S6 kinase (RSK) regulates phosphorylation of filamin A on an important regulatory site. *Molecular and Cellular Biology* **24** 3025–3035. (doi:10.1128/MCB.24.7.3025-3035.2004)

Xu Y, Bismar TA, Su J, Xu B, Kristiansen G, Varga Z, Teng L, Ingber DE, Mammoto A, Kumar R *et al.* 2010 Filamin A regulates focal adhesion disassembly and suppresses breast cancer cell migration and invasion. *Journal of Experimental Medicine* **207** 2421–2437. (doi:10.1084/jem.20100433)

Zhang Y, Zhong S, Dong Z, Chen N, Bode AM & Ma W 2001 UVA induces Ser381 phosphorylation of p90RSK/MAPKAP-K1 via ERK and JNK pathways. *Journal of Biological Chemistry* **276** 14572–14580. (doi:10.1074/jbc.M004615200)

Zhang Y, Zhu G, Gu S, Chen X, Hu H & Weng S 2010 Genistein inhibits osteolytic bone metastasis and enhances bone mineral in nude mice. *Environmental Toxicology and Pharmacology* **30** 37–44. (doi:10.1016/j.etap.2010.03.016)

Zhao R, Xiang N, Domann FE & Zhong W 2009 Effects of selenite and genistein on G2/M cell cycle arrest and apoptosis in human prostate cancer cells. *Nutrition and Cancer* **61** 397–407. (doi:10.1080/01635580802582751)

Received in final form 30 August 2012
Accepted 18 September 2012
Made available online as an Accepted Preprint
19 September 2012

FELLOWSHIP APPLICANT BIOGRAPHICAL SKETCH

USE ONLY FOR INDIVIDUAL PREDOCTORAL and POSTDOCTORAL FELLOWSHIPS. DO NOT EXCEED FOUR PAGES.

NAME OF FELLOWSHIP APPLICANT	POSITION TITLE
Rosalinda Savoy	Graduate Student Researcher
eRA COMMONS USER NAME (credential, e.g., agency login) rmsavoy	

EDUCATION/TRAINING (Begin with baccalaureate or other initial professional education, such as nursing, and include postdoctoral training.)

INSTITUTION AND LOCATION	DEGREE *(if applicable)*	YEAR(s)	FIELD OF STUDY
Rutgers, the State University of New Jersey	B.S.	01/2009	Genetics
University of California, Davis	Ph.D.	Exp 06/2014	Genetics

A. Personal Statement

My ongoing research interests involve using cutting edge technology in genetics and genomics to gain a comprehensive understanding of key pathways in the development and progression of cancer. I am interested in elucidating how alterations in gene expression contribute to cancer. My academic training and research experience have provided me with an excellent background in multiple biological disciplines including molecular biology, biochemistry, and genetics. I was able to start my collegiate career during high school by taking several AP classes and taking advantage of a partnership between Rensselaer Polytechnic Institute and local high schools to complete Calculus II during my final year in high school. As an undergraduate, I was able to conduct research with Dr. Randall Kerstetter on the gene funciton of a family of genes in Arabidopsis related to the RADIALIS gene in Antirrhinum. I gained valuable experience in developing a research project and learning techniques in recombinant DNA technology. During my undergraduate career I received several academic awards that helped further my research. As a predoctoral student with Dr. Paramita Ghosh, my research has focused on the regulation of transcription in prostate cancer by the androgen receptor.
My sponsor Dr. Paramita Ghosh is a leading researcher in the prostate cancer field and has a successful record for training predoctoral fellows. The proposed research will provide me with new conceptual and technical training in cancer biology and high throughput sequencing analysis. In addition, the proposed training plan outlines a set of career development activities and workshops – e.g. grant writing, public speaking, lab management, and mentoring students – designed to enhance my ability to be an independent investigator. My choice of sponsor, research project, and training will give me a solid foundation to reach my goal of studying cancer development.

B. Positions and Honors

ACTIVITY/OCCUPATION	BEGINNING DATE (mm/yy)	ENDING DATE (mm/yy)	FIELD	INSTITUTION/COMPANY	SUPERVISOR/ EMPLOYER
Undergraduate Research Assistant	09/06	05/08	Genetics, Plant Biology	Rutgers, the State University of New Jersey	Dr. Randall Kerstetter
ARESTY Peer Mentor	09/07	05/08		Rutgers, the State University of New Jersey	Aresty Research Center for Undergraduates
Graduate Research Assistant	06/10	Present	Genetics, Cancer Biology	University of California, Davis	Dr. Paramita Ghosh
Teaching Assistant	04/11	06/11	Molecular Biology	University of California, Davis	Dr. Valley Stewart

Academic and Professional Honors
National Society of Collegiate Scholars, 2006
ARESTY Research Assistant Program ($1,000), 2006-2007
Waksman Undergraduate Research Fellowship ($3,000), 2007
Graduate Studies Block Grant ($46,000), 2009-2010

Memberships in professional societies:
American Association for Cancer Researchers, 2010
Phi Sigma Honors Society, 2011
Society of Endocrinology, 2013

C. Publications
Research Papers
Mooso, B.A., Vinall, R.L., Tepper, C.G., **Savoy, R.M.**, Cheung, J.P., Singh, S., Siddiqui, S., Wang, Y., Bedolla, R.G., Martinez, A., Mudryj, M., Kung, H.J., deVere White, R.W., and Ghosh, P.M. 2012. Enhancing the effectiveness of androgen deprivation in prostate cancer by inducing Filamin A nuclear localization. Endocrine-Related Cancer, 19(6), 759-77

Savoy, R.M., Chen, L., Siddiqui, S., Melgoza, F.U., Durbin-Johnson, B., Roy, M., Jathal, M.K., Bose, S., Wang, Y., Mooso, B.A., D'Abronzo, L., Fry, W.H., Carraway, K.L.III, and Ghosh, P.M. 2013. Androgen Receptor targeting of Nrdp1, a negative regulator of ErbB3, restored by Filamin A nuclear localization in prostate cancer (In submission)

Abstracts
Savoy, R.M. and Kerstetter, R. Functional genomics of RADIALIS-like transcription factors in Arabidopsis leaf development. Abstract for poster presentation. 3rd Annual ARESTY Undergraduate Research Symposium 2007

Savoy, R.M., Mooso, B.A., Cheung, J.P., Wang, Y., Vinall, R.L., deVere White, R.W., and Ghosh, P.M. Abstract for poster presentation. Genestein Combined Polusaccharide-induced apoptosis is mediated by Filamin A cleavage. UC Davis Cancer Center: 16th Annual Cancer Research Symposium 2010

Chen, L., Fry, W.H., Savoy, R.M., Jathal, M.K., Bose, S., Mooso, B.A., Singh, S., Carraway, K.L.III, and Ghosh, P.M. Abstract for poster presentation. Loss of Angdrogen Receptor Transcriptional Regulation of Nrdp1, a negative regulator ofErbB3, results in Castration Resistant Growth of Prostate Cancer cells. AACR Targeting PI3K/mTOR Signaling in Cancer Conference 2011

Savoy, R.M., Chen, L., Siddiqui, S., Roy, M., Ryan, R.E., Jathal, M.K., Bose, S., Wang, Y., Fry, W.H., Carraway, K.L.III, and Ghosh, P.M. Abstract for poster presentation. Identification of Nrdp1 as a Novel Androgen Receptor Transcription Target Differentially Regulated in Androgen-Dependent and Independent Prostate Cancer. AACR Molecular Targeted Therapies: Mechanisms of Resistance Conference 2012

Savoy, R.M., Chen, L., Siddiqui, S., Roy, M., Ryan, R.E., Jathal, M.K., Bose, S., Wang, Y., Fry, W.H., Carraway, K.L.III, and Ghosh, P.M. Abstract for poster presentation. Identification of Nrdp1 as a Novel Androgen Receptor Transcription Target Differentially Regulated in Androgen-Dependent and Independent Prostate Cancer. UC Davis Interdisciplinary Graduate and Professional Symposium 2013

Review
Savoy, R.M. and Ghosh, P.M. 2013. Filamin A: Role in Cancer Development. In Preparation.

D. Scholastic Performance

YEAR	SCIENCE COURSE TITLE	GRADE
2005	AP Biology	5
	RUTGERS, THE STATE UNIVERSITY OF NEW JERSEY	
2005	Intro to Experimentation	A
2005	General Chemistry I	A
2006	General Chemistry II	B+
2006	General Physics	A
2006	General Physics Lab	A
2006	General Physics	B
2006	General Physics Lab	A
2006	Organic Chemistry I	B
2006	Genetic Analysis I	A
2007	Organic Chemistry II	B+
2007	Genetic Analysis II	A
2007	Behavioral and Neural Genetics	A
2007	Intro to Biochemistry and Molecular Biology	B+
2008	Organic Chemistry Lab	B+
	UNIVERSITY OF CALIFORNIA, DAVIS	
2009	Genetic Analysis	A
2010	Quantitative and Population Genetics	A
2010	Molecular Biology	A
2010	Functional Genomics	A
2010	Genomics	B+
2010	Cell Proliferation and Cancer Genes	A-
2011	Apoptosis and Disease	A-

YEAR	OTHER COURSE TITLE	GRADE
2004	AP Calculus AB	5
2004	AP American History	5
	RENSSELAER POLYTECHNIC INSTITUTE	
2004	Calculus II (taken during high school)	B
	RUTGERS, THE STATE UNIVERSITY OF NEW JERSEY	
2005	Expository Writing I	B
2005	Development of Europe I	A
2005	Intro to Sociology	B
2006	Current Moral and Social Issues	B+
2006	General Psychology	A
2006	Abnormal Psychology	A
2007	Social Psychology	A
2007	Religions of the Eastern World	A
2007	Gene and Evolution: Historical Perspective	A
2007	Seminar in Genetics	B
2007	Topics in Molecular Genetics	A
2007	Intro to Modern Philosophy	A
2007	Physiological Psych	B+
2008	Seminar in Genetics	A
2008	Topics in Human Genetics	A
2008	Special Topics in Genetics	A
2008	Adolescent Development	A
2008	Italian	A
2008	Italian Renaissance History	A
2008	Italian Renaissance Art History	A
2008	Italian Literature	A
	UNIVERSITY OF CALIFORNIA, DAVIS	
2009	Seminar in History of Genetics	A
2010	Seminar in Human Genetics	A-
2010	Literature in Molecular and Cell Biology	S
2011	Seminar in Cell Signaling	S